

Design, Synthesis and Study of the Bridged and Cofacially-Arrayed Poly-P-Phenylene Molecular Wires

Matthew J. Modjewski
Marquette University

Recommended Citation

Modjewski, Matthew J., "Design, Synthesis and Study of the Bridged and Cofacially-Arrayed Poly-P-Phenylene Molecular Wires" (2009). *Master's Theses (2009 -)*. Paper 21.
http://epublications.marquette.edu/theses_open/21

**DESIGN, SYNTHESIS AND STUDY OF THE BRIDGED AND COFACIALLY-
ARRAYED POLY-*P*-PHENYLENE MOLECULAR WIRES**

by

Matthew J. Modjewski

A Thesis Submitted to the Faculty of the Graduate School,

Marquette University,

in Partial Fulfillment of the Requirements for

the Degree of

Master of Science

Milwaukee, Wisconsin

December 2009

Abstract

Two novel series of bridged and cofacially-arrayed poly-*p*-phenylenes have been designed synthesized and studied. The bridged poly-*p*-phenylenes have been synthesized from a readily available diacetylenic precursor utilizing three high yielding steps, and their structures were determined by $^1\text{H}/^{13}\text{C}$ NMR spectroscopy as well as X-ray crystallography. The racemization barrier between the two atropoisomers was found to be ~ 12 Kcal mol $^{-1}$; the versatility of the synthesis employed was extended to synthesis a triply bridged tetra-*p*-phenylene and a quadruply bridged penta-*p*-phenylene.

The cofacially-arrayed poly-*p*-phenylenes have shown that the X-ray crystal structures of the neutral compounds are largely dominated by C-H-- π -interactions interactions while the dicationic species display an almost perfect parallel arrangement of the cofacially-arrayed poly-*p*-phenylene moieties. Electrochemistry of the cofacially-arrayed poly-*p*-phenylenes and their model compounds consistently met the reversibility criteria. Electronic absorption spectra show that the two series are strikingly similar; however the emission spectra show that the cofacially-arrayed poly-*p*-phenylenes are significantly broader and bathochromically shifted in comparison to the model compounds.

Electrochemical oxidation of 2,3,6,7-tetramethoxy-9,10-dimethylantra-cene showed that it undergoes a highly reversible electrochemical oxidation ($E_{\text{ox}} = 0.81$ V vs. SCE) and forms a modestly stable cation-radical salt in solution. The X-ray crystal structure showed the presence of a dicationic homotrimer that decomposes in the spiro adduct when allowed to sit at ambient temperatures.

Acknowledgements

- I would like to thank *Dr. Rajendra Rathore* for giving me the opportunity to work in his laboratory for these past two years and for his constant support and advice throughout my academic career here at Marquette.
- I would also like to express my thanks to my committee members; *Dr. Mark Steinmetz* and *Dr. James Gardinier*
- I would also like to thank all of my group members for their constant friendship, advice and support.

Dedication

- I would like to dedicate this thesis to my wife *Erin Modjewski* and to all of my family for their constant support, love and encouragement all throughout my life.

Table of Contents

List of Tables	iv
List of Figures	vi
List of Schemes	ix
Chapter 1 A Versatile Preparation of Geländer-Type <i>p</i>-Terphenyls from a Readily Available Diacetylenic Precursor	
1.1 Introduction.....	2
1.2 Results and Discussion	3
1.3 Summary and Conclusion	15
1.4 Experimental Section	16
1.5 Experimental Spectra	49
Chapter 2 Isolation and X-Ray Structural Characterization of a Dicationic Homotrimer of 2,3,6,7-Tetramethoxy-9,10-Dimethylanthracene Cation Radical	
2.1 Introduction.....	91
2.2 Results and Discussion	92
2.3 Summary and Conclusion	103
2.4 Experimental Section	104

**Chapter 3 Synthesis and Optoelectronic Properties of Cofacially-Stacked
Poly-*p*-Phenylene Derivatives: X-Ray Crystallographic Evidence of
Through-Space Charge Delocalization**

3.1 Introduction.....	112
3.2 Results and Discussion	117
3.3 Summary and Conclusion.....	134
3.4 Experimental Section.....	135
3.5 Experimental Spectra.....	152

List of Tables

Table 1.	Molecular structures of various doubly-bridged <i>p</i> -terphenyls obtained by X-ray crystallography.....	6
Table 2.	Crystal data and structure refinement of 4a	79
Table 3.	Crystal data and structure refinement of 4b	80
Table 4.	Crystal data and structure refinement of 4c	81
Table 5.	Crystal data and structure refinement of 4d	82
Table 6.	Crystal data and structure refinement of 5d	83
Table 7.	Crystal data and structure refinement of 4e	84
Table 8.	Crystal data and structure refinement of 4f	85
Table 9.	Crystal data and structure refinement of 4g	86
Table 10.	Crystal data and structure refinement of 4h	87
Table 11.	Crystal data and structure refinement of 5i	88
Table 12.	Crystal data and structure refinement of the bischromiumtricarbonyl complex of 4a	89
Table 13.	DFT calculations of the bond length changes between neutral and cation radical 1	99
Table 14.	Crystal data and structure refinement of neutral 1	107
Table 15.	Crystal data and structure refinement of 1⁺ SbCl₆⁻	108
Table 16.	Crystal data and structure refinement of [5²⁺ (SbCl₆⁻)₂].....	109

Table 17.	The optical and electrochemical data of F2-Ar and F1-Ar derivatives.....	124
Table 18.	Crystal data and structure refinement for F2-Ph	162
Table 19.	Crystal data and structure refinement for F2-Tol	163
Table 20.	Crystal data and structure refinement for F1-Tol	164
Table 21.	Crystal data and structure refinement for F2-BP	165
Table 22.	Crystal data and structure refinement for F2-BPH	166
Table 23.	Crystal data and structure refinement for F2-An	167
Table 24.	Crystal data and structure refinement for F2-DMT	168
Table 25.	Crystal data and structure refinement for $[(\text{F2-Ph})^{2+} (\text{SbCl}_6^-)_2]$.	169
Table 26.	Crystal data and structure refinement for $[(\text{F2-Tol})^{2+} (\text{SbCl}_6^-)_2]$	170
Table 27.	Crystal data and structure refinement for $[(\text{F2-DMT})^{2+} (\text{SbCl}_6^-)_2]$	171
Table 28.	Crystal data and structure refinement for F2-Ver-Cl	172
Table 29.	Crystal data and structure refinement for F2-Ph-Br6	173

List of Figures

Figure 1.	Showing the similarity of the shape of doubly-bridged <i>p</i> -terphenyl with the helical ribbons and the banister of a helical staircase	2
Figure 2.	Showing the two isoenergetic atropoisomers of <i>p</i> -terphenyl 4a as obtained by DFT calculations.....	9
Figure 3.	Isoenergetic conformers of 4g obtained within a single crystalline sample.....	10
Figure 4.	VT ¹ H NMR spectra of the aliphatic region of 4e	11
Figure 5.	X-ray crystal structure of the neutral 2,3,6,7-tetramethoxy-9,10-dimethylantracene (1) including the extended packing.....	93
Figure 6.	Cyclic voltammograms of 1 showing reversibility at scan rates of 50-600 mV/s.....	94
Figure 7.	Spectral changes attendant upon the reduction of MA ⁺ * cation radical by addition of substoichiometric amounts of 1	96
Figure 8.	X-Ray crystal structure of the dicationic homotrimer of 1	97
Figure 9.	DFT calculations of the dicationic homotrimer of 1	99
Figure 10.	ORTEP and stick diagram of the dicationic spiro adduct [5 ²⁺ (SbCl ₆ ⁻) ₂].....	101
Figure 11.	Spacing diagram of [5 ²⁺ (SbCl ₆ ⁻) ₂] showing that the molecules do not overlap with each other.....	110

- Figure 12.** Line diagrams of bichromophoric electron donors showing the interplanar angles between a pair of veratrole moieties.....112
- Figure 13.** The molecular structures of representative cation radical salts established by X-ray crystallography113
- Figure 14.** The crystal structure of $\text{QP}^{+\bullet} \text{SbCl}_6^-$ cation radical showing the stacked dimeric pairs.....114
- Figure 15.** Structure and naming scheme of cofacially-arrayed pimer cation radical precursors (**F2-Ar**) and the corresponding model compounds (**F1-Ar**).....116
- Figure 16.** Electronic absorption spectra of various **F2-Ar** and **F1-Ar**119
- Figure 17.** Emission and excitation spectra of various **F2-Ar** and **F1-Ar**120
- Figure 18.** Cyclic voltammograms of **F1-Ph** and **F2-Ph** at scan rates between 50 and 500 mV/s.....122
- Figure 19.** Cyclic and square wave voltammograms of various **F2-Ar** and **F1-Ar** at a scan rate of 200 mV/s.....123
- Figure 20.** The structures and redox potentials of the aromatic oxidants used for the generation of pimeric dications.....125
- Figure 21.** Spectral changes obtained upon the redox titrations of **F2-Ar** and **F1-Ar**126
- Figure 22.** A comparison of the absorption spectra of **F2-Ar**²⁺ and **F1-Ar**⁺127

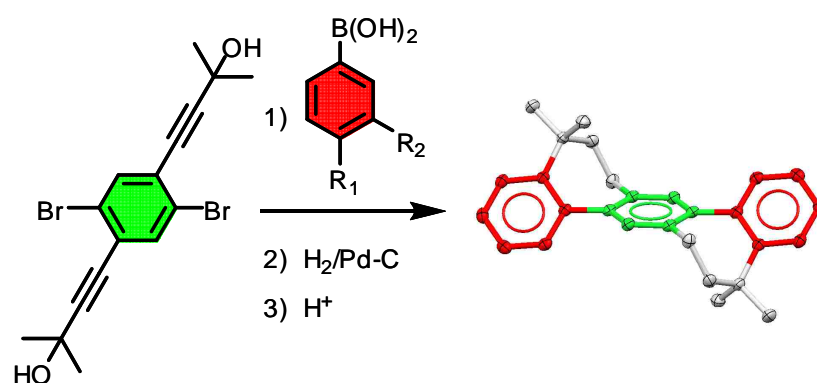
- Figure 23.** Typical aromatic-acromatic interactions observed in the solid state128
- Figure 24.** The molecular structures of various (neutral) **F2-Ar** and a model **F1-Ar** derivative (**F1-Tol**), obtained by X-ray crystallography, are compared129
- Figure 25.** The representative structures of **F2-Tol** and **F2-An** showing that the conformations of various **F2-Ar** are controlled, in part by effective intramolecular CH-- π interactions130
- Figure 26.** Conformations of **F2-Bp** and **F2-BPH** showing that while the conformation of **F2-BP** is dominated by CH-- π interactions, the **F2-BPH** is controlled by efficient stacking of the nonpolar hexyl groups connected to the polyphenylenes130
- Figure 27.** The molecular dicationic [**F2-Ph**²⁺ (SbCl₆⁻)₂], [**F2-Tol**²⁺ (SbCl₆⁻)₂], and [**F2-DMT**²⁺ (SbCl₆⁻)₂], obtained by X-ray crystallography ..131
- Figure 28.** The packing arrangement of [**F2-DMT**²⁺ (SbCl₆⁻)₂]133
- Figure 29.** Comparing the neutral **F2-DMT** and the dicationic [**F2-DMT**²⁺ (SbCl₆⁻)₂] X-ray crystal structures134

List of Schemes

Scheme 1.	Synthesis of diacetylenic precursor 1	3
Scheme 2.	A 3 step synthetic protocol of Geländer-type <i>p</i> -terphenyls	4
Scheme 3.	Preparation of biscyclohexyl derivative 4h	5
Scheme 4.	Intramolecular Friedel-Crafts cyclizations leading to both the 5 and 7 membered carbocycles	7
Scheme 5.	Preparation of the quadruply-bridged penta- <i>p</i> -phenylene	13
Scheme 6.	Preparation of the singly-bridged biphenyl and the triply-bridged tetra- <i>p</i> -phenylene	14
Scheme 7.	Proposed mechanism for the formation of the dicationic spiro adduct [5 ²⁺ (SbCl ₆ ⁻) ₂]	102
Scheme 8.	Synthetic scheme for the preparation of various F2-Ar and F1-Ar derivatives.....	118
Bibliography	174

CHAPTER 1

A Versatile Preparation of Geländer-Type *p*-Terphenyls from a Readily Available Diacetylenic Precursor



Abstract: A series of doubly bridged *p*-terphenyls (**4**) have been synthesized utilizing a facile three step synthesis starting from the readily available diacetylenic precursor (**1**) in excellent overall yields and their structures were confirmed by $^1\text{H}/^{13}\text{C}$ NMR Spectroscopy as well as by X-ray Crystallography. The racemization barriers between the meso and chiral atropoisomers of the **4** were found to be ~ 12 Kcal/mol by variable temperature NMR Spectroscopy. The versatility of the protocol developed herein was further demonstrated by the preparation of a singly-bridged biphenyl, a triply-bridged tetra-*p*-phenylene and a quadruply-bridged penta-*p*-phenylene derivative.

1.1 INTRODUCTION

The doubly-bridged *p*-terphenyls are helical ribbon-shaped molecules which have been coined the name “Geländer” owing to the similarity of their shape with the banister of a spiral staircase, i.e. Figure 1.¹⁻³

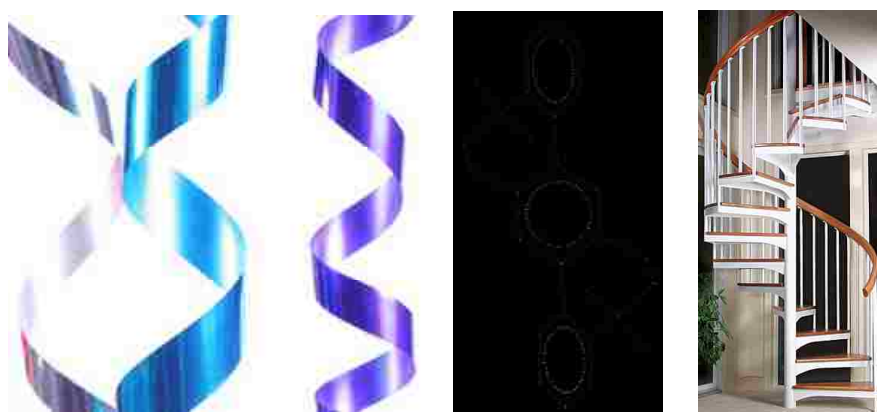


Figure 1. Showing the similarity of the shape of doubly-bridged *p*-terphenyl with the helical ribbons and the banister of a helical staircase.

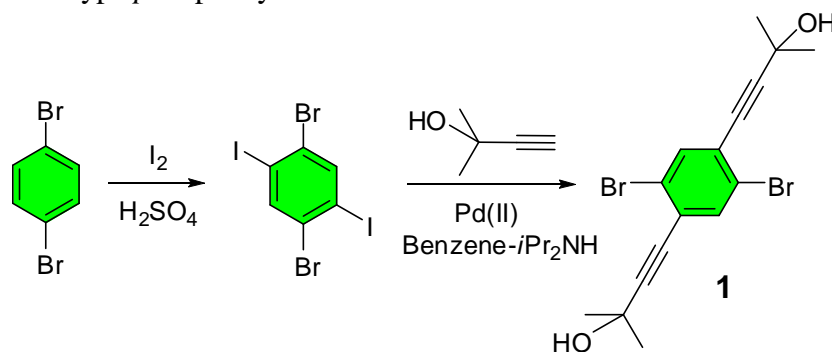
The helical biaryls, such as binaphthyls and biphenyls, have found widespread usage as chiral ligands in modern asymmetric catalysis.⁴⁻⁷ Although, a multi-step synthesis of Geländer-type terphenyls has been reported by Vögtle and coworkers,¹ their potential either in asymmetric catalysis or for materials' applications, thus far, remains unexplored. The lack of applications may arise, in part, owing to the unavailability of a simple general synthesis of such doubly-bridged *p*-terphenyls as well as bridged biphenyls.⁸⁻¹⁰

Herein we report a versatile synthesis of a variety of doubly-bridged *p*-terphenyls from a readily available diacetylenic precursor via a simple three-step route which involves high-yielding reactions, such as Suzuki coupling, catalytic hydrogenation, and intramolecular Friedel-Crafts alkylation (see Scheme 2). Various doubly-bridged terphenyls, obtained in excellent overall yields, were characterized by NMR spectroscopy and by X-ray crystallography. Moreover, it is shown that these doubly-bridged *p*-terphenyls, similar to the singly-bridged biphenyls,¹¹⁻¹² undergo a ready racemization at room temperature as probed by variable temperature ¹H NMR spectroscopy and by DFT calculations. The details of these findings are described herein.

1.2 RESULTS and DISCUSSION

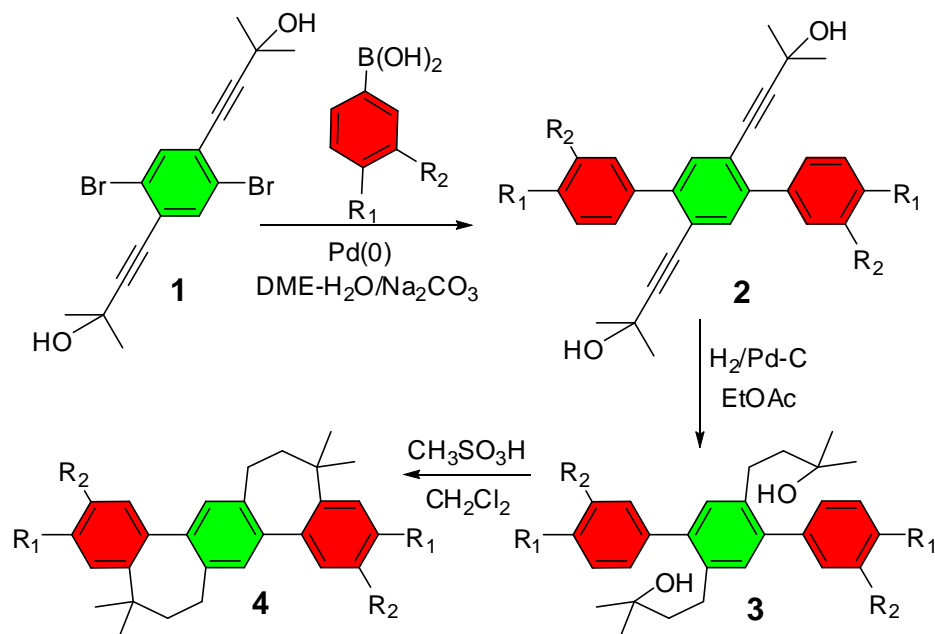
Thus, the common diacetylenic precursor **1** for the synthesis of doubly-bridged *p*-terphenyls was easily obtained in excellent yield via a standard Sonogashira coupling¹³ of the readily available 1,4-dibromo-2,5-diiodo-benzene¹⁴ and 2-methyl-3-butyn-2-ol, i.e. Scheme 1.

Scheme 1. Synthesis of diacetylenic precursor **1** for the preparation of Geländer-type *p*-terphenyls.



Syntheses of the various doubly-bridged *p*-terphenyls from **1** were accomplished via a three-step route as follows. Thus, a standard Suzuki coupling¹⁵⁻¹⁶ of the diacetylenic precursor **1** with various aryl boronic acids (see Table 1) in the presence of a Pd(0) catalyst afforded the diacetylenic *p*-terphenyls (**2**), which in most cases were easily purified by a simple filtration over a short pad of silica gel using a hexanes/ethyl acetate mixture as the eluent. The resulting diacetylenic *p*-terphenyls (**2**) were then subjected to catalytic hydrogenation in ethyl acetate in the presence of 10% palladium on activated carbon as the catalyst. The resulting reduced terphenyls (**3**) were then treated with methanesulfonic acid in dichloromethane at room temperature to afford the doubly-bridged *p*-terphenyls via two facile intramolecular Friedel-Crafts cyclizations¹⁷ (Scheme 2).

Scheme 2. A 3-step synthetic protocol for the preparation of Geländer-type *p*-terphenyls from diacetylenic precursor **1**.



With the use of the protocol developed in Scheme 2, a variety of doubly-bridged *p*-terphenyls were prepared in excellent overall yields (see Table 1) and their structures were established by $^1\text{H}/^{13}\text{C}$ NMR spectroscopy and further confirmed by X-ray crystallography (see Table 1).

It is noteworthy that the usage of 1-ethynyl-1-cyclohexanol instead of 2-methyl-3-butyn-2-ol (in Scheme 1) easily allows for the preparation of a bis-cyclohexyl derivative **4h** instead of the corresponding tetramethyl derivative **4e** (see Table 1 and Scheme 3).

Scheme 3. Preparation of bis-cyclohexyl derivative **4h**.

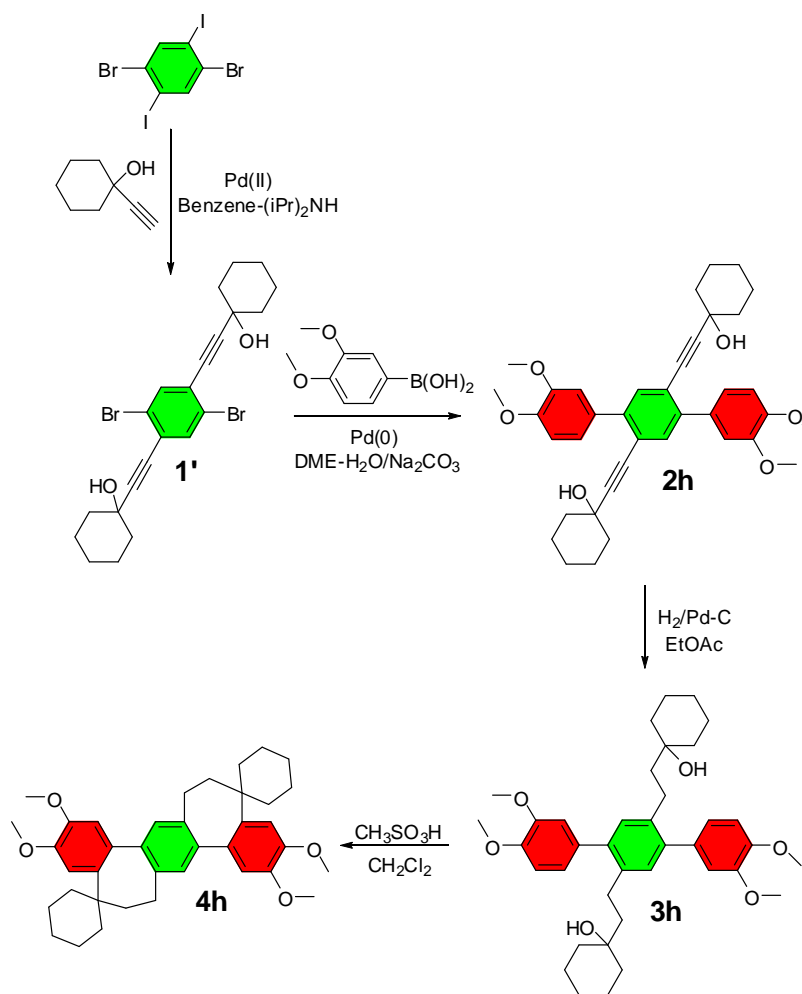
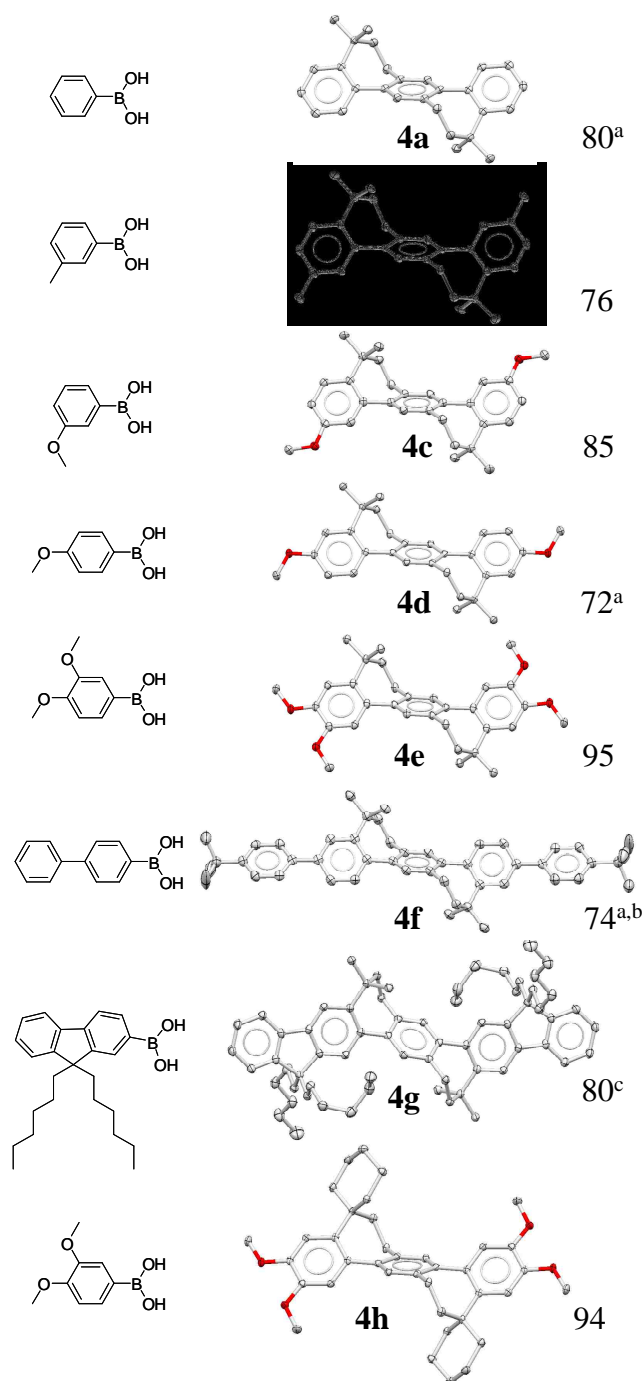
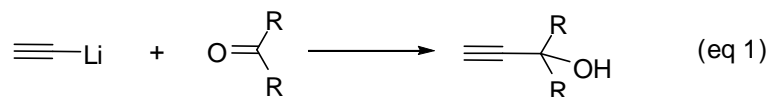


Table 1. Molecular structures of various doubly bridged *p*-terphenyls obtained by X-ray crystallography and their overall yields in 3-steps.



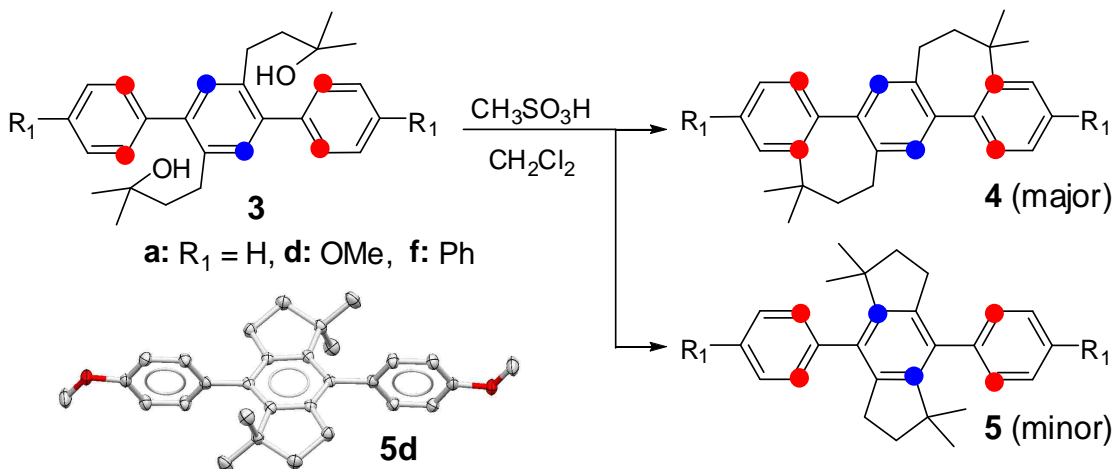
^aYields include both of the doubly-bridged *p*-terphenyls **4** and the centrally cyclized isomer **5** (vide infra), i.e. **4a/5a**: 83:17; **4d/5d**: 38:62; **4f/5f**: 58:42. ^b**4f** did not afford single crystals and thus a *tert*-butyl derivative was prepared by a reaction of **4f** with *tert*-butyl chloride and a catalytic amount of FeCl₃ (see Experimental Section).¹⁸ ^cA single crystal of **4g** contained a 1:1 mixture of meso (shown) and d/l mixture (see text below).

As such, the preparation of **4h** also demonstrates that the bridge substituents (i.e. dimethyl and cyclohexyl in **4e** and **4h**, respectively) can be easily varied by employing an appropriate acetylenic tertiary alcohol, which, in turn, can be readily prepared by a reaction of the acetylene monoanion with the corresponding ketone, e.g. eq 1.



As shown in Scheme 4, the final step of the synthesis of the doubly-bridged *p*-terphenyls (**4**) required that the Friedel-Crafts cyclization must occur at the terminal aryls producing a pair of entropically less-accessible 7-membered carbocycles. Indeed, the substrates which contained an activating para-substituent (i.e. at carbon 3) on the terminal aryls (i.e. **3b**, **3c**, **3e**, **3g** and **3h**) exclusively produced the doubly-bridged *p*-terphenyls (**4**), without contamination from the products (i.e. **5**) formed via an alternative Friedel-Crafts cyclization to the central aromatic ring producing the entropically favored 5-membered carbocycles (i.e. Scheme 4).

Scheme 4. Intramolecular Friedel-Crafts cyclizations leading to 7-membered versus 5-membered isomers.



Expectedly, in the case of *p*-terphenyl substrates (i.e. **3a**, **3d**, and **3f**), which do not contain an activating substituent at carbon 3 of the terminal aryl groups (i.e. para to the carbons indicated by the red dots), the Friedel-Crafts cyclization also produced significant amounts of bis-indano products (i.e. **5a**, **5d**, and **5f**) where the cyclization occurred at the central aromatic ring (see Scheme 4 and Table 1). Furthermore, the structure of a representative bis-indano product (i.e. **5d**) was confirmed by X-ray crystallography (see Scheme 4).

In order to further confirm that the preferential formation of doubly-bridged *p*-terphenyls (**4**), containing 7-membered carbocycles in Scheme 4, did not occur via an acid catalyzed rearrangement of **5** to **4** or vice versa, samples of both **4a** and **5a** were subjected to the same acidic conditions employed for the Friedel-Crafts intramolecular cyclizations and the course of the reactions were monitored by ¹H NMR spectroscopy over several days. Under these conditions, both **4a** and **5a** showed no signs of interconversion as judged by the ¹H NMR spectroscopic analysis of the aliquots after 3 and 6 days.

The DFT calculations at the B3LYP/6-31G* level showed that two atropoisomers of the doubly bridged *p*-terphenyls, i.e. the chiral syn atropoisomer (*C*₂) or the achiral anti (meso) atropoisomer (*C*_i), are isoenergetic (see Figure 2).

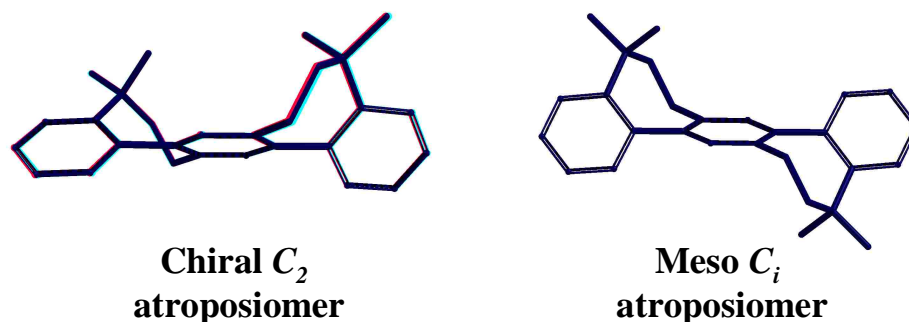


Figure 2. The structures of the two isoenergetic atropisomers of the doubly bridged *p*-terphenyl **4a** as obtained by DFT calculations at the B3LYP/6-31G* level.

Interestingly, however, in the solid state almost all doubly-bridged *p*-terphenyls showed the presence of only the centrosymmetric anti (meso) conformer with the dihedral angles between the central and peripheral aryl rings varying only in a very narrow range, i.e. 45.6-49.5°, as determined by X-ray crystallography (see Table 1). The exception being the fluoranyl containing **4g** which contained a 1:1 mixture of both syn and anti atropisomers in a single crystal, i.e. the meso and chiral atropisomers (see Figure 3). The co-crystallization of both syn and anti conformers may, in part, arise owing to the fact that each half of the syn-**4g** was structurally identical to that of the anti-**4g** (see Figure 3) with the dihedral angles of 47.6 and 46.9° between the central aryl and fluoranyl rings.

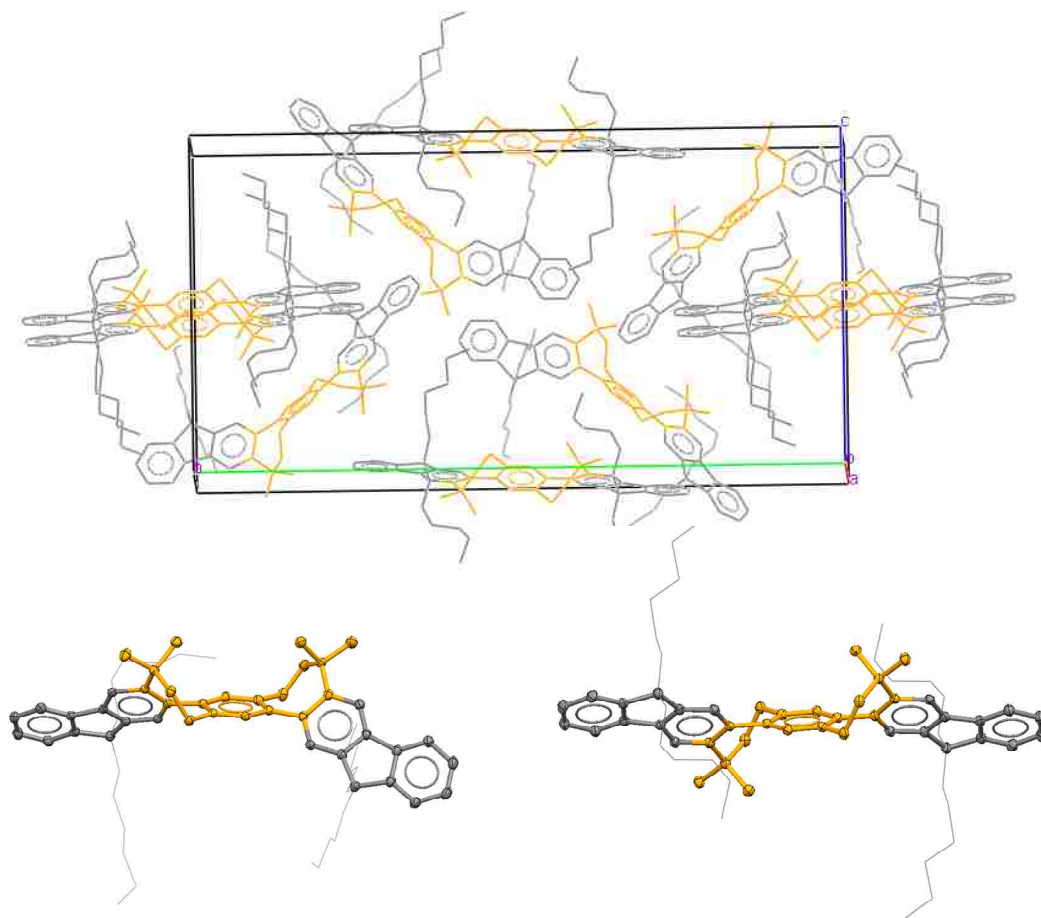


Figure 3. Isoenergetic conformers of **4g** obtained within a single crystalline sample.

The low activation barriers for the interconversion between the (isoenergetic) syn and anti conformers of the various doubly-bridged *p*-terphenyls was apparent by the presence of broadened methyl signals in their ^1H NMR spectra at ambient temperatures (see Experimental Spectra and Figure 4).

Variable temperature ^1H NMR spectroscopy of a representative doubly-bridged *p*-terphenyl (**4e**) in dichloromethane- d_2 over a temperature range of +20 to -90 $^\circ\text{C}$ showed that the interchange between the two isoenergetic conformers can be frozen at ~ -60 $^\circ\text{C}$; and the activation energy for the interchange into syn and anti conformers¹⁹ was

estimated to be $E_a \sim 12 \text{ Kcal mol}^{-1}$ by line-shape analysis of the signals in the variable temperature ^1H NMR spectra in Figure 4 (see additional spectra in the Experimental Spectra Section).

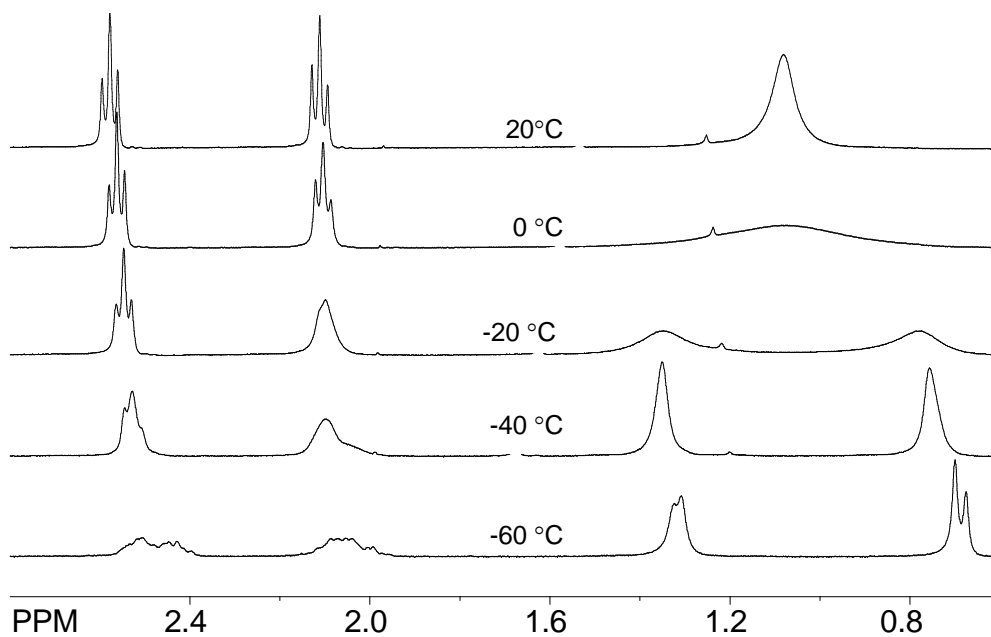


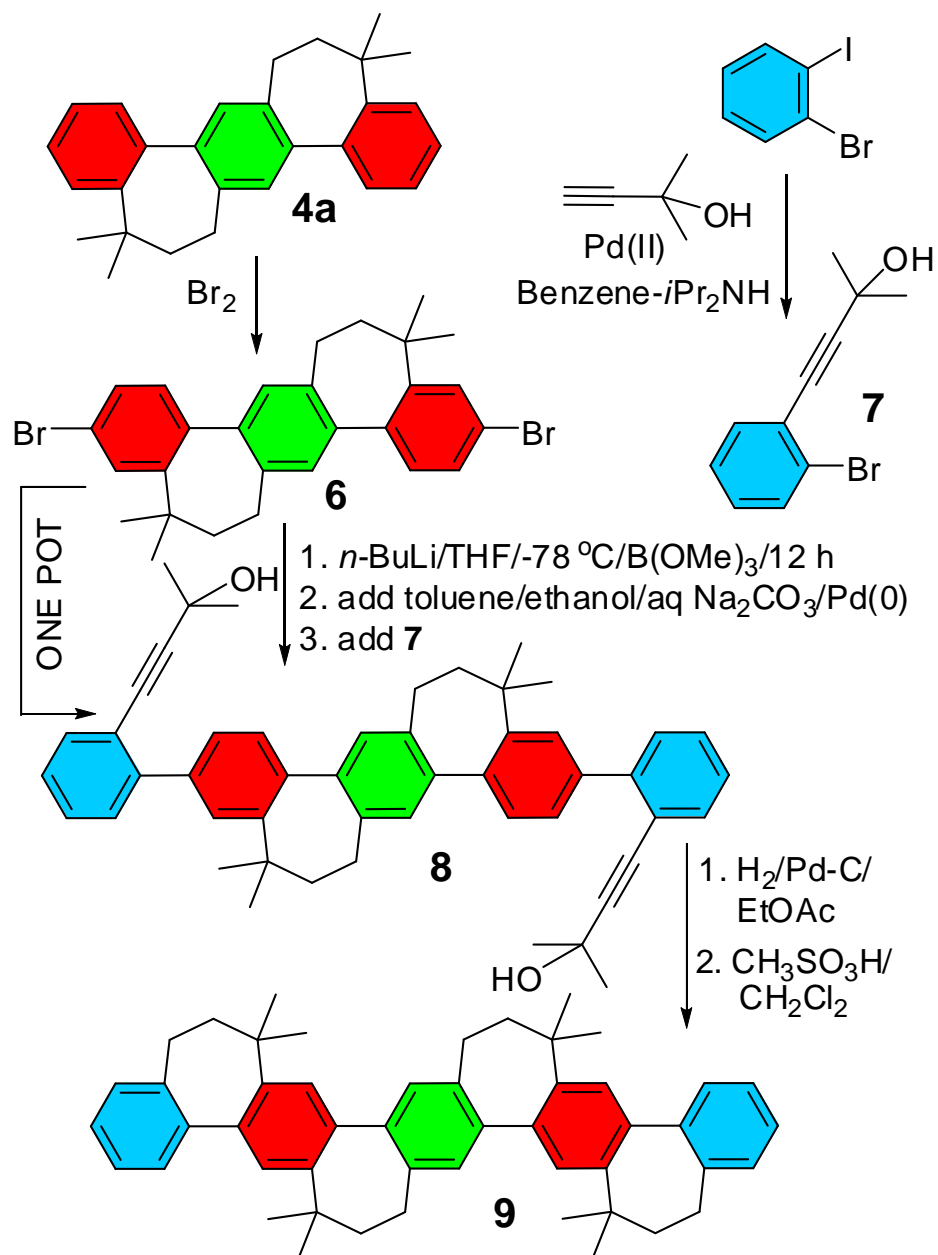
Figure 4. ^1H NMR spectra of the aliphatic region of *p*-terphenyl **4e** which shows that the broadened signal due to 4 methyl groups (at ~ 1.1 ppm) and the methylene protons (at 2.1 and 2.5 ppm) split into two sets of peaks at ~ -60 °C.

A substitution of the methyl groups in *p*-terphenyl **4e** with cyclohexyl groups (i.e. **4h**) did not change the activation barrier for the interconversion between the two atropoisomers. The broadened signals attributed to the cyclohexyl moiety, the methoxy peaks, and the aromatic peaks of **4h** resolved into two sets of signals at low temperatures (see Experimental Spectra for VT ^1H NMR spectra of **4h**).

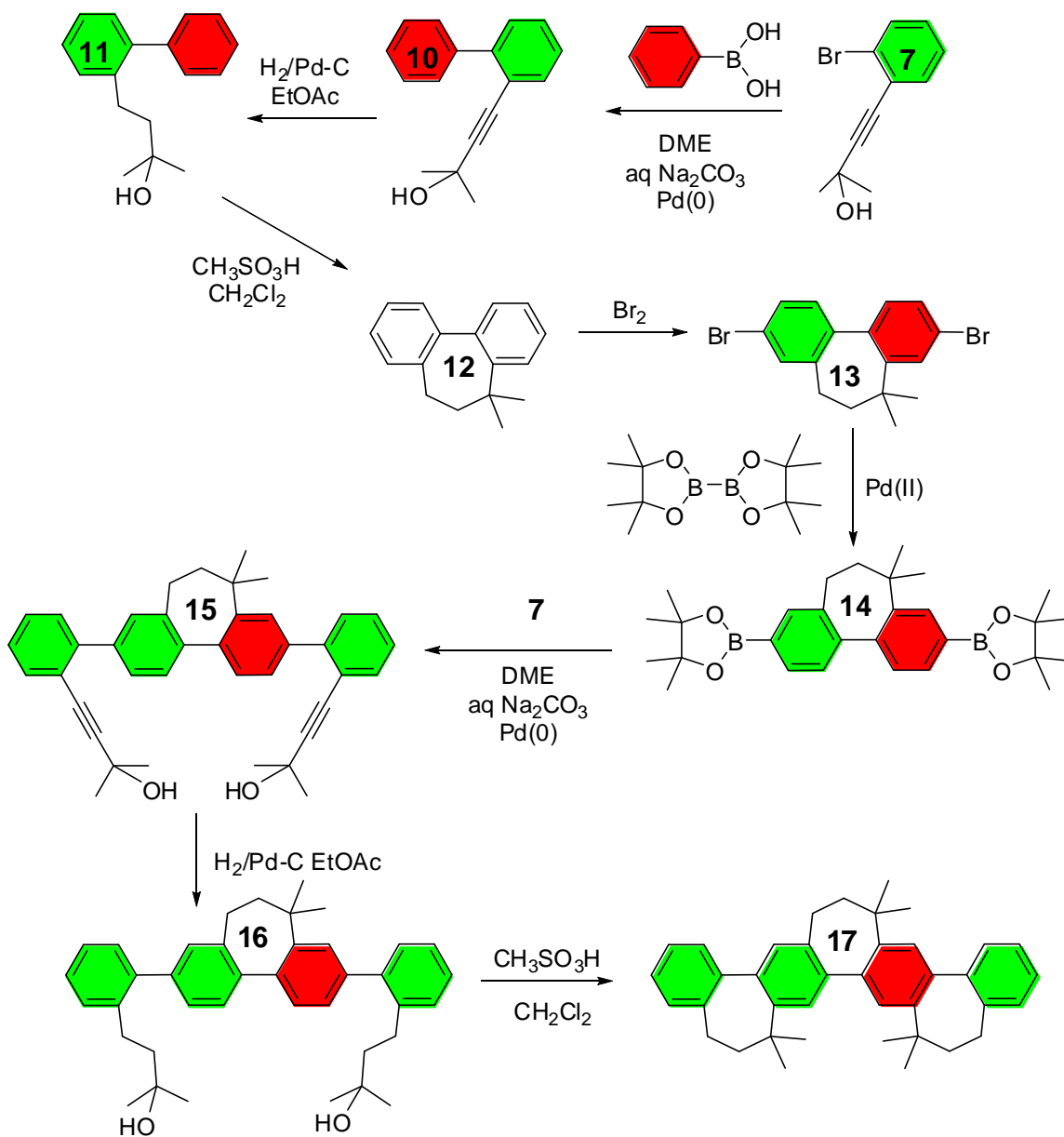
The versatility of the synthetic protocol in Schemes 1 and 2 for the preparation of various doubly-bridged *p*-terphenyls, was readily extended for the preparation of a higher poly-*p*-phenylene homologue with fixed dihedral angles (Scheme 5).²⁰ For example, a quadruply-bridged penta-*p*-phenylene **9** was obtained in good overall yield by a one-pot Suzuki coupling of the dibromo derivative **6** with monoacetylenic precursor **7** to afford **8** followed by a simple hydrogenation and a reaction with methanesulfonic acid (Scheme 5). The dibromo derivative **6** was, in turn, obtained by a bromination of **4a** while **7** was prepared by Sonogashira coupling according to Scheme 1.

In order to complete the series of bridged poly-*p*-phenylenes containing up to 5 phenylene moieties, a singly-bridged biphenyl and triply-bridged tetra-*p*-phenylene were also prepared by adaptation of the synthetic protocol in Schemes 1 and 2. Thus, Suzuki coupling of phenylboronic acid with monoacetylenic precursor **7** afforded **10**. A simple hydrogenation of **10** followed by an acid-catalyzed cyclization furnished the singly-bridged biphenyl **12** in good yield. The singly-bridged biphenyl **12** was converted to triply-bridged tetra-*p*-phenylene **17** (see Scheme 6) using a protocol similar to that described for the preparation of quadruply-bridged penta-*p*-phenylene **9** (compare Scheme 5).

Scheme 5. Preparation of quadruply-bridged penta-*p*-phenylene.



Scheme 6. Preparation of singly-bridged biphenyl (**12**) and triply-bridged tetra-*p*-phenylene (**17**).



1.3 SUMMARY and CONCLUSIONS

In summary, we have developed a facile synthesis of the doubly bridged *p*-terphenyls from the readily available diacetylenic precursor (**1**) via three high-yielding synthetic steps. In most cases, the X-ray crystal structure analysis showed that the achiral (meso) atropisomer preferentially crystallizes with the exception of **4g** whose crystalline samples contained both the achiral and chiral atropisomers within the same crystal. It was also shown by variable temperature ¹H NMR spectroscopy that the interchange between the two atropisomers can be prevented at low temperatures. Successful syntheses of singly-bridged biphenyl **12**, triply-bridged tetra-*p*-phenylene **15** and quadruply-bridged penta-*p*-phenylene **9** were also accomplished which further demonstrates the versatility of the synthetic protocol in Schemes 1 and 2. The availability of these homologues of bridged poly-*p*-phenylenes will allow the study of their optoelectronic properties in comparison to the simple poly-*p*-phenylenes.²⁰

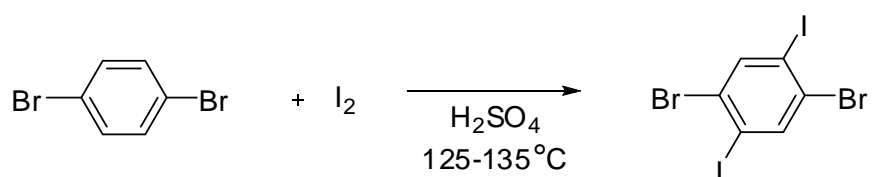
1.4 EXPERIMENTAL SECTION

General Experimental Methods and Materials. All reactions were performed under an argon atmosphere unless otherwise stated. 1,4-dibromobenzene, 2-methyl-3-butyn-2-ol, 3,4-dimethoxyphenylboronic acid, phenylboronic acid, 4-biphenylboronic acid, 1-ethynyl-1-cyclohexanol, anhydrous benzene, anhydrous toluene, anhydrous ethanol, sulfuric acid, diisopropylamine, anhydrous 1,2-dimethoxyethane, ethyl acetate, methanesulfonic acid, copper(I) iodide, *bis*(triphenylphosphine)palladium(II) dichloride, 3-bromoanisole, 3-bromotoluene, sodium carbonate, *tetrakis*(triphenylphosphine)palladium(0), 10% palladium on activated carbon, *n*-butyllithium, anhydrous ferric chloride, 2-chloro-2-methylpropane, trimethylborate, and triisopropylborate were all commercially available and used without further purification. 4-methoxyphenylboronic acid, and 9,9-dihexylfluoren-2-ylboronic acid were prepared according to standard literature procedures.

Anhydrous tetrahydrofuran (THF) was prepared by refluxing the commercial tetrahydrofuran over lithium tetrahydroaluminate under an argon atmosphere for 24 hours followed by distillation. It was stored under an argon atmosphere in a Schlenk flask equipped with a Teflon valve fitted with Viton *O*-rings. NMR spectra were recorded on 300 and 400 MHz NMR spectrometers.

Synthetic details for the preparation of various intermediates for the synthesis of *p*-terphenyls

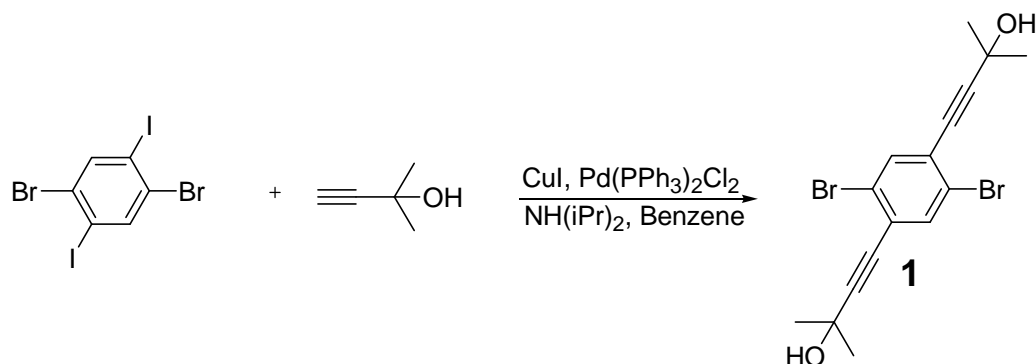
1,4-Dibromo-2,5-diiodobenzene.



In a 500-mL 3-neck flask equipped with a thermometer adapter and condenser, 1,4-dibromobenzene (19.5 g, 82.7 mmol) was dissolved in 250 mL concentrated sulfuric acid with heating. Elemental iodine (46.2 g, 181.9 mmol) was added to the solution portion wise while heating. The resulting purple mixture was stirred at 125-135 °C for 2 days during which the sublimated iodine was washed into the reaction mixture by shaking the flask after every 2 hours. The resulting mixture was cooled to room temperature and poured into ice water (300 mL), and extracted with dichloromethane (3 x 30 mL). The dichloromethane layer was then stirred with a dilute solution of sodium hydroxide (300 mL) in order to remove any excess iodine. The dichloromethane layer was separated and the aqueous sodium hydroxide layer was extracted once with dichloromethane (30 mL), and the combined organic layers were dried over anhydrous magnesium sulfate, evaporated, and dried under vacuum. A large portion of the product remained as a solid mass in the original reaction mixture which was broken up, triturated with dilute sodium hydroxide solution (300 mL), and filtered. Both portions combined gave a yellow solid which was recrystallized from a dichloromethane/methanol mixture. Yield (33.9 g, 84%);

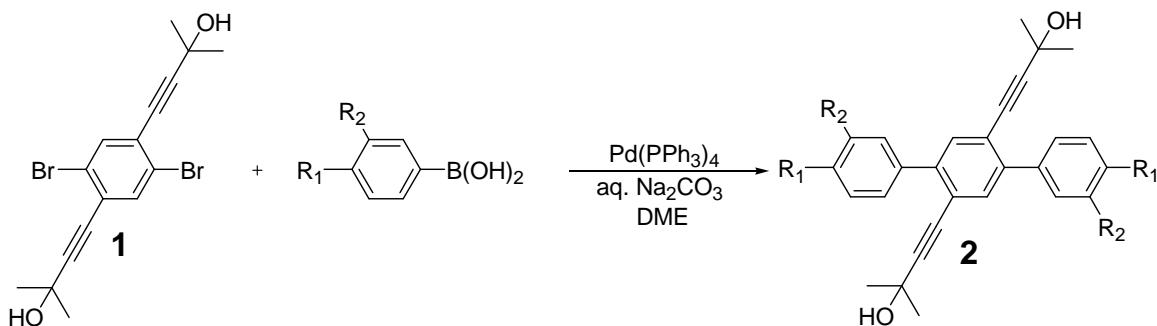
mp: 160-162 °C; ^1H NMR (CDCl_3) δ : 8.04 (s, 2H). ^{13}C NMR (CDCl_3) δ : 101.57, 129.42, 142.51.

Preparation of Diacetylenic Precursor 1.



1,4-Dibromo-2,5-diiodobenzene (8.0 g, 16.4 mmol) was dissolved in anhydrous benzene (80 mL) and diisopropylamine (48 mL) in an oven dried Schlenk flask under an argon atmosphere and the flask was evacuated and filled with argon (3x). Then, CuI (120 mg) and $\text{Pd}(\text{PPh}_3)_2\text{Cl}_2$ (100 mg) were added to the flask under an argon atmosphere and the flask was again evacuated and filled with argon (3x). Finally, 2-methyl-3-butyn-2-ol (3.2 mL, 32.8 mmol) was added to the flask via syringe and the flask was evacuated and filled with argon (3x) once more. The resulting solution was allowed to stir at room temperature overnight. The resulting yellow solution was diluted with water (100 mL) and extracted with ether (3 x 30 mL). The ether layer was washed with water (100 mL), extracted, dried over anhydrous magnesium sulfate, evaporated, and dried under vacuum to give a bright orange solid. The resulting solid was filtered over a short pad of silica gel using 30% ethyl acetate/hexanes as eluent to afford **1** as a pale orange solid. Yield (6.4 g, 98%); mp: 133-136 °C; ^1H NMR (CDCl_3) δ : 1.62 (s, 12H), 2.42 (s, 2H), 7.59 (s, 2H). ^{13}C NMR (CDCl_3) δ : 31.37, 65.90, 79.74, 101.30, 123.94, 126.13, 136.22.

General Procedure (a) for the Preparation of Various Diacetylenic Terphenyls (2).



Solid **1** and the corresponding aryl boronic acid (3 equiv.) were dissolved in anhydrous 1,2-dimethoxyethane (DME) (30 mL) in an oven dried Schlenk flask under an argon atmosphere and the flask was evacuated and filled with argon (3x). In another oven dried Schlenk flask a solution of anhydrous sodium carbonate (5.0 g) in water (20 mL) was prepared under an argon atmosphere and the flask was also evacuated and filled with argon (3x). To the DME solution, $\text{Pd(PPh}_3)_4$ (50 mg) and the salt solution were added sequentially under a strict argon atmosphere followed by evacuation and filling the flask with argon (3x) after each addition. The flask was covered with foil and the solution was allowed to reflux overnight. The resulting solution was cooled to room temperature, quenched with water (50 mL) and extracted with dichloromethane (3 x 20 mL). The organic layer was dried over anhydrous magnesium sulfate, evaporated and dried under vacuum. The various **2** were either filtered over a short pad of silica gel with a hexanes/ethyl acetate mixture as eluent or purified by column chromatography using a hexanes/ethyl mixture to give the pure **2**.

2a: Yield (0.97 g, 98%) beige solid; mp; 176-178 °C; ^1H NMR (CDCl_3) δ : 1.47 (s, 12H), 1.91 (s, 2H), 7.36-7.47 (m, 6H), 7.55 (s, 2H), 7.59-7.62 (m, 4H). ^{13}C NMR (CDCl_3) δ : 31.21, 65.81, 81.78, 98.19, 121.40, 127.97, 128.11, 129.38, 133.92, 139.47, 142.71.

2d: Yield (0.85 g, >99%) beige solid; mp: 182-184 °C; ^1H NMR (CDCl_3) δ : 1.49 (s, 12H), 1.99 (s, 2H), 3.85 (s, 6H), 6.95 (d, 4H, $J = 8.8$ Hz), 7.50 (s, 2H), 7.55 (d, 4H, $J = 8.8$ Hz). ^{13}C NMR (CDCl_3) δ : 31.28, 55.53, 65.83, 82.04, 97.92, 113.49, 121.14, 130.53, 131.90, 133.91, 141.74, 159.45

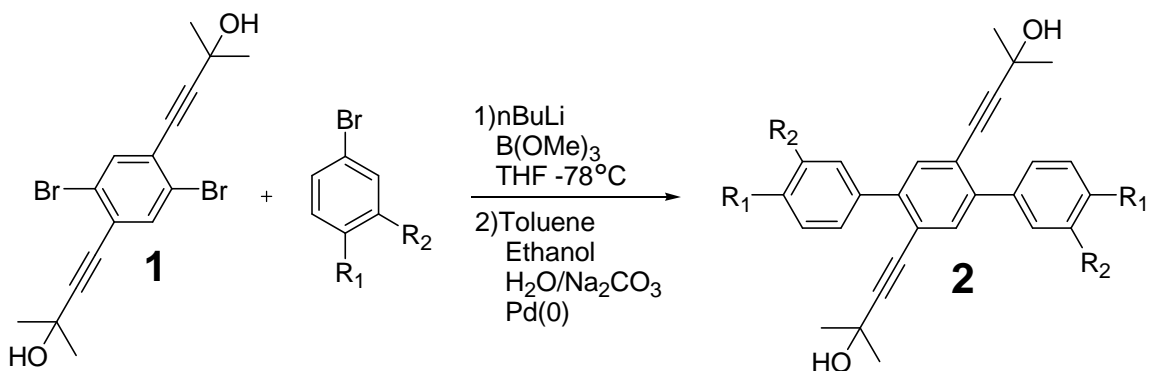
2e: Yield (0.91 g, >99%) brown solid; mp: 149-152 °C; ^1H NMR (CDCl_3) δ : 1.50 (s, 12H), 1.88 (s, 2H), 3.94 (s, 6H), 3.96 (s, 6H), 6.93 (d, 2H, $J = 8.2$ Hz), 7.16 (d, 4H, $J = 8.2$ Hz), 7.52 (s, 2H). ^{13}C NMR (CDCl_3) δ : 31.36, 56.10, 56.14, 65.75, 81.84, 98.13, 110.74, 112.69, 121.13, 121.78, 132.16, 134.07, 141.98, 148.46, 148.89

2f: Yield (0.95 g, 91%) beige solid; mp: 257-260 °C; ^1H NMR (CDCl_3) δ : 1.51 (s, 12H), 1.93 (s, 2H), 7.38 (d, 2H, $J = 7.3$ Hz), 7.48 (t, 4H, $J = 7.3$ Hz), 7.63 (s, 2H), 7.65-7.70 (m, 8H), 7.71-7.73 (m, 4H). ^{13}C NMR (CDCl_3) δ : 31.27, 65.88, 81.81, 98.36, 121.40, 126.83, 127.32, 127.69, 129.07, 129.82, 134.09, 138.36, 140.80, 142.18.

2g: Yield (1.13 g, 93%) yellow solid; mp: 102-105 °C; ^1H NMR (CDCl_3) δ : 0.69-0.80 (m, 20H), 1.07-1.14 (m, 24H), 1.46 (s, 12H), 1.83 (s, 2H), 2.02 (t, 8H), 7.32-7.38 (m, 6H), 7.45 (s, 2H), 7.60 (s, 2H), 7.65 (d, 2H, $J = 7.9$ Hz), 7.75 (d, 4H, $J = 7.9$ Hz). ^{13}C NMR (CDCl_3) δ : 14.24, 22.77, 24.01, 29.87, 31.37, 31.72, 40.51, 55.45, 65.85, 82.05, 98.26,

118.96, 120.03, 121.44, 123.21, 123.42, 127.02, 127.36, 128.51, 134.18, 138.56, 140.89, 140.95, 143.31, 151.10, 151.19.

General Procedure (b) for the Preparation of Various Diacetylenic Terphenyls (2).



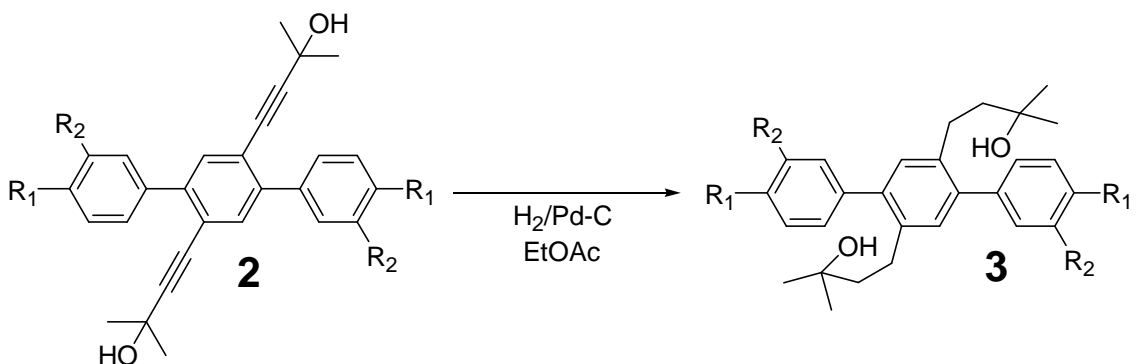
In an oven dried Schlenk flask under an argon atmosphere the aryl bromide (5 equiv.) was dissolved in dry THF (20 mL) and cooled to -78°C , n-butyllithium (6 equiv., 2.5 M in hexane) was added dropwise and the solution was allowed to stir for one hour while the temperature was maintained at -78°C . Then, trimethylborate (8 equiv.) was added via syringe and the mixture was allowed to come to room temperature overnight. In a separate Schlenk flask, a salt solution was made with water (8 mL) and anhydrous sodium carbonate (6 equiv.), at the same time, toluene (20 mL) and ethanol (20 mL) were added to the reaction mixture via syringe so that the toluene:ethanol:water ratio is 3:3:1. Next, solid **1** was added to the reaction flask and a condenser attached to a bubbler was placed on the reaction vessel and the flask was evacuated and filled with argon (3x). To the reaction mixture, Pd(PPh₃)₄ (50 mg) and the salt solution were added sequentially under a strict argon atmosphere followed by evacuation and filling the flask with argon (3x) after each addition. The flask was covered with foil and the solution was allowed to reflux overnight. The resulting solution was cooled to room temperature, quenched with

water (50 mL) and extracted with dichloromethane (3 x 20 mL). The organic layer was dried over anhydrous magnesium sulfate, evaporated and dried under vacuum. The various **2** were purified by column chromatography over silica gel using a hexanes/ethyl acetate mixture as the eluent to afford the pure various **2**.

2b: Yield (0.81 g, 76%) yellow solid; mp: 139-142 °C; $^1\text{H NMR}$ (CDCl_3) δ : 1.48 (s, 12H), 2.06 (s, 2H), 2.42 (s, 6H), 7.18 (m, 2H), 7.31 (m, 2H), 7.41 (m, 4H), 7.54 (s, 2H). $^{13}\text{C NMR}$ (CDCl_3) δ : 21.66, 31.22, 65.75, 81.87, 98.03, 121.25, 126.45, 128.01, 128.62, 130.07, 133.95, 137.56, 139.34, 142.58

2c: Yield (1.09 g, 94%) pale brown oil; $^1\text{H NMR}$ (CDCl_3) δ : 1.48 (s, 12H), 2.03 (s, 2H), 3.86 (s, 6H), 6.92 (d, 2H, $J = 8.0$ Hz), 7.17 (d, 4H, $J = 7.7$ Hz), 7.34 (t, 2H, $J = 7.7, 8.0$ Hz) $^{13}\text{C NMR}$ (CDCl_3) δ : 31.24, 55.53, 65.80, 81.69, 98.40, 113.41, 115.17, 121.33, 121.86, 129.13, 133.89, 140.75, 142.54, 159.34

General Procedure for the Catalytic Hydrogenation of Various Diacetylenic Terphenyls.



The corresponding **2** from above was placed into a Parr apparatus along with a stir bar and dissolved in ethyl acetate. To the solution, 10% Palladium on activated Carbon catalyst (100 mg) was added. The vessel was then put under hydrogen pressure (3 bar) for 24 hours after which time the solution was filtered over a short pad of silica gel. The silica gel was washed with ethyl acetate (2 x 20 mL), the solvent was evaporated and the resulting **3** was dried under vacuum and used without further purification.

3a: Yield (0.89 g, 90%) yellow solid; mp: 160-161 °C; ¹H NMR (CDCl₃) δ: 1.01 (s, 2H), 1.07 (s, 12H), 1.63 (m, 4H), 2.67 (m, 4H), 7.15 (s, 2H), 7.33-7.46 (m, 10H). ¹³C NMR (CDCl₃) δ: 27.87, 29.07, 45.89, 71.00, 127.15, 128.32, 129.45, 131.29, 137.45, 141.20, 141.66

3b: Yield (0.83 g, >99%) yellow oil; ¹H NMR (CDCl₃) δ: 1.01 (s, 12H), 1.57 (m, 4H), 1.97 (s, 2H), 2.33 (s, 6H), 2.58 (m, 4H), 7.06-7.26 (m, 10H). ¹³C NMR (CDCl₃) δ: 21.68, 27.87, 29.06, 45.94, 71.02, 126.49, 127.79, 128.17, 130.17, 131.23, 137.34, 137.85, 141.16, 141.65.

3c: Yield (1.08 g, 97%) yellow oil; ¹H NMR (CDCl₃) δ: 1.09 (s, 12H), 1.65 (m, 4H), 2.67 (m, 4H), 3.85 (s, 6H), 6.89-6.97 (m, 6H), 7.15 (s, 2H), 7.31-7.36 (m, 2H). ¹³C NMR (CDCl₃) δ: 27.86, 29.11, 45.94, 55.50, 71.01, 112.65, 115.10, 121.90, 129.29, 131.15, 137.39, 141.10, 143.07, 159.53

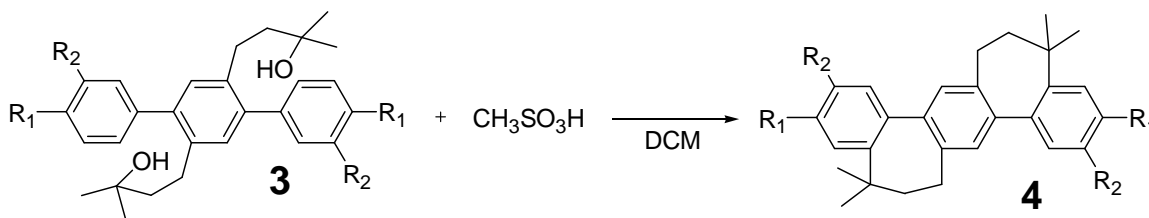
3d: Yield (0.83 g, 95%) yellow solid; mp: 151-153 °C; ^1H NMR (CDCl_3) δ : 1.06 (s, 2H), 1.10 (s, 12H), 1.64 (m, 4H), 2.66 (m, 4H), 3.86 (s, 6H), 6.95 (d, 4H, $J = 8.4$ Hz), 7.12 (s, 2H), 7.29 (d, 4H, $J = 8.4$ Hz). ^{13}C NMR (CDCl_3) δ : 27.88, 29.14, 45.90, 55.53, 71.05, 113.73, 130.49, 131.46, 134.12, 137.58, 140.57, 158.80

3e: Yield (0.90 g, 96%) yellow solid; mp: 152-155 °C; ^1H NMR (CDCl_3) δ : 1.10 (s, 12H), 1.49 (s, 2H), 1.66 (m, 4H), 2.68 (m, 4H), 3.90 (s, 6H), 3.93 (s, 6H), 6.90-6.95 (m, 6H), 7.14 (s, 2H). ^{13}C NMR (CDCl_3) δ : 27.91, 29.21, 31.41, 45.89, 56.13, 70.97, 110.99, 112.77, 121.56, 131.37, 134.36, 137.59, 140.86, 148.19, 148.64

3f: Yield (0.83 g, 86%) yellow solid; mp: 229-231°C; ^1H NMR (CDCl_3) δ : 1.10 (s, 2H), 1.12 (s, 12H), 1.71 (m, 4H), 2.75 (m, 4H), 7.23 (s, 2H), 7.35-7.40 (m, 2H), 7.46-7.51 (m, 8H), 7.66-7.70 (m, 8H). ^{13}C NMR (CDCl_3) δ : 27.93, 29.15, 45.96, 71.06, 127.04, 127.29, 127.55, 129.04, 129.90, 131.40, 137.61, 139.99, 140.69, 140.86, 140.99.

3g: Yield (0.74 g, 94%) yellow oil; ^1H NMR (CDCl_3) δ : 0.68-0.79 (m, 22H), 1.05-1.16 (m, 36H), 1.66 (m, 4H), 1.99 (t, 8H), 2.77 (m, 4H), 7.23 (s, 2H), 7.32-7.37 (m, 10H), 7.73-7.77 (t, 4H, $J = 7.3$ Hz). ^{13}C NMR (CDCl_3) δ : 14.24, 22.83, 24.08, 28.03, 29.18, 29.95, 31.73, 40.59, 45.80, 55.30, 70.95, 119.46, 119.92, 123.12, 124.07, 126.99, 127.21, 128.08, 131.45, 137.66, 140.10, 140.47, 141.03, 141.76, 150.93, 151.05.

General Procedure for the Intramolecular Friedel-Crafts Cyclization.



To a stirred solution of **3** (1-2 mmol; without additional purification) in dichloromethane (15-30 mL) at room temperature was added methanesulfonic acid (1-2 mL). The reaction progress was monitored by ^1H NMR, and when it was deemed complete, the solution was quenched with aqueous sodium bicarbonate (50-100 mL). The organic layer was separated and the aqueous layer was further extracted with dichloromethane (3 x 20 mL). The combined organic extracts were dried over anhydrous magnesium sulfate, evaporated and dried under vacuum. The various solid **4** were purified by recrystallization from a dichloromethane/methanol mixture to give the solid **4**.

4a: Yield (0.50 g, 76%), pale-yellow solid; mp: 200-202 °C; ^1H NMR (CDCl_3) δ : 1.12 (broad s, 12H), 2.14 (t, 4H), 2.61 (t, 4H), 7.21 (s, 2H), 7.31-7.38 (m, 4H), 7.44-7.50 (m, 4H). ^{13}C NMR (CDCl_3) δ : 31.76, 32.49, 37.99, 49.04, 125.64, 126.59, 127.36, 127.66, 130.55, 138.07, 140.69, 142.25, 146.37.

5a (centrally cyclized isomer): Yield (0.10 g, 15%), pale-yellow solid; mp: 249-251 °C; ^1H NMR (CDCl_3) δ : 0.92 (s, 12H), 1.67 (t, 4H), 2.35 (t, 4H), 7.18-7.22 (m, 4H), 7.28-7.34 (m, 10H). ^{13}C NMR (CDCl_3) δ : 28.81, 28.97, 43.57, 45.71, 126.74, 127.87, 129.81, 134.99, 140.74, 141.65, 146.35.

4b: Yield (0.67 g, >99%) yellow solid; mp: 250-253 °C; ^1H NMR (CDCl_3) δ : 1.11 (broad s, 12H), 2.12 (t, 4H), 2.43 (s, 6H), 2.61 (t, 4H), 7.16 (d, 2H, $J = 7.9$ Hz), 7.21 (s, 2H), 7.28 (s, 2H), 7.37 (d, 2H, $J = 7.9$ Hz). ^{13}C NMR (CDCl_3) δ : 21.08, 31.88, 32.54, 37.61, 48.93, 125.61, 127.59, 127.95, 131.35, 135.94, 138.09, 140.53, 142.18, 143.44.

4c: Yield (0.73 g, 93%) yellow solid; mp: 231-234 °C; ^1H NMR (CDCl_3) δ : 1.09 (broad s, 12H), 2.09 (t, 4H), 2.61 (t, 4H), 3.87 (s, 6H), 6.87 (d, 2H, $J = 8.6$ Hz), 7.01 (s, 2H), 7.21 (s, 2H), 7.38 (d, 2H, $J = 8.6$ Hz). ^{13}C NMR (CDCl_3) δ : 32.02, 32.52, 37.30, 48.82, 55.55, 112.01, 116.27, 126.69, 127.62, 138.21, 138.73, 141.79, 142.21, 158.08.

4d: Yield (0.17 g, 29%) yellow solid; mp: 239-240 °C; ^1H NMR (CDCl_3) δ : 1.09 (broad s, 12H), 2.10 (t, 4H), 2.58 (t, 4H), 3.87 (s, 6H), 6.87 (dd, 2H, $J_1 = 2.5$ Hz, $J_2 = 8.4$ Hz), 7.04 (d, 2H, $J = 2.5$ Hz), 7.14 (s, 2H), 7.37 (d, 2H, $J = 8.4$ Hz). ^{13}C NMR (CDCl_3) δ : 31.71, 32.52, 38.12, 48.68, 55.44, 110.20, 112.99, 127.41, 131.45, 133.40, 137.91, 141.49, 148.03, 158.85.

5d (centrally cyclized isomer): Yield (0.28 g, 48%) pale-yellow solid; mp: 264-266 °C; ^1H NMR (CDCl_3) δ : 1.01 (s, 12H), 1.75 (t, 4H), 2.43 (t, 4H), 3.87 (s, 6H), 6.94 (d, 4H, $J = 8.7$ Hz), 7.19 (d, 4H, $J = 8.7$ Hz). ^{13}C (CDCl_3) δ : 28.84, 29.01, 43.53, 45.73, 55.39, 113.22, 130.74, 133.00, 134.56, 142.10, 146.73, 158.42.

4e: Yield (0.47 g, >99%) white solid; mp: 281-283 °C; ^1H NMR (CDCl_3) δ : 1.11 (broad s, 12H), 2.12 (t, 4H), 2.61 (t, 4H), 3.95 (s, 6H), 3.96 (s, 6H), 6.97 (s, 2H), 7.02 (s, 2H),

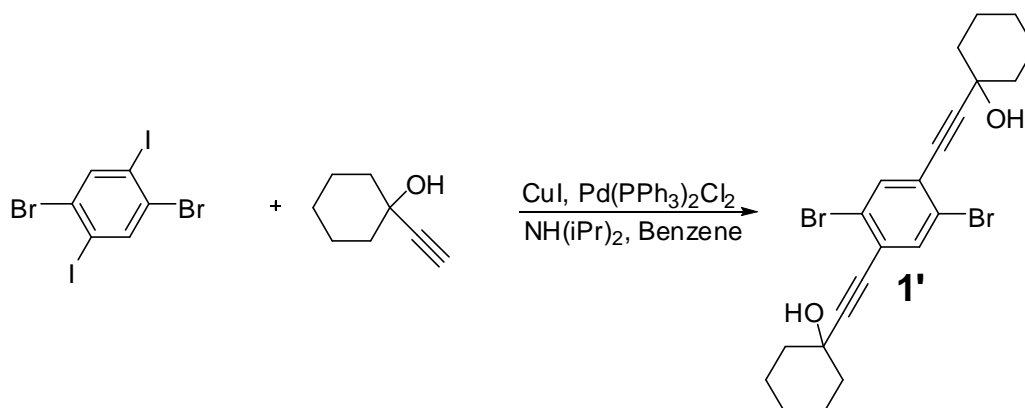
7.18 (s, 2H). ^{13}C NMR (CDCl_3) δ : 32.01, 32.56, 37.66, 49.15, 56.22, 56.25, 109.90, 114.03, 127.40, 132.89, 138.23, 138.94, 141.75, 147.18, 147.63.

4f: Yield (0.43 g, 55%) white solid; mp: 337-338 °C; ^1H NMR (CDCl_3) δ : 1.18 (broad s, 12H), 2.18 (t, 4H), 2.67 (t, 4H), 7.27 (s, 2H), 7.37 (t, 2H, $J = 7.7$ Hz), 7.48 (t, 4H, $J = 7.7$ Hz), 7.53 (d, 2H, $J = 8.0$ Hz), 7.58 (d, 2H, $J = 7.7$ Hz), 7.68 (m, 6H). ^{13}C NMR (CDCl_3) δ : 31.85, 32.56, 38.21, 49.01, 124.79, 125.24, 127.37, 127.42, 127.69, 128.99, 131.02, 138.21, 139.77, 140.07, 141.77, 141.99, 146.80

5f (centrally cyclized isomer): Yield (0.31 g, 40%) white solid; mp: 356-358 °C; ^1H NMR (CDCl_3) δ : 1.05 (s, 12H), 1.78 (t, 4H), 2.49 (t, 4H), 7.36 (m, 6H), 7.47 (t, 4H, $J = 7.6$ Hz), 7.65 (d, 4H, $J = 7.9$ Hz), 7.70 (d, 4H, $J = 7.9$ Hz). ^{13}C NMR (CDCl_3) δ : 28.91, 29.08, 43.61, 45.78, 126.53, 127.22, 127.40, 128.99, 130.23, 134.70, 139.42, 139.81, 141.15, 141.80, 146.57.

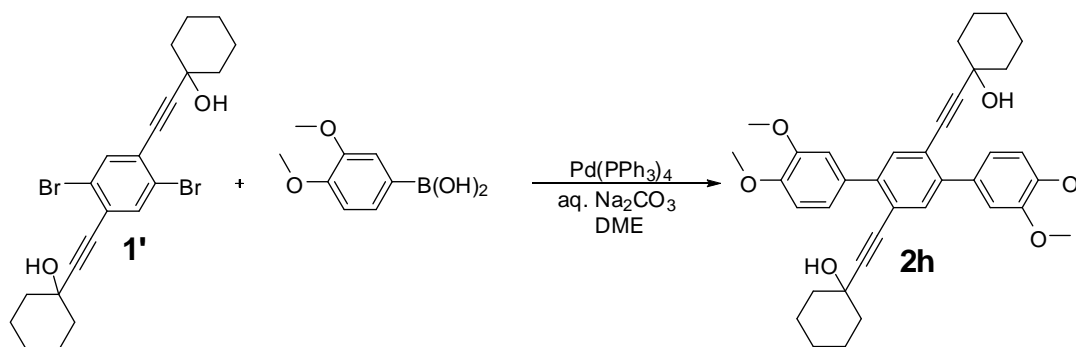
4g: Yield (0.65 g, 92%) beige solid; mp: 163-165 °C; ^1H NMR (CDCl_3) δ : 0.77 (m, 24H), 1.08 (broad s, 32H), 1.99 (m, 8H) 2.21 (t, 4H), 2.68 (t, 4H), 7.24-7.37 (m, 10H), 7.77 (d, 2H, $J = 7.3$ Hz), 7.82 (s, 2H). ^{13}C NMR (CDCl_3) δ : 14.25, 22.81, 24.05, 29.95, 31.74, 32.69, 38.13, 40.52, 48.96, 54.33, 55.11, 116.85, 119.60, 123.09, 125.18, 126.89, 126.91, 127.62, 138.32, 139.77, 140.04, 141.63, 143.07, 145.10, 148.78, 151.45.

Preparation of Diacetylenic Biscyclohexyl Derivative 1'.



1,4-Dibromo-2,5-diiodobenzene (1.86 g, 3.8 mmol) was dissolved in anhydrous benzene (20 mL) and diisopropylamine (12 mL) in an oven dried Schlenk flask under an argon atmosphere and the flask was evacuated and filled with argon (3x). Then, CuI (120 mg) and Pd(PPh₃)₂Cl₂ (100 mg) were added to the flask under an argon atmosphere and the flask was again evacuated and filled with argon (3x). Finally, 1-ethynyl-1-cyclohexanol (0.95 g, 7.6 mmol) was added to the flask which was then evacuated and filled with argon (3x) once more. The solution was allowed to stir at room temperature overnight. The resulting solution was diluted with water (100 mL) and extracted with ether (3 x 30 mL). The ether layer was washed with water (100 mL), extracted, dried over anhydrous magnesium sulfate, evaporated, and dried under vacuum to give a yellow solid which was purified by column chromatography using a 15% ethyl acetate/hexanes mixture as the eluent to afford **1'** as a pale yellow solid. Yield (1.6 g, 87%); mp: 166-168 °C; ¹H NMR (CDCl₃) δ: 1.26 (m, 4H), 1.59-1.75 (m, 8H), 2.04 (m, 8H), 2.12 (s, 2H), 7.64 (s, 2H). ¹³C NMR (CDCl₃) δ: 23.54, 25.33, 40.03, 69.63, 81.89, 100.43, 123.96, 126.28, 136.31.

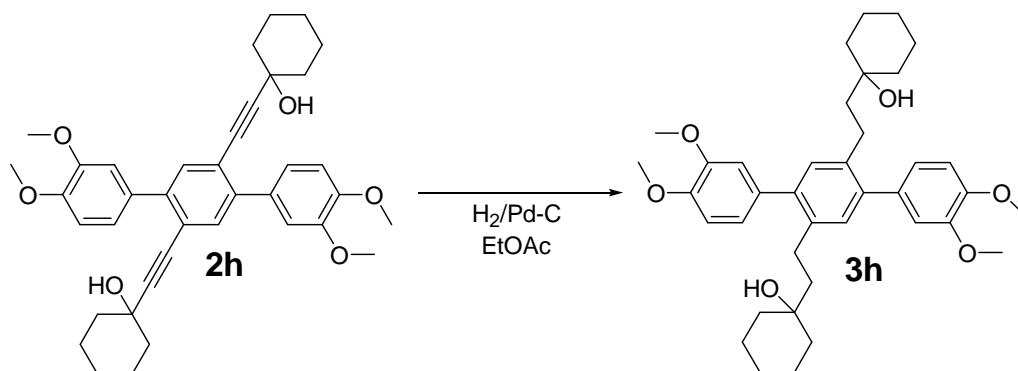
Preparation of 2h via Suzuki Coupling.



Solid **1'** (0.80 g, 1.7 mmol) and 3,4-dimethoxyphenylboronic acid (0.91 g, 5.0 mmol) were dissolved in anhydrous 1,2-dimethoxyethane (DME) (30 mL) in an oven dried Schlenk flask under an argon atmosphere and the flask was evacuated and filled with argon (3x). In another oven dried Schlenk flask a solution of anhydrous sodium carbonate (5.0 g) in water (20 mL) was prepared under an argon atmosphere and the flask was also evacuated and filled with argon (3x). To the DME solution, $\text{Pd(PPh}_3)_4$ (50 mg) and the salt solution were added sequentially under a strict argon atmosphere followed by evacuation and filling the flask with argon (3x) after each addition. The flask was covered with foil and the solution was allowed to reflux for 2 days. The resulting solution was cooled to room temperature, quenched with water (50 mL) and extracted with dichloromethane (3 x 20 mL). The organic layer was dried over anhydrous magnesium sulfate, evaporated and dried under vacuum. The resulting yellow solid was filtered over a small pad of silica gel using an 80% ethyl acetate/hexanes mixture as the eluent to afford **2h** as a yellow solid. Yield (0.99 g, >99%); mp: 172-175 °C; $^1\text{H NMR}$ (CDCl_3) δ : 1.10-1.1.65 (broad m, 16H), 1.85 (m, 4H), 2.00 (s, 2H), 3.92 (s, 6H), 3.93 (s, 6H), 6.90 (d, 2H, $J = 8.3$ Hz), 7.09 (d, 2H, $J = 1.8$ Hz), 7.13 (dd, 2H, $J = 8.3, 1.8$ Hz). $^{13}\text{C NMR}$

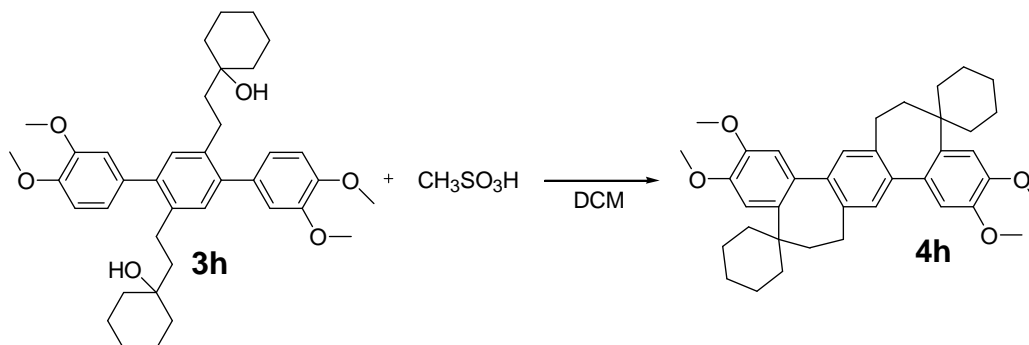
(CDCl₃) δ : 23.36, 25.27, 40.04, 56.17, 69.42, 83.86, 97.22, 110.82, 112.65, 121.40, 121.81, 132.44, 134.08, 142.22, 148.58, 148.88.

Procedure for the Preparation of 3h via Catalytic Hydrogenation.



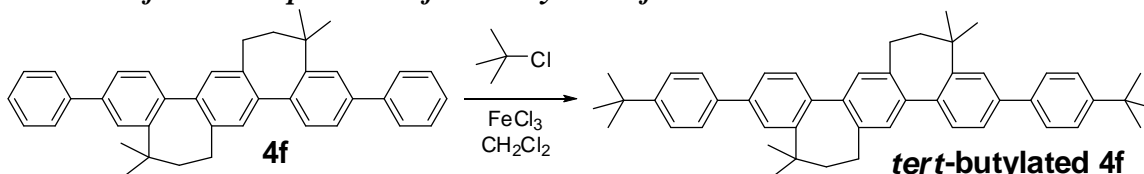
The corresponding **2h** (0.95 g, 1.6 mmol) from above was placed into a Parr apparatus along with a stir bar and dissolved in ethyl acetate (50 mL). To the solution, 10% Palladium on activated Carbon catalyst (100 mg) was added. The vessel was then put under hydrogen pressure (3 bar) for 24 hours after which time the solution was filtered over a short pad of silica gel. The silica gel was washed with ethyl acetate (2 x20 mL), the solvent was evaporated and the resulting **3h** was dried under vacuum to afford a yellow solid which was used without further purification. Yield (0.91 g, 95%); mp: 134-137 °C; ¹H NMR (CDCl₃) δ : 1.03 (s, 2H), 1.15-1.51 (broad m, 20H), 1.62 (m, 4H), 2.68 (m, 4H), 3.90 (s, 6H), 3.93 (s, 6H), 6.91 (d, 6H), 7.14 (s, 2H). ¹³C NMR (CDCl₃) δ : 22.34, 25.88, 26.51, 37.48, 44.18, 56.12, 56.13, 71.48, 110.99, 112.80, 121.56, 131.42, 134.42, 137.84, 140.86, 148.16, 148.63.

Intramolecular Friedel – Crafts Cyclization of 3h.



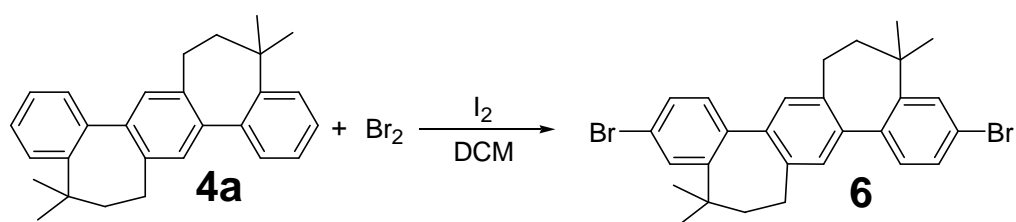
To a stirred solution of **3h** (0.91 g, 1.51 mmol) in dichloromethane (30 mL) at room temperature was added methanesulfonic acid (2 mL). The solution was allowed to stir for 1 hour after which time the solution was quenched with aqueous sodium bicarbonate (100 mL) and extracted with dichloromethane (3 x 20 mL). The combined organic extracts were dried over anhydrous magnesium sulfate, evaporated and dried under vacuum resulting in a yellow solid which was recrystallized from a dichloromethane/methanol mixture to afford **4h** as a white solid. Yield (0.85 g, 99%); mp: 239-241 °C; ¹H NMR (CDCl₃) δ: 0.80-2.40 (broad m, 24H), 2.55 (m, 4H), 3.93 (s, 6H), 3.96 (s, 6H), 6.93 (s, 2H), 7.06 (s, 2H), 7.16 (s, 2H). ¹³C NMR (CDCl₃) δ: 22.57, 26.36, 32.20, 40.58, 44.93, 53.58, 56.10, 56.15, 110.97, 113.97, 126.51, 133.01, 138.41, 138.63, 141.83, 146.87, 147.41.

Procedure for the Preparation of tert-butylated 4f.



To a stirred solution of **4f** (0.10 g, 0.19 mmol) in dichloromethane (20 mL) was added 2-chloro-2-methylpropane (0.18 g, 1.9 mmol) and anhydrous ferric chloride (0.31 g, 0.05 mmol). The solution was stirred with gentle heating for 10 minutes after which time it was quenched with methanol (20 mL) and poured into water (50 mL). The organic layer was extracted with dichloromethane (3 x 20 mL), washed with aqueous sodium bicarbonate (50 mL), and dried over anhydrous magnesium sulfate. The combined organic extracts were evaporated and dried under vacuum to afford a yellow solid which was purified by column chromatography using a hexane/ethyl acetate mixture as the eluent to give a bright orange solid. Yield (0.09 g, 75%); mp: 310-313 °C; ¹H NMR (CDCl₃) δ: 1.16 (s, 12H), 1.39 (s, 18H), 2.17 (t, 4H), 2.66 (t, 4H), 7.26 (s, 2H), 7.49-7.52 (m, 6H), 7.57 (dd, 2H, *J* = 7.9, 1.7 Hz), 7.62 (d, 4H, *J* = 8.3 Hz), 7.69 (d, 2H, *J* = 1.7 Hz). ¹³C NMR (CDCl₃) δ: 31.61, 31.81, 32.56, 34.74, 38.17, 49.01, 124.69, 125.09, 125.91, 127.06, 127.65, 130.94, 138.15, 138.90, 139.45, 139.93, 141.98, 146.63, 150.29.

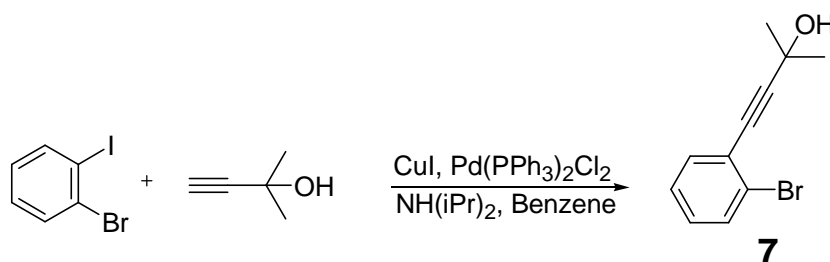
Procedure for the Preparation of the Dibromo Derivative 6.



In an oven dried Schlenk flask equipped with a dropping funnel attached to a bubbler solid **4a** (1.5 g, 4.1 mmol) and a catalytic amount of iodine were dissolved in dichloromethane (25 mL) at room temperature. A solution of bromine (1.38 g, 8.6 mmol) in dichloromethane (5 mL) was added dropwise over the course of 10 minutes and the resulting dark red solution was allowed to stir for 3 hours after which time the reaction

was quenched with aqueous potassium hydroxide (50 mL) and extracted with dichloromethane (3 x 20 mL). The combined organic extracts were dried over anhydrous magnesium sulfate, evaporated, and dried under vacuum to afford a beige solid which was used without further purification. Yield (1.92 g, 89%); mp: 268-270 °C; ^1H NMR (CDCl_3) δ : 1.08 (broad s, 12H), 2.11 (t, 4H), 2.58 (t, 4H), 7.15 (s, 2H), 7.28 (d, 2H, $J = 8.2$ Hz), 7.47 (dd, 2H, $J = 8.2$ Hz, 2.0 Hz), 7.58 (d, 2H, $J = 2.0$ Hz). ^{13}C NMR (CDCl_3) δ : 31.51, 32.30, 38.17, 48.73, 121.67, 127.60, 129.04, 129.56, 132.07, 138.10, 139.47, 141.52, 148.63.

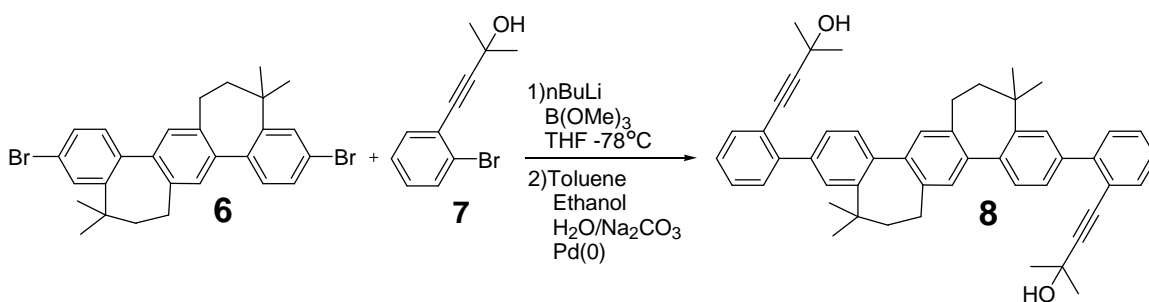
Procedure for the Preparation of the Monoacetylenic Precursor 7.



1-Bromo-2-iodobenzene (3.1 g, 11.0 mmol) was dissolved in anhydrous benzene (20 mL) and diisopropylamine (12 mL) in an oven dried Schlenk flask under an argon atmosphere and the flask was evacuated and filled with argon (3x). Then, CuI (120 mg) and $\text{Pd}(\text{PPh}_3)_2\text{Cl}_2$ (100 mg) were added to the flask under an argon atmosphere and the flask was again evacuated and filled with argon (3x). Finally, 2-methyl-3-butyn-2-ol (1.1 mL, 11.0 mmol) was added to the flask via syringe and the flask was evacuated and filled with argon (3x) once more. The resulting solution was allowed to stir at room temperature overnight. The resulting brown solution was diluted with water (100 mL) and extracted with ether (3 x 30 mL). The ether layer was washed with water (100 mL), extracted, dried

over anhydrous magnesium sulfate, evaporated, and dried under vacuum to give a black oil. The resulting oil was filtered over a short pad of silica gel using 30% ethyl acetate/hexanes as eluent to afford **7** as a dark orange oil. Yield (2.61 g, 99%); ^1H NMR (CDCl_3) δ : 1.64 (s, 6H), 2.80 (s, 2H), 7.11 (t, 1H, $J = 7.8$ Hz), 7.21 (t, 1H, $J = 8.0$ Hz), 7.41 (d, 1H, $J = 7.8$ Hz), 7.54 (d, 1H, $J = 8.0$ Hz). ^{13}C NMR (CDCl_3) δ : 31.46, 65.86, 81.00, 98.69, 124.96, 125.85, 127.11, 129.57, 132.48, 133.37.

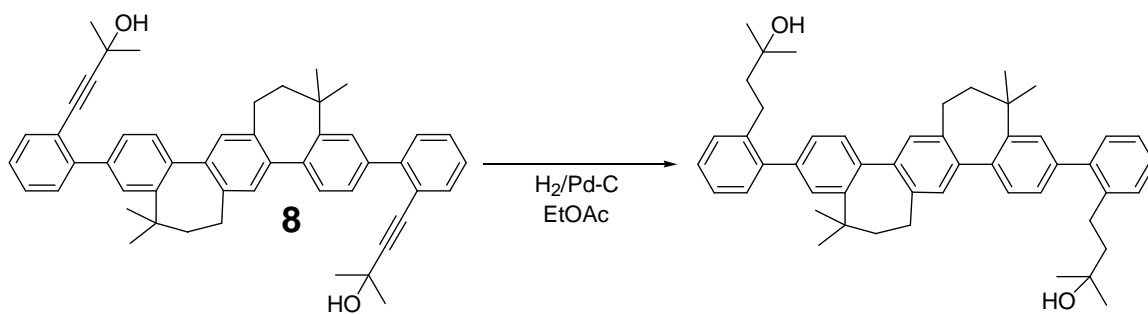
Procedure for the Preparation of Penta-*p*-Phenylene Precursor 8.



In an oven dried Schlenk flask under an argon atmosphere **7** (2.3 g, 9.6 mmol) was dissolved in dry THF (20 mL) and cooled to -78°C , n-butyllithium (11.5 mL, 28.9 mmol, 2.5 M in hexane) was added dropwise and the solution was allowed to stir for one hour while the temperature was maintained at -78°C . Then, triisopropylborate (5.79 g, 30.8 mmol) was added via syringe and the mixture was allowed to come to room temperature overnight. In a separate Schlenk flask, a salt solution was made with water (8 mL) and anhydrous sodium carbonate (1.53 g, 14.4 mmol), at the same time, toluene (20 mL) and ethanol (20 mL) were added to the reaction mixture via syringe so that the toluene:ethanol:water ratio is 3:3:1. Next, solid **6** (1.68 g, 3.2 mmol) was added to the reaction flask and a condenser attached to a bubbler was placed on the reaction vessel and the flask was evacuated and filled with argon (3x). To the reaction mixture, $\text{Pd}(\text{PPh}_3)_4$ (50

mg) and the salt solution were added sequentially under a strict argon atmosphere followed by evacuation and filling the flask with argon (3x) after each addition. The flask was covered with foil and the solution was allowed to reflux overnight. The resulting solution was cooled to room temperature, quenched with water (50 mL) and extracted with dichloromethane (3 x 20 mL). The organic layer was dried over anhydrous magnesium sulfate, evaporated, and dried under vacuum to afford a brown oil which was purified by column chromatography using a hexane/ethyl acetate mixture as the eluent to afford a yellow solid. Yield (0.78 g, 36%); mp: 170-173 °C; ^1H NMR (CDCl_3) δ : 1.17 (broad s, 12H), 1.52 (s, 12H), 2.18 (t, 4H), 2.67 (t, 4H), 7.27 (s, 2H), 7.31 (t, 2H, $J = 7.4$ Hz), 7.41 (t, 2H, $J = 7.4$ Hz), 7.47 (d, 2H, $J = 7.4$ Hz), 7.51 (d, 2H, $J = 7.7$ Hz), 7.57 (d, 4H, $J = 7.7$ Hz), 7.67 (s, 2H). ^{13}C NMR (CDCl_3) δ : 31.51, 31.79, 32.55, 38.16, 48.98, 65.78, 82.36, 96.61, 121.19, 126.97, 127.06, 127.21, 127.69, 128.73, 129.78, 130.08, 133.31, 138.17, 139.43, 139.79, 142.06, 144.55, 145.78.

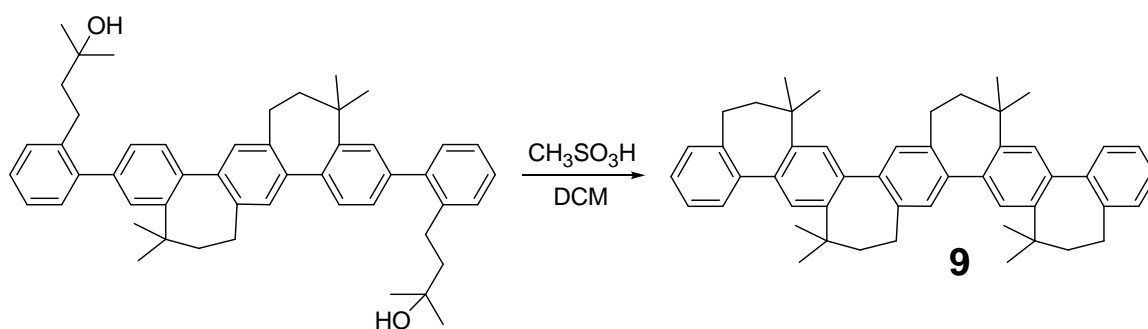
Procedure for the Preparation of Reduced Penta-*p*-Phenylene.



The corresponding **8** (0.40 g, 0.59 mmol) from above was placed into a Parr apparatus along with a stir bar and dissolved in ethyl acetate (50 mL). To the solution, 10% Palladium on activated Carbon catalyst (100 mg) was added. The vessel was then put under hydrogen pressure (3 bar) for 24 hours after which time the solution was filtered

over a short pad of silica gel. The silica gel was washed with ethyl acetate (2 x 20 mL), the solvent was evaporated and the resulting reduced penta-*p*-phenylene was dried under vacuum to afford a white solid which was used without further purification. Yield (0.40 g, >99%); mp: 207-209 °C; ¹H NMR (CDCl₃) δ: 1.05 (broad m, 24H), 1.59 (m, 4H), 1.97 (s, 2H), 2.10 (t, 4H), 2.59 (t, 4H), 2.67 (m, 4H), 7.21-7.26 (m, 12H), 7.37 (s, 2H), 7.43 (d, 2H, *J* = 7.7 Hz). ¹³C NMR (CDCl₃) δ: 28.59, 29.14, 31.83, 32.54, 38.08, 45.95, 49.01, 70.97, 126.04, 126.71, 127.26, 127.66, 129.64, 130.32, 130.35, 138.11, 139.22, 140.27, 140.59, 142.00, 142.43, 145.98.

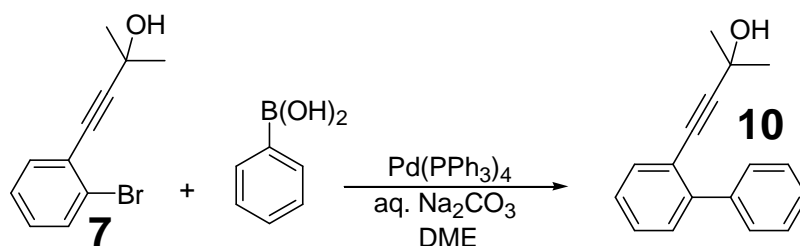
Procedure for the Preparation of Quadruply-Bridged Penta-*p*-phenylene 9



To a stirred solution of the reduced penta-*p*-phenylene (0.40 g, 0.58 mmol) in dichloromethane (30 mL) at room temperature was added methanesulfonic acid (2 mL). The solution was allowed to stir for 30 minutes after which time the solution was quenched with aqueous sodium bicarbonate (100 mL) and extracted with dichloromethane (3 x 20 mL). The combined organic extracts were dried over anhydrous magnesium sulfate, evaporated and dried under vacuum to afford a brown solid which was purified by precipitation from an ethanol/dichloromethane mixture to afford a white solid. Yield (0.38 g, >99%) mp: 377-379 °C; ¹H NMR (CDCl₃) at 50 °C δ: 1.14 (s, 12H), 1.18 (s, 12H), 2.17 (m, 8H), 2.64 (t, 4H), 2.71 (t, 4H), 7.23 (d, 2H, *J* = 7.4 Hz), 7.28 (t,

2H, $J = 7.4$ Hz), 7.32 (s, 2H), 7.36 (t, 2H, $J = 7.4$ Hz), 7.44 (m, 4H), 7.51 (s, 2H). ^{13}C NMR (CDCl_3) at 50 °C δ : 31.00, 31.96, 32.81, 33.06, 37.69, 37.75, 49.15, 49.34, 127.05, 127.36, 127.81, 127.90, 127.96, 128.18, 128.26, 138.51, 139.19, 139.27, 140.10, 142.62, 143.81, 144.13, 144.30.

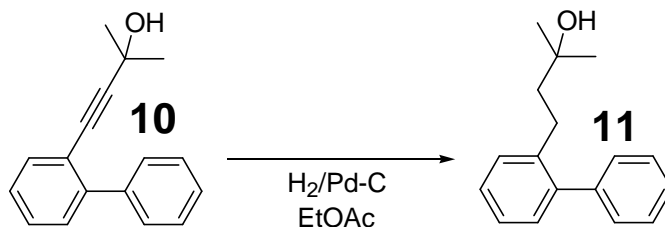
Procedure for the Preparation of Biphenyl Acetylenic Precursor 10.



The liquid monacetylenic precursor **7** (4.81 g, 20.1 mmol) and phenylboronic acid (4.91 g, 40.2 mmol) were dissolved in anhydrous 1,2-dimethoxyethane (DME) (50 mL) in an oven dried Schlenk flask under an argon atmosphere and the flask was evacuated and filled with argon (3x). In another oven dried Schlenk flask a solution of anhydrous sodium carbonate (5.0 g) in water (20 mL) was prepared under an argon atmosphere and the flask was also evacuated and filled with argon (3x). To the DME solution, $\text{Pd}(\text{PPh}_3)_4$ (100 mg) and the salt solution were added sequentially under a strict argon atmosphere followed by evacuation and filling the flask with argon (3x) after each addition. The flask was covered with foil and the solution was allowed to reflux overnight. The resulting solution was cooled to room temperature, quenched with water (50 mL) and extracted with dichloromethane (3 x 20 mL). The organic layer was dried over anhydrous magnesium sulfate, evaporated and dried under vacuum. The resulting brown oil was purified by column chromatography over silica gel using a 5% ethyl acetate/hexanes mixture as the eluent to afford an orange oil. Yield (4.75 g, >99%); ^1H NMR (CDCl_3) δ :

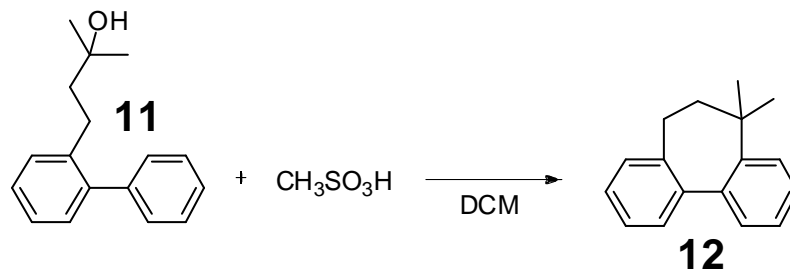
1.35 (s, 6H), 2.07 (s, 1H), 7.16 (m, 1H), 7.24-7.32 (m, 5H), 7.42, (d, 1H, $J = 7.7$ Hz), 7.47 (m, 2H). ^{13}C NMR (CDCl_3) δ : 31.18, 65.65, 82.05, 96.72, 121.18, 127.13, 127.58, 127.95, 128.66, 129.44, 129.50, 132.94, 140.62, 144.14.

Procedure for the Preparation of the Reduced Biphenyl Precursor 11



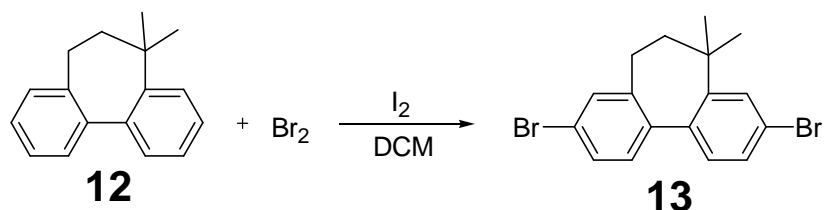
The corresponding **10** (4.75 g, 20.1 mmol) from above was placed into a Parr apparatus along with a stir bar and dissolved in ethyl acetate (100 mL). To the solution, 10% Palladium on activated Carbon catalyst (200 mg) was added. The vessel was then put under hydrogen pressure (3 bar) for 24 hours after which time the solution was filtered over a short pad of silica gel. The silica gel was washed with ethyl acetate (2 x 20 mL), the solvent was evaporated and the resulting reduced biphenyl precursor (**11**) was dried under vacuum to afford a colorless oil which was used without further purification. Yield (4.83 g, >99%); ^1H NMR (CDCl_3) δ : 0.98 (s, 6H), 1.13 (s, 1H), 1.51 (m, 2H), 2.58 (m, 2H), 7.15-7.33 (broad m, 9H). ^{13}C NMR (CDCl_3) δ : 28.35, 29.03, 45.80, 70.99, 125.99, 127.09, 127.71, 128.26, 129.40, 129.53, 130.26, 140.11, 141.89, 142.02.

Procedure for the Preparation of the Singly- Bridged Biphenyl 12



To a stirred solution of **11** (4.21 g, 17.5 mmol) in dichloromethane (75 mL) at room temperature was added methanesulfonic acid (4 mL). The solution was allowed to stir for 90 minutes after which time the solution was quenched with aqueous sodium bicarbonate (100 mL) and extracted with dichloromethane (3 x 20 mL). The combined organic extracts were dried over anhydrous magnesium sulfate, evaporated and dried under vacuum resulting in a brown oil which was filtered over a short pad of silica gel using an ethyl acetate/hexanes mixture as the eluent to afford the singly-bridged biphenyl (**12**) as a clear oil. Yield (3.12 g, 74%); $^1\text{H NMR}$ (CDCl_3) δ : 0.97 (broad s, 6H), 2.01 (t, 2H), 2.46 (t, 2H), 7.10, (d, 1H, $J = 7.1$ Hz), 7.16 (td, 1H, $J = 7.1$ Hz, 1.9 Hz), 7.21-7.29 (broad m, 5H), 7.37 (m, 1H). $^{13}\text{C NMR}$ (CDCl_3) δ : 31.72, 32.75, 37.91, 48.83, 125.55, 126.65, 127.02, 127.48, 127.81, 128.19, 130.62, 139.64, 140.73, 143.24, 146.22.

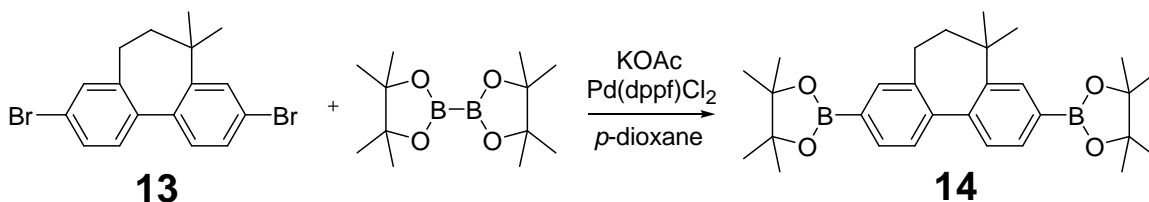
Procedure for the Synthesis of the Dibromo Singly-Bridged Biphenyl 13



To a stirred solution of **12** (3.12 g, 14.0 mmol) and a catalytic amount of iodine in dichloromethane (40 mL) a solution of bromine (4.9 g, 30.9 mmol) in dichloromethane (5

mL) is added dropwise. The resulting dark red solution is allowed to stir for 3 hours after which time it is quenched with aqueous potassium hydroxide (100 mL) and extracted with dichloromethane (3 x 20 mL). The combined organic extracts were filtered over anhydrous magnesium sulfate, evaporated, and dried under vacuum to afford a beige solid which was purified by recrystallization from a dichloromethane/methanol mixture to afford the dibromo singly-bridged biphenyl (**13**) as a colorless solid. Yield (3.56 g, 67%); mp: 125-127 °C; ¹H NMR (CDCl₃) δ: 1.05 (broad s, 6H), 2.09 (t, 2H), 2.50 (t, 2H), 7.15 (d, 1H, *J* = 3.9 Hz), 7.17 (d, 1H, *J* = 3.7 Hz), 7.35 (d, 1H, *J* = 1.9 Hz), 7.45 (m, 2H), 7.57 (d, 1H, *J* = 2.1 Hz). ¹³C NMR (CDCl₃) δ: 31.51, 32.40, 38.05, 48.24, 121.55, 122.12, 129.13, 129.55, 129.75, 130.19, 130.87, 131.96, 138.51, 141.11, 141.62, 148.40.

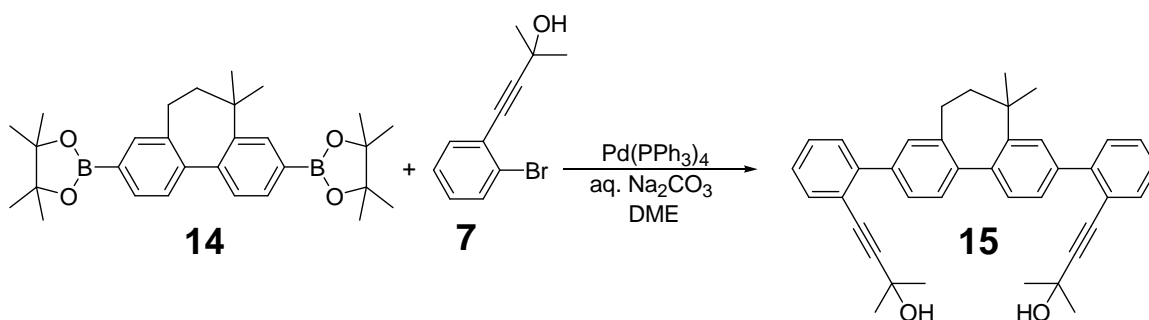
Procedure for the Preparation of the Bridged Biphenyl Diboronic Ester 14



In an oven dried Schlenk flask equipped with a condenser attached to a bubbler, **13** (2.73 g, 7.2 mmol), bis(pinacolato)diboron (5.47 g, 21.6 mmol), and potassium acetate (3.17 g, 32.3 mmol) were dissolved in anhydrous *p*-dioxane (50 mL) under argon and the flask was evacuated and filled with argon (3x). To this solution Pd(dppf)Cl₂ (0.10 g, 0.14 mmol) was added and the flask was again evacuated and filled with argon (3x). The resulting solution was allowed to reflux for 4 hours after which time the solvent was evaporated and the residue was taken up in dichloromethane (50 mL) and washed with water. The organic layer was separated and dried over anhydrous magnesium sulfate,

evaporated, and dried under vacuum to afford a black oil which was purified by filtering over a short pad of anhydrous magnesium sulfate using hexanes as the eluent to afford a yellow semisolid that was used without further purification. Yield (3.4 g, >99%); ^1H NMR (CDCl_3) δ : 1.10 (broad s, 6H), 1.36 (s, 24H), 2.09 (t, 2H), 2.54 (t, 2H), 7.36 (dd, 2H, $J = 7.5$ Hz, 2.8 Hz), 7.63 (s, 1H), 7.77 (m, 2H), 7.89 (s, 1H). ^{13}C NMR (CDCl_3) δ : 25.09, 25.21, 31.78, 32.51, 37.97, 48.70, 83.93, 83.97, 127.58, 130.09, 131.75, 133.24, 133.57, 134.12, 138.94, 143.61, 145.59, 146.29.

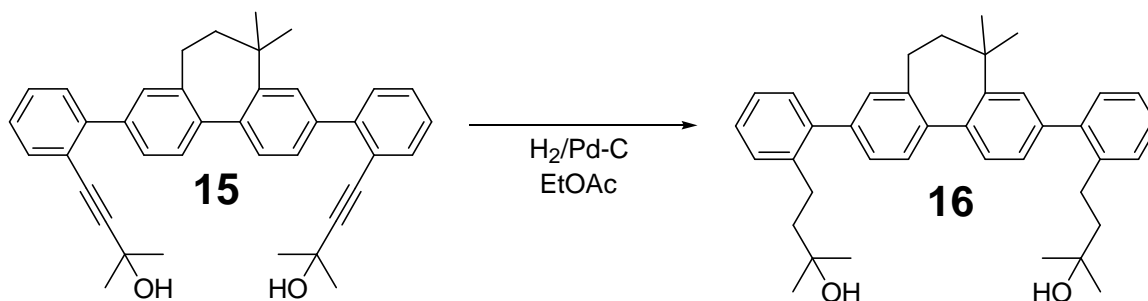
Procedure for the Preparation of the Quarterphenyl Acetylenic Precursor 15



The liquid **7** (3.43 g, 14.3 mmol) and **14** (3.4 g, 7.2 mmol) were dissolved in anhydrous 1,2-dimethoxyethane (DME) (40 mL) in an oven dried Schlenk flask under an argon atmosphere and the flask was evacuated and filled with argon (3x). In another oven dried Schlenk flask a solution of anhydrous sodium carbonate (5.0 g) in water (20 mL) was prepared under an argon atmosphere and the flask was also evacuated and filled with argon (3x). To the DME solution, $\text{Pd}(\text{PPh}_3)_4$ (50 mg) and the salt solution were added sequentially under a strict argon atmosphere followed by evacuation and filling the flask with argon (3x) after each addition. The flask was covered with foil and the solution was allowed to reflux overnight. The resulting solution was cooled to room temperature, quenched with water (50 mL) and extracted with dichloromethane (3 x 20 mL). The

organic layer was dried over anhydrous magnesium sulfate, evaporated and dried under vacuum. The resulting brown oil was purified by column chromatography over silica gel using an ethyl acetate/hexanes mixture as the eluent to afford the tetra-*p*-phenylene acetylenic precursor (**15**) as a yellow solid. Yield (1.88 g, 49%); mp: 108-110 °C; ¹H NMR (CDCl₃) δ: 1.16 (broad s, 6H), 1.49 (s, 6H), 1.50 (s, 6H), 2.00 (s, 2H), 2.18 (s, 2H), 2.66 (s, 2H), 7.28-7.33 (m, 2H), 7.38-7.43 (m, 2H), 7.44-7.48 (m, 5H), 7.55-7.59 (m, 4H), 7.68 (d, 1H, *J* = 1.6 Hz). ¹³C NMR (CDCl₃) δ: 31.38, 31.48, 31.82, 32.85, 38.16, 48.64, 65.75, 65.78, 82.28, 82.29, 96.63, 96.64, 121.08, 121.20, 126.94, 127.11, 127.32, 127.64, 128.12, 128.74, 129.66, 129.73, 130.14, 133.17, 133.32, 139.12, 139.56, 139.64, 139.78, 142.17, 143.96, 144.43, 145.73,

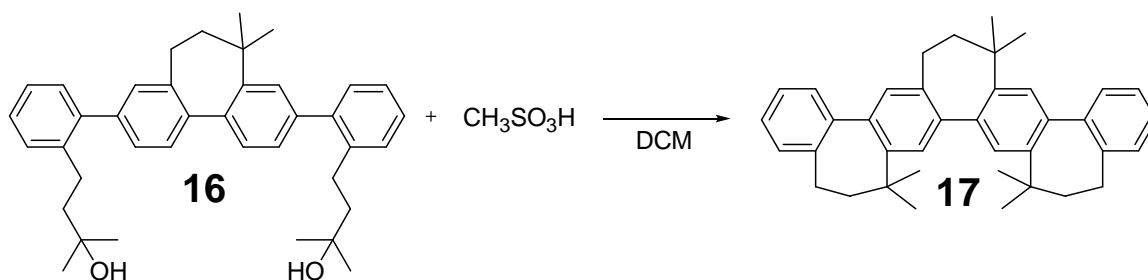
Procedure for the Preparation of the Reduced Tetra-*p*-Phenylene 16



The corresponding **15** (1.48 g, 2.75 mmol) from above was placed into a Parr apparatus along with a stir bar and dissolved in ethyl acetate (75 mL). To the solution, 10% Palladium on activated Carbon catalyst (200 mg) was added. The vessel was then put under hydrogen pressure (3 bar) for 24 hours after which time the solution was filtered over a short pad of silica gel. The silica gel was washed with ethyl acetate (2 x 20 mL), the solvent was evaporated and the resulting reduced tetra-*p*-phenylene (**16**) was dried

under vacuum and used without further purification. Yield (1.38 g, 92%); mp: 129-132 °C; ^1H NMR (CDCl_3) δ : 0.99 (s, 9H), 1.03 (s, 9H), 1.57 (m, 4H), 2.06 (t, 2H), 2.54 (t, 2H), 2.65 (m, 4H), 7.10 (d, 1H, $J = 1.4$ Hz), 7.17-7.24 (broad m, 10H), 7.34-7.38 (m, 3H). ^{13}C NMR (CDCl_3) δ : 28.51, 28.59, 29.11, 29.17, 31.14, 31.89, 32.83, 38.06, 45.94, 48.86, 70.94, 71.03, 125.99, 126.05, 126.73, 127.37, 127.67, 127.68, 127.86, 127.88, 128.74, 129.62, 129.66, 130.31, 130.37, 130.41, 138.97, 139.39, 140.10, 140.28, 140.76, 141.08, 141.58, 141.85, 142.33, 145.86.

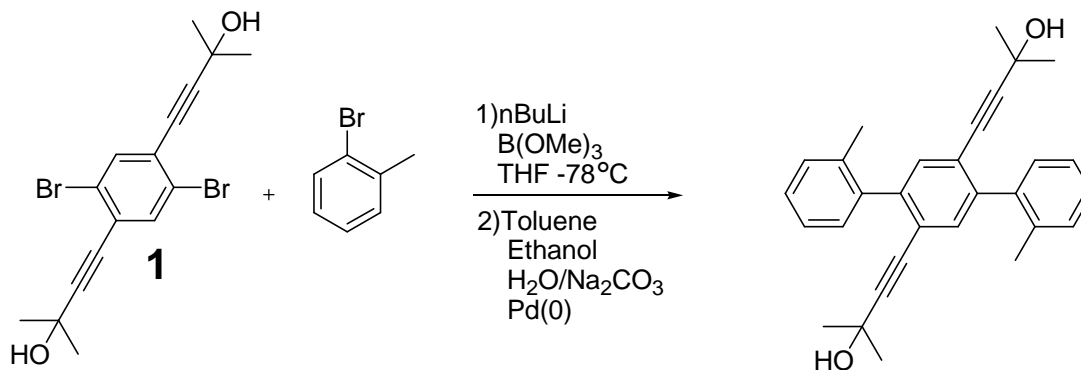
Procedure for the Preparation of Triply-Bridged Tetra-*p*-Phenylene



To a stirred solution of **16** (1.18 g, 2.16 mmol) in dichloromethane (40 mL) at room temperature was added methanesulfonic acid (2 mL). The solution was allowed to stir for 30 minutes after which time the solution was quenched with aqueous sodium bicarbonate (100 mL) and extracted with dichloromethane (3 x 20 mL). The combined organic extracts were dried over anhydrous magnesium sulfate, evaporated and dried under vacuum to afford a brown solid which was purified by column chromatography over silica gel using an ethyl acetate/hexanes mixture as the eluent to afford the pure **17** as a white solid. Yield (0.77 g, 70%); mp: 211-212 °C; ^1H NMR (CDCl_3) δ : 1.15 (broad s, 18H), 2.17 (m, 6H), 2.66 (m, 6H), 7.23-7.32 (broad m, 5H), 7.35 (d, 1H, $J = 6.8$ Hz), 7.39 (d, 1H, $J = 6.8$ Hz), 7.46 (m, 3H), 7.53 (s, 2H). ^{13}C NMR (CDCl_3) δ : 31.92, 32.28,

32.93, 33.01, 37.59, 37.71, 37.81, 48.90, 125.47, 126.99, 127.00, 127.33, 127.36, 127.90, 127.93, 128.00, 128.11, 128.17, 128.19, 130.22, 137.73, 139.03, 139.40, 139.50, 139.82, 139.98, 142.05, 143.20, 143.61, 143.99, 144.12, 144.79.

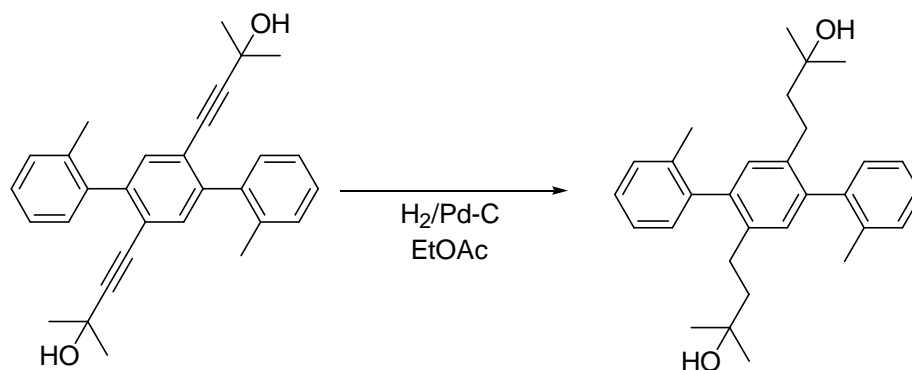
Procedure for the Preparation of *o*-Tolyl Terphenyl Diacetylenic Precursor (2i).



In an oven dried Schlenk flask under an argon atmosphere *o*-bromotoluene (1.28 g, 7.5 mmol.) was dissolved in dry THF (20 mL) and cooled to -78°C, n-butyllithium (4.5 mL, 11.25 mmol, 2.5 M in hexane) was added dropwise and the solution was allowed to stir for one hour while the temperature was maintained at -78°C. Then, trimethylborate (1.56 g, 15.0 mmol) was added via syringe and the mixture was allowed to come to room temperature overnight. In a separate Schlenk flask, a salt solution was made with water (8 mL) and anhydrous sodium carbonate (1.59 g, 15.0 mmol), at the same time, toluene (20 mL) and ethanol (20 mL) were added to the reaction mixture via syringe so that the toluene:ethanol:water ratio is 3:3:1. Next, solid **1** was added to the reaction flask and a condenser attached to a bubbler was placed on the reaction vessel and the flask was evacuated and filled with argon (3x). To the reaction mixture, Pd(PPh₃)₄ (50 mg) and the salt solution were added sequentially under a strict argon atmosphere followed by evacuation and filling the flask with argon (3x) after each addition. The flask was

covered with foil and the solution was allowed to reflux overnight. The resulting solution was cooled to room temperature, quenched with water (50 mL) and extracted with dichloromethane (3 x 20 mL). The organic layer was dried over anhydrous magnesium sulfate, evaporated and dried under vacuum. The resulting brown solid was purified by column chromatography over silica gel using a hexanes/ethyl acetate mixture as the eluent to afford the pure *o*-tolyl terphenyl diacetylenic precursor **2i** as a yellow solid. Yield (0.73 g, 92%); mp: 189-191 °C; ^1H NMR (CDCl_3) δ : 1.22 (s, 12H), 1.67 (s, 2H), 2.15 (s, 6H), 7.13-7.16 (m, 4H), 7.19 (m, 4H), 7.29 (s, 2H). ^{13}C (CDCl_3) δ : 20.17, 31.07, 65.59, 81.33, 98.37, 122.40, 125.53, 127.93, 129.76, 129.83, 132.38, 136.40, 139.93, 143.77.

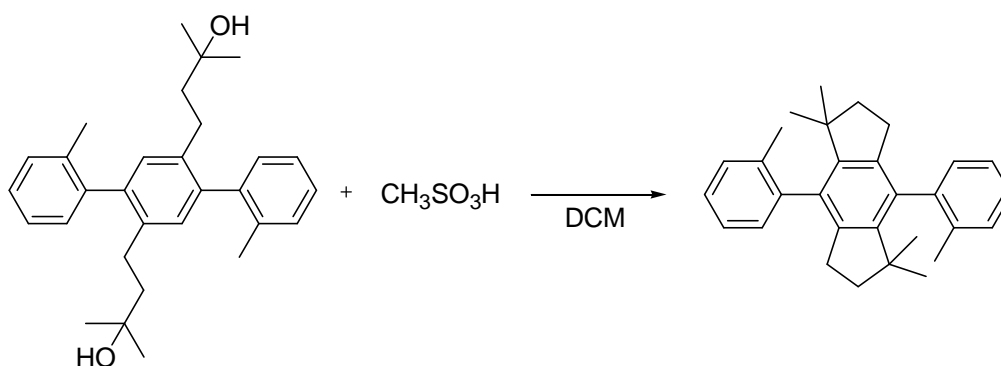
Procedure for the Preparation of *o*-Tolyl Terphenyl Alkane 3i via Catalytic Hydrogenation.



The corresponding **2i** (0.70 g, 1.66 mmol) from above was placed into a Parr apparatus along with a stir bar and dissolved in ethyl acetate (75 mL). To the solution, 10% Palladium on activated Carbon catalyst (100 mg) was added. The vessel was then put under hydrogen pressure (3 bar) for 24 hours after which time the solution was filtered over a short pad of silica gel. The silica gel was washed with ethyl acetate (2 x 20 mL),

the solvent was evaporated and the resulting *o*-tolyl terphenyl alkane **3i** was dried under vacuum to afford a yellow solid which was used without further purification. Yield (0.70 g, 99%); mp: 146-149 °C; ^1H NMR (CDCl_3) δ : 0.93 (s, 12H), 1.14 (broad s, 2H), 1.47 (m, 4H), 2.04 (s, 3H), 2.06 (s, 3H), 2.28 (m, 2H), 2.41 (m, 2H), 6.94 (s, 1H), 6.95 (s, 1H), 7.15-7.20 (m, 8H). ^{13}C (CDCl_3) δ : 20.28, 20.47, 27.90, 28.93, 45.49, 70.93, 125.54, 125.56, 127.44, 127.46, 129.83, 129.94, 130.09, 130.36, 136.16, 136.22, 137.46, 137.55, 140.24, 140.29, 141.23, 141.28.

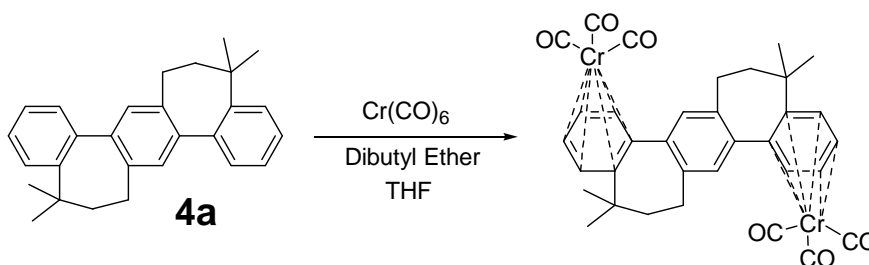
Intramolecular Friedel – Crafts Cyclization of *o*-Tolyl Terphenyl Alkane 3i to 5i



To a stirred solution of the *o*-tolyl terphenyl alkane **3i** (0.65 g, 1.51 mmol) in dichloromethane (30 mL) at room temperature was added methanesulfonic acid (2 mL). The solution was allowed to stir for 2 hours after which time the solution was quenched with aqueous sodium bicarbonate (100 mL) and extracted with dichloromethane (3 x 20 mL). The combined organic extracts were dried over anhydrous magnesium sulfate, evaporated and dried under vacuum resulting in a brown solid which was purified by column chromatography using a hexanes/ethyl acetate mixture as the eluent to afford the centrally cyclized *o*-tolyl terphenyl **5i** as a yellow solid. Yield (0.28 g, 47%); mp: 228-230 °C; ^1H NMR (CDCl_3) δ : 0.75 (d, 6H), 1.00 (d, 6H), 1.66 (m, 4H), 1.96 (s, 3H), 2.01

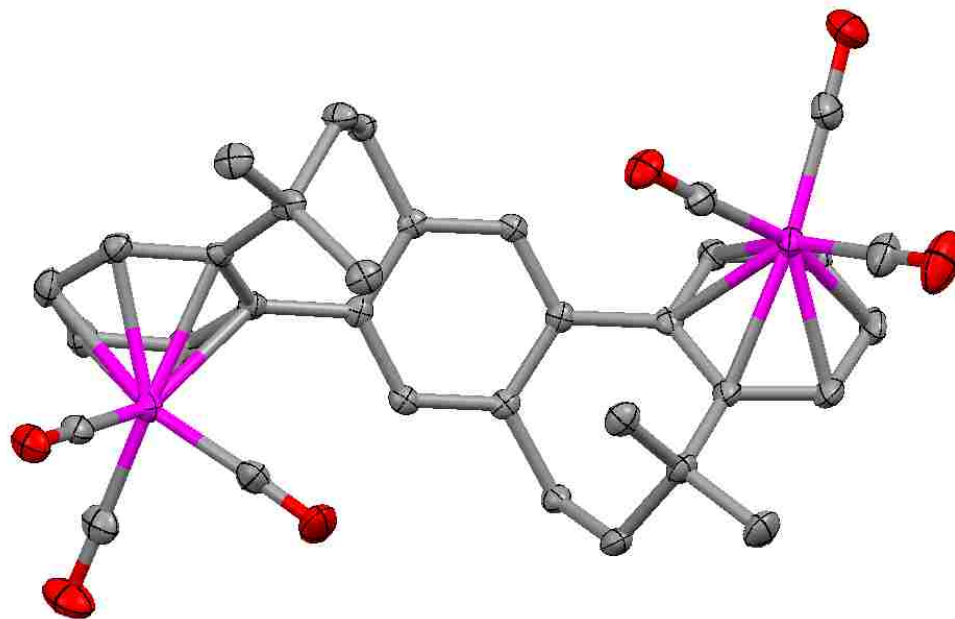
(s, 3H), 2.19 (m, 2H), 2.29 (m, 2H), 7.12-7.17 (m, 8H). ^{13}C (CDCl_3) δ : 20.09, 20.36, 26.84, 27.33, 28.52, 28.68, 29.06, 29.24, 43.34, 43.39, 45.62, 45.64, 125.15, 125.22, 127.04, 127.09, 129.80, 129.83, 129.92, 130.07, 133.70, 133.75, 136.21, 136.65, 140.08, 140.23, 141.37, 141.54, 145.91, 145.94. [Note that none of the desired product from cyclization on the terminal rings was obtained.]

Procedure for the Preparation of the Bischromiumtricarbonyl Complex of 4a

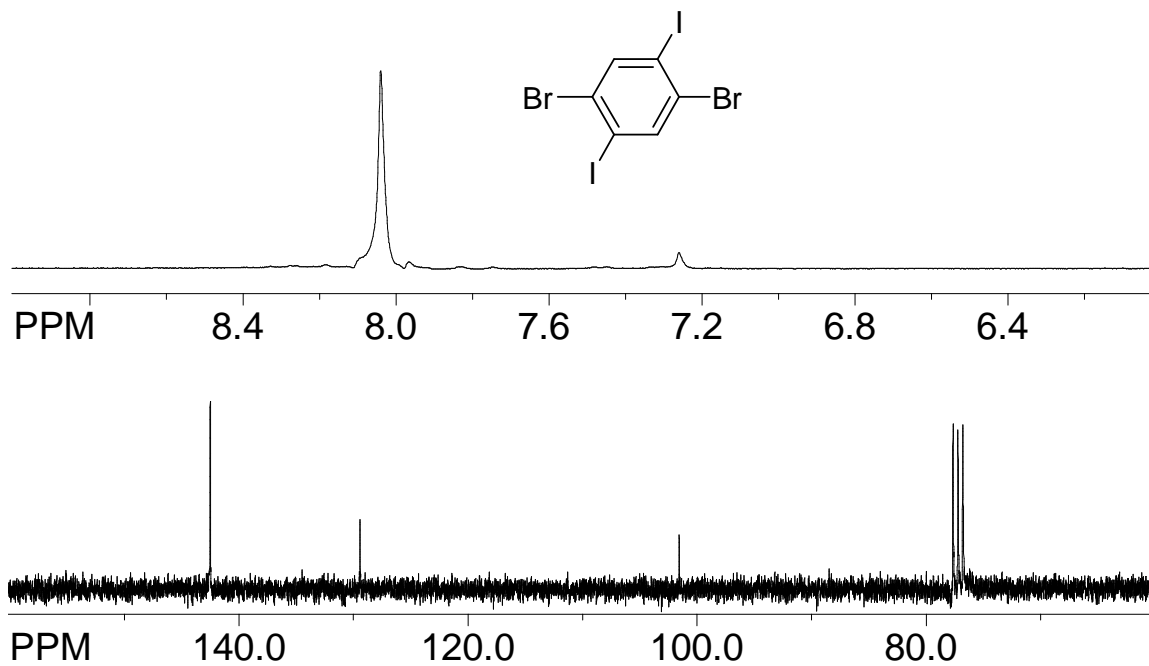
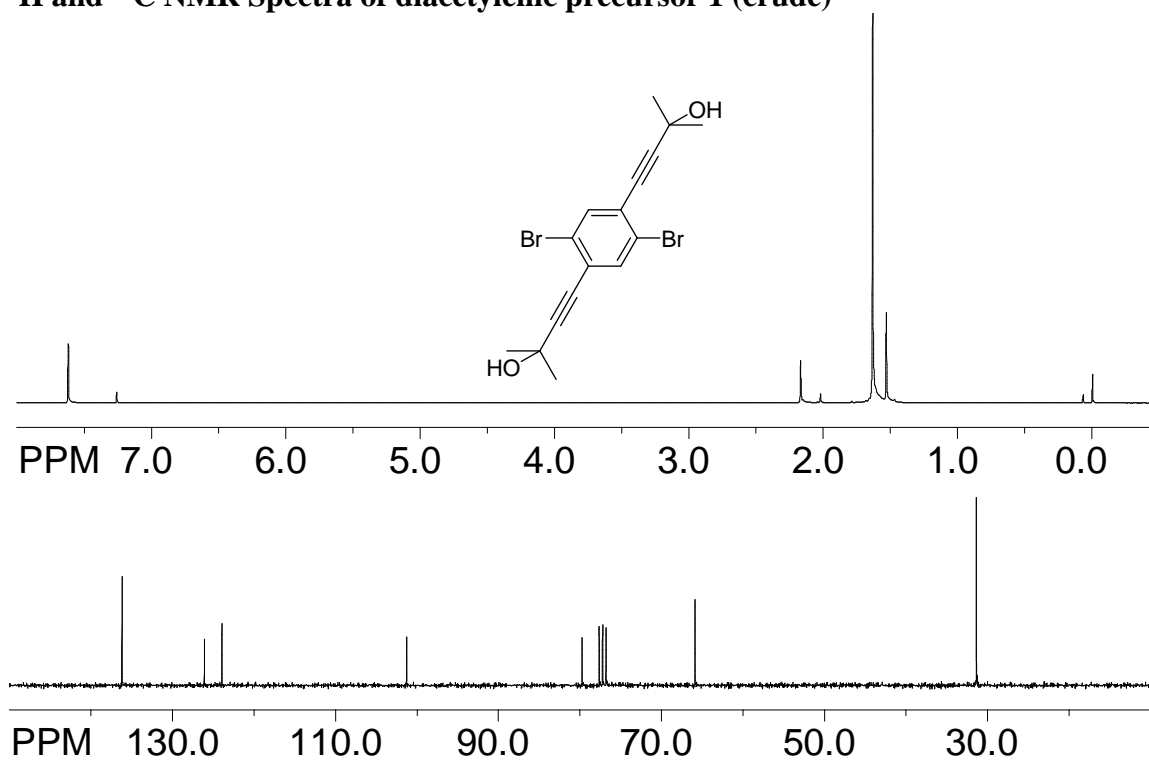


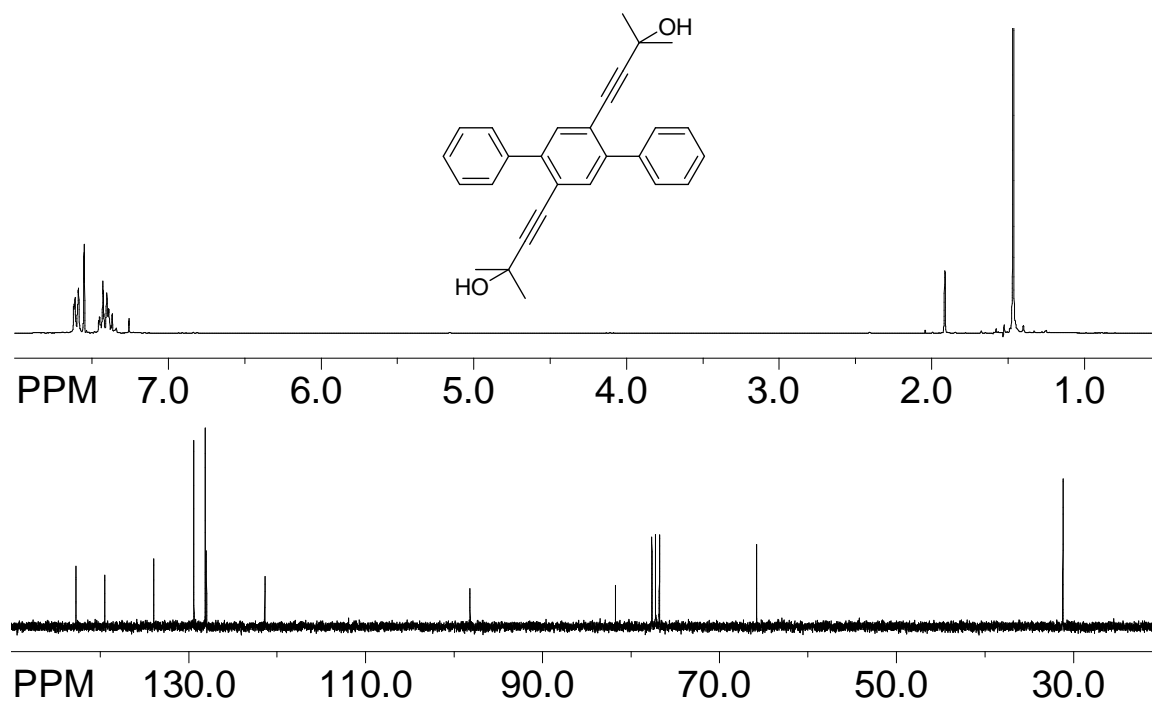
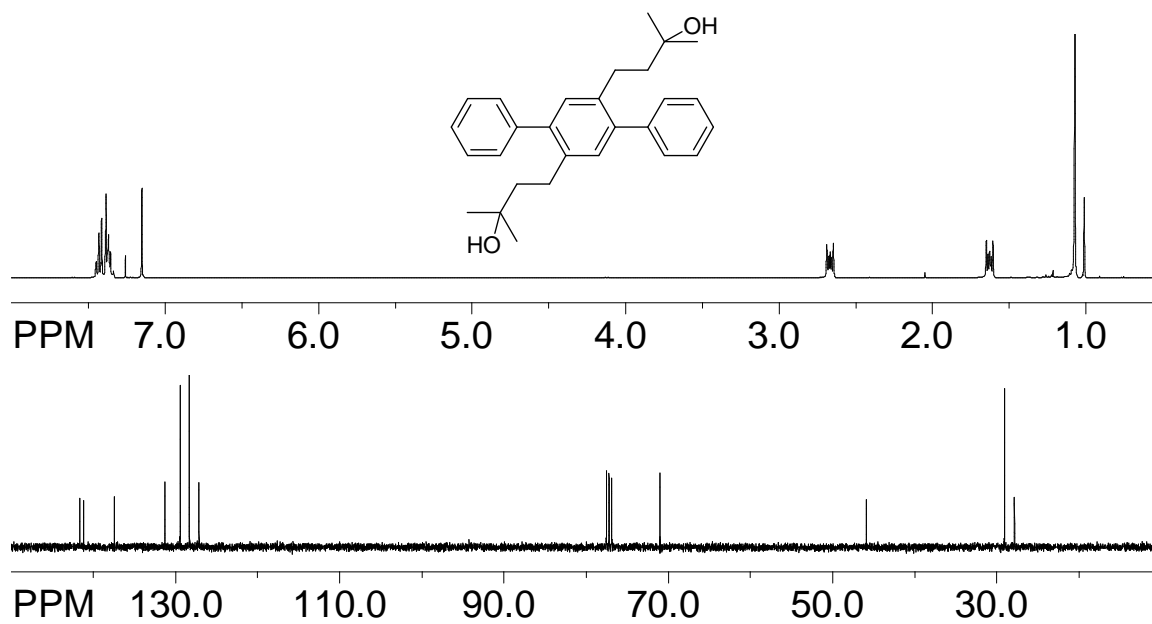
Solid terphenyl **4a** (0.17 g, 0.45 mmol) and hexacarbonylchromium (0.10 g, 0.45 mmol) were dissolved in anhydrous dibutyl ether (20 mL) and dry THF (2 mL) in an oven dried Schlenk flask equipped with a condenser attached to a bubbler under an argon atmosphere and the flask was evacuated and backfilled with argon (3x). The resulting yellow solution was allowed to reflux for 24 hours after which time the flask was cooled to room temperature and allowed to sit for 2 days after which time yellow single crystals that were suitable for X-ray crystallography were formed. Yield (0.16 g, 70%); mp: 178-180°C.

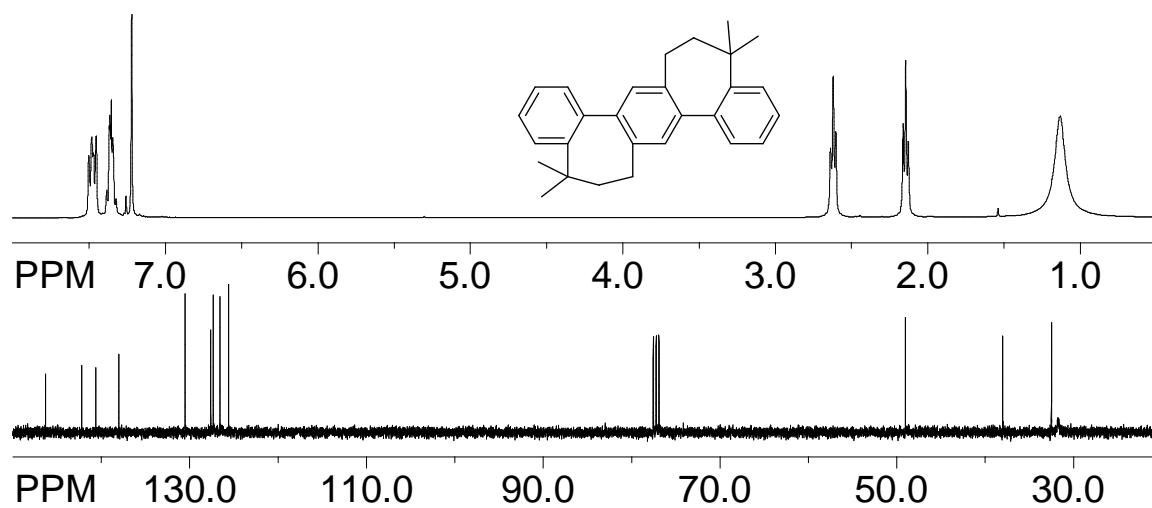
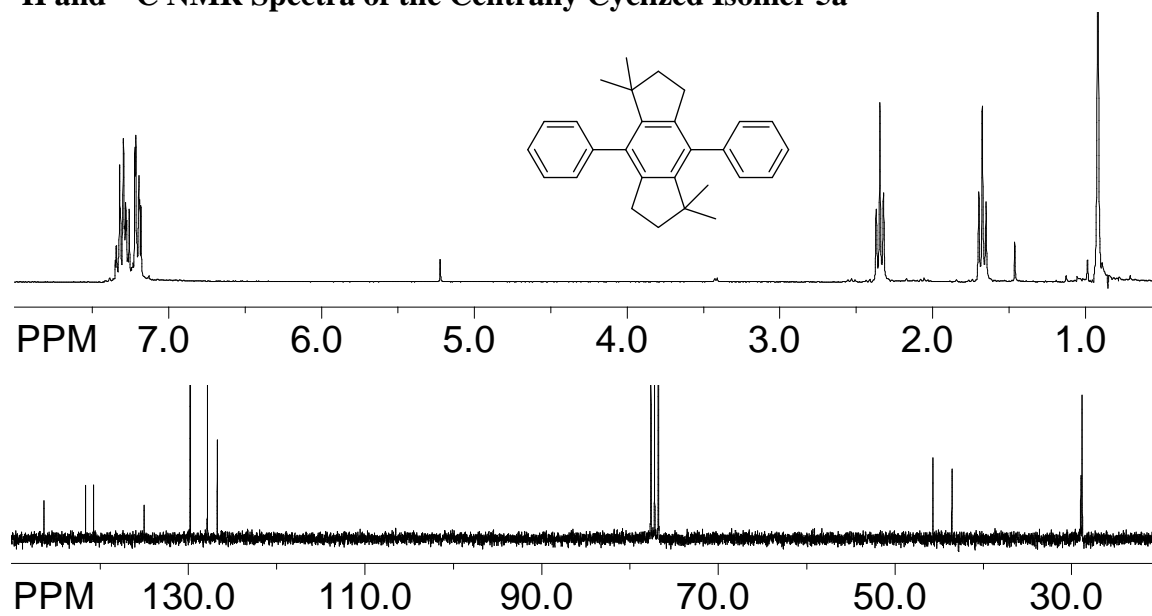
The X-ray structure of bis-chromiumtricarbonyl Complex of **4a** showed that its conformation is frozen into chiral (syn) conformation (see below its molecular structure obtained by X-ray crystallography).

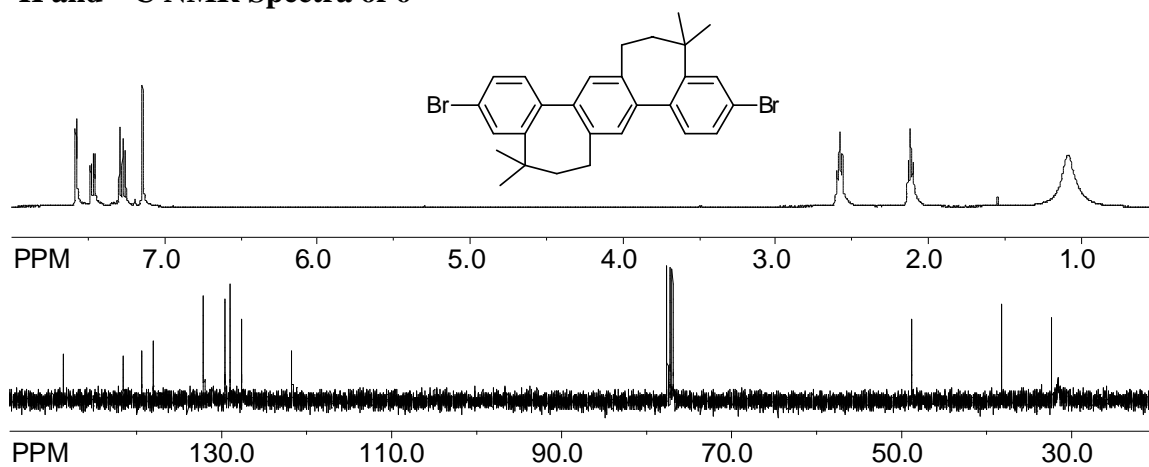
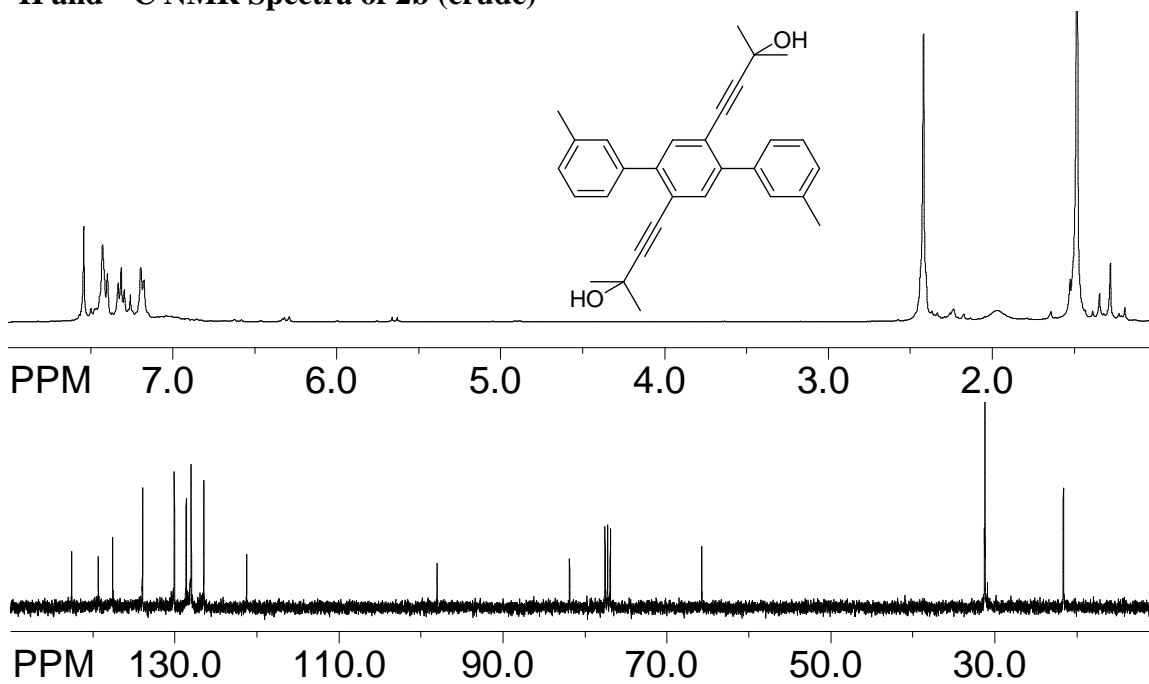


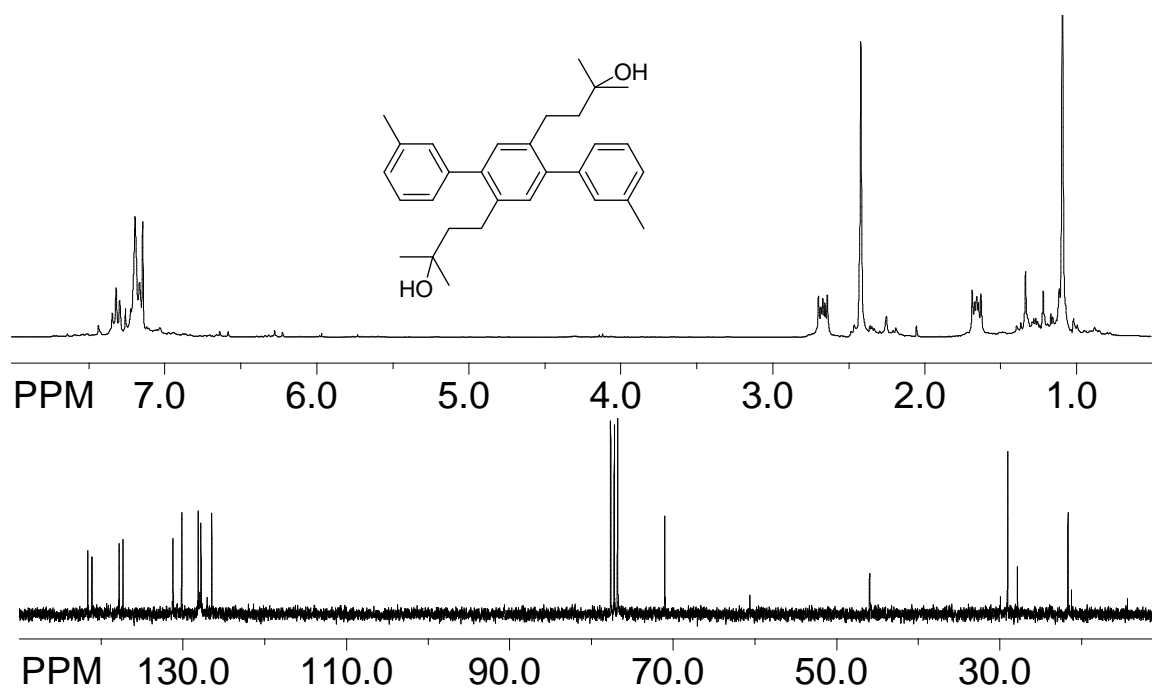
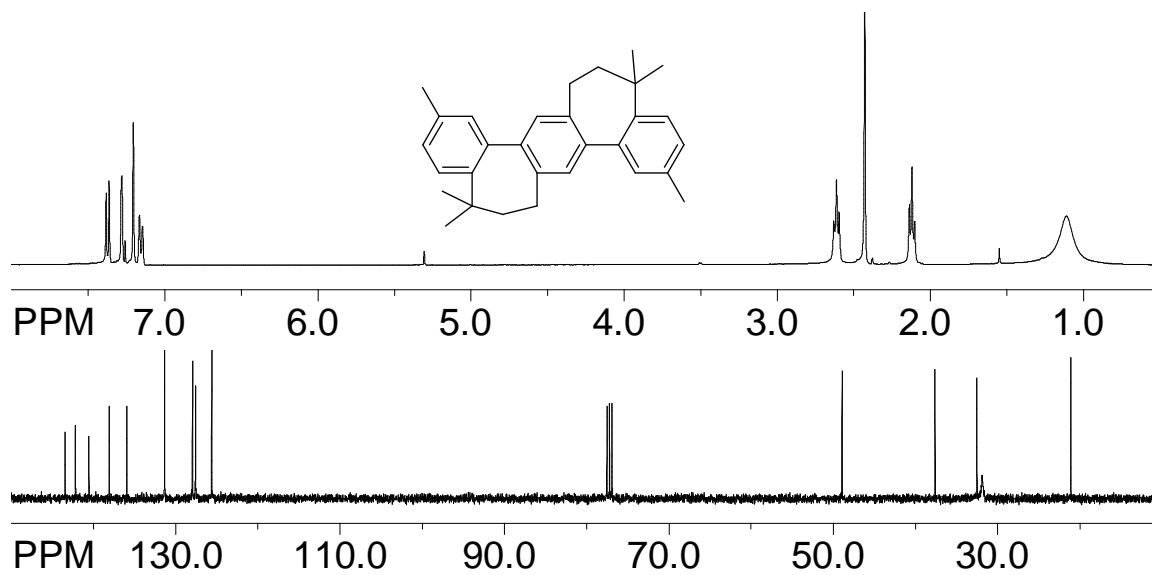
1.5 EXPERIMENTAL SPECTRA

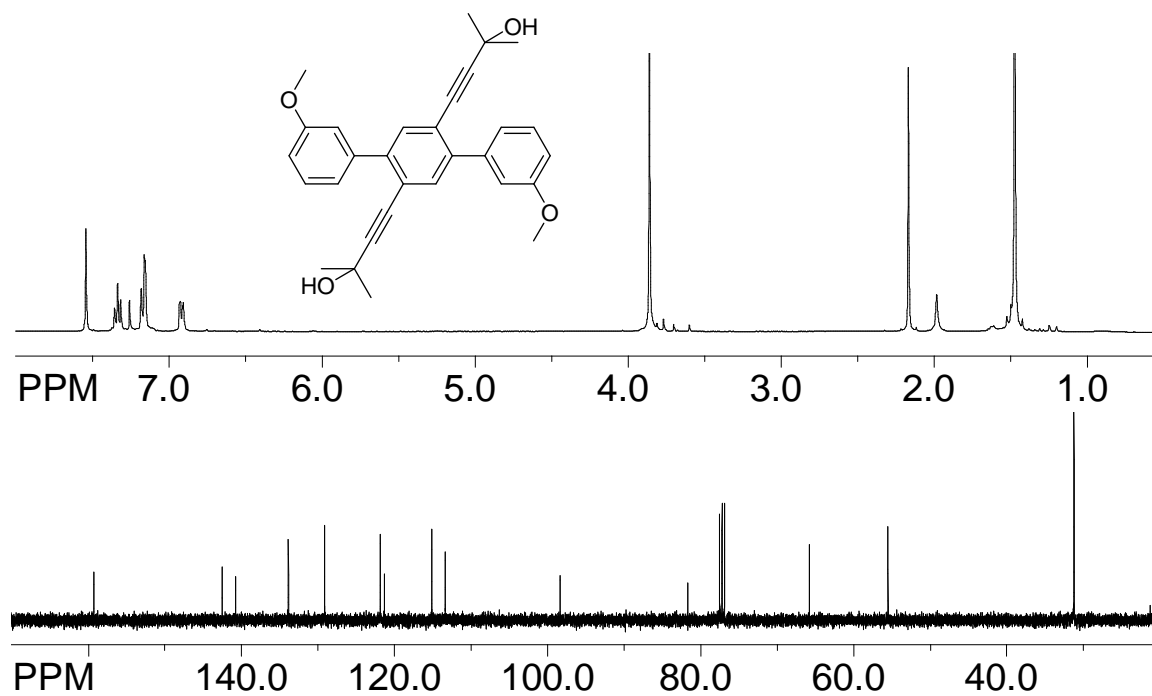
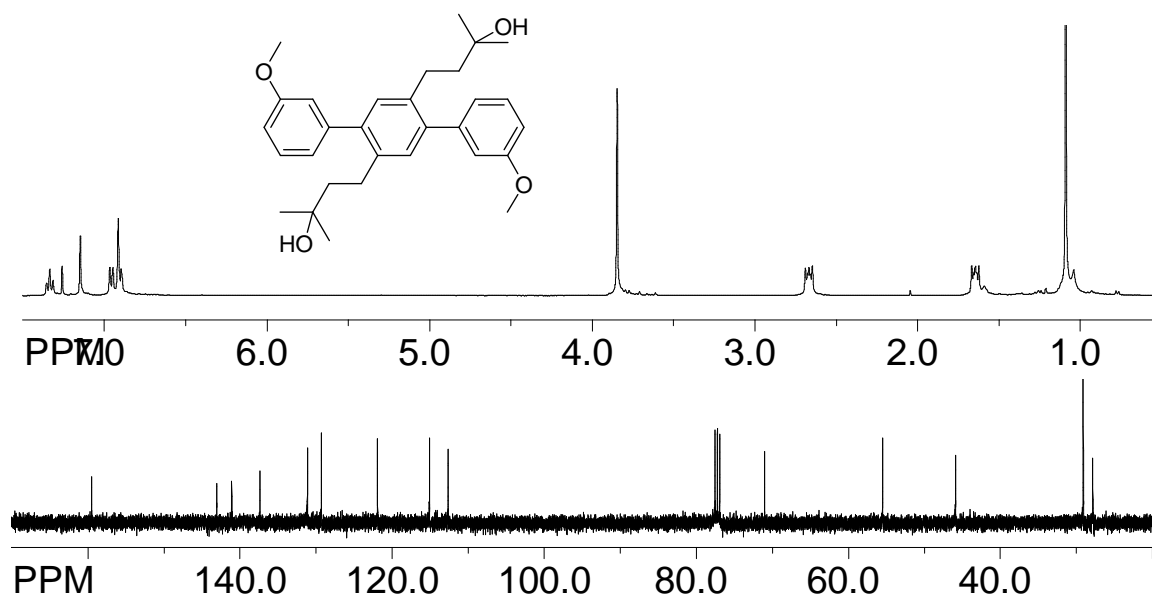
 ^1H and ^{13}C NMR Spectra of 1,4-dibromo-2,5-diiodobenzene **^1H and ^{13}C NMR Spectra of diacetylenic precursor 1 (crude)**

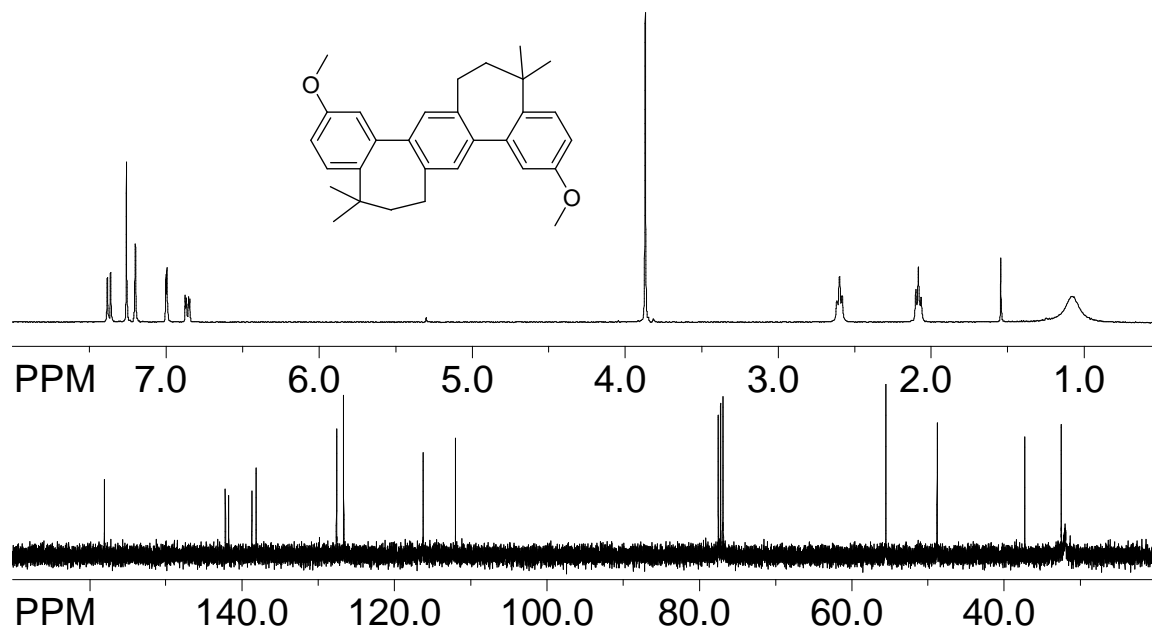
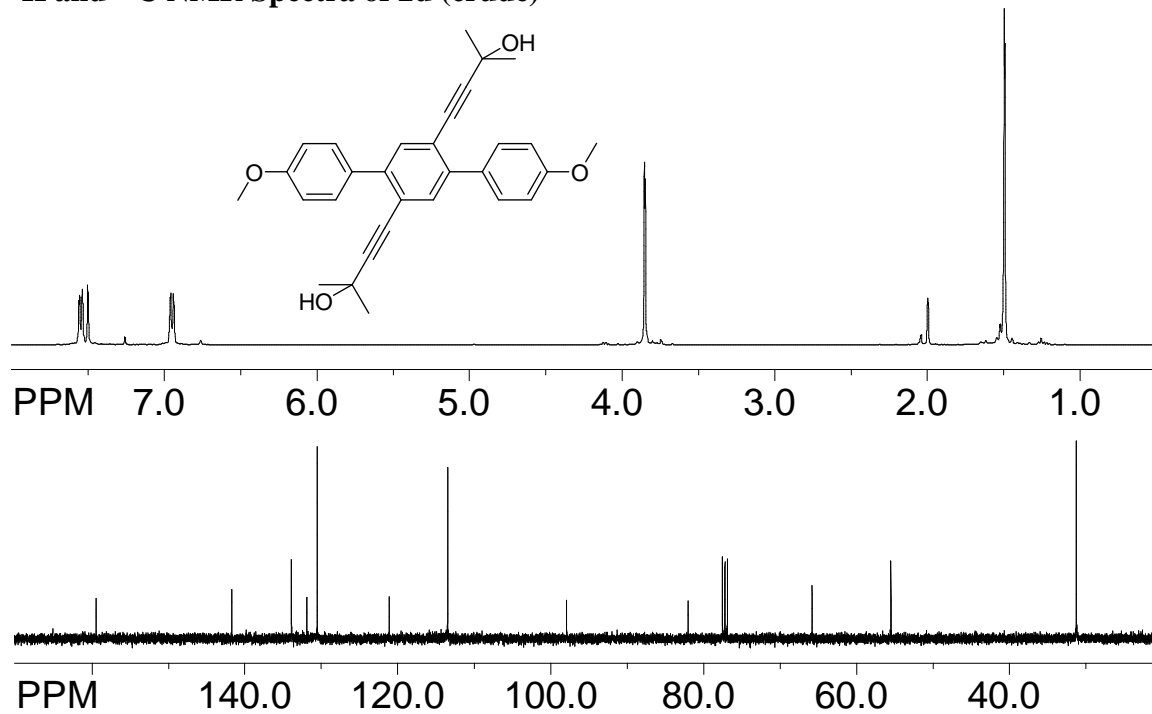
^1H and ^{13}C NMR Spectra of 2a (crude) **^1H and ^{13}C NMR Spectra of 3a (crude)**

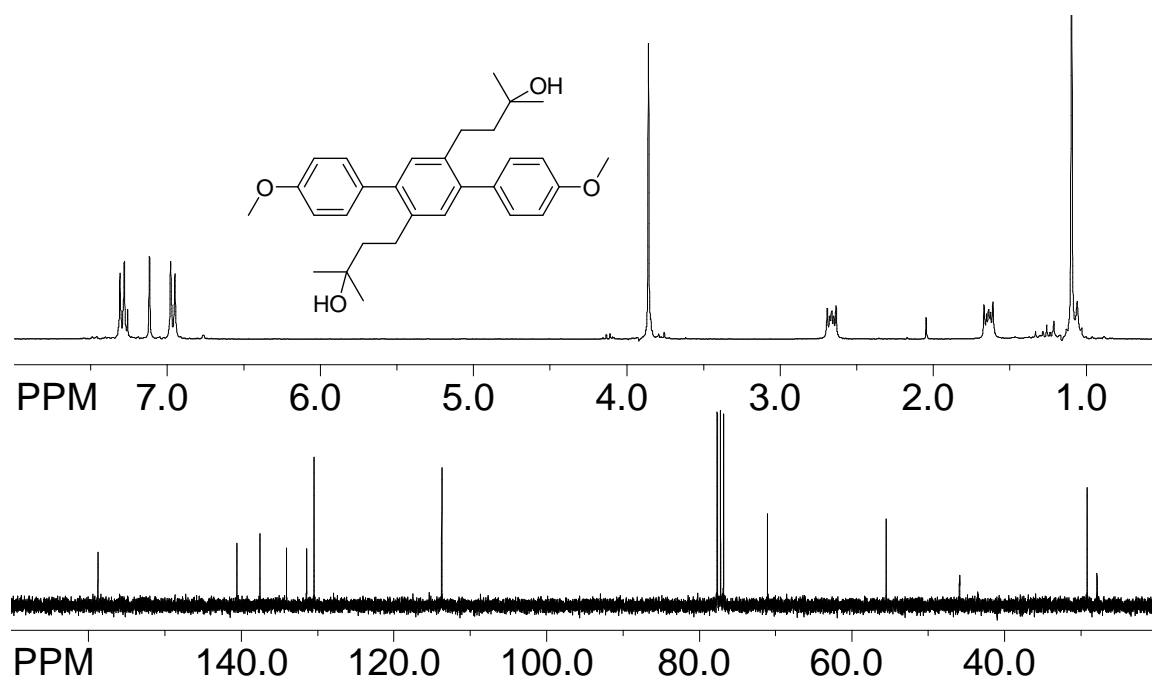
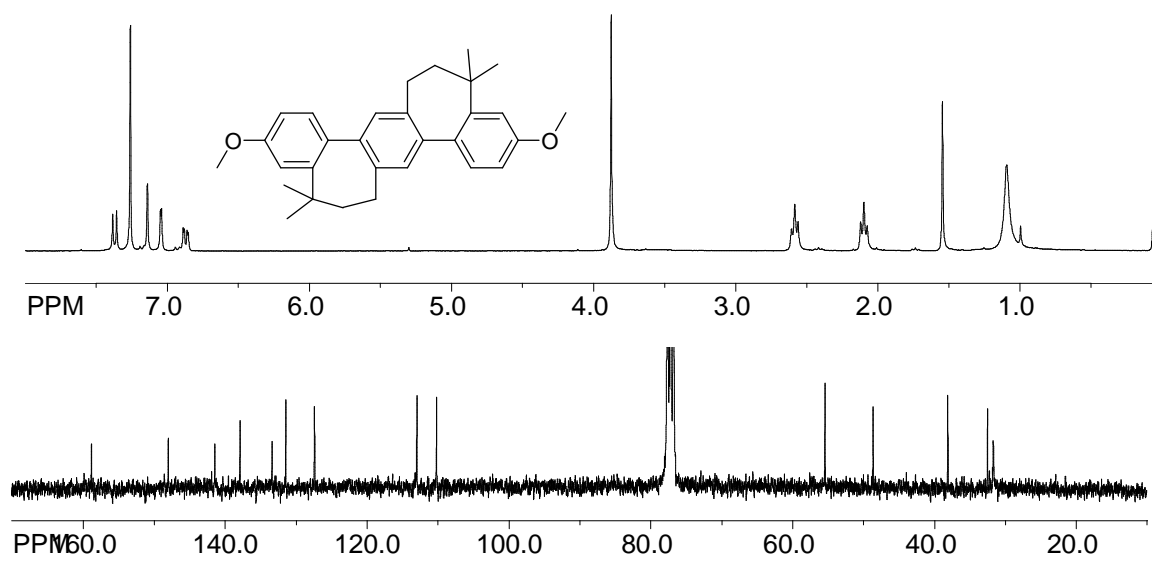
^1H and ^{13}C NMR Spectra of 4a **^1H and ^{13}C NMR Spectra of the Centrally Cyclized Isomer 5a**

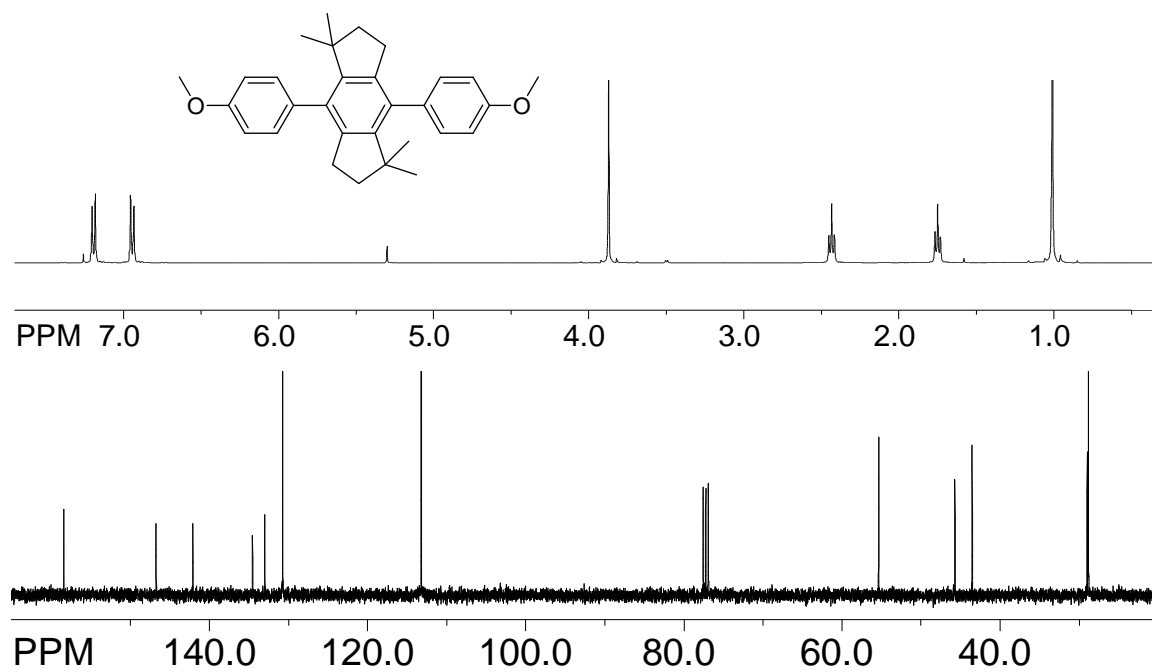
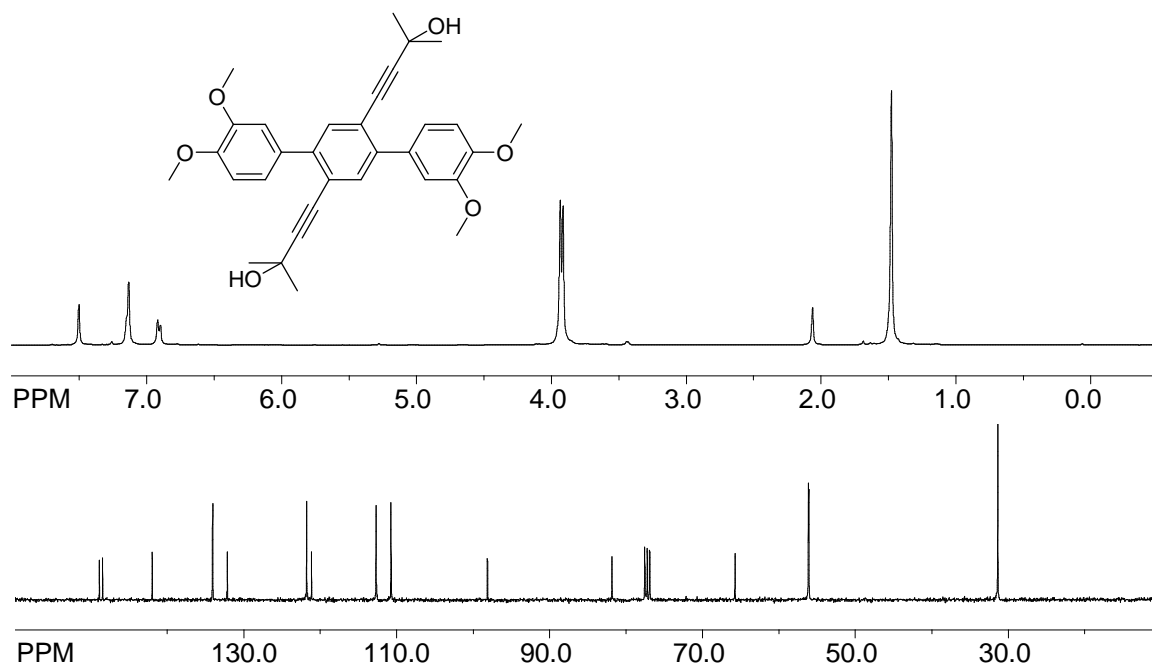
^1H and ^{13}C NMR Spectra of 6 **^1H and ^{13}C NMR Spectra of 2b (crude)**

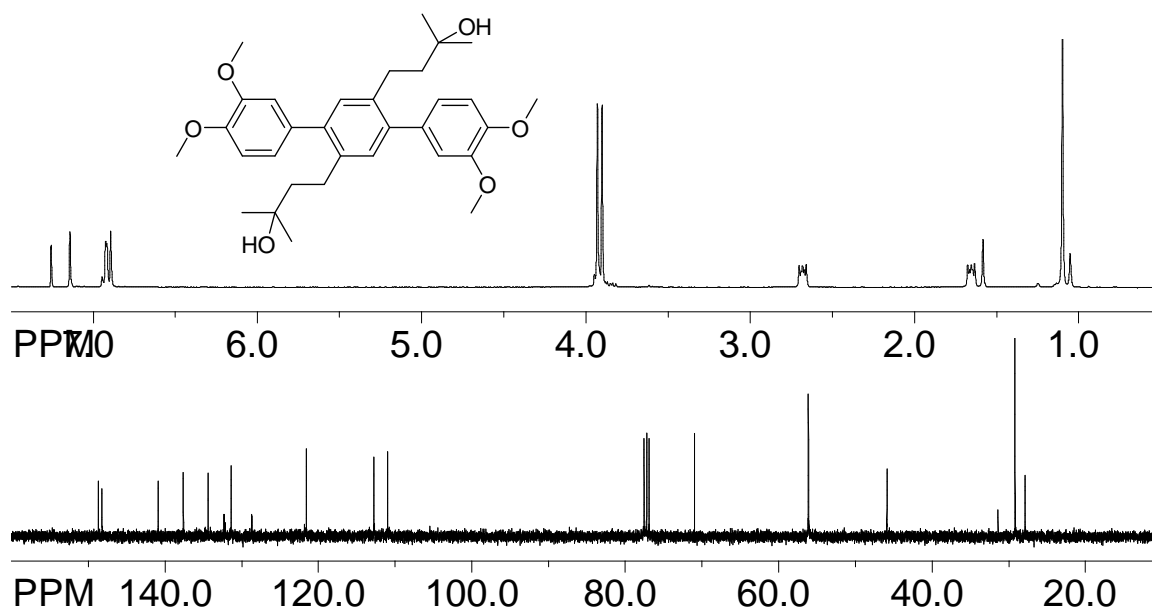
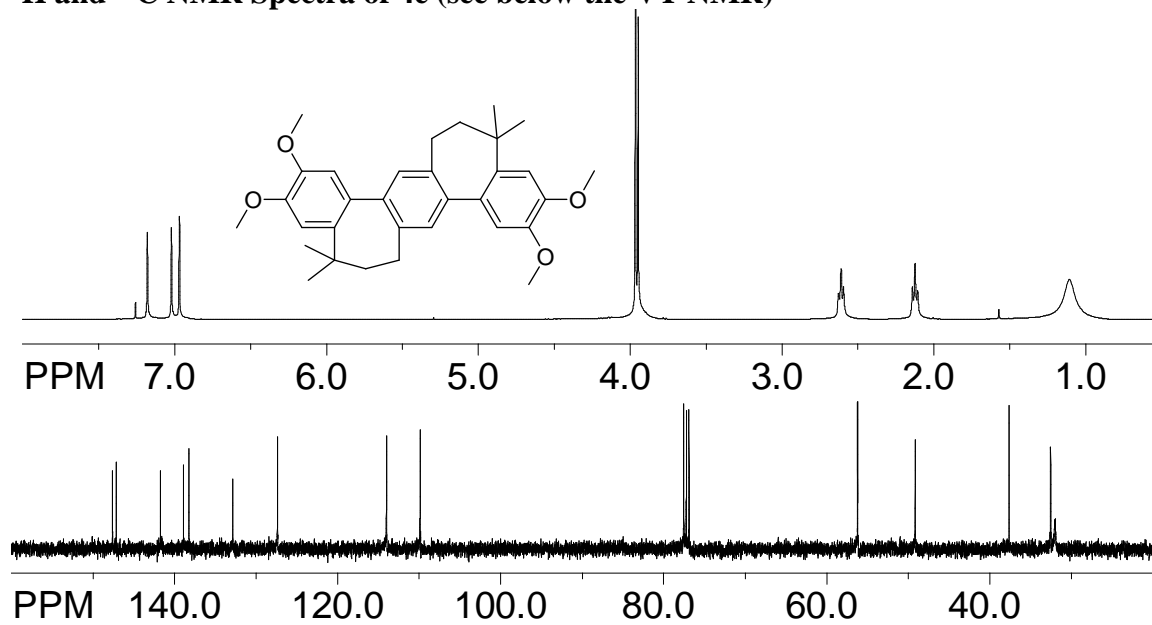
^1H and ^{13}C NMR Spectra of 3b (crude) **^1H and ^{13}C NMR Spectra of 4b**

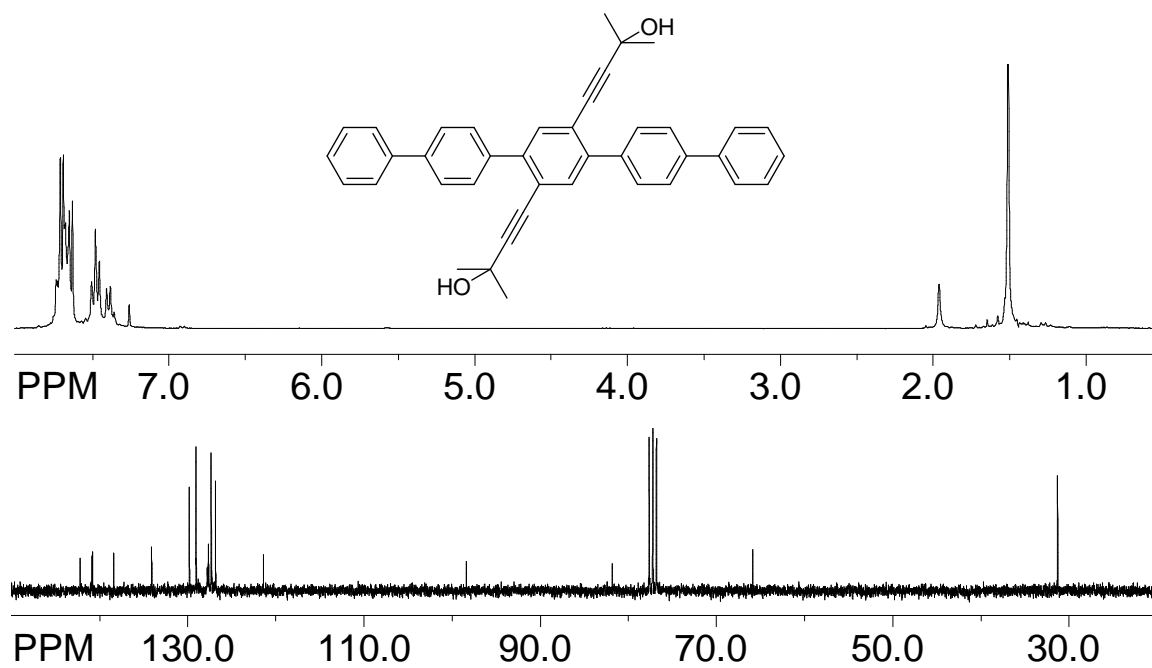
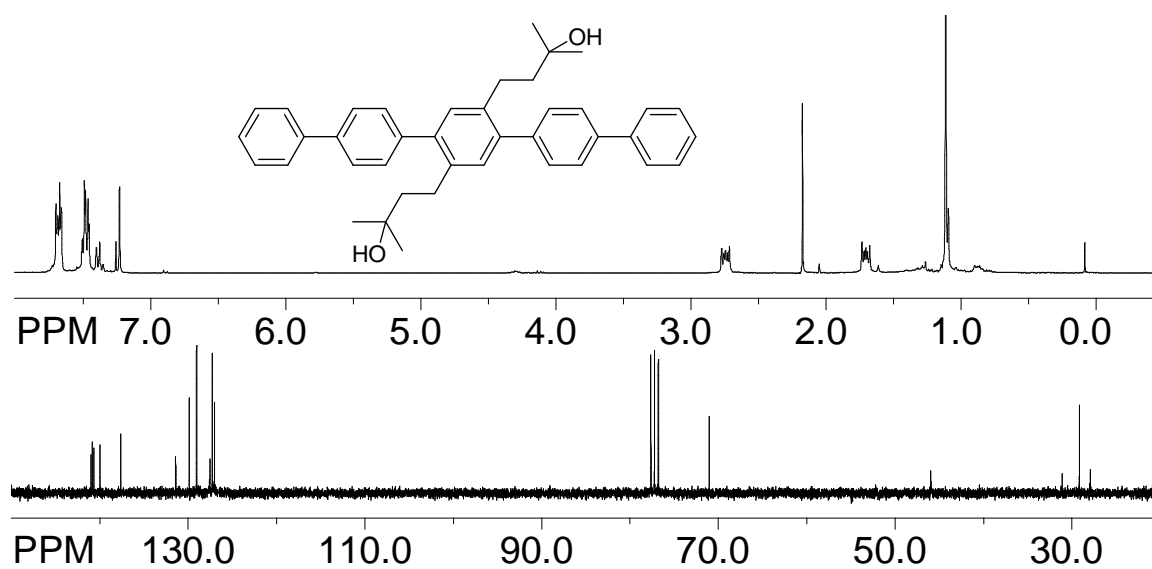
^1H and ^{13}C NMR Spectra of 2c (crude) **^1H and ^{13}C NMR Spectra of 3c (crude)**

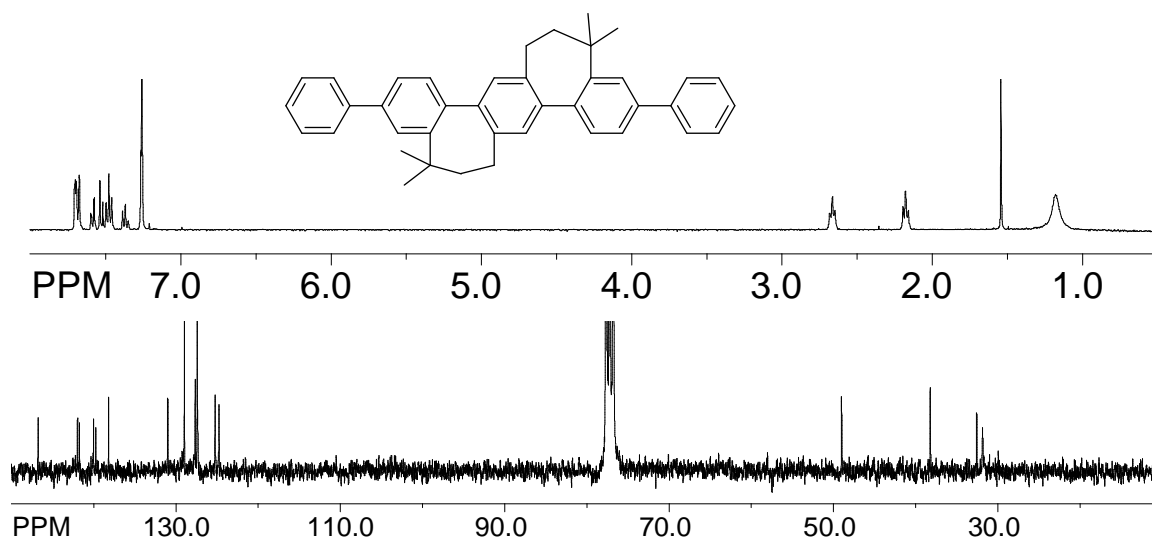
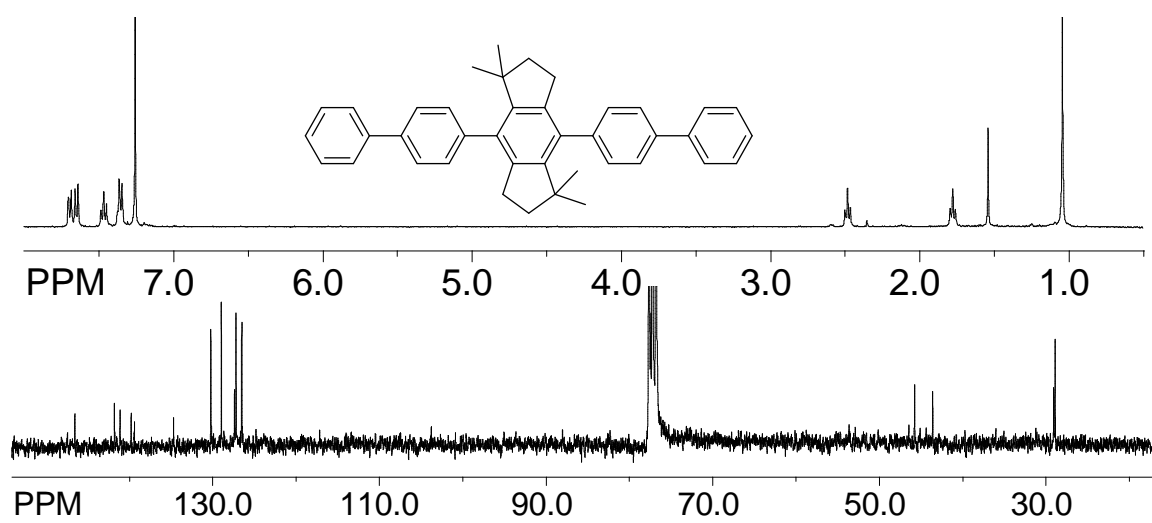
^1H and ^{13}C NMR Spectra of 4c **^1H and ^{13}C NMR Spectra of 2d (crude)**

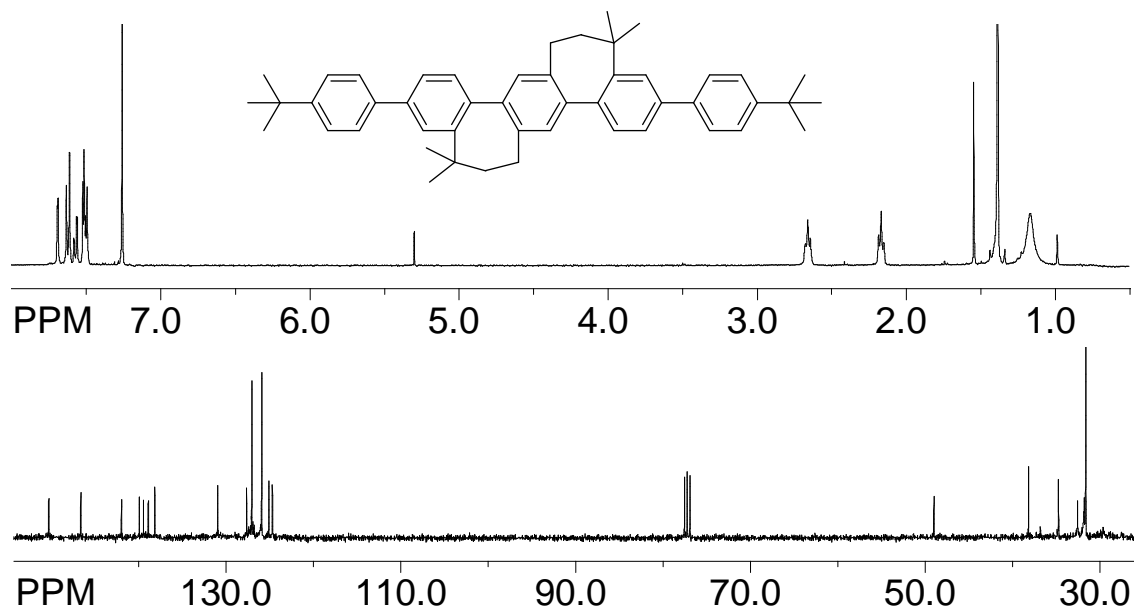
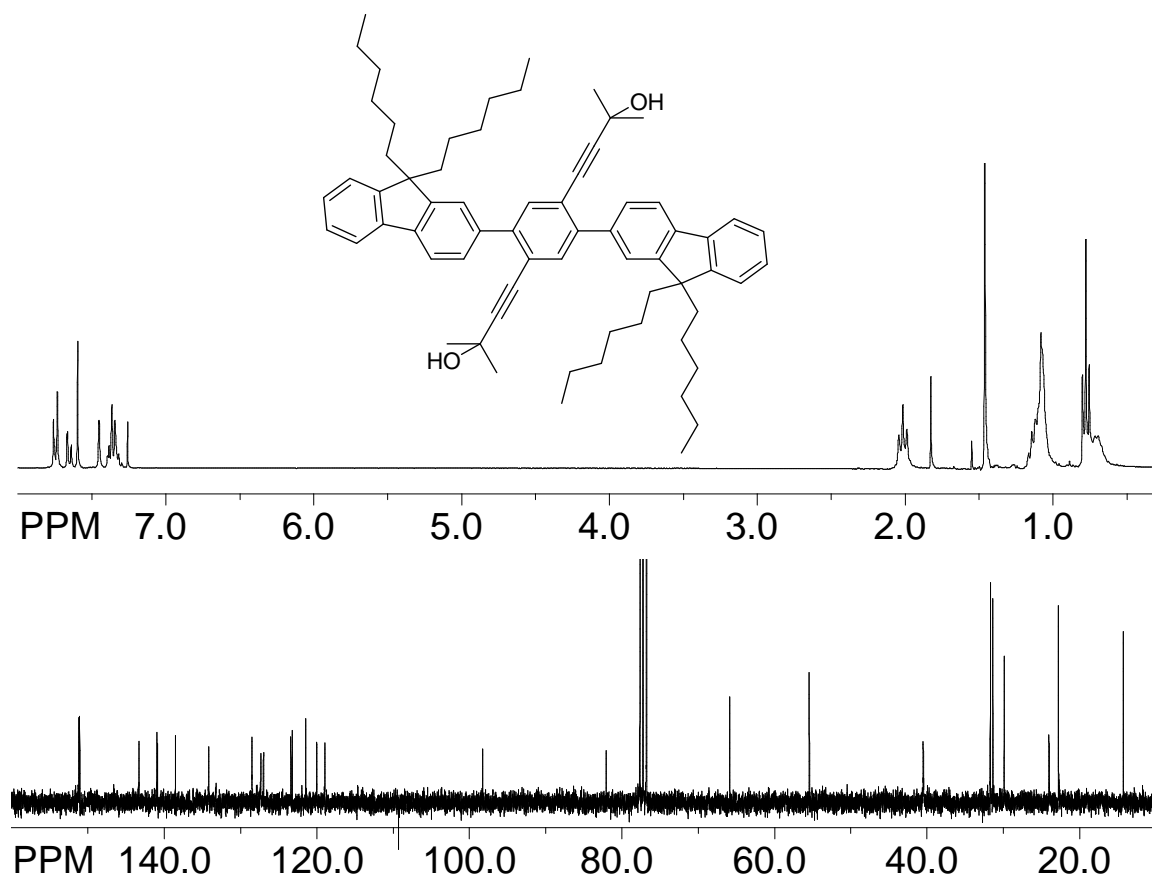
^1H and ^{13}C NMR Spectra of 3d (crude) **^1H and ^{13}C NMR Spectra of 4d**

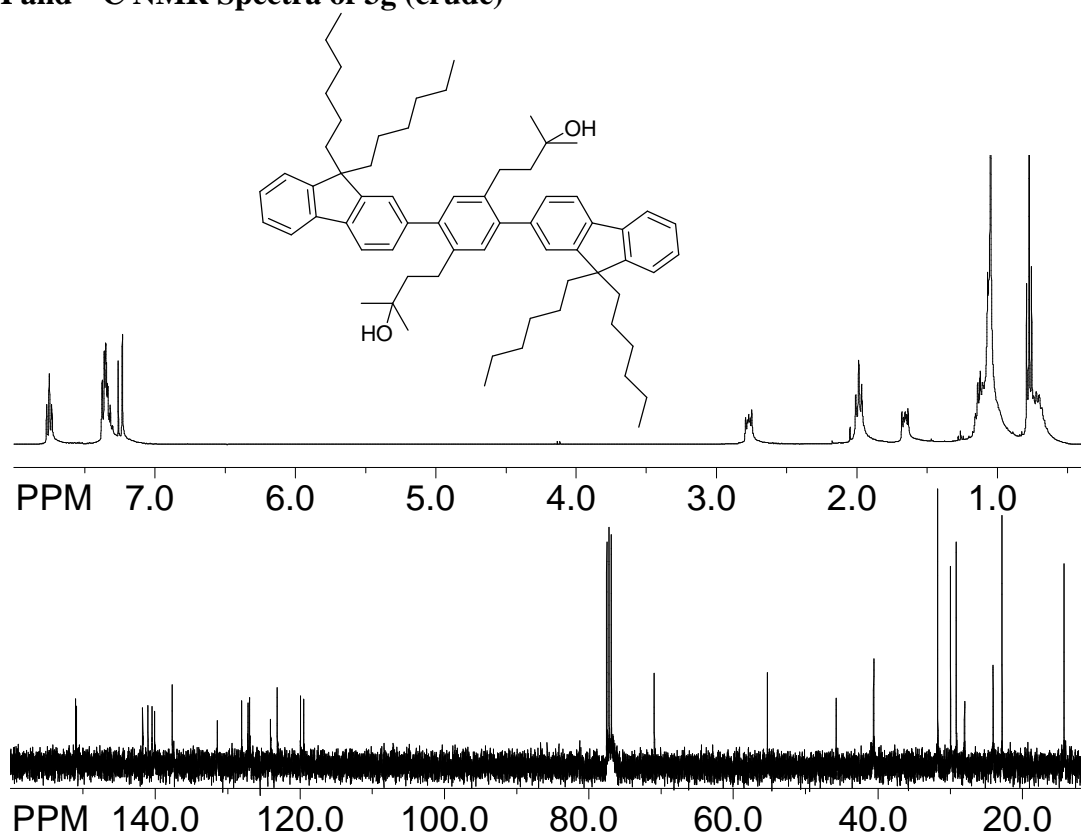
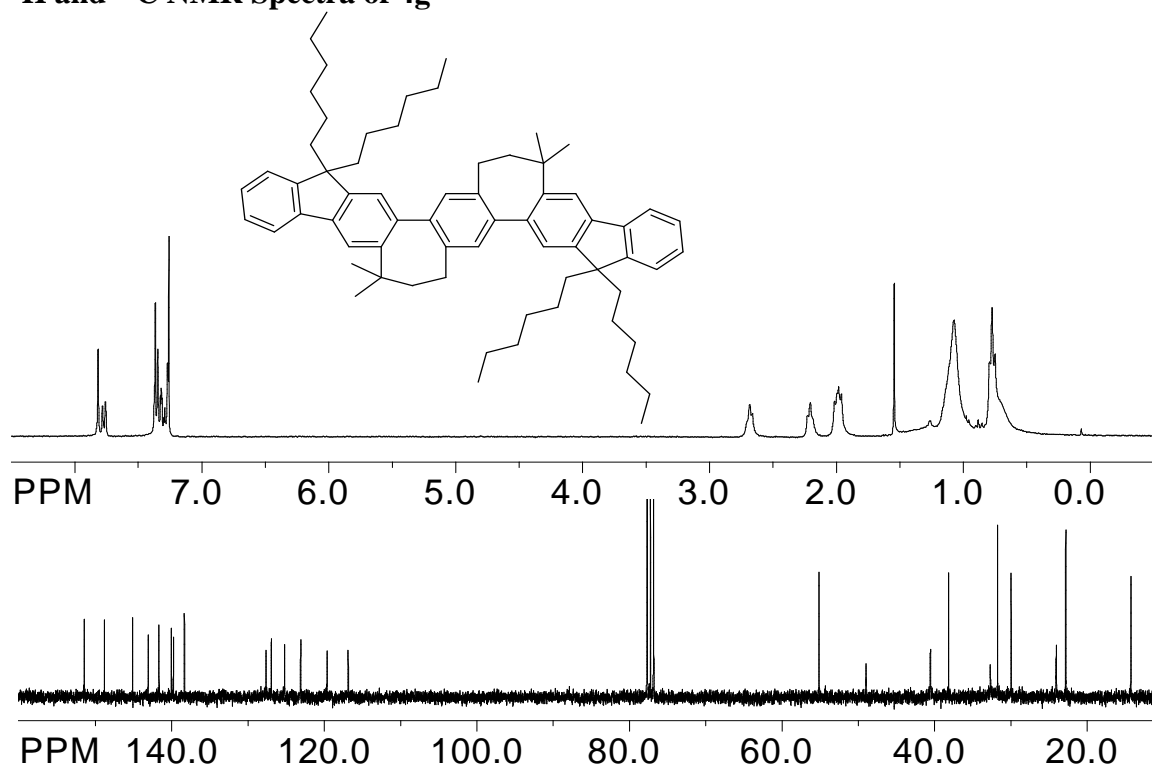
^1H and ^{13}C NMR Spectra of the Centrally Cyclized Isomer 5d **^1H and ^{13}C NMR Spectra of 2e (crude)**

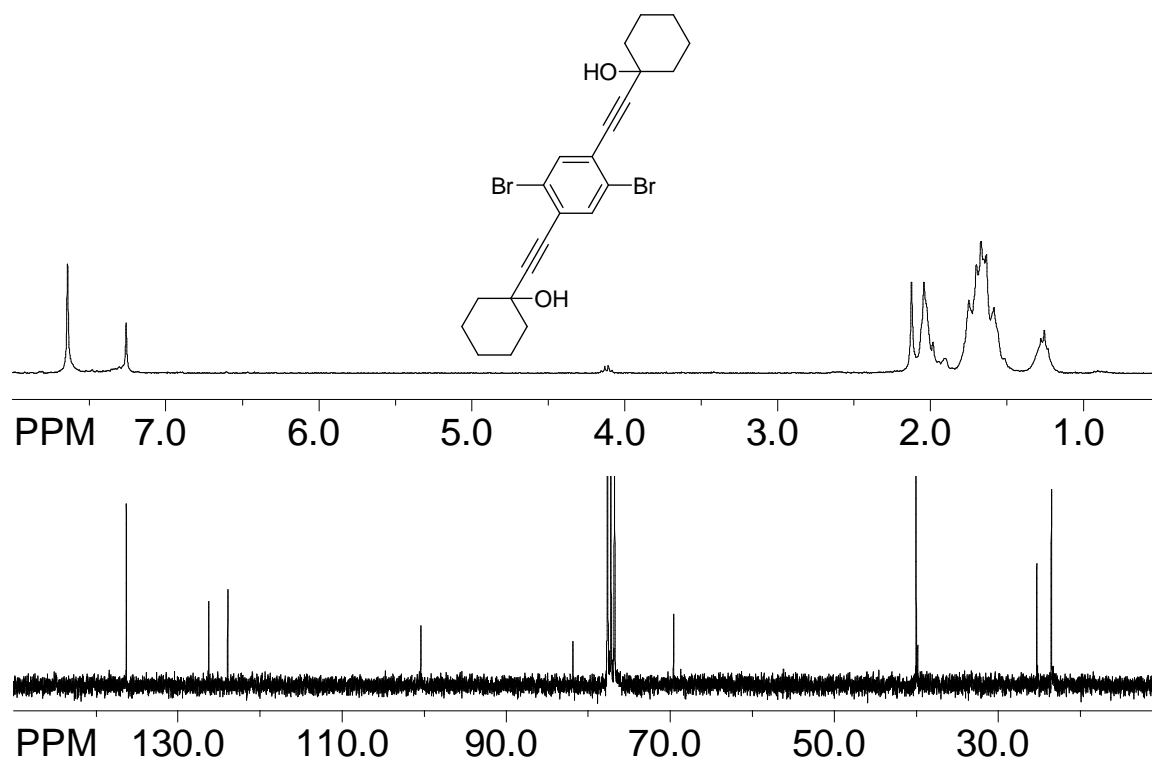
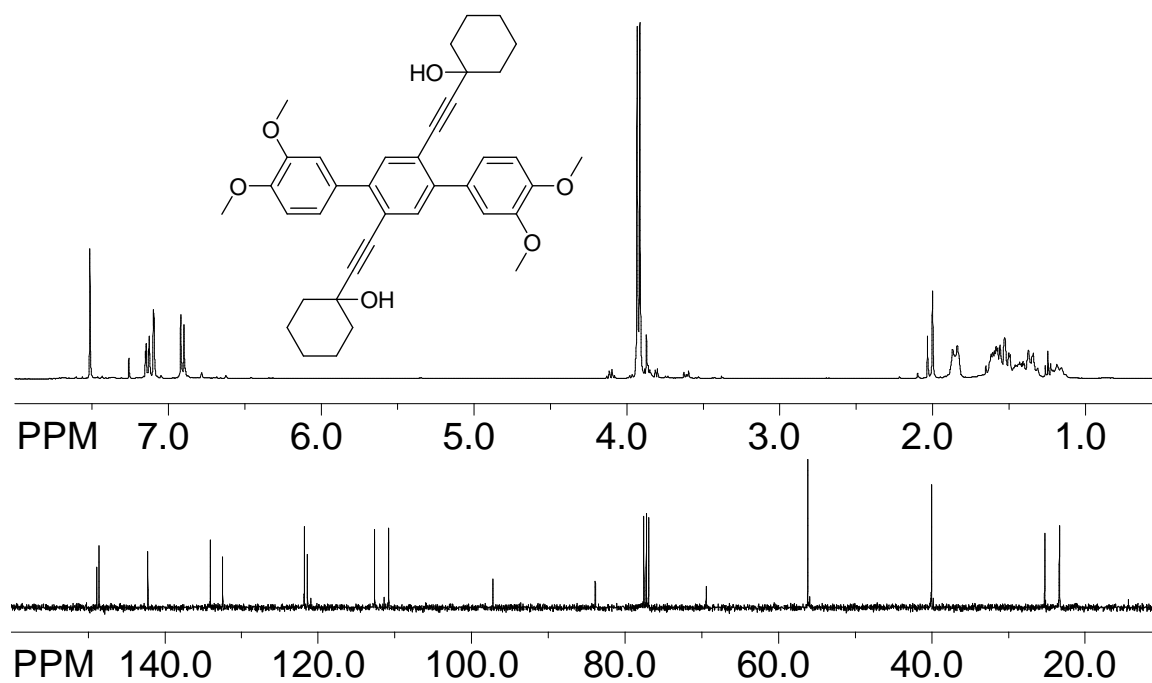
^1H and ^{13}C NMR Spectra of 3e (crude) **^1H and ^{13}C NMR Spectra of 4e (see below the VT NMR)**

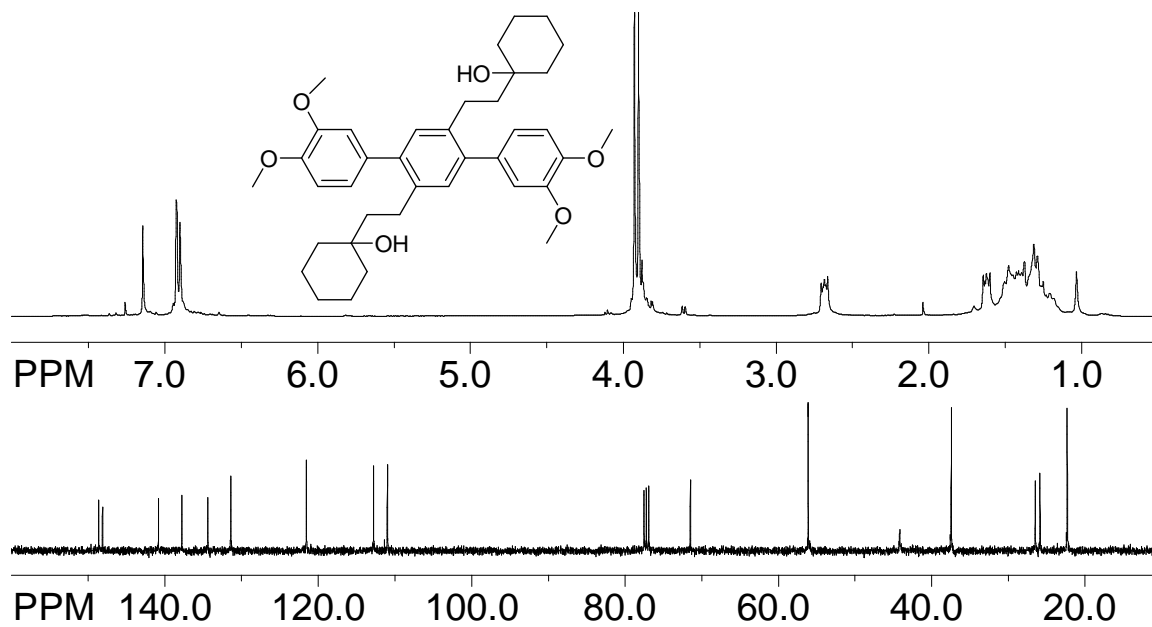
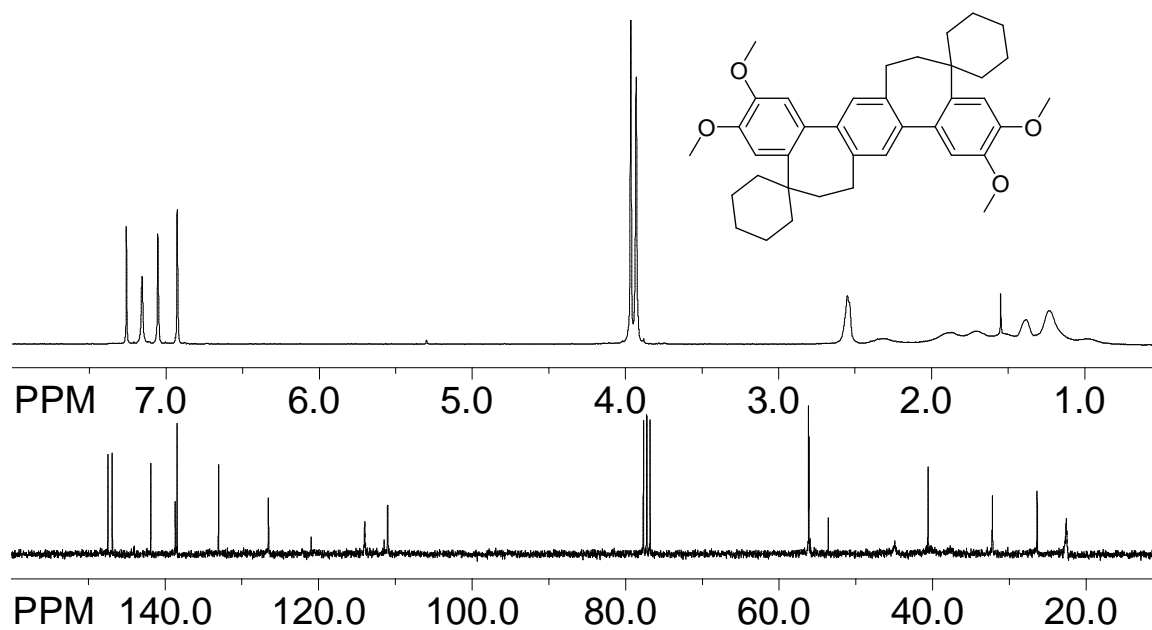
^1H and ^{13}C NMR Spectra of 2f (crude) **^1H and ^{13}C NMR Spectra of 3f (crude)**

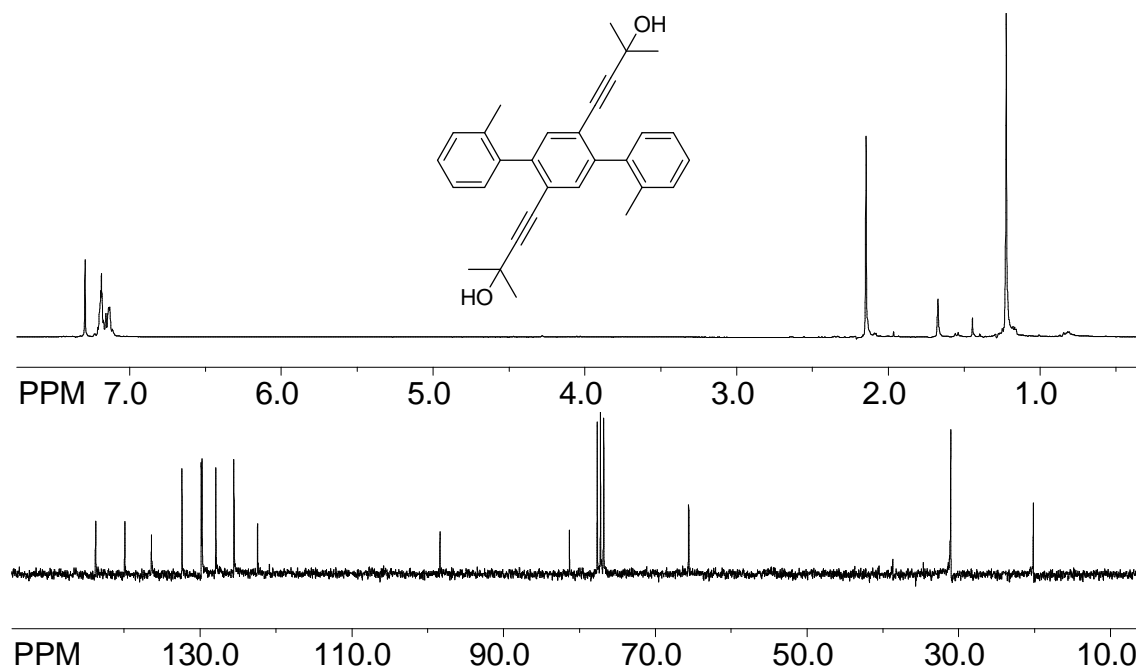
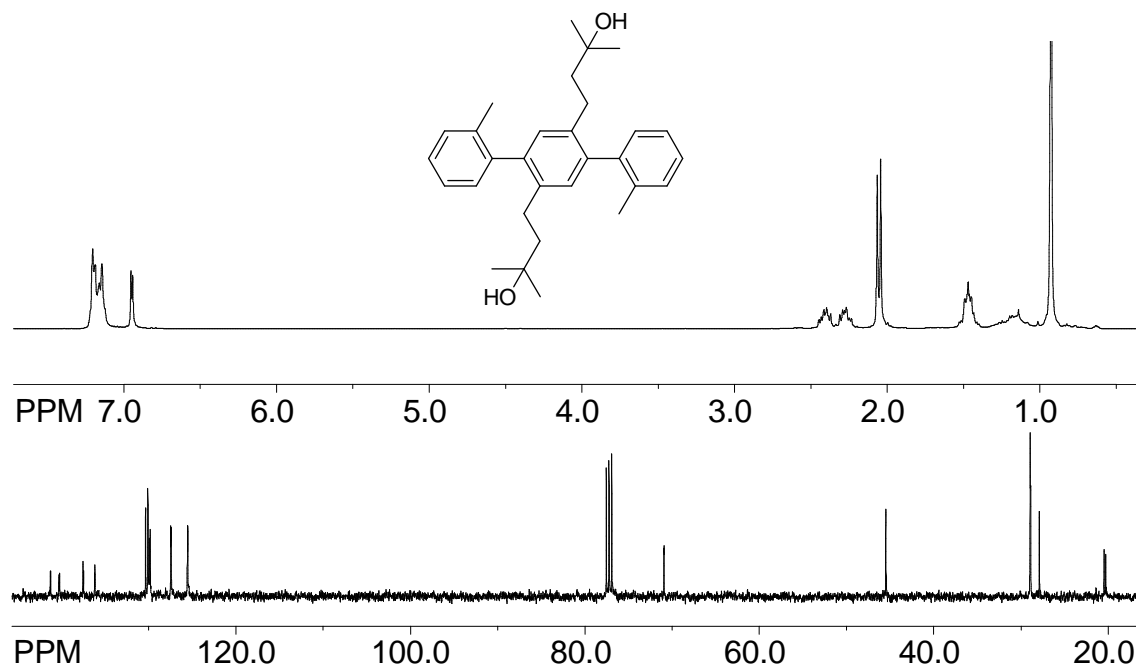
^1H and ^{13}C NMR Spectra of 4f **^1H and ^{13}C NMR Spectra of the Centrally Cyclized Isomer 5f**

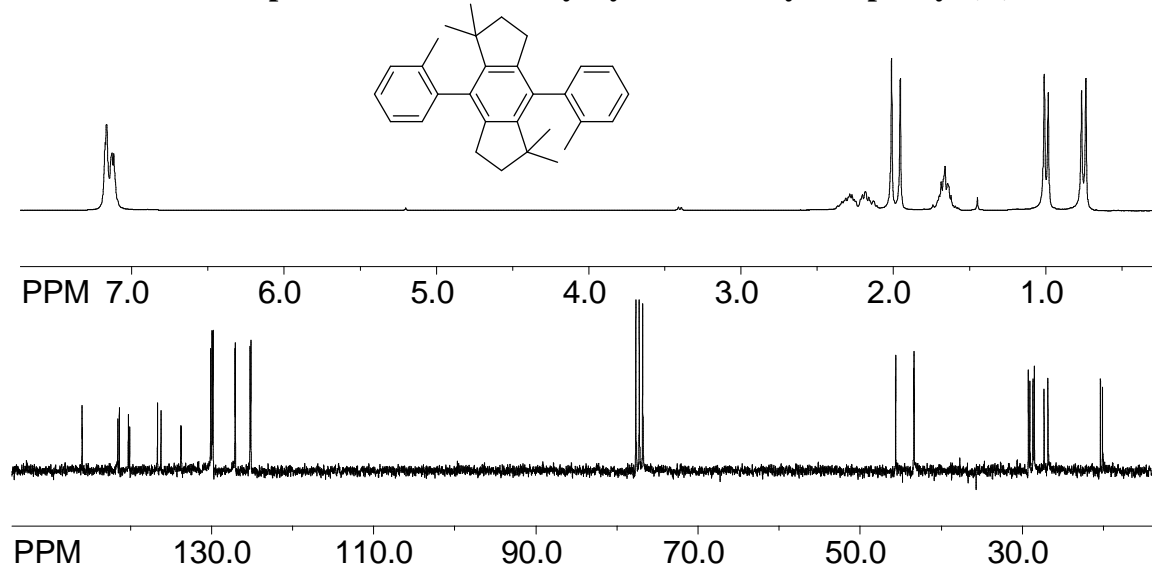
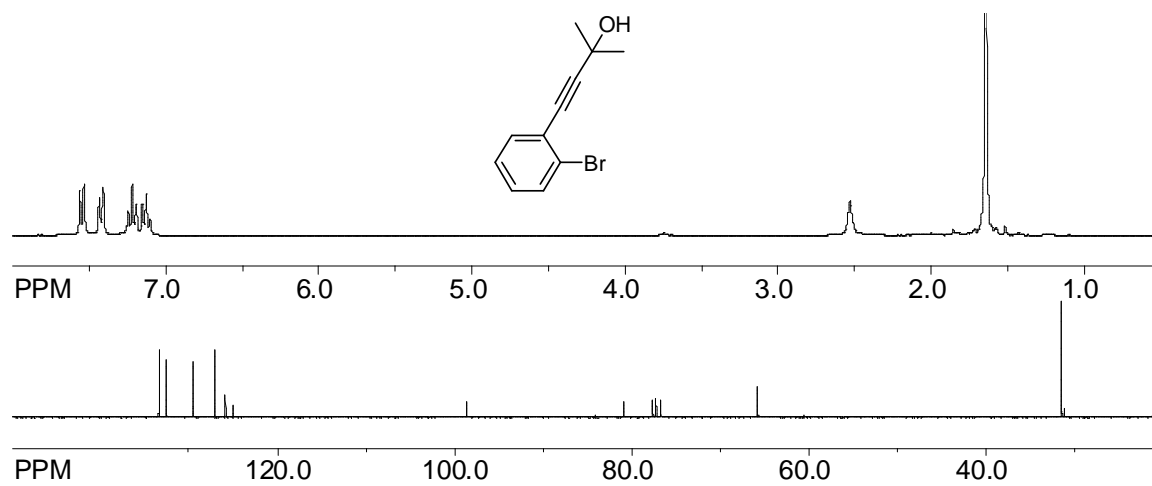
^1H and ^{13}C NMR Spectra of *tert*-butylated 4f **^1H and ^{13}C NMR Spectra of 2g (crude)**

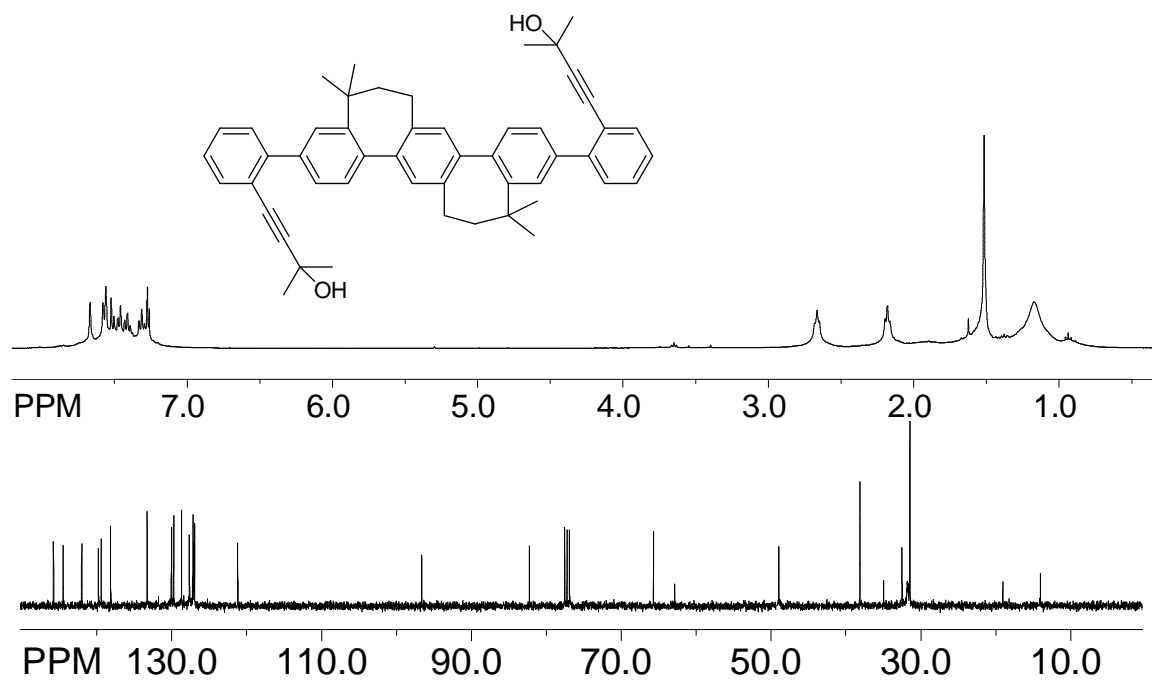
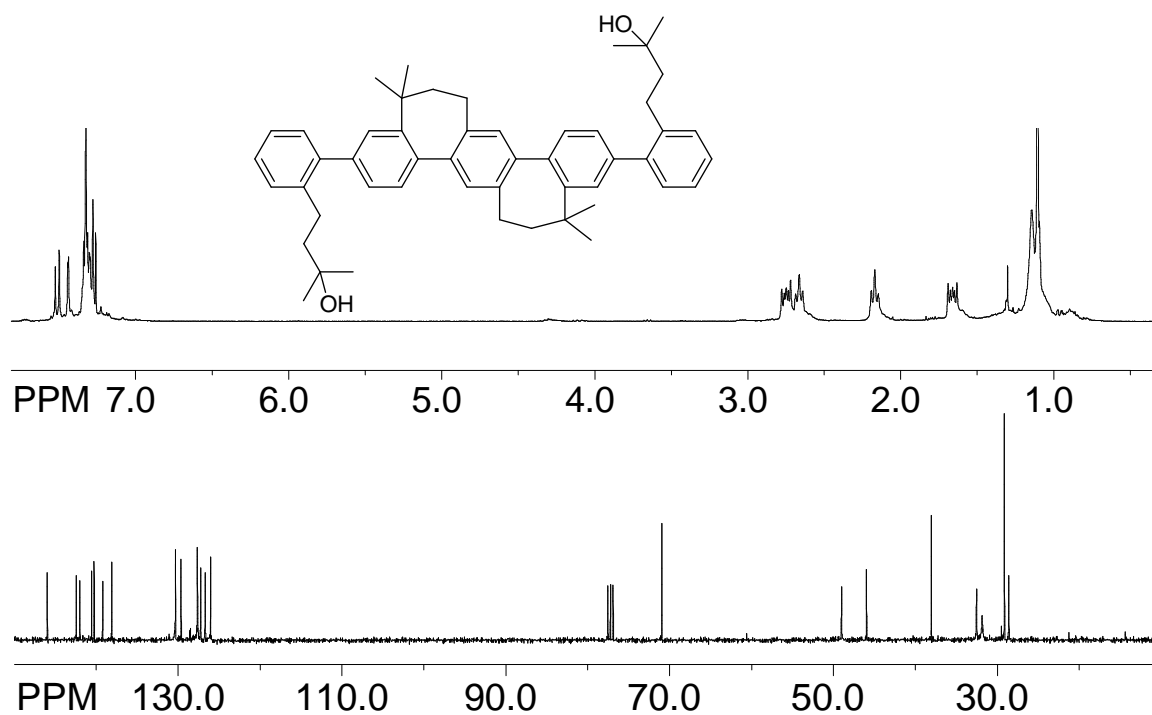
^1H and ^{13}C NMR Spectra of 3g (crude) **^1H and ^{13}C NMR Spectra of 4g**

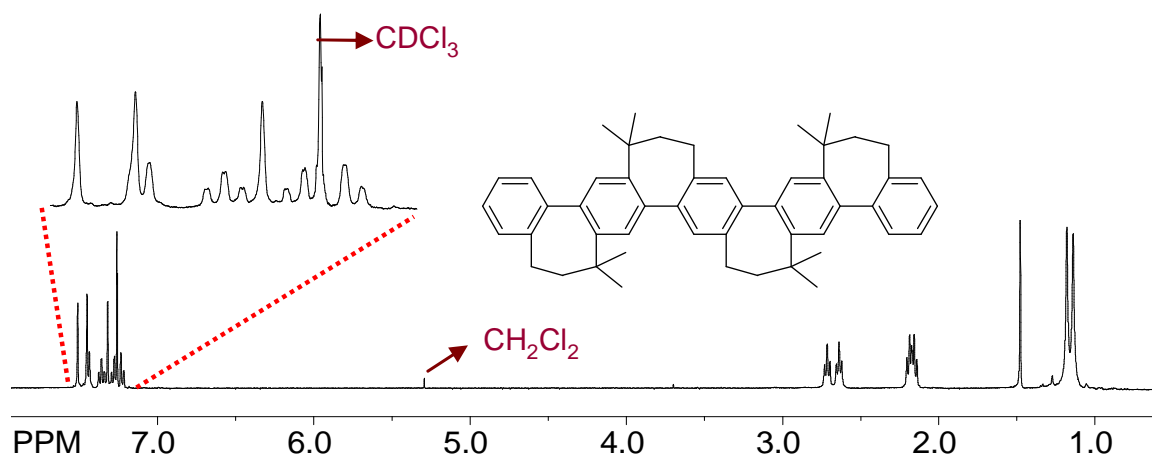
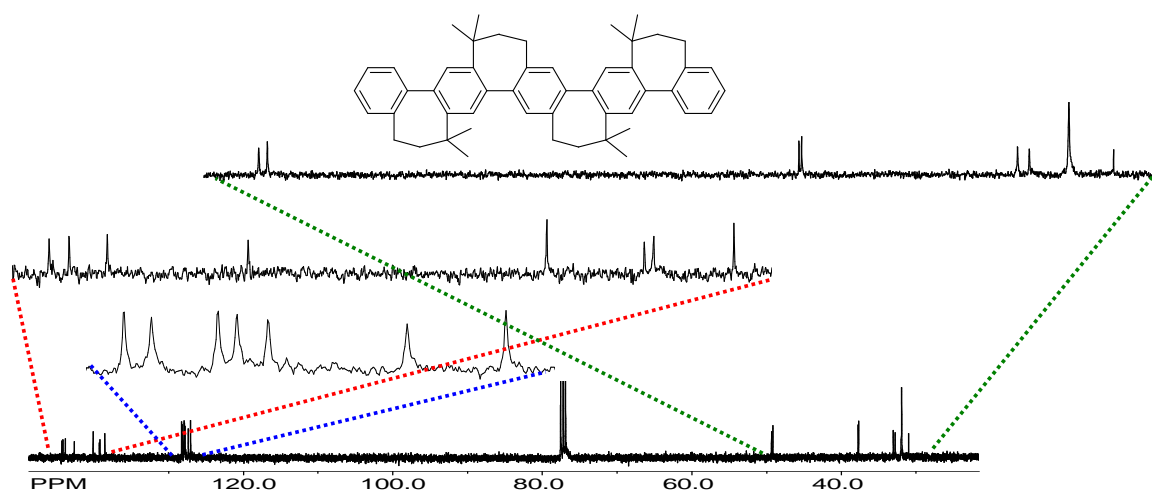
^1H and ^{13}C NMR Spectra of diacetylenic biscyclohexyl derivative 1' **^1H and ^{13}C NMR Spectra of 2h (crude)**

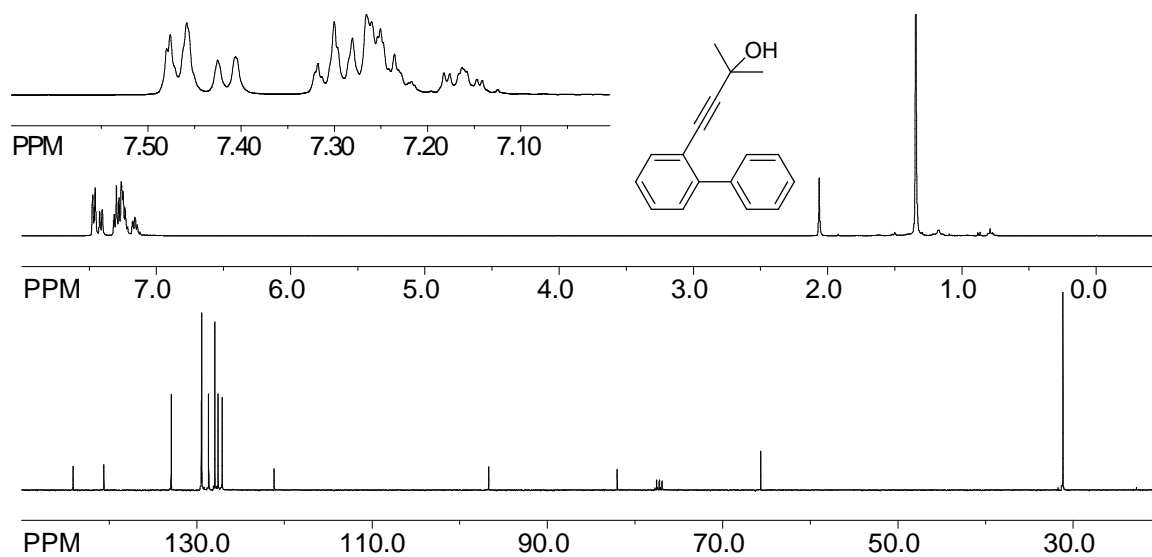
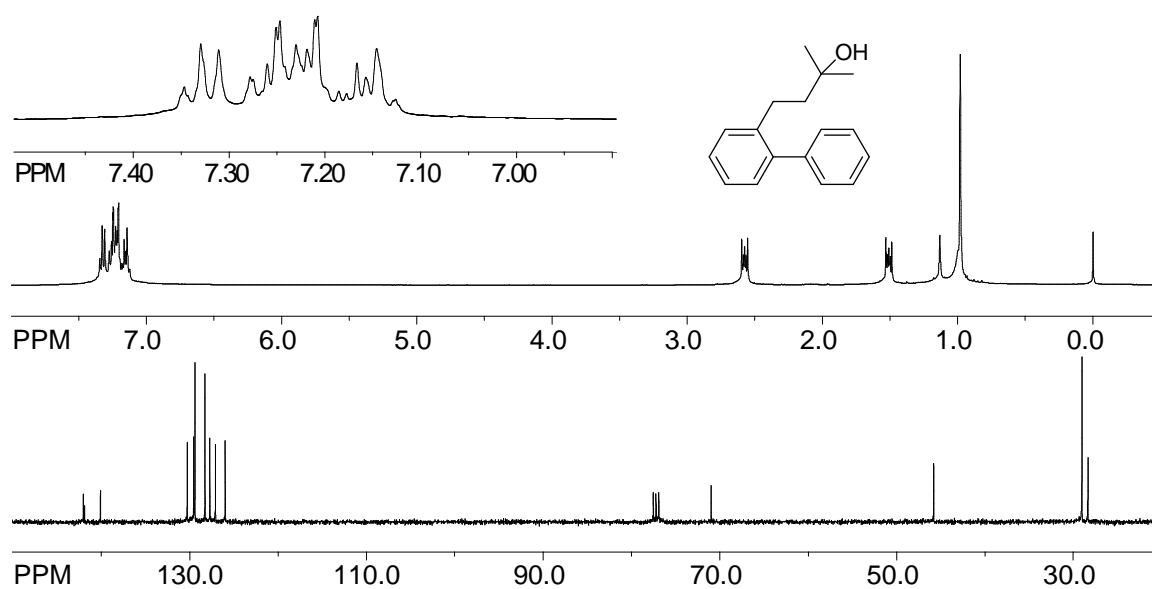
^1H and ^{13}C NMR Spectra of 3h (crude) **^1H and ^{13}C NMR Spectra of 4h (see below the VT NMR)**

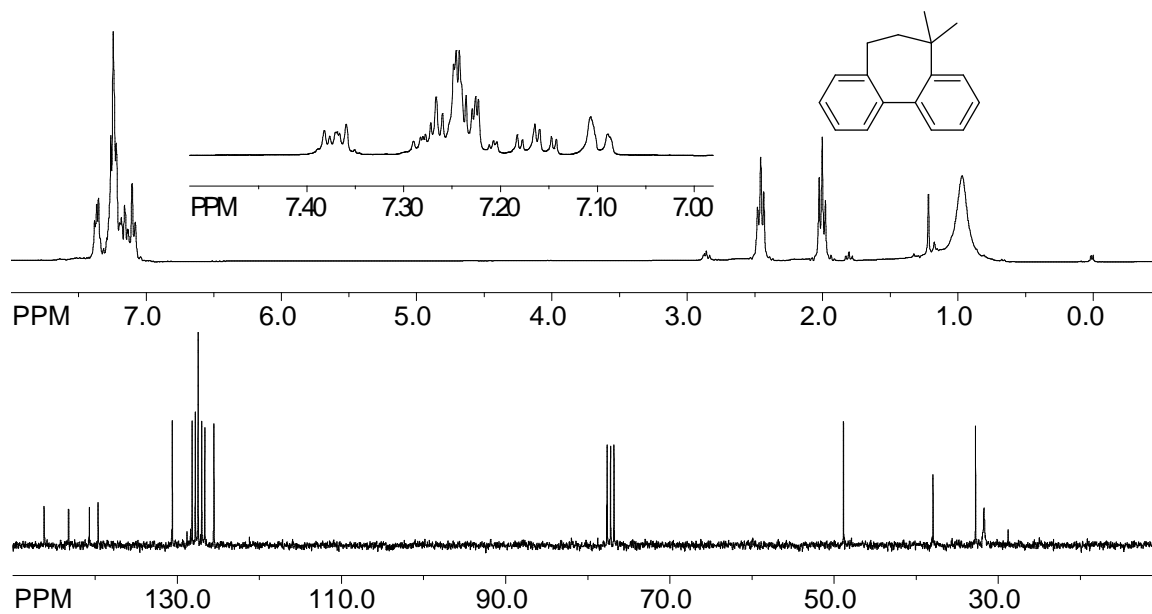
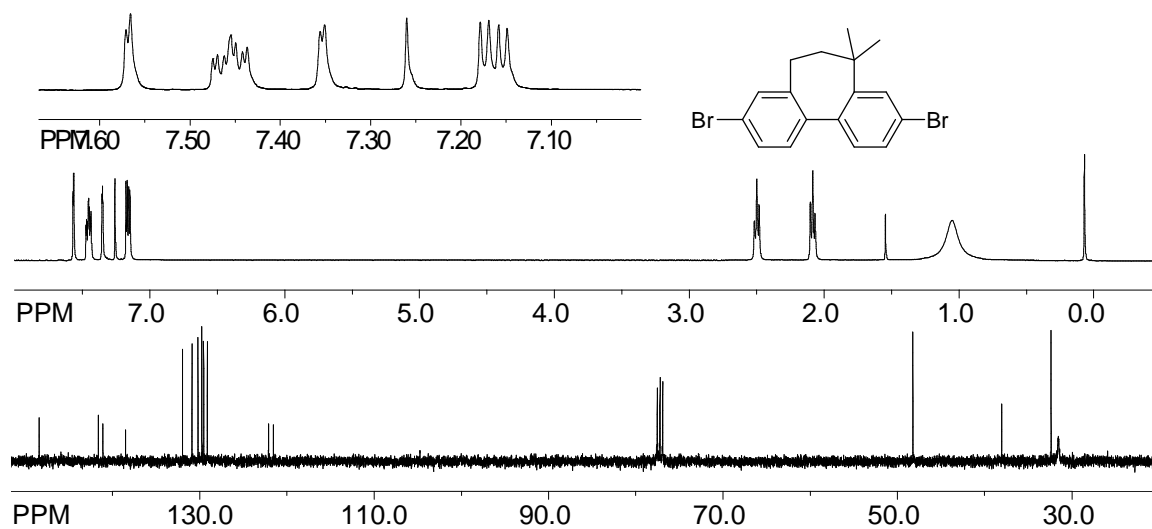
^1H and ^{13}C NMR Spectra of *o*-Tolyl Terphenyl Diacetylenic Precursor (2i) **^1H and ^{13}C NMR Spectra of *o*-Tolyl Terphenyl Alkane (3i)**

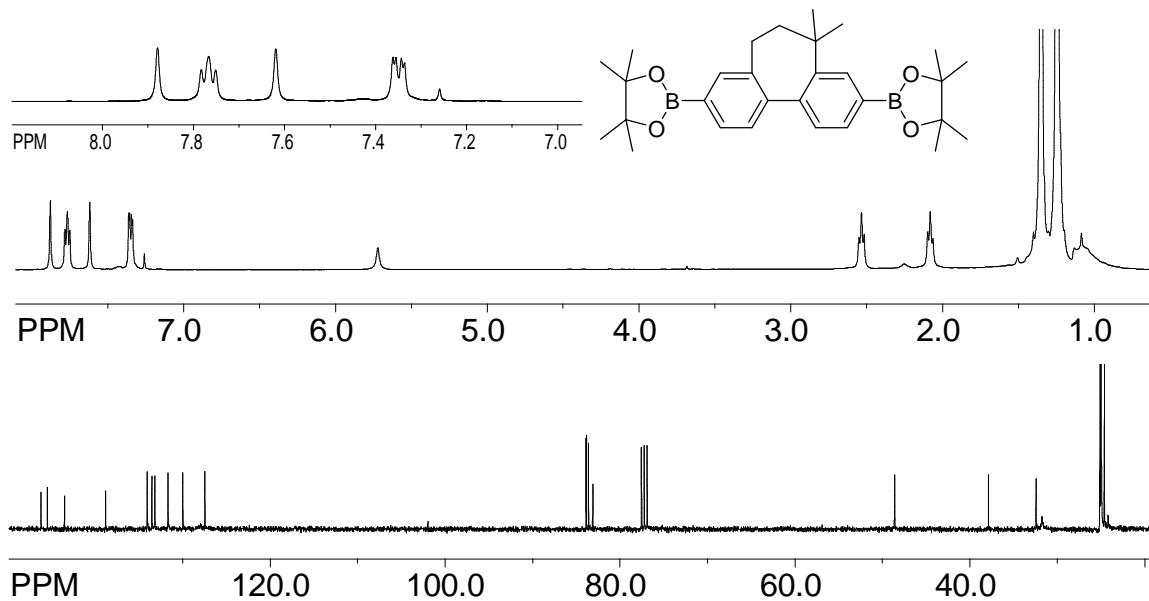
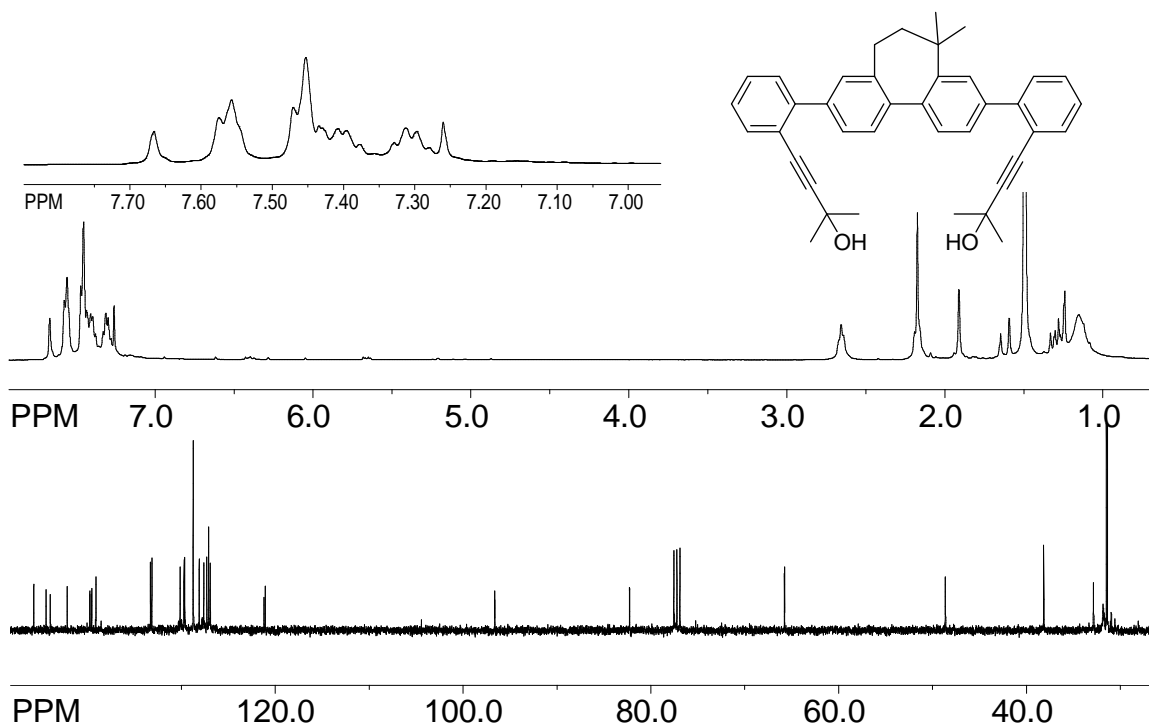
^1H and ^{13}C NMR Spectra of the Centrally Cyclized *o*-Tolyl Terphenyl (5i) **^1H and ^{13}C NMR Spectra of 7**

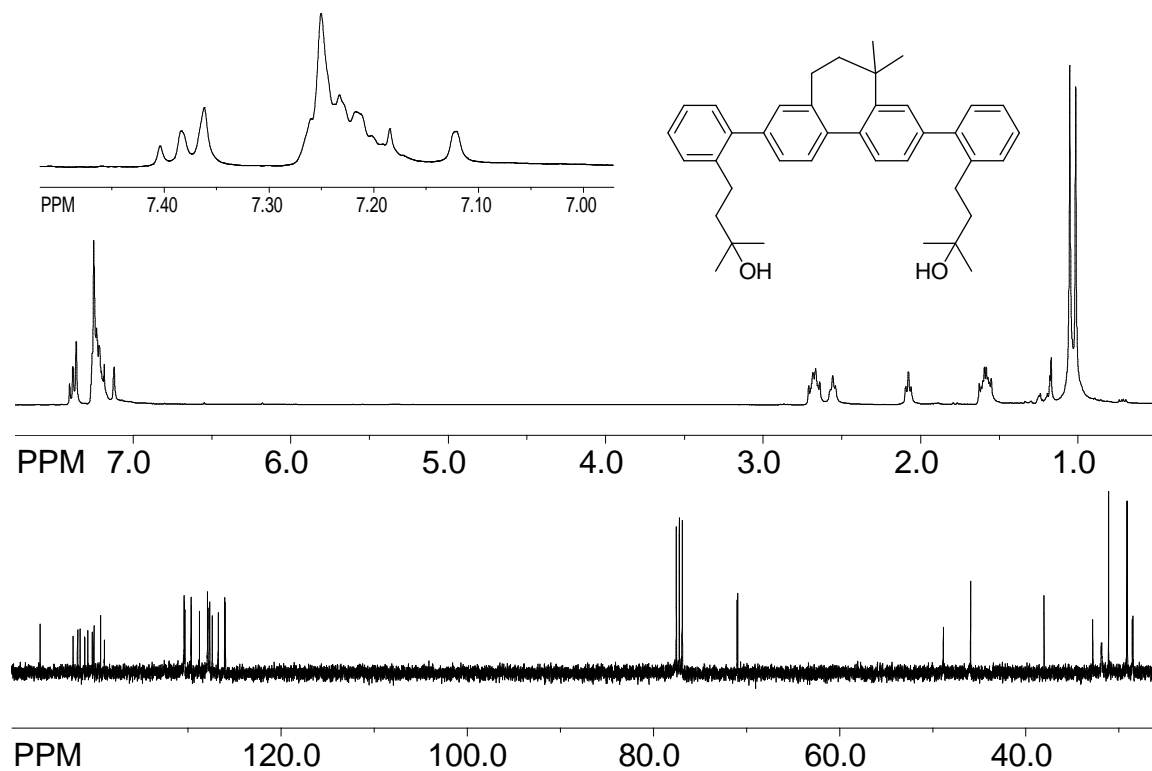
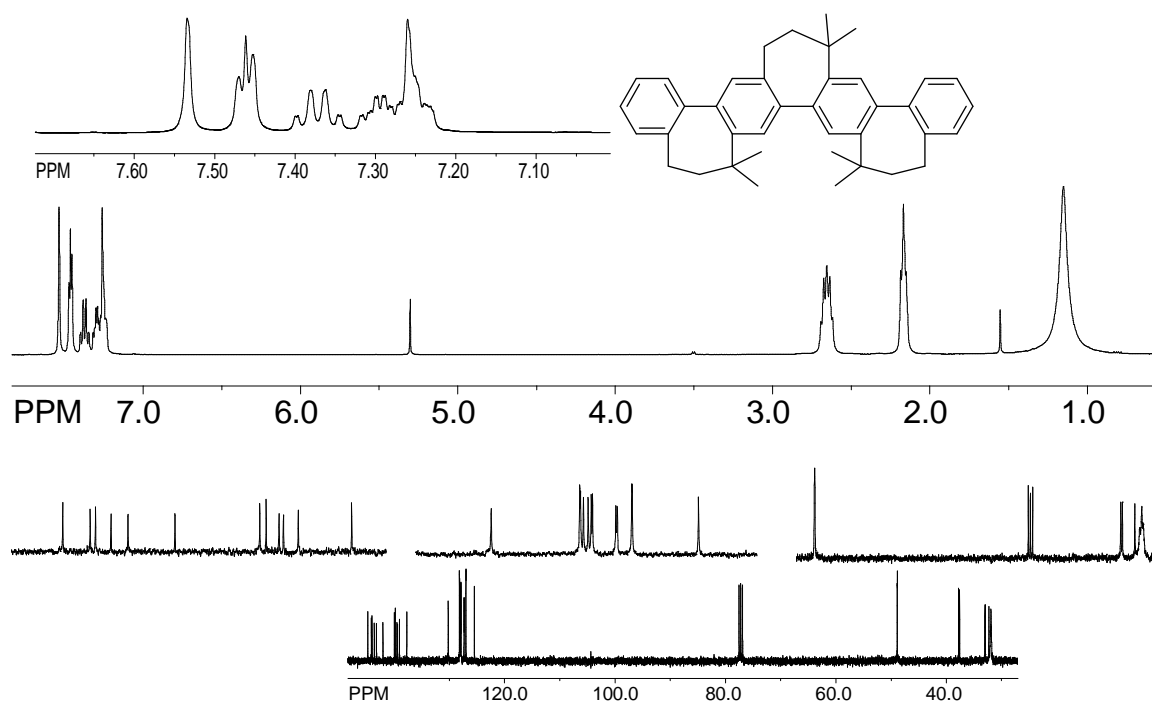
^1H and ^{13}C NMR Spectra of 8 **^1H and ^{13}C NMR Spectra of Reduced Penta-*p*-Phenylene**

^1H NMR Spectra of 9 **^{13}C NMR Spectra of 9**

^1H and ^{13}C NMR Spectra of Biphenyl Acetylenic Precursor 10 **^1H and ^{13}C NMR Spectra of the Reduced Biphenyl Precursor 11**

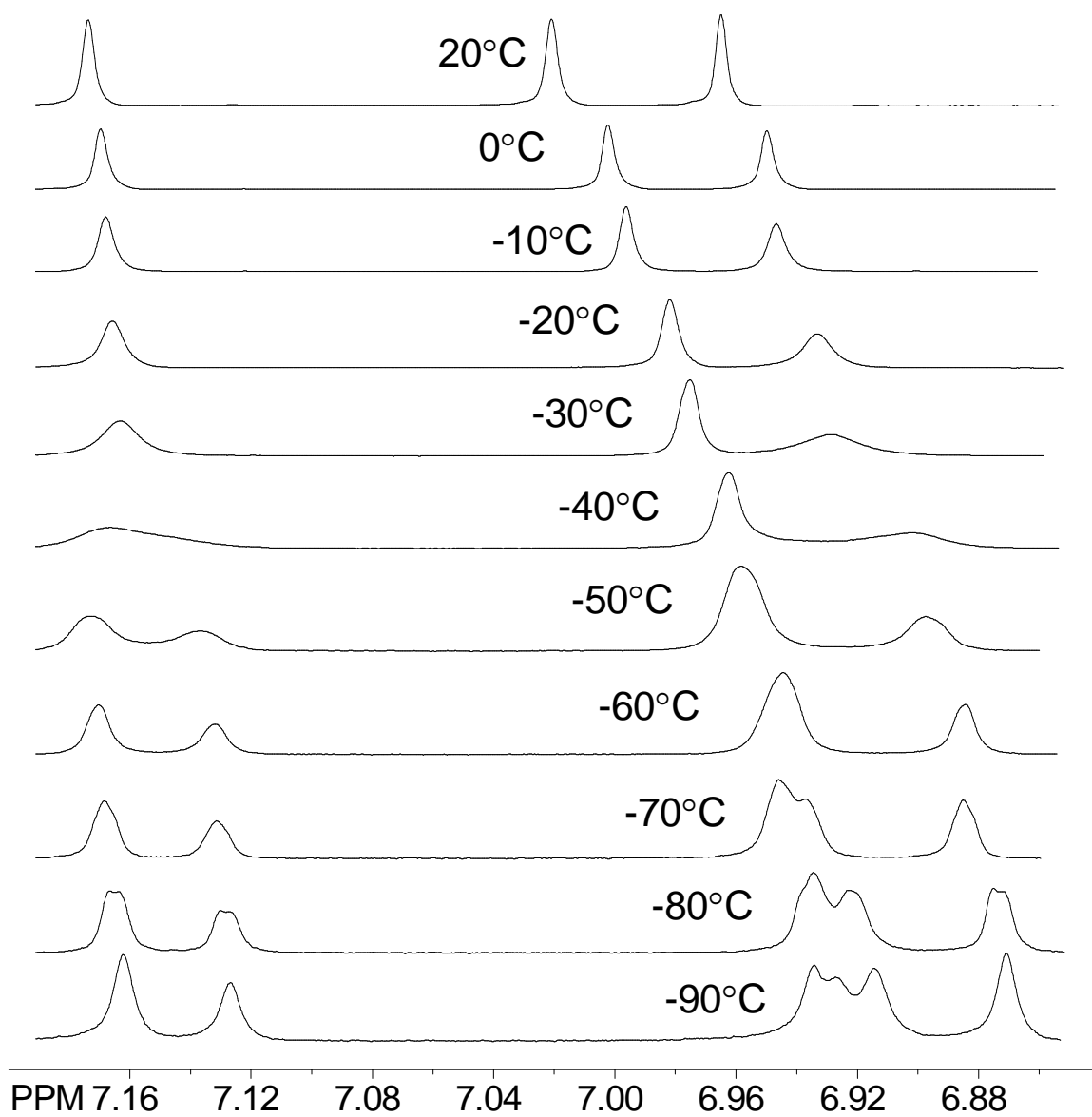
^1H and ^{13}C NMR Spectra of Bridged Biphenyl 12 **^1H and ^{13}C NMR Spectra of the Dibromo Bridged Biphenyl 13**

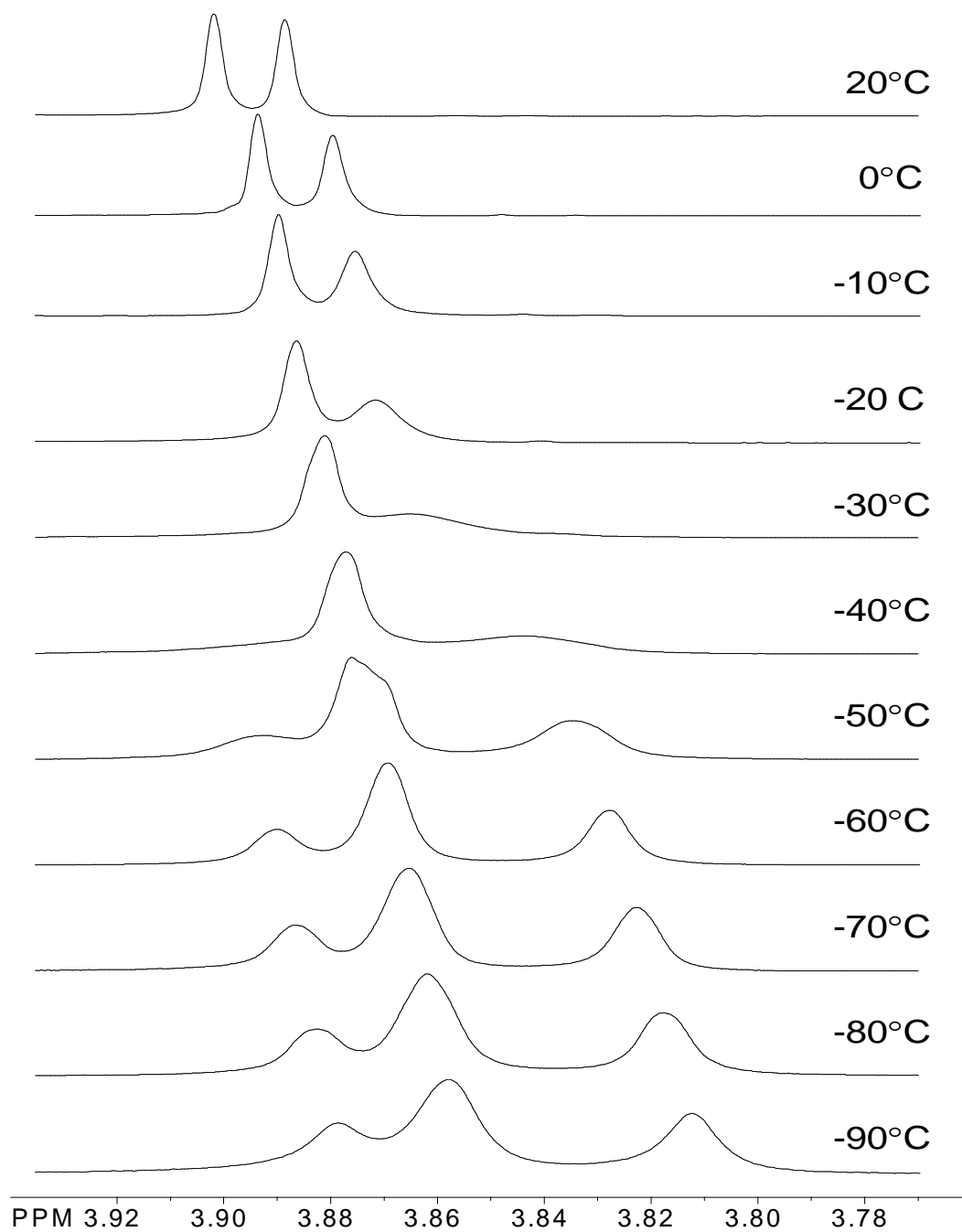
^1H and ^{13}C NMR Spectra of Bridged Biphenyl Diboronic Ester 14 **^1H and ^{13}C NMR Spectra of the Tetra-*p*-Phenylene Acetylenic Precursor 15**

^1H and ^{13}C NMR Spectra of the Reduced Tetra-*p*-Phenylene Precursor 16 **^1H and ^{13}C NMR of Tetra-*p*-Phenylene 17**

Variable Temperature ^1H NMR of 4e in CD_2Cl_2

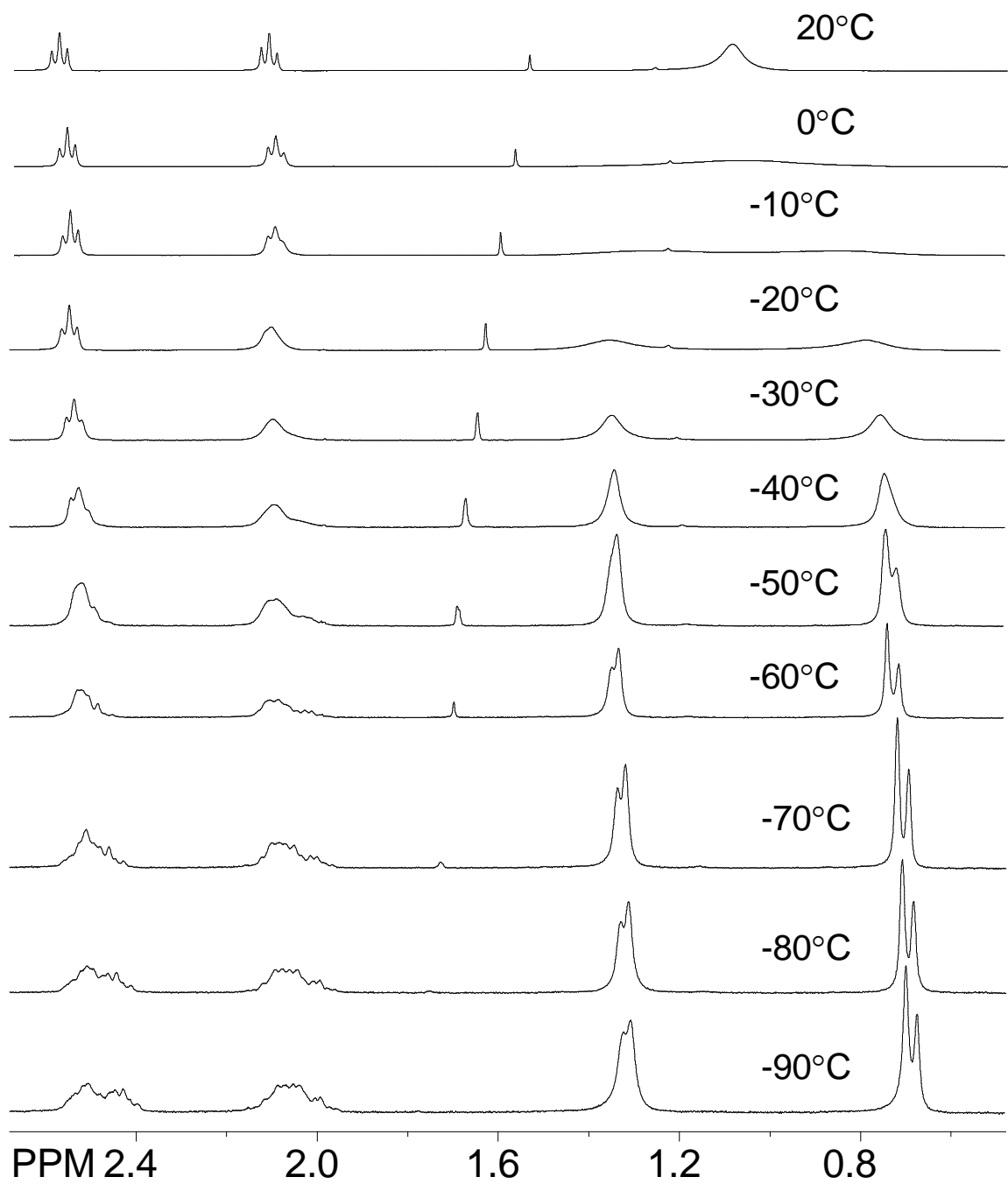
Aromatic Region (4e)

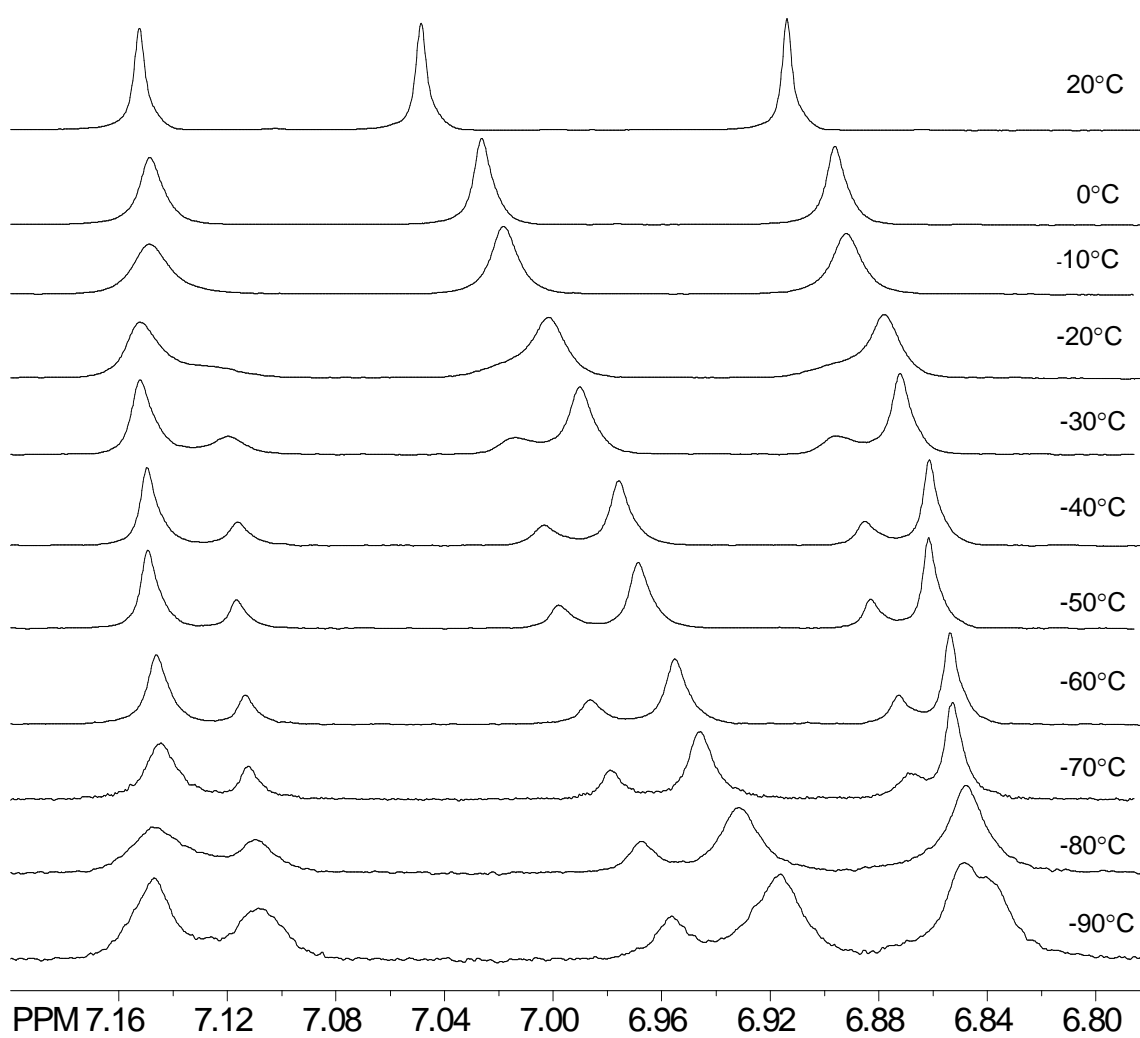


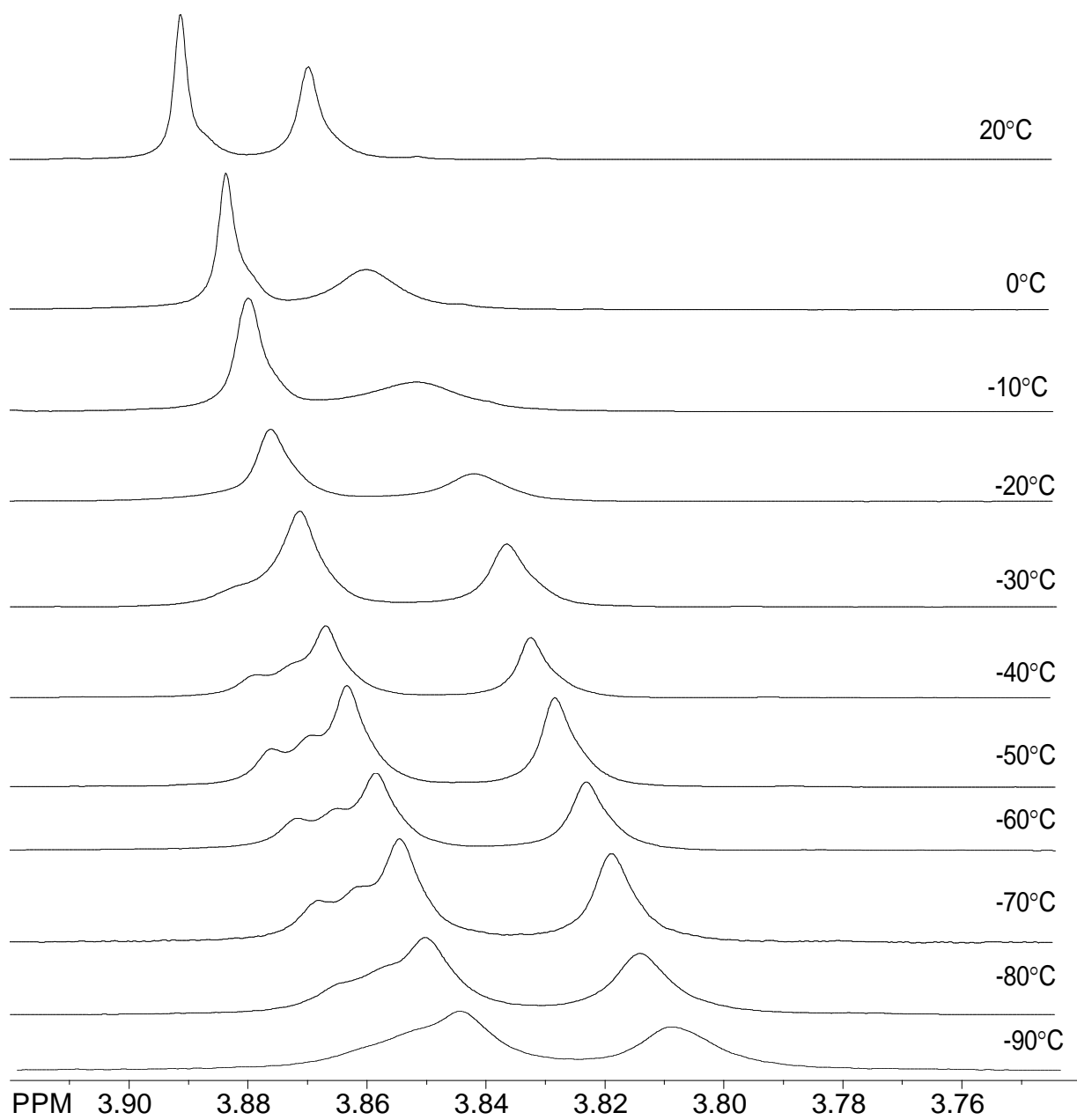
Variable Temperature ^1H NMR of 4e in CD_2Cl_2 **Methoxy Region (4e)**

Variable Temperature ^1H NMR of 4e in CD_2Cl_2

Aliphatic Region (4e)



Variable Temperature ^1H NMR of 4h in CD_2Cl_2 **Aromatic Region**

Variable Temperature ^1H NMR of 4h in CD_2Cl_2 **Methoxy Region (4h)**

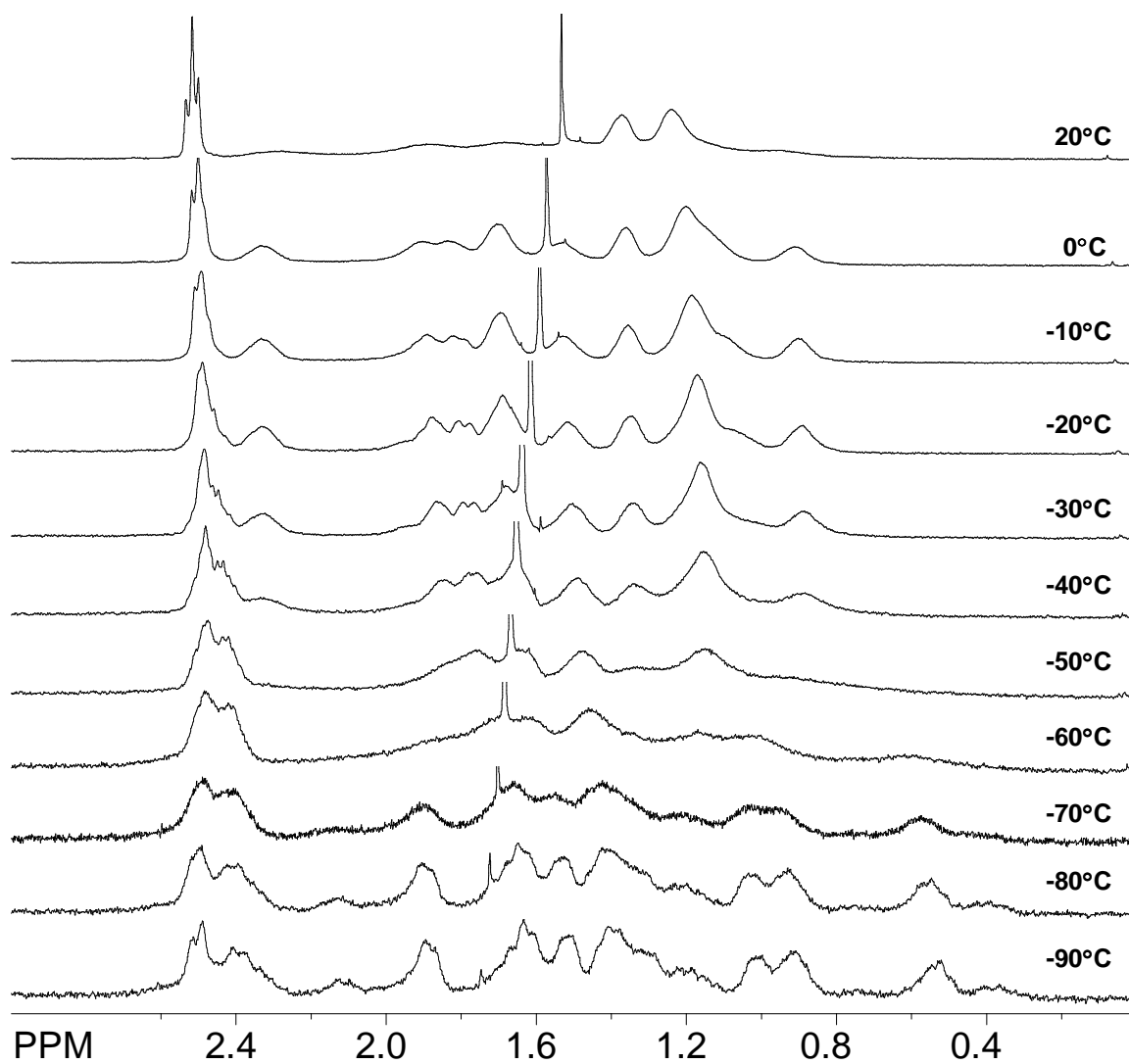
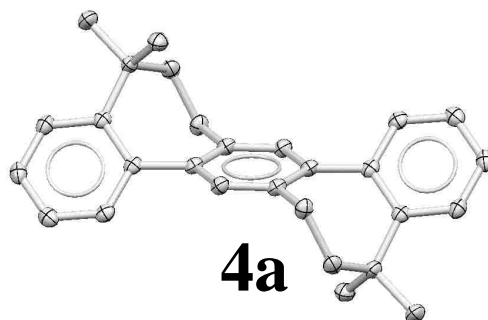
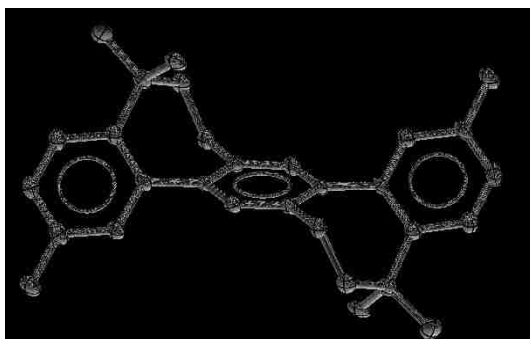
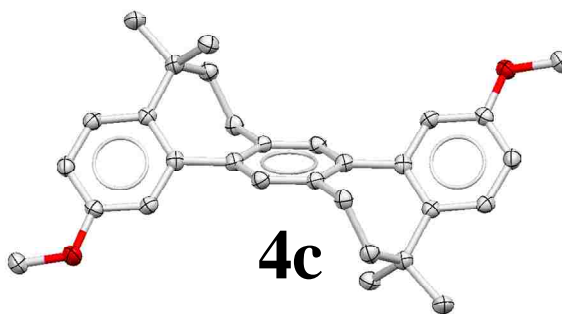
Variable Temperature ^1H NMR of 4h in CD_2Cl_2 **Aliphatic Region (4h)**

Table 2. Crystal data and structure refinement for raj13h (4a)

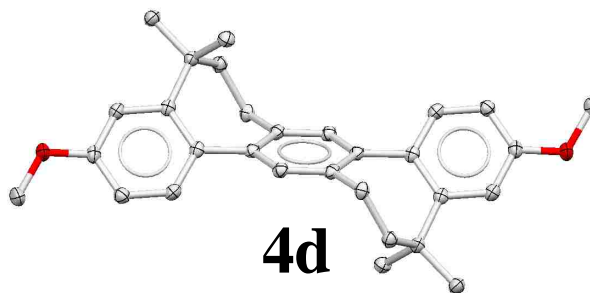
Identification code	raj13h	
Empirical formula	C _{28.50} H ₃₁ Cl	
Formula weight	408.98	
Temperature	100(2) K	
Wavelength	1.54178 Å	
Crystal system	Monoclinic	
Space group	C 2/c	
Unit cell dimensions	a = 25.9973(4) Å	α = 90°.
	b = 12.3802(2) Å	β = 93.7240(10)°.
	c = 13.8796(2) Å	γ = 90°.
Volume	4457.74(12) Å ³	
Z	8	
Density (calculated)	1.219 Mg/m ³	
Absorption coefficient	1.583 mm ⁻¹	
F(000)	1752	
Crystal size	0.25 x 0.19 x 0.12 mm ³	
Theta range for data collection	3.41 to 68.01°.	
Index ranges	-31 ≤ h ≤ 31, 0 ≤ k ≤ 14, 0 ≤ l ≤ 16	
Reflections collected	18639	
Independent reflections	4001 [R(int) = 0.0178]	
Completeness to theta = 68.01°	98.2 %	
Absorption correction	Semi-empirical from equivalents	
Max. and min. transmission	0.8327 and 0.6930	
Refinement method	Full-matrix least-squares on F ²	
Data / restraints / parameters	4001 / 2 / 286	
Goodness-of-fit on F ²	1.013	
Final R indices [I > 2σ(I)]	R1 = 0.0397, wR2 = 0.1076	
R indices (all data)	R1 = 0.0427, wR2 = 0.1101	
Extinction coefficient	0.00010(3)	
Largest diff. peak and hole	0.240 and -0.340 e.Å ⁻³	

Table 3. Crystal data and structure refinement for raj14j4 (4b)

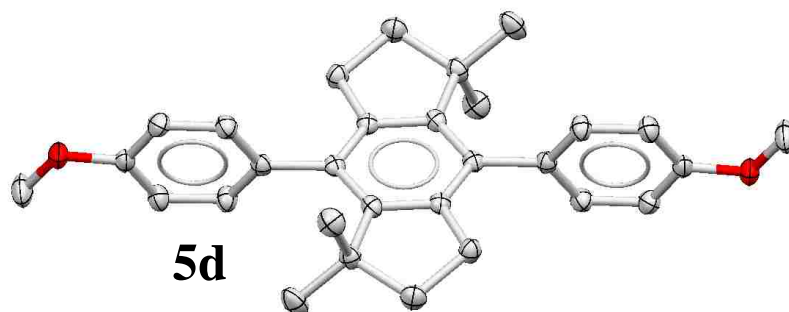
Identification code	raj14j4	
Empirical formula	C ₃₀ H ₃₄	
Formula weight	394.57	
Temperature	100(2) K	
Wavelength	1.54178 Å	
Crystal system	Triclinic	
Space group	P -1	
Unit cell dimensions	a = 11.075(3) Å	α = 118.089(11)°.
	b = 14.841(3) Å	β = 91.405(14)°.
	c = 15.693(4) Å	γ = 92.655(12)°.
Volume	2270.1(9) Å ³	
Z	4	
Density (calculated)	1.155 Mg/m ³	
Absorption coefficient	0.479 mm ⁻¹	
F(000)	856	
Crystal size	0.16 x 0.14 x 0.10 mm ³	
Theta range for data collection	3.20 to 69.87°.	
Index ranges	-13 ≤ h ≤ 13, -17 ≤ k ≤ 15, 0 ≤ l ≤ 18	
Reflections collected	27474	
Independent reflections	7875 [R(int) = 0.1460]	
Completeness to theta = 69.87°	98.8 %	
Absorption correction	Semi-empirical from equivalents	
Max. and min. transmission	0.9536 and 0.9273	
Refinement method	Full-matrix least-squares on F ²	
Data / restraints / parameters	7875 / 0 / 553	
Goodness-of-fit on F ²	1.846	
Final R indices [I > 2σ(I)]	R1 = 0.0993, wR2 = 0.2565	
R indices (all data)	R1 = 0.1270, wR2 = 0.2693	
Largest diff. peak and hole	0.501 and -0.420 e.Å ⁻³	

Table 4. Crystal data and structure refinement for raj14d (**4c**).

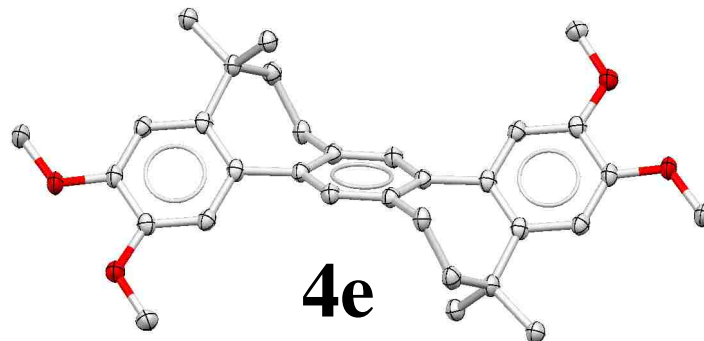
Identification code	raj14d	
Empirical formula	C ₃₀ H ₃₄ O ₂	
Formula weight	426.57	
Temperature	100(2) K	
Wavelength	1.54178 Å	
Crystal system	Monoclinic	
Space group	P 21/c	
Unit cell dimensions	a = 10.6975(6) Å	α = 90°.
	b = 10.0435(6) Å	β = 101.430(3)°.
	c = 10.8065(6) Å	γ = 90°.
Volume	1138.03(11) Å ³	
Z	2	
Density (calculated)	1.245 Mg/m ³	
Absorption coefficient	0.585 mm ⁻¹	
F(000)	460	
Crystal size	0.15 x 0.12 x 0.04 mm ³	
Theta range for data collection	4.22 to 67.48°.	
Index ranges	-12 ≤ h ≤ 12, 0 ≤ k ≤ 11, 0 ≤ l ≤ 12	
Reflections collected	9187	
Independent reflections	2009 [R(int) = 0.0275]	
Completeness to theta = 67.48°	97.8 %	
Absorption correction	Semi-empirical from equivalents	
Max. and min. transmission	0.9770 and 0.9174	
Refinement method	Full-matrix least-squares on F ²	
Data / restraints / parameters	2009 / 0 / 149	
Goodness-of-fit on F ²	1.036	
Final R indices [I > 2σ(I)]	R1 = 0.0367, wR2 = 0.0961	
R indices (all data)	R1 = 0.0440, wR2 = 0.1005	
Extinction coefficient	0.0023(6)	
Largest diff. peak and hole	0.241 and -0.173 e.Å ⁻³	

Table 5. Crystal data and structure refinement for raj14a (4d).

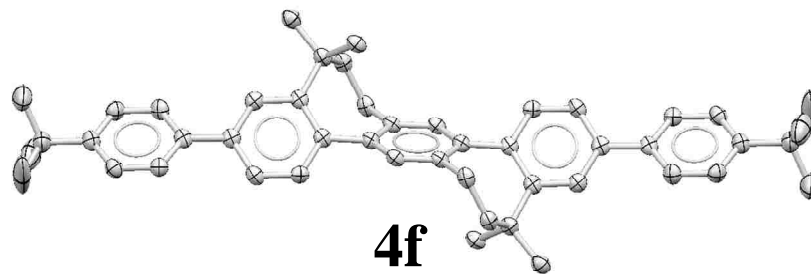
Identification code	raj14a	
Empirical formula	C ₃₀ H ₃₄ O ₂	
Formula weight	426.57	
Temperature	100(2) K	
Wavelength	1.54178 Å	
Crystal system	Monoclinic	
Space group	P 21/c	
Unit cell dimensions	a = 14.0575(3) Å	α = 90°.
	b = 10.3006(2) Å	β = 99.5330(10)°.
	c = 8.0732(2) Å	γ = 90°.
Volume	1152.86(4) Å ³	
Z	2	
Density (calculated)	1.229 Mg/m ³	
Absorption coefficient	0.577 mm ⁻¹	
F(000)	460	
Crystal size	0.32 x 0.26 x 0.15 mm ³	
Theta range for data collection	3.19 to 67.69°.	
Index ranges	-16 ≤ h ≤ 16, 0 ≤ k ≤ 12, 0 ≤ l ≤ 9	
Reflections collected	9572	
Independent reflections	2055 [R(int) = 0.0162]	
Completeness to theta = 67.69°	98.4 %	
Absorption correction	Semi-empirical from equivalents	
Max. and min. transmission	0.9184 and 0.8368	
Refinement method	Full-matrix least-squares on F ²	
Data / restraints / parameters	2055 / 0 / 149	
Goodness-of-fit on F ²	1.002	
Final R indices [I > 2σ(I)]	R1 = 0.0358, wR2 = 0.0921	
R indices (all data)	R1 = 0.0368, wR2 = 0.0928	
Extinction coefficient	0.0030(6)	
Largest diff. peak and hole	0.223 and -0.175 e.Å ⁻³	

Table 6. Crystal data and structure refinement for raj13p (5d).

Identification code	raj13p	
Empirical formula	C ₃₀ H ₃₄ O _{2.96}	
Formula weight	441.86	
Temperature	100(2) K	
Wavelength	1.54178 Å	
Crystal system	Trigonal	
Space group	R -3	
Unit cell dimensions	a = 21.0561(3) Å	α = 90°.
	b = 21.0561(3) Å	β = 90°.
	c = 14.3941(2) Å	γ = 120°.
Volume	5526.76(14) Å ³	
Z	9	
Density (calculated)	1.195 Mg/m ³	
Absorption coefficient	0.589 mm ⁻¹	
F(000)	2139	
Crystal size	0.26 x 0.24 x 0.12 mm ³	
Theta range for data collection	4.20 to 67.72°.	
Index ranges	-25 ≤ h ≤ 12, 0 ≤ k ≤ 25, 0 ≤ l ≤ 17	
Reflections collected	15234	
Independent reflections	2211 [R(int) = 0.0150]	
Completeness to theta = 67.72°	99.1 %	
Absorption correction	Semi-empirical from equivalents	
Max. and min. transmission	0.9327 and 0.8619	
Refinement method	Full-matrix least-squares on F ²	
Data / restraints / parameters	2211 / 0 / 159	
Goodness-of-fit on F ²	1.030	
Final R indices [I > 2σ(I)]	R1 = 0.0433, wR2 = 0.1127	
R indices (all data)	R1 = 0.0450, wR2 = 0.1139	
Extinction coefficient	0.00008(2)	
Largest diff. peak and hole	0.552 and -0.185 e.Å ⁻³	

Table 7. Crystal data and structure refinement for raj13u (4e).

Identification code	raj13u	
Empirical formula	C ₃₂ H ₃₈ O ₄	
Formula weight	486.62	
Temperature	100(2) K	
Wavelength	1.54178 Å	
Crystal system	Monoclinic	
Space group	P 21/n	
Unit cell dimensions	a = 9.6612(4) Å	α = 90°.
	b = 6.9042(3) Å	β = 94.574(3)°.
	c = 19.3657(9) Å	γ = 90°.
Volume	1287.63(10) Å ³	
Z	2	
Density (calculated)	1.255 Mg/m ³	
Absorption coefficient	0.640 mm ⁻¹	
F(000)	524	
Crystal size	0.22 x 0.16 x 0.10 mm ³	
Theta range for data collection	4.58 to 67.64°.	
Index ranges	-11 ≤ h ≤ 11, 0 ≤ k ≤ 8, 0 ≤ l ≤ 22	
Reflections collected	10386	
Independent reflections	2282 [R(int) = 0.0435]	
Completeness to theta = 67.64°	98.0 %	
Absorption correction	Semi-empirical from equivalents	
Max. and min. transmission	0.9388 and 0.8721	
Refinement method	Full-matrix least-squares on F ²	
Data / restraints / parameters	2282 / 0 / 167	
Goodness-of-fit on F ²	1.033	
Final R indices [I > 2σ(I)]	R1 = 0.0442, wR2 = 0.1215	
R indices (all data)	R1 = 0.0480, wR2 = 0.1253	
Largest diff. peak and hole	0.282 and -0.206 e.Å ⁻³	

Table 8. Crystal data and structure refinement for raj14t (**4f**).

Identification code	raj14t	
Empirical formula	C ₄₈ H ₅₄	
Formula weight	630.91	
Temperature	100(2) K	
Wavelength	1.54178 Å	
Crystal system	Monoclinic	
Space group	P 21/c	
Unit cell dimensions	a = 21.8162(14) Å	α = 90°.
	b = 9.4664(6) Å	β = 90.648(4)°.
	c = 8.9027(6) Å	γ = 90°.
Volume	1838.5(2) Å ³	
Z	2	
Density (calculated)	1.140 Mg/m ³	
Absorption coefficient	0.473 mm ⁻¹	
F(000)	684	
Crystal size	0.23 x 0.21 x 0.04 mm ³	
Theta range for data collection	4.05 to 66.99°.	
Index ranges	-24 ≤ h ≤ 24, 0 ≤ k ≤ 11, 0 ≤ l ≤ 10	
Reflections collected	14075	
Independent reflections	3161 [R(int) = 0.0488]	
Completeness to theta = 66.99°	96.3 %	
Absorption correction	Semi-empirical from equivalents	
Max. and min. transmission	0.9813 and 0.8989	
Refinement method	Full-matrix least-squares on F ²	
Data / restraints / parameters	3161 / 0 / 223	
Goodness-of-fit on F ²	1.005	
Final R indices [I > 2σ(I)]	R1 = 0.0690, wR2 = 0.1722	
R indices (all data)	R1 = 0.0996, wR2 = 0.1935	
Extinction coefficient	0.0010(3)	
Largest diff. peak and hole	0.555 and -0.278 e.Å ⁻³	

Table 9. Crystal data and structure refinement for raj13z (4g).

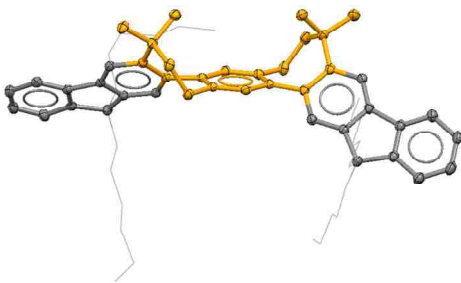
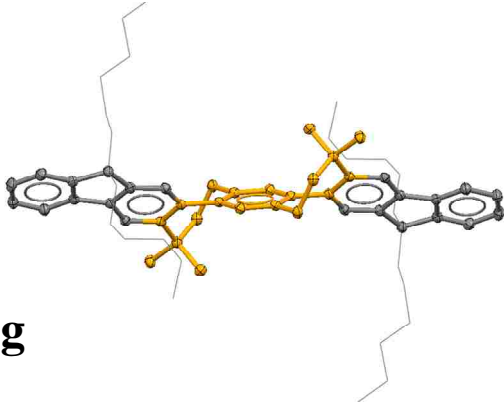
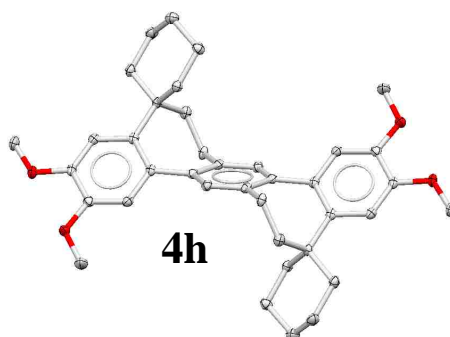
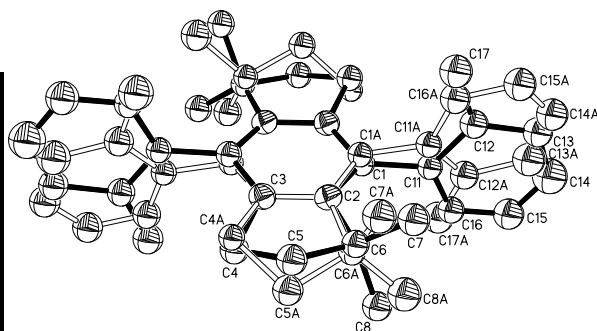
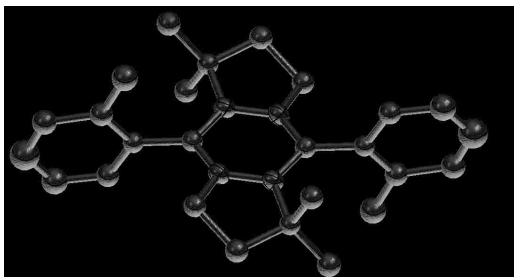
		
		4g
Identification code	raj13z	
Empirical formula	C ₆₆ H ₈₆	
Formula weight	879.35	
Temperature	100(2) K	
Wavelength	1.54178 Å	
Crystal system	Monoclinic	
Space group	P 2 ₁ /n	
Unit cell dimensions	a = 11.9837(2) Å	α = 90°.
	b = 36.2583(5) Å	β = 95.0130(10)°.
	c = 18.6597(3) Å	γ = 90°.
Volume	8076.8(2) Å ³	
Z	6	
Density (calculated)	1.085 Mg/m ³	
Absorption coefficient	0.445 mm ⁻¹	
F(000)	2892	
Crystal size	0.32 x 0.27 x 0.25 mm ³	
Theta range for data collection	2.44 to 68.05°.	
Index ranges	-14 ≤ h ≤ 14, 0 ≤ k ≤ 43, 0 ≤ l ≤ 22	
Reflections collected	67930	
Independent reflections	14519 [R(int) = 0.0187]	
Completeness to theta = 68.05°	98.4 %	
Absorption correction	Semi-empirical from equivalents	
Max. and min. transmission	0.8969 and 0.8707	
Refinement method	Full-matrix least-squares on F ²	
Data / restraints / parameters	14519 / 0 / 904	
Goodness-of-fit on F ²	1.013	
Final R indices [I > 2σ(I)]	R1 = 0.0421, wR2 = 0.1054	
R indices (all data)	R1 = 0.0465, wR2 = 0.1089	
Largest diff. peak and hole	0.298 and -0.276 e.Å ⁻³	

Table 10. Crystal data and structure refinement for raj14q (4h).

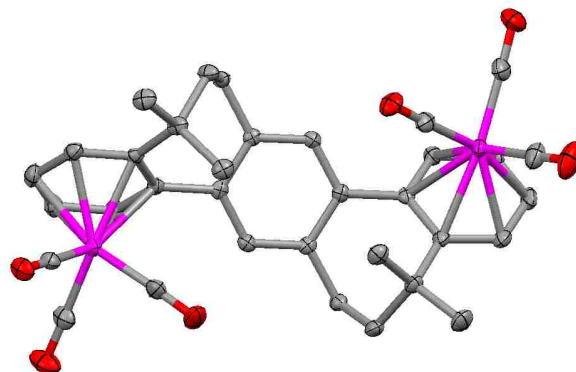
Identification code	raj14q	
Empirical formula	C ₄₀ H ₅₀ Cl ₄ O ₄	
Formula weight	736.60	
Temperature	100(2) K	
Wavelength	1.54178 Å	
Crystal system	Monoclinic	
Space group	P 21/c	
Unit cell dimensions	a = 12.5705(2) Å	α = 90°.
	b = 9.62430(10) Å	β = 106.3470(10)°.
	c = 15.9960(2) Å	γ = 90°.
Volume	1857.00(4) Å ³	
Z	2	
Density (calculated)	1.317 Mg/m ³	
Absorption coefficient	3.210 mm ⁻¹	
F(000)	780	
Crystal size	0.16 x 0.12 x 0.10 mm ³	
Theta range for data collection	3.66 to 68.05°.	
Index ranges	-15 ≤ h ≤ 14, 0 ≤ k ≤ 11, 0 ≤ l ≤ 19	
Reflections collected	15545	
Independent reflections	3314 [R(int) = 0.0193]	
Completeness to theta = 68.05°	98.0 %	
Absorption correction	Semi-empirical from equivalents	
Max. and min. transmission	0.7396 and 0.6277	
Refinement method	Full-matrix least-squares on F ²	
Data / restraints / parameters	3314 / 0 / 220	
Goodness-of-fit on F ²	1.015	
Final R indices [I > 2σ(I)]	R1 = 0.0304, wR2 = 0.0815	
R indices (all data)	R1 = 0.0312, wR2 = 0.0821	
Extinction coefficient	0.00094(16)	
Largest diff. peak and hole	0.299 and -0.198 e.Å ⁻³	

Table 11. Crystal data and structure refinement for 5i (raj16e).



Identification code	raj16e	
Empirical formula	C ₃₀ H ₃₄	
Formula weight	394.57	
Temperature	100(2) K	
Wavelength	1.54178 Å	
Crystal system	Monoclinic	
Space group	P 2 ₁ /n	
Unit cell dimensions	a = 10.2322(5) Å	α = 90°.
	b = 9.3059(4) Å	β = 102.173(2)°.
	c = 12.0581(5) Å	γ = 90°.
Volume	1122.35(9) Å ³	
Z	2	
Density (calculated)	1.168 Mg/m ³	
Absorption coefficient	0.485 mm ⁻¹	
F(000)	428	
Crystal size	0.20 x 0.18 x 0.15 mm ³	
Theta range for data collection	5.16 to 67.75°.	
Index ranges	-12 ≤ h ≤ 11, 0 ≤ k ≤ 11, 0 ≤ l ≤ 14	
Reflections collected	9193	
Independent reflections	1992 [R(int) = 0.0186]	
Completeness to theta = 67.75°	98.5 %	
Absorption correction	Semi-empirical from equivalents	
Max. and min. transmission	0.9309 and 0.9093	
Refinement method	Full-matrix least-squares on F ²	
Data / restraints / parameters	1992 / 35 / 128	
Goodness-of-fit on F ²	1.012	
Final R indices [I > 2σ(I)]	R1 = 0.0886, wR2 = 0.1966	
R indices (all data)	R1 = 0.0910, wR2 = 0.1981	
Extinction coefficient	0.0042(9)	
Largest diff. peak and hole	0.515 and -0.303 e.Å ⁻³	

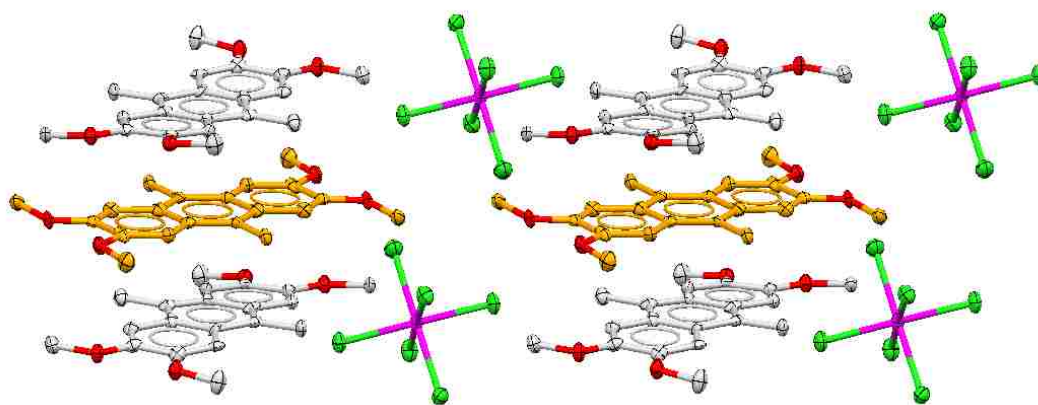
Table 12. Crystal data and structure refinement for raj16ia (bis-chromiumtricarboxyl complex of 4a).



Identification code	raj16ia	
Empirical formula	C ₃₄ H ₃₀ Cr ₂ O ₆	
Formula weight	638.58	
Temperature	100(2) K	
Wavelength	1.54178 Å	
Crystal system	Monoclinic	
Space group	P 21/c	
Unit cell dimensions	a = 6.9910(2) Å	α = 90°.
	b = 18.8426(6) Å	β = 92.012(2)°.
	c = 21.7466(7) Å	γ = 90°.
Volume	2862.88(15) Å ³	
Z	4	
Density (calculated)	1.482 Mg/m ³	
Absorption coefficient	6.637 mm ⁻¹	
F(000)	1320	
Crystal size	0.52 x 0.32 x 0.09 mm ³	
Theta range for data collection	3.10 to 67.79°.	
Index ranges	-8 ≤ h ≤ 8, 0 ≤ k ≤ 22, 0 ≤ l ≤ 25	
Reflections collected	23525	
Independent reflections	4980 [R(int) = 0.0243]	
Completeness to theta = 67.79°	98.8 %	
Absorption correction	Numerical	
Max. and min. transmission	0.5928 and 0.1289	
Refinement method	Full-matrix least-squares on F ²	
Data / restraints / parameters	4980 / 0 / 423	
Goodness-of-fit on F ²	1.022	
Final R indices [I > 2σ(I)]	R1 = 0.0360, wR2 = 0.0959	
R indices (all data)	R1 = 0.0395, wR2 = 0.0987	
Largest diff. peak and hole	0.392 and -0.445 e.Å ⁻³	

CHAPTER 2

Isolation and X-ray Structural Characterization of a Dicationic Homotrimer of 2,3,6,7-Tetramethoxy-9,10-Dimethylantracene Cation Radical



Abstract: Electrochemical oxidation of 2,3,6,7-tetramethoxy-9,10-dimethylantracene (**1**) showed that it undergoes a highly reversible electrochemical oxidation ($E_{\text{ox}} = 0.81$ V vs. SCE) and forms a modestly stable cation-radical salt in solution. X-ray crystallography established that $\mathbf{1}^{+\bullet} \text{SbCl}_6^-$ crystallizes as a (centrosymmetric) dicationic homotrimer via a close cofacial association of a pair of cationic and one neutral molecule of **1** with an interplanar separation of ~ 3.2 Å. The structure of the dicationic homotrimer was also reproduced by DFT calculations. Furthermore, the structure of a dicationic spiro adduct, formed by a slow decomposition of a solution of $\mathbf{1}^{+\bullet} \text{SbCl}_6^-$, was also established by X-ray crystallography.

2.1 INTRODUCTION

The stable organic cation radicals are not only critical reaction intermediates when (poly)aromatic electron donors are exposed to various oxidants or subjected to different electrochemical, photoinduced, and radiolytic (activation) methodologies,²¹⁻²³ they also pertain directly to the contemporary interest in organic materials science for molecular devices such as electrical and photoconductors, ferromagnets, sensors, optical and electrochemical switches, etc.²⁴⁻²⁹

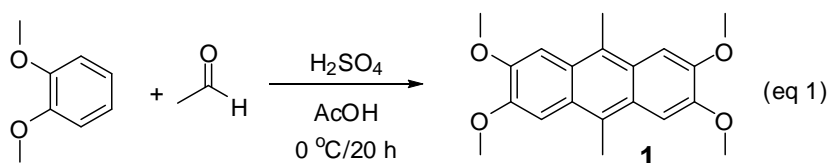
Our continued interest in the design and synthesis of various (poly)aromatic hydrocarbons (such as substituted benzenes, naphthalenes, anthracenes, pyrenes, poly-*p*-phenylenes, hexa-*peri*-hexabenzocoronenes, etc.),^{20,30} which form stable cation radicals (or hole carriers) prompted us to examine the possibility of isolation and X-ray crystallographic characterization of the cation radical of 2,3,6,7-tetramethoxy-9,10-dimethylanthracene (**1**),³¹ whose derivatives have been extensively explored for various modern materials³²⁻³³ owing to the potential applications in the emerging areas of molecular electronics and nanotechnology.³⁴⁻³⁵

Herein, we now report that anthracene **1** can be quantitatively oxidized to its cation radical using either a stable aromatic oxidant³⁶ or inorganic oxidant such as NO^+ SbCl_6^- .³⁷ The cation radical of **1** was found to be stable at low-temperatures and allows the isolation of single crystals of a unique dicationic homotrimer, formally represented as a sandwich of a neutral molecule of **1** between the two cationic molecules of $\mathbf{1}^{+\bullet}$, as established by X-ray crystallography and corroborated by DFT calculations. Moreover, it is shown that the cation radical of anthracene **1** undergoes a slow multi-step

transformation to a novel dicationic spiro product ($\mathbf{5}^{2+}$), at room temperature, whose structure was also determined by X-ray crystallography. The details of these preliminary findings are discussed herein.

2.2 RESULTS and DISCUSSION

The tetramethoxy-9,10-dimethylantracene (**1**) was readily obtained by a simple condensation of 1,2-dimethoxybenzene with acetaldehyde in a mixture of sulfuric acid and acetic acid at 0 °C, i.e. eq 1.³¹



The structure of anthracene **1** was established by $^1\text{H}/^{13}\text{C}$ NMR spectroscopy and was further confirmed by X-ray crystallography (see Figure 5). In the crystals, the molecules of anthracene **1** occupy a crystallographic inversion center and have an ideal planar geometry. Moreover, the molecules of **1** form layers along the crystallographic ‘ab’ plane, and within these layers, neighboring parallel anthracene moieties are separated at van-der-Waals distances of ~ 3.4 Å. Based on the observation of the limited π,π -overlap of the molecules of **1** in the layers, it is suggested that the crystal packing is largely dominated by C-H... π contacts (see Figure 5).

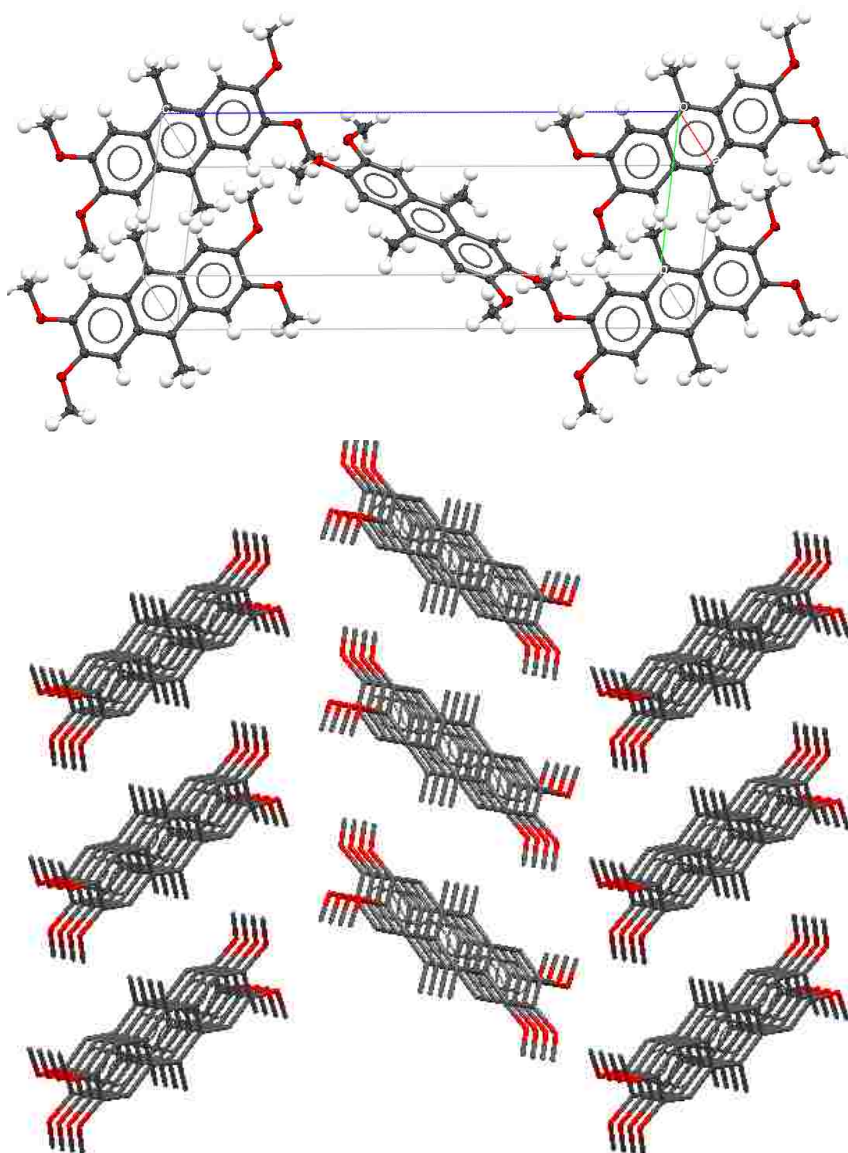


Figure 5. The unit cell of anthracene **1** showing the limited π , π -overlap between the molecules of **1** (top) and its extended packing arrangement in the crystals (bottom) largely dominated by C-H... π contacts.

The electron donor strength and the initial indication of the cation radical stability of **1** were evaluated by electrochemical oxidation at a platinum electrode as a 1×10^{-3} M solution in dichloromethane containing 0.1 M *n*-Bu₄NPF₆ as the supporting electrolyte. The cyclic voltammograms of **1** (Figure 6) consistently met the reversibility criteria at various scan rates of 50-600 mV/s, as they all showed cathodic/anodic peak current ratios

of $i_a/i_c = 1.0$ (theoretical) as well as the differences between anodic and cathodic peak potentials of $E_{pa}-E_{pc} = 70$ mV at 22 °C. The reversible oxidation potential of **1** ($E_{ox} = 0.81$ V vs. SCE) was calibrated with added ferrocene ($E_{ox} = 0.45$ V vs. SCE as an internal standard. It is also noted that under similar conditions as above, the parent 9,10-dimethylantracene undergoes an electrochemical oxidation at $E_{ox} = 1.16$ V vs. SCE owing to the absence of 4 electron donating methoxy groups.

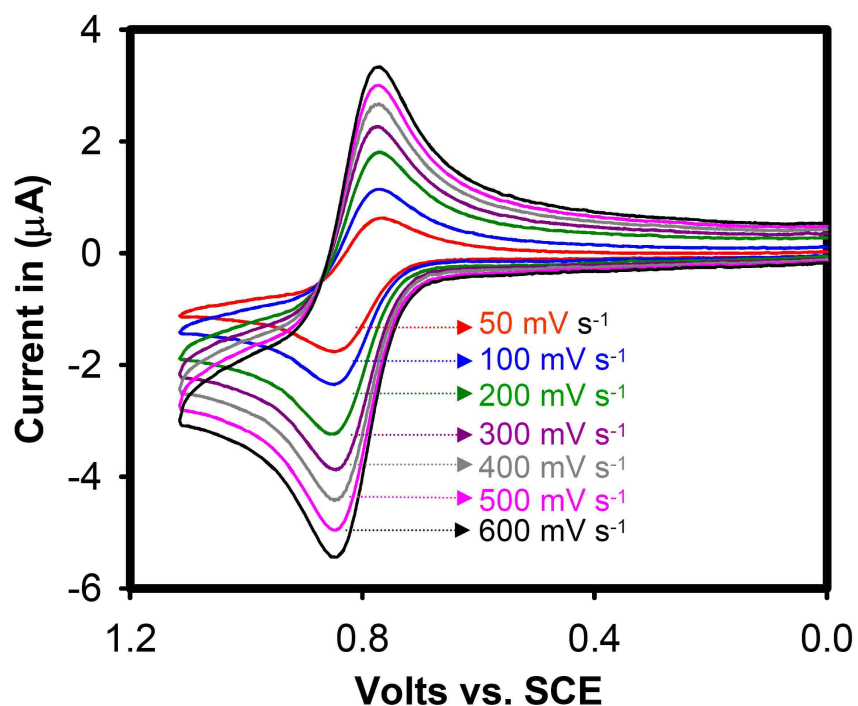
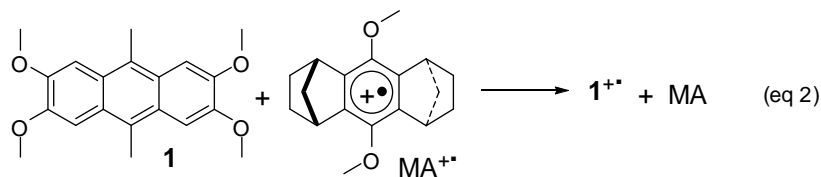


Figure 6. Cyclic voltammograms of 1×10^{-3} M **1** in CH_2Cl_2 containing 0.1 M tetra-*n*-butylammonium hexafluorophosphate [$(n\text{-Bu})_4\text{NPF}_6$] at 22 °C at scan rates between 50 and 600 mV s^{-1} .

The electrochemical reversibility and relatively low oxidation potential of **1**, prompted us to generate its cation radical by electrochemical oxidation using a stable aromatic cation radical ($\text{MA}^{+\bullet} \text{SbCl}_6^-$; $E_{\text{red}} = 1.11$ V vs. SCE) as a one-electron oxidant.³⁶

Thus Figure 7 shows the spectral changes attendant upon an incremental addition of sub-stoichiometric amounts of **1** to a 3.4×10^{-5} M $\text{MA}^{+\bullet}$ [$\lambda_{\text{max}} (\log \epsilon) = 518 \text{ nm} (3.86)$] in dichloromethane at 22 °C. It is noted that the formation of green-colored $\mathbf{1}^{+\bullet}$ (i.e. increase in the absorbance at 700 nm) and concomitant disappearance of $\text{MA}^{+\bullet}$ (i.e. decrease in the absorbance at 518 nm) was complete after the addition of 1 equiv. of **1**; and the resulting highly structured absorption spectrum of $\mathbf{1}^{+\bullet}$ [$\lambda_{\text{max}} = 277, 387, 409 (\log \epsilon = 4.61), 497, 473, 627, \text{ and } 706 \text{ nm}$] remained unchanged upon further addition of neutral **1** (i.e. eq 2). Furthermore, the presence of (multiple) well-defined isosbestic points (i.e. $\lambda = 294, 334, 503, \text{ and } 508 \text{ nm}$) in Figure 7 attest to an uncluttered character of electron transfer from **1** to $\text{MA}^{+\bullet}$ (i.e. eq 2).



It is also noted that the $\mathbf{1}^{+\bullet}$ did not show either the self aggregation (i.e. pimer formation) or the formation of dimer cation radical [i.e. $\mathbf{1} + \mathbf{1} \leftrightarrow (\mathbf{1})_2^{+\bullet}$] in the presence of excess neutral **1** in dichloromethane solutions, as judged by the singular absence of any new absorption band in the near infrared region. The dichloromethane solution of the cation radical of anthracene **1** showed modest stability at ambient temperatures but was stable for several days at -10 °C, as discerned by the periodic monitoring of the solutions of $\mathbf{1}^{+\bullet}$ by UV-vis spectroscopy.

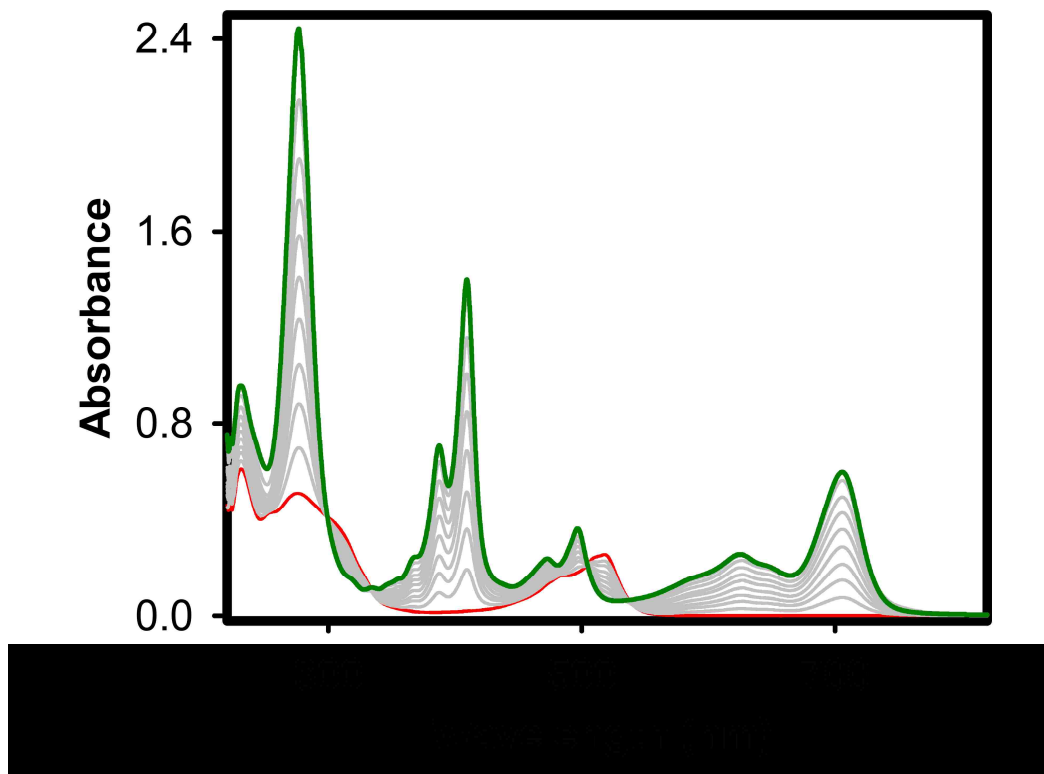
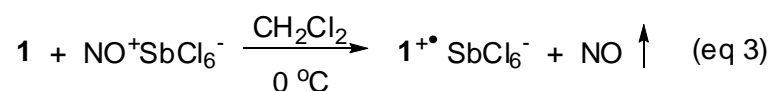


Figure 7. Spectral changes observed upon the reduction of 3.4×10^{-5} M $\text{MA}^{\bullet+}$ (red line) by addition of sub-stoichiometric increments of 1.0×10^{-3} M anthracene **1** to its radical cation (gray lines) in anhydrous dichloromethane at 22 °C. The final plot (green line) of $\mathbf{1}^{\bullet+}$ obtained after the addition of one equivalent of **1** which remained unchanged upon further addition of neutral **1**.

In order to isolate crystalline salts of $\mathbf{1}^{\bullet+}$, a solution of sufficient amounts of $\mathbf{1}^{\bullet+}$ was prepared by chemical oxidation using nitrosonium hexachloroantimonate³⁷ as a 1- e^- oxidant according to the stoichiometry in eq 3.



Thus, a solution of **1** in anhydrous dichloromethane was added to crystalline $\text{NO}^+ \text{SbCl}_6^-$ under an argon atmosphere at ~ 0 °C. The gaseous nitric oxide produced was entrained by bubbling argon through the solution to yield a dark green solution, which upon

spectrophotometric analysis indicated the formation of $\mathbf{1}^{+\bullet}$ SbCl_6^- (see Figure 7). Repeated attempts to isolate single crystals of $\mathbf{1}^{+\bullet}$ SbCl_6^- by a slow diffusion of toluene or hexane into the solution of $\mathbf{1}^{+\bullet}$ in dichloromethane, during a period of 4 days at $-10\text{ }^\circ\text{C}$, did not result in suitable single crystals. However, a solution of a 1:1 mixture of neutral $\mathbf{1}$ and $\mathbf{1}^{+\bullet}$ SbCl_6^- in dichloromethane afforded dark-colored crystals, suitable for X-ray crystallographic studies, by a slow diffusion of hexanes at $-10\text{ }^\circ\text{C}$.

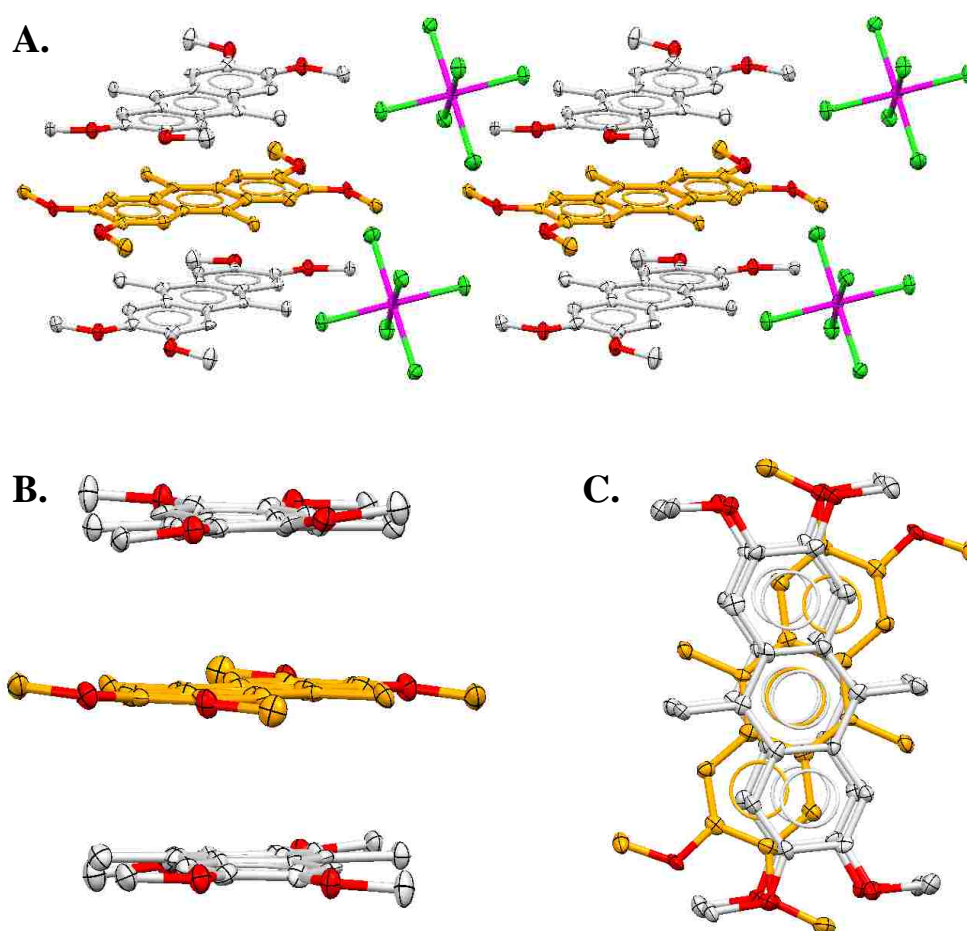


Figure 8. Crystal structure of the tetramethoxydimethylantracene cation radical with the packing diagram (A) showing that it crystallizes as a centrosymmetric homotrimer (B and C) with a pair of cationic charges [$(\mathbf{1})_3^{2+\bullet} (\text{SbCl}_6^-)_2$]. The thermal ellipsoids are shown in 50% probability and the hydrogens and solvent molecules (CH_2Cl_2) are omitted for the sake of clarity.

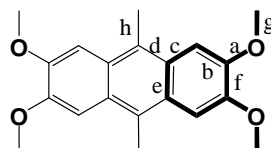
The crystal structure of 2,3,6,7-tetramethoxy-9,10-dimethylantracene (**1**) cation radical revealed that it forms isolated (centrosymmetric) dicationic homotrimers resulting from a close cofacial association of a pair of cationic $\mathbf{1}^{+\bullet}$ SbCl_6^- and one neutral molecule of **1** (see Figure 8) with an interplanar distance of ~ 3.2 Å, which is considerably shorter than the van-der-Waal's contact. Within a homotrimer, the central anthracene ring is found to be completely planar whereas the two outer anthracene molecules are bent inward by ~ 7 deg. (see Figure 8). Unfortunately, the limited precision of the structure of the dicationic homotrimer (i.e. esd = 1 pm) did not allow an accurate estimation of the distribution of the cationic charges onto the three anthracene molecules. However, a pair of counter anions (SbCl_6^-) associated with each homotrimer are located in closer proximity to the outer anthracene molecules than to the central anthracene molecules (see Figure 8A), and thus suggest that the charge distribution may not be similar amongst the three anthracene moieties in the dicationic homotrimer. Calculation of the molecular structure of the dicationic (triplet) homotrimer using DFT calculations at the B3LYP/6-31G* level reproduced a similar arrangement of the three anthracene molecules. Furthermore, an examination of the bond length changes in various anthracene molecules (see Figure 9 and Table 13A-C) showed that the cationic charge was largely ($\sim 70\%$) localized onto the outer (bent) anthracene molecules whereas the central (planar) anthracene molecule contained only a partial cation charge ($\sim 30\%$).³⁸⁻³⁹

From the calculated bond length data in Tables 13A-13C, it is apparent that the central molecule of **1** undergoes much less shortening/lengthening of various bonds as compared to the top and bottom (BENT) molecules of **1** in the centrosymmetric dicationic (triplet) homotrimer obtained by DFT calculations.



Figure 9. Three different vies of the calculated molecular structure of the dicationic (triplet) homotrimer obtained by DFT calculations at the B3LYP/6-31G* level (Spartan '08). The calculated structure reproduces the structure obtained by X-ray crystallography (see Figure8).

Table 13A. Theoretical bond lengths of the neutral and cation radical of **1** presented in picometers (pm) by DFT calculations at the B3LYP/6-31G* level (Spartan '08).



B3LYP/6-31G*			
Bond ¹	1	1 ^{••}	Δ (1 ^{••} -1)
a	136.1	133.8	-2.3
b	137.0	138.7	+1.7
c	143.5	142.0	-1.5
d	141.2	142.6	+1.4
e	144.3	143.7	-0.6
f	143.9	143.2	-0.7
g	141.7	143.0	+1.3
h	151.7	150.8	-0.9

¹Average of equivalent bonds

Table 13B. Bond lengths (in picometers) of the top and bottom (BENT) molecules of **1** in the centrosymmetric dicationic (triplet) homotrimer obtained by DFT calculations at the B3LYP/6-31G* level (Spartan '08). Bond lengths of neutral **1** were taken from Table 13A.

B3LYP/6-31G*		
<u>Bond</u> ¹	$1_{T/B}^{+}$	$\Delta (1_{T/B}^{+}-1)$
a	134.4	-1.7
b	138.5	+1.5
c	142.1	-1.4
d	142.4	+1.2
e	143.8	-0.5
f	143.2	-0.7
g	143.4	+1.7
h	150.7	-0.7
σ	--	--

¹Average of equivalent bonds

Table 13C. Bond lengths (in picometers) of the central (PLANAR) molecule of **1** in the centrosymmetric dicationic (triplet) homotrimer obtained by DFT calculations at the B3LYP/6-31G* level (Spartan '08). Bond lengths of neutral **1** were taken from Table 13A.

B3LYP/6-31G*		
<u>Bond</u> ¹	1_C^{+}	$\Delta (1_C^{+}-1)$
a	135.4	-0.7
b	137.5	+0.5
c	143.2	-0.3
d	141.6	+0.4
e	144.2	-0.1
f	143.9	0.0
g	142.8	+1.1
h	151.1	-0.6
σ	--	--

¹Average of equivalent bonds

The instability of 1^{+}SbCl_6^{-} at ambient temperatures was further probed by allowing its dichloromethane solution to stand for a period of 1-2 days at 22 °C. After which time, the solution deposited shiny dark-colored needles which were analyzed by X-ray crystallography as follows.

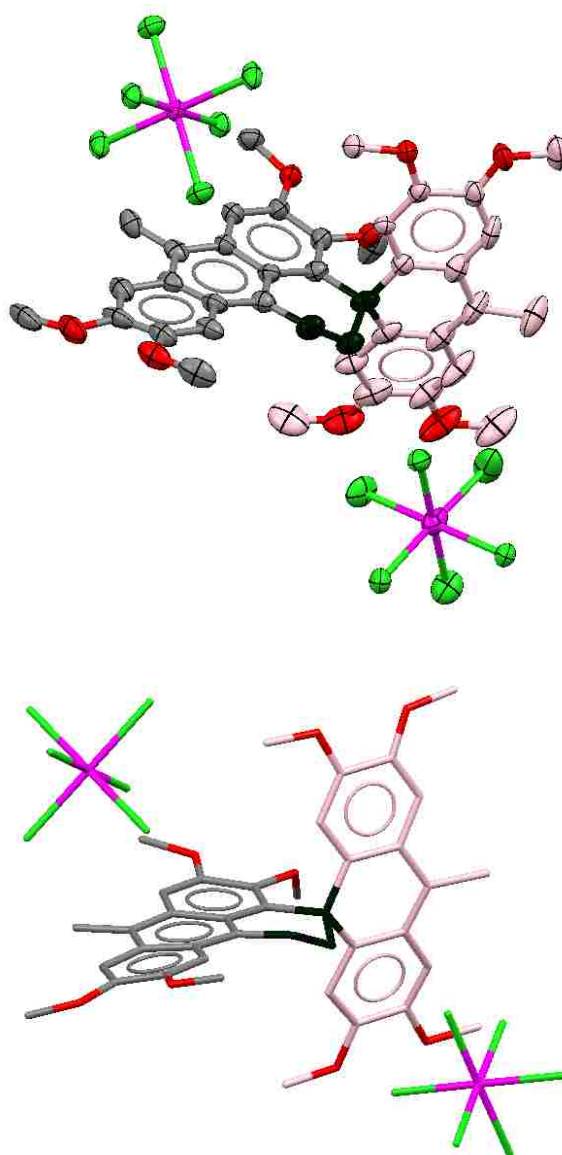
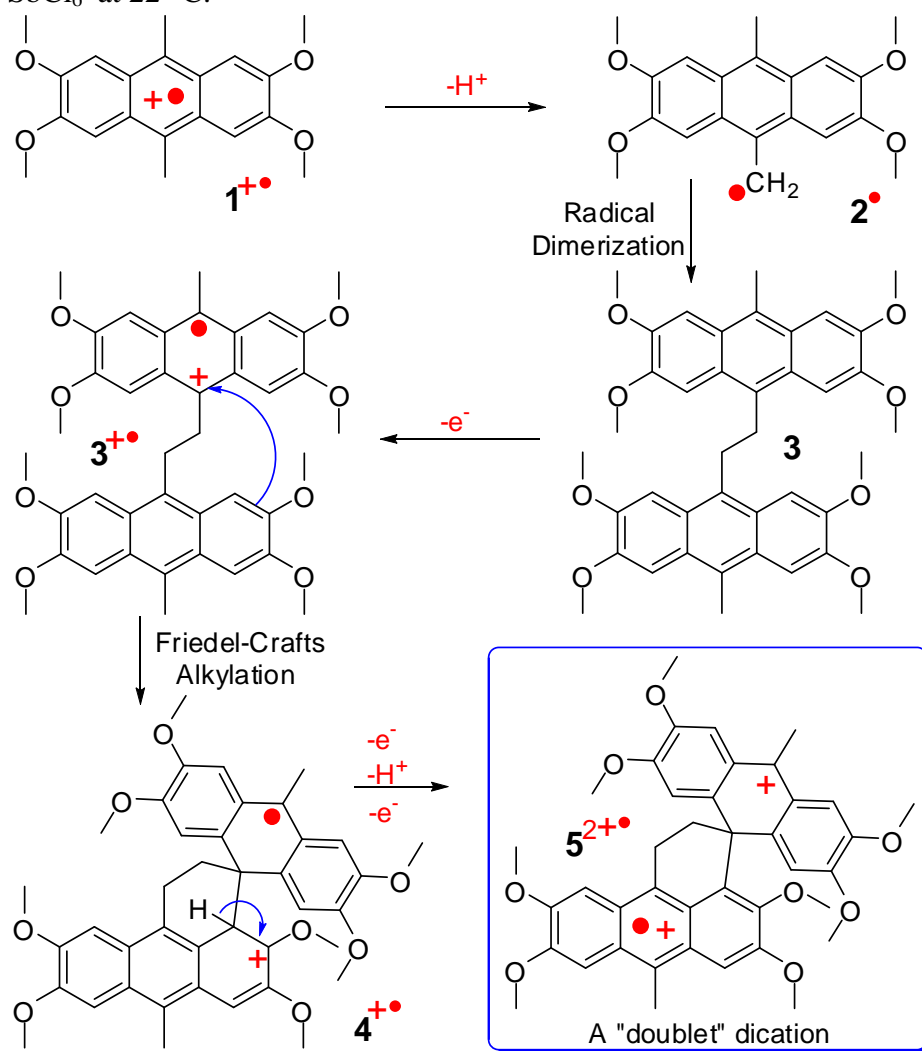


Figure 10. ORTEP (top) and stick (bottom) diagrams of a (doublet) dicationic spiro adduct $[5^{2+} (\text{SbCl}_6^{-})_2]$ formed via the decomposition of a CH_2Cl_2 solution of 1^{+}SbCl_6^{-} at 22 °C. The thermal ellipsoids are shown in 30% probability and the hydrogens and solvent molecules (CH_2Cl_2) are omitted for the sake of clarity.

The X-ray structure in Figure 10 showed that the decomposition of a dichloromethane solution of $1^{+\bullet}$ SbCl_6^- at 22 °C produces a (doublet) dicationic spiro adduct $[5^{2+\bullet} (\text{SbCl}_6^-)_2]$ via a multi-step transformation. The decomposition of $1^{+\bullet}$ SbCl_6^- to the dicationic spiro adduct in Figure 10 can be reconciled by a sequence of transformations as elucidated in Scheme 7.

Scheme 7. Proposed mechanism for the formation of dicationic spiro adduct $[5^{2+\bullet} (\text{SbCl}_6^-)_2]$ by a decomposition of a CH_2Cl_2 solution of $1^{+\bullet}$ SbCl_6^- at 22 °C.



The 1-e⁻ oxidation of a methylbenzene to its cation radical is known to enhance the acidity of methyl protons by several orders of magnitude.⁴⁰ Thus, a loss of H⁺ from **1**^{•+} SbCl₆⁻ generates a benzyl-type radical **2**[•] which undergoes self dimerization to produce an electron-rich dianthrylethane **3**.⁴¹⁻⁴² The 1-e⁻ oxidation of **3** with **1**^{•+} SbCl₆⁻ affords **3**^{•+} which undergoes an efficient intramolecular Friedel-Crafts-type alkylation to form a distonic cation radical⁴³ **4**^{•+}. A facile loss of a proton and a pair of electrons then furnishes the dicationic spiro adduct [**5**²⁺ (SbCl₆⁻)₂] shown in Figure 10.⁴⁴

2.3 SUMMARY and CONCLUSIONS

In summary, we have demonstrated that the readily-available 2,3,6,7-tetramethoxy-9,10-dimethylantracene (**1**) cation radically crystallizes as a unique dicationic homotrimer with the stoichiometry [(**1**)₃²⁺ (SbCl₆⁻)₂] as established by X-ray crystallography. The molecular structure of the dicationic homotrimer was reproduced by DFT calculations at the B3LYP/6-31G* level which provided evidence that the charge distribution is dissimilar amongst the three anthracene moieties and that central anthracene molecule bears only a partial charge in the dicationic homotrimer. It was also shown that prolonged storage of **1**^{•+} SbCl₆⁻ at 22 °C leads to its decomposition to a (double) dicationic spiro adduct [**5**²⁺ (SbCl₆⁻)₂] as established by X-ray crystal structure analysis. Studies will continue for a more comprehensive investigation of the structure modulation of the anthracene ring system for the preparation and study of a covalently-linked homotrimer and their homologues.

2.4 EXPERIMENTAL SECTION

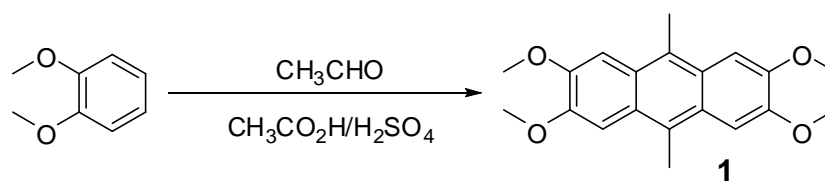
General Experimental Methods and Materials. All reactions were performed under an argon atmosphere unless otherwise noted. All commercial reagents were used without further purification unless otherwise noted. Dichloromethane (Aldrich) was repeatedly stirred with fresh aliquots of concentrated sulfuric acid (~10% by volume) until the acid layer remained colorless. After separation it was washed successively with water, aqueous sodium carbonate, water, and aqueous sodium chloride and dried over anhydrous calcium chloride. The dichloromethane was distilled twice from P₂O₅ under an argon atmosphere and stored in a Schlenk flask equipped with a Teflon valve fitted with Viton O-rings. The hexanes and toluene were distilled from P₂O₅ under an argon atmosphere and then refluxed over calcium hydride (~12 h). After distillation from CaH₂, the solvents were stored in Schlenk flasks under an argon atmosphere. NMR spectra were recorded on Varian 300 and 400 MHz NMR spectrometers.

Cyclic Voltammetry (CV). The CV cell was of an air-tight design with high vacuum Teflon valves and Viton O-ring seals to allow an inert atmosphere to be maintained without contamination by grease. The working electrode consisted of an adjustable platinum disk embedded in a glass seal to allow periodic polishing (with a fine emery cloth) without changing the surface area (~1 mm²) significantly. The reference SCE electrode (saturated calomel electrode) and its salt bridge were separated from the catholyte by a sintered glass frit. The counter electrode consisted of a platinum gauze that was separated from the working electrode by ~3 mm. The CV measurements were carried out in a solution of 0.1 M supporting electrolyte (tetra-*n*-butylammonium

hexafluorophosphate, TBAH) and 1.0×10^{-3} M substrate in dry dichloromethane under an argon atmosphere. All the cyclic voltammograms were recorded at a sweep rate of 200 mV sec^{-1} , unless otherwise specified and were IR compensated. The oxidation potentials ($E_{1/2}$) were referenced to SCE, which was calibrated with added (equimolar) ferrocene ($E_{1/2} = 0.45$ V vs. SCE) the $E_{1/2}$ values were calculated by taking the average of anodic and cathodic peak potentials in the reversible cyclic voltammograms.

Procedure for the Spectra Titration of $\text{MA}^{+\bullet} \text{SbCl}_6^-$ with 2,3,6,7-tetramethoxy-9,10-dimethylantracene. An orange-red solution of $\text{MA}^{+\bullet} \text{SbCl}_6^-$ in dichloromethane (3 mL, 3.4×10^{-5} M) was transferred under an argon atmosphere in a 1-cm quartz cuvette at room temperature. A dichloromethane solution (1×10^{-3} M of) **1** in 10 μL increments was added to this solution. The UV-vis spectra of the resulting solutions, after the addition of each increment, were recorded at 22 $^\circ\text{C}$.

Synthesis of 2,3,6,7-tetramethoxy-9,10-dimethylantracene (**1**).



To a cooled solution (~ 0 $^\circ\text{C}$) of veratrole (32 mL, 250 mmol) in acetic acid (125 mL) was slowly added an ice-cold solution of acetaldehyde (21 mL, 375 mmol) in methanol (20 mL). The resulting mixture was then stirred for 1 h and concentrated H_2SO_4 (95%, 125 mL) was added dropwise over 2 h. The reaction mixture was then stirred at 0 $^\circ\text{C}$ for 20 h and pured onto ice-water which precipitated the product out as a beige solid and collected by vacuum filtration. The product was further purified by recrystallization in chloroform to afford the final product as a yellow solid. Yield (8.4 g, 20%): mp: >350

°C; ^1H NMR (CDCl_3) δ : 2.95 (s, 6H), 4.08 (s, 12H), 7.40 (s, 4H); ^{13}C NMR (CDCl_3) δ : 15.00, 55.90, 102.80, 124.08, 125.99, 148.90. [Reference: Chung, Y.; Duerr, B. F.; McKelvey, T. A.; Nanjappan, P.; Czarnik, A. W. *J. Org. Chem.* **1989**, *54*, 1018-32.]

^1H NMR spectrum of 2,3,6,7-tetramethoxy-9,10-dimethylantracene (1)



^{13}C NMR spectrum of 2,3,6,7-tetramethoxy-9,10-dimethylantracene (1)

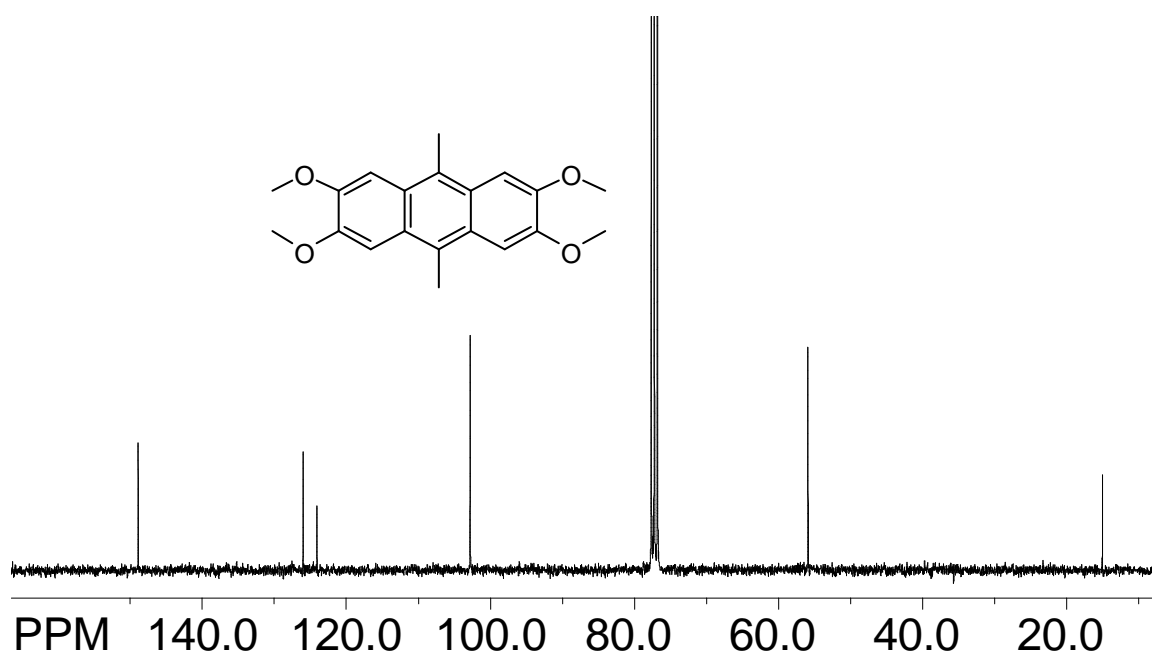
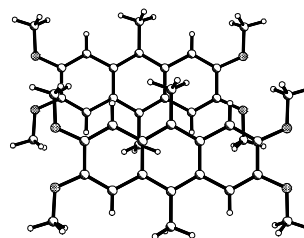
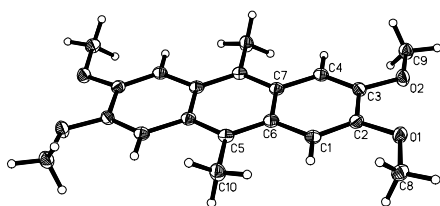
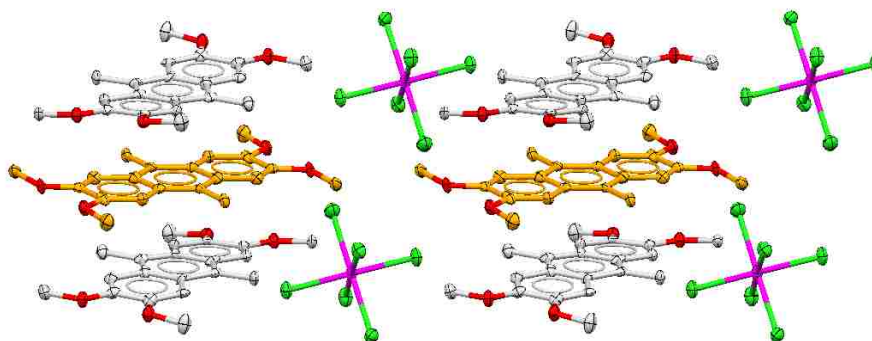
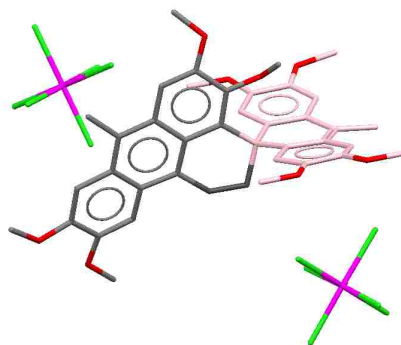


Table 14. Crystal data and structure refinement for neutral 1 (raj15c).

Identification code	raj15c	
Empirical formula	C ₂₀ H ₂₂ O ₄	
Formula weight	326.38	
Temperature	100(2) K	
Wavelength	1.54178 Å	
Crystal system	Monoclinic	
Space group	P 21/c	
Unit cell dimensions	a = 5.01890(10) Å	α = 90°.
	b = 7.3462(2) Å	β = 92.9410(10)°.
	c = 21.7143(4) Å	γ = 90°.
Volume	799.55(3) Å ³	
Z	2	
Density (calculated)	1.356 Mg/m ³	
Absorption coefficient	0.758 mm ⁻¹	
F(000)	348	
Crystal size	0.12 x 0.07 x 0.06 mm ³	
Theta range for data collection	4.08 to 67.56°.	
Index ranges	-6 ≤ h ≤ 6, 0 ≤ k ≤ 8, 0 ≤ l ≤ 26	
Reflections collected	6572	
Independent reflections	1422 [R(int) = 0.0200]	
Completeness to theta = 67.56°	99.0 %	
Absorption correction	Semi-empirical from equivalents	
Max. and min. transmission	0.9560 and 0.9146	
Refinement method	Full-matrix least-squares on F ²	
Data / restraints / parameters	1422 / 0 / 113	
Goodness-of-fit on F ²	1.002	
Final R indices [I > 2σ(I)]	R1 = 0.0381, wR2 = 0.1059	
R indices (all data)	R1 = 0.0419, wR2 = 0.1098	
Extinction coefficient	0.0021(6)	
Largest diff. peak and hole	0.376 and -0.292 e.Å ⁻³	

Table 15. Crystal data and structure refinement for $[(1)_3^{2+}(\text{SbCl}_6)_2]$ (raj14y).

Identification code	raj14y5	
Empirical formula	C ₆₃ H ₇₂ Cl ₁₈ O ₁₂ Sb ₂	
Formula weight	1902.81	
Temperature	100(2) K	
Wavelength	1.54178 Å	
Crystal system	Triclinic	
Space group	P -1	
Unit cell dimensions	a = 10.8352(16) Å	α = 65.447(6)°.
	b = 13.4975(19) Å	β = 76.831(7)°.
	c = 14.690(2) Å	γ = 73.988(7)°.
Volume	1862.5(5) Å ³	
Z	1	
Density (calculated)	1.696 Mg/m ³	
Absorption coefficient	12.171 mm ⁻¹	
F(000)	954	
Crystal size	0.11 x 0.04 x 0.02 mm ³	
Theta range for data collection	3.34 to 67.81°.	
Index ranges	-12 ≤ h ≤ 12, -14 ≤ k ≤ 15, 0 ≤ l ≤ 17	
Reflections collected	28451	
Independent reflections	6280 [R(int) = 0.1630]	
Completeness to theta = 67.81°	98.8 %	
Absorption correction	Semi-empirical from equivalents	
Max. and min. transmission	0.8385 and 0.3478	
Refinement method	Full-matrix least-squares on F ²	
Data / restraints / parameters	6280 / 3 / 448	
Goodness-of-fit on F ²	1.009	
Final R indices [I > 2σ(I)]	R1 = 0.0651, wR2 = 0.1398	
R indices (all data)	R1 = 0.1095, wR2 = 0.1595	
Extinction coefficient	0.00057(12)	
Largest diff. peak and hole	1.778 and -0.857 e.Å ⁻³	

Table 16. Crystal data and structure refinement for $[5^{2+}(\text{SbCl}_6)_2]$ (raj15ga).

Identification code	raj15ga	
Empirical formula	C ₄₄ H ₄₉ Cl _{17.5} O ₈ Sb ₂	
Formula weight	1569.70	
Temperature	100(2) K	
Wavelength	1.54178 Å	
Crystal system	Triclinic	
Space group	P -1	
Unit cell dimensions	a = 10.8843(9) Å	α = 108.194(3)°.
	b = 16.9006(14) Å	β = 104.146(3)°.
	c = 19.2674(16) Å	γ = 96.119(3)°.
Volume	3200.0(5) Å ³	
Z	2	
Density (calculated)	1.629 Mg/m ³	
Absorption coefficient	13.789 mm ⁻¹	
F(000)	1553	
Crystal size	0.62 x 0.09 x 0.03 mm ³	
Theta range for data collection	4.27 to 67.86°.	
Index ranges	-12 ≤ h ≤ 12, -19 ≤ k ≤ 19, 0 ≤ l ≤ 23	
Reflections collected	25909	
Independent reflections	10858 [R(int) = 0.0804]	
Completeness to theta = 67.86°	98.5 %	
Absorption correction	Numerical	
Max. and min. transmission	0.6988 and 0.0429	
Refinement method	Full-matrix least-squares on F ²	
Data / restraints / parameters	10858 / 21 / 732	
Goodness-of-fit on F ²	0.997	
Final R indices [I > 2σ(I)]	R1 = 0.0775, wR2 = 0.2106	
R indices (all data)	R1 = 0.1521, wR2 = 0.2707	
Largest diff. peak and hole	1.570 and -0.788 e.Å ⁻³	

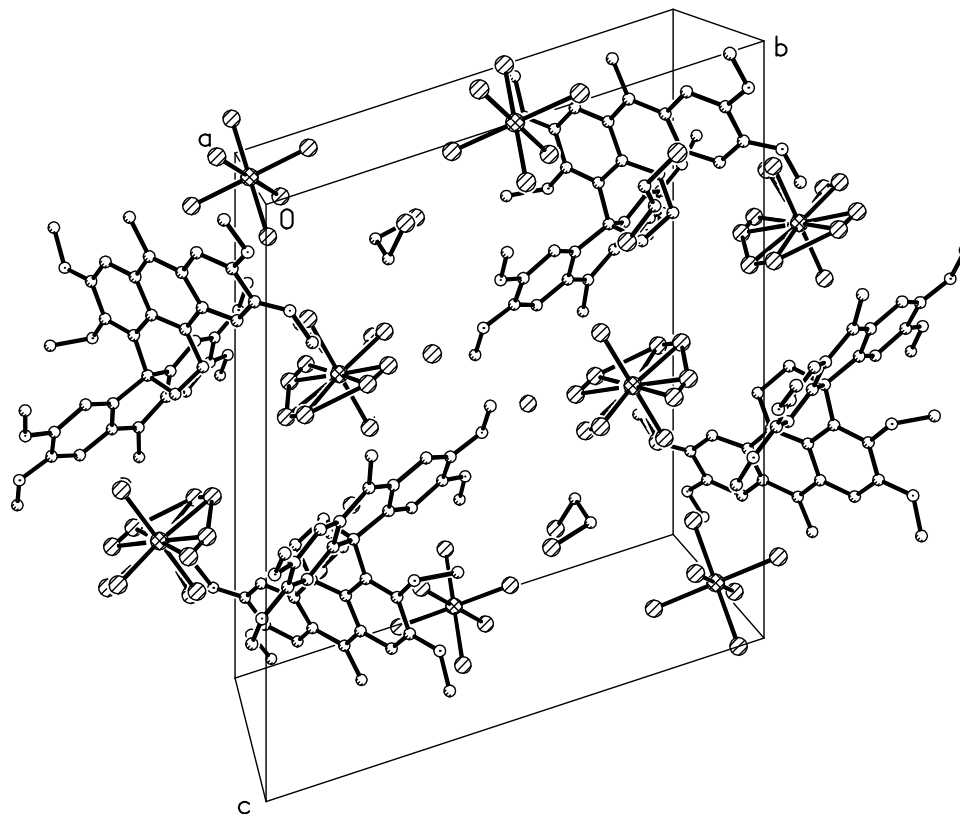
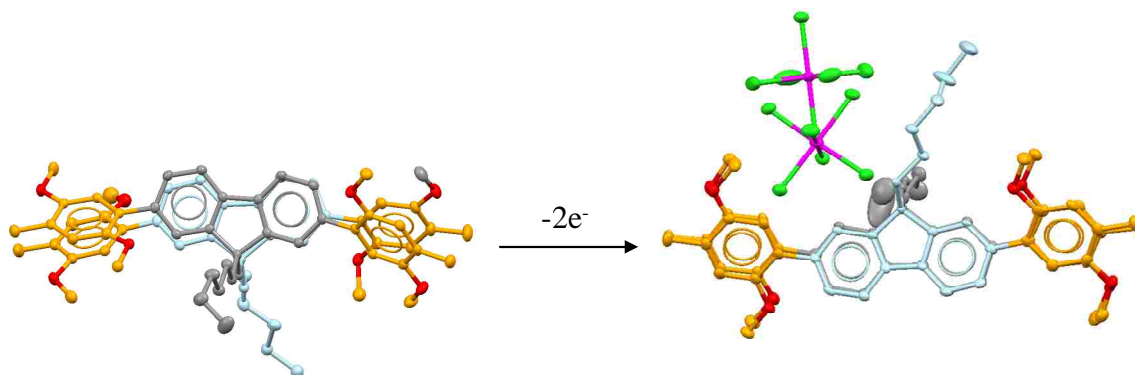


Figure 11. The packing diagram shows that molecules of dicationic $[5^{2+}(\text{SbCl}_6^-)_2]$ do not overlap with each other. Instead, they are surrounded by counter ions and disordered solvent (CH_2Cl_2) molecules. The structure contains large channels along the x axis that are filled out by the disordered solvent (CH_2Cl_2) molecules.

CHAPTER 3

Synthesis and Optoelectronic Properties of Cofacially-Stacked Poly-*p*-phenylene Derivatives: X-ray Crystallographic Evidence of Through-Space Charge Delocalization



Abstract: A novel series of cofacially-arrayed poly-*p*-phenylenes (**F2-Ar**) has shown that the X-ray structural characterization of the neutral molecules are largely dominated by effective intramolecular C-H-- π interactions while the dicationic species display an almost perfect parallel arrangement of the cofacial poly-*p*-phenylene moieties. Electrochemistry of the various **F2-Ar** and **F1-Ar** consistently met the reversibility criteria and the first 2 e⁻ oxidation event of the various **F2-Ar** occurred at a relatively lower potential ($\sim 170 \pm 10$ mV) as compared to the corresponding **F1-Ar**. The electronic absorption spectra of **F2-Ar** and **F1-Ar** were strikingly similar as opposed to their emission spectra which showed that the **F2-Ar** derivatives were relatively broad and bathochromically shifted in comparison to the model **F1-Ar** derivatives.

3.1 INTRODUCTION

Interactions between aromatic rings *via* cofacial stacking are at the origin of many phenomena of organic material science and biological chemistry; including the electron transport in DNA through stacked π -bases.⁴⁵⁻⁵³ Through space aromatic-aromatic interaction also controls the spatial relationship between the molecular subunits in bulk materials and thus plays a critical role in controlling their bulk optoelectronic and materials' properties. In this context, it is also noteworthy that numerous pentacene derivatives with different substituents are continually synthesized and studied⁵⁴⁻⁵⁵ in order to influence their packing in solid-state devices. Pentacene and its derivatives have enjoyed unprecedented attention owing to their successful usage for the preparation and study of modern functioning photovoltaic devices.

Studies in our laboratory using well-defined polyaromatic architectures have demonstrated that the effective electronic coupling amongst cofacially oriented aryl moieties can occur with drastically varied interplanar angles, from 0-120 degrees (Figure 12), which suggested that a minimal orbital overlap between the interacting π -systems is sufficient for electronic coupling to occur.²⁹⁻³⁰

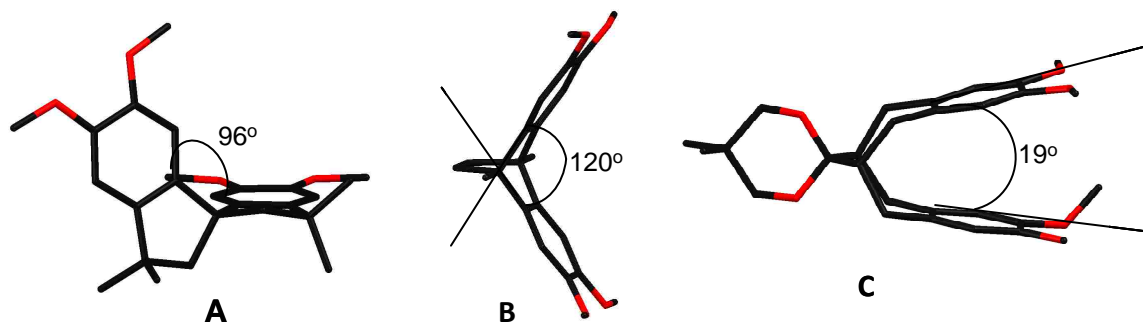


Figure 12. Line diagrams of bichromophoric electron donors **A**, **B** and **C** showing the interplanar (dihedral) angles between a pair of veratrole moieties as obtained by X-ray crystallography

The extent of electronic coupling amongst the cofacially oriented aryl moieties in various polychromophoric molecules can be gauged by the significant lowering of their oxidation potentials as compared to the monochromophoric model donors (such as 3,4-dimethyl-1,2-dimethoxybenzene for **A-C**). Furthermore, the isolation and X-ray crystal structure determination of the neutral and cation radicals of various polychromophoric donors (such as **A-C** and many others) provide unequivocal evidence as to the extent of charge (or polaron) distribution over the cofacially-oriented aryl moieties, e.g. Figure 13.

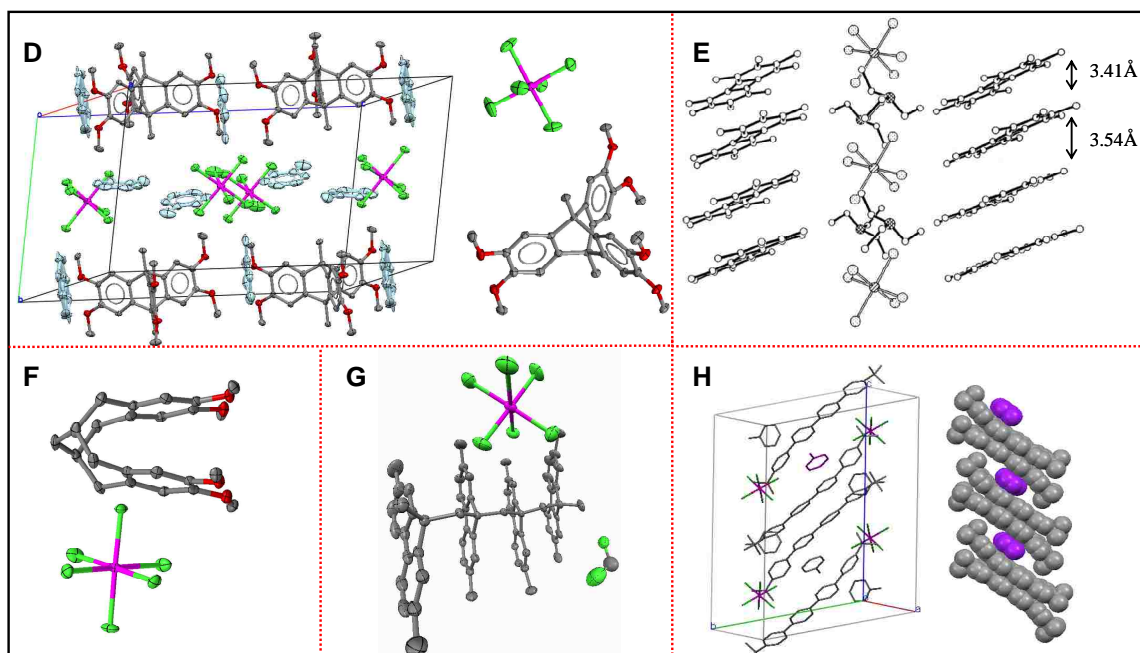
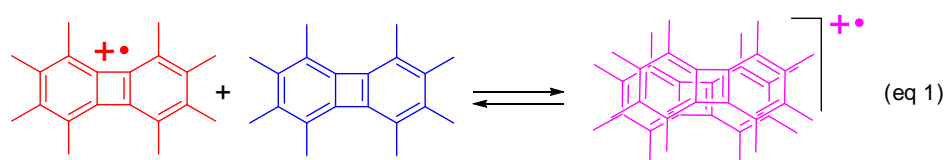


Figure 13. The molecular structures of representative cation radical salts established by X-ray crystallography: **(D)** A single charge resides on the three cofacially oriented veratrole rings (at an angle of $\sim 120^\circ$) in the hexamethoxytryptcene cation radical. **(E)** Dimeric octamethylbiphenylene SbCl_6^- salt. **(F)** A single charge is delocalized onto the two cofacially oriented veratrole moieties in a bichromophoric system built on the [4.4.1]undecane framework. **(G)** An ORTEP diagram of the cofacially-arrayed tetrafluorene (**F4**) cation radical salt showed that a single charge is delocalized onto all four fluorene moieties. **(H)** Self-association of the di-*tert*-butylquaterphenyl cation radical salt.

Importantly, a one-electron oxidation of an organic electron donor (**D**) generates the paramagnetic cation-radical, which spontaneously associates with its neutral counterpart to form a stabilized dimeric cation-radical with a single charge (entry '**E**' in Figure 13, referred to hereafter as dimer cation radicals), i.e. eq. 1.



Also noteworthy is the entry '**H**' in Figure 13 in which a quarter-*p*-phenylene cation radical, which existed largely as a monomer in solution, due to the presence of bulky *tert*-butyl groups, crystallizes in dimeric pairs bearing a pair of charges (referred to hereafter as pimer cation radicals), despite the presence of bulky *tert*-butyl groups, i.e. Figure 14.^{20,56}

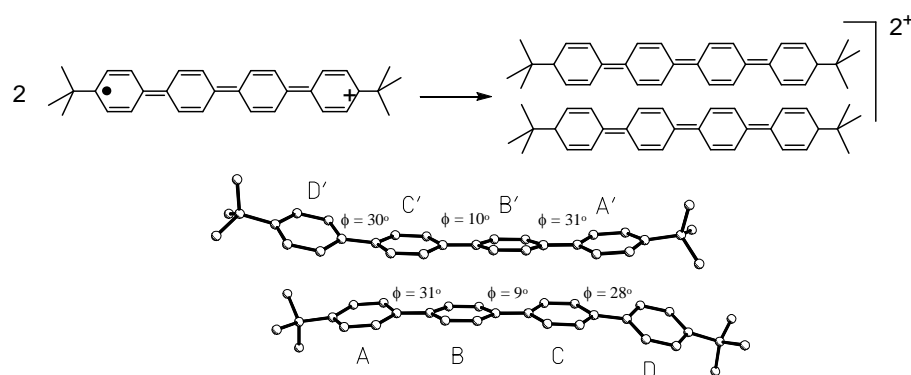


Figure 14. The crystal structure of $\text{QP}^{2+} \text{SbCl}_6^-$ cation radical showing the stacked dimeric pairs.

In order to evaluate the cause and effect of the formation of such pimer cation radicals (i.e. Figure 14), it was conjectured that if a series of soluble polyp-*p*-phenylene derivatives are constructed using cofacially stacked polyfluorenes (such as **F2**), i.e. Figure 15, these materials with well-defined polyphenylene-polyphenylene interactions both in neutral and oxidized forms, may mimic the charge-delocalization characteristics in a pimer cation radical. Note that the study of π -conjugated organic polymers, such as poly-*p*-phenylenes,^{20,56} has attracted considerable attention owing to their potential applications as functional materials in the emerging areas of molecular electronics and nanotechnology.^{34, 57-60} Moreover, the synthesis of the necessary difluorene (**F2**) platform for the construction of cofacially-arrayed pimer cation radical precursors have been earlier developed in our laboratories using readily available precursors i.e. fluorene and formaldehyde (see Figures 13G and 15).¹⁷

Accordingly, herein we will describe the syntheses of a series of soluble poly-*p*-phenylene derivatives (**F2-Ar**) containing up to six phenylene moieties (i.e. **F2-BP**). The availability of various **F2-Ar** derivatives allows us to evaluate the optoelectronic and electrochemical properties of these cofacially-arrayed polyphenylenes. Moreover, the generation and comparison of the spectral characteristics of their cation radical salts as well as their X-ray crystallography is investigated. The details of these finding are described herein.

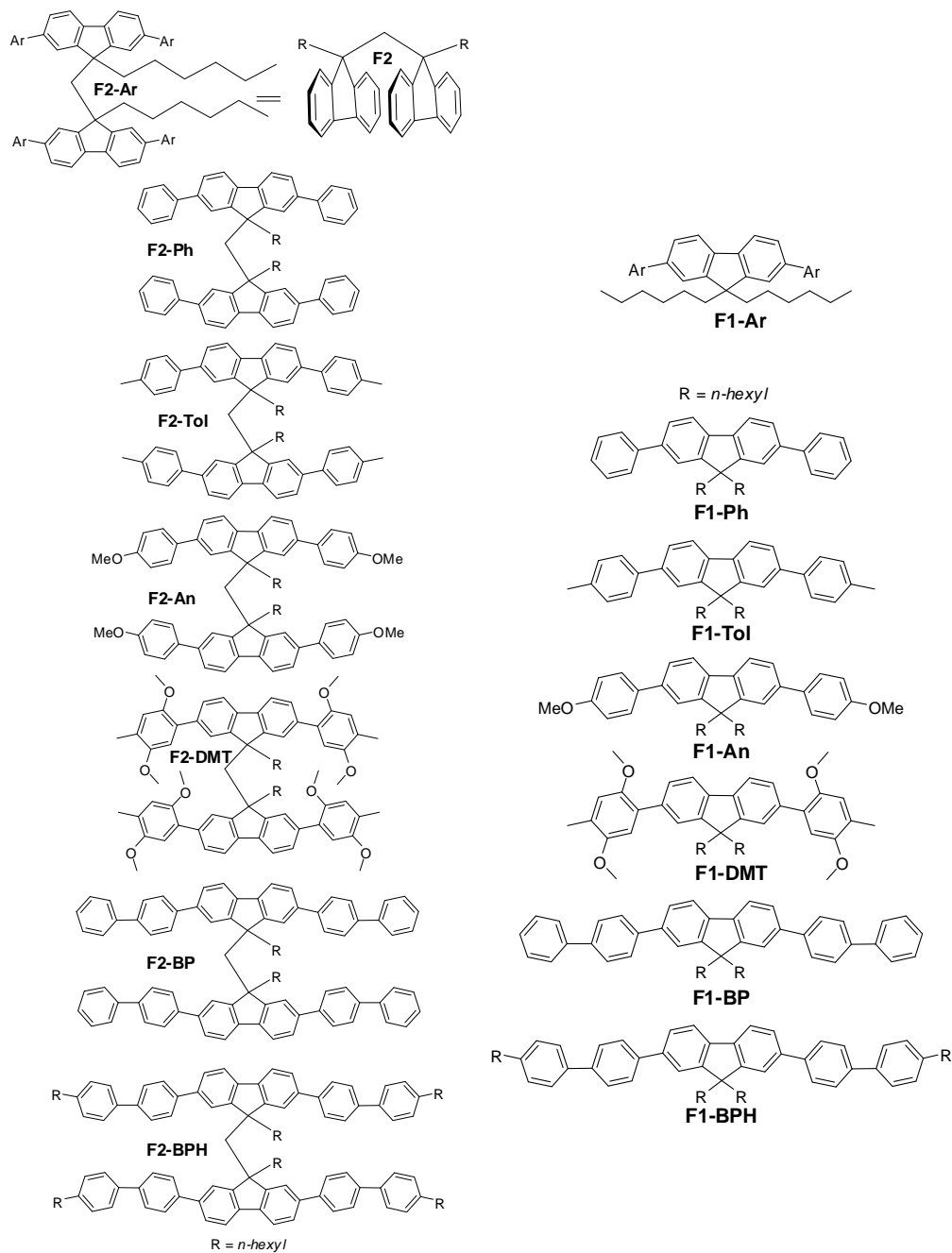


Figure 15. Structures and naming scheme of cofacially-arrayed pimer cation radical precursors (**F2-Ar**) and the corresponding model compounds (**F1-Ar**).

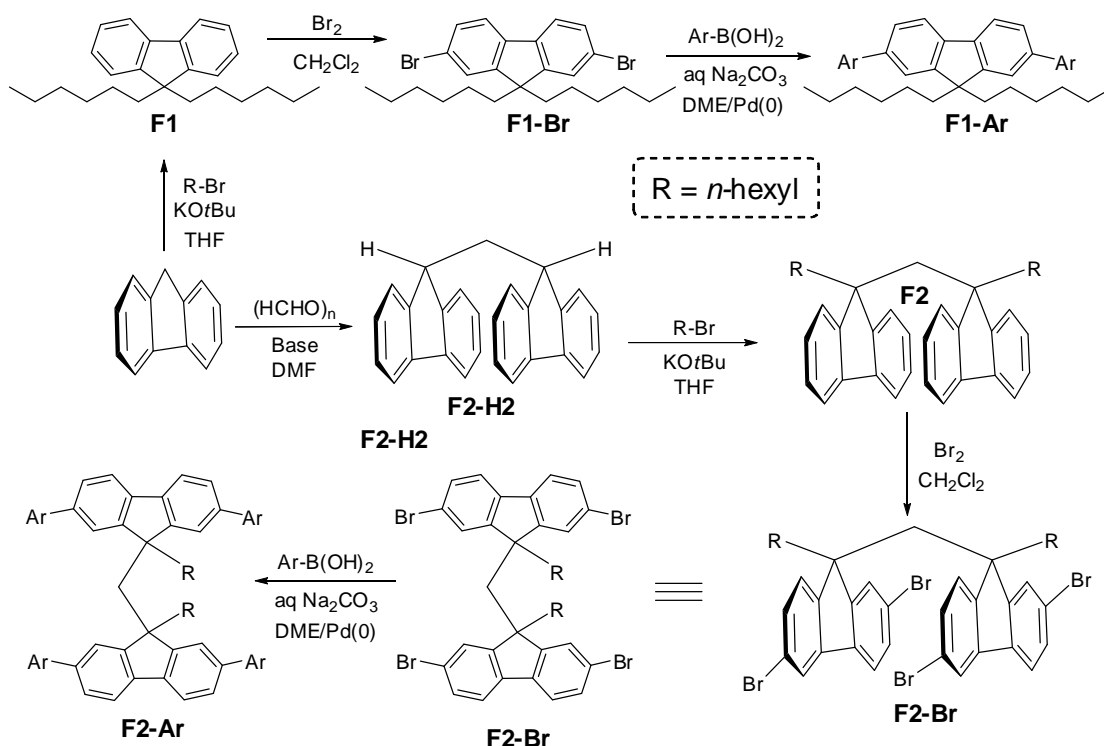
3.2 RESULTS and DISCUSSION

Synthesis of F2-Ar. In order to obtain the desired **F2-Ar**, we have resorted to the Pd-catalyzed Suzuki reaction, which has emerged as a favored reaction for aryl-aryl bond formation particularly in the synthesis of π -conjugated systems.¹⁵ The starting difluorene tetrabromide (**F2-Br**) was prepared from difluorene (**F2**)¹⁷ by a simple two-step sequence, i.e. alkylation of **F2** using 1-bromohexane and potassium *tert*-butoxide in THF followed by a simple bromination in dichloromethane (Scheme 8). The various boronic acids were prepared according to a standard literature procedure from the readily-available arylbromides with the exception of 4-bromo-4'-hexylbiphenyl which was synthesized starting from 4-bromobiphenyl by a sequence of Friedel-Crafts acylation with hexanoyl chloride followed by a standard Wolf-Kishner reduction. Thus a standard Suzuki coupling¹⁵ of **F2-Br** with various aryl boronic acids in the presence of a Pd(0) catalyst afforded the corresponding **F2-Ar** which were purified by column chromatography over silica gel using an ethyl acetate/hexanes mixture as the eluent. This simple protocol produced the various **F2-Ar** in good overall yields and their structures were established by ¹H/¹³C NMR spectroscopy as well as X-ray crystallography.

Synthesis of F1-Ar. In an analogous manner to the synthesis employed for the preparation of the various **F2-Ar**, a Pd-catalyzed Suzuki coupling reaction was utilized for the synthesis of the various **F1-Ar**. The **F1-Br** precursor was also prepared in a simple two step manner in which fluorene was first subjected to alkylation with 1-

bromohexane and potassium *tert*-butoxide in THF followed by a simple bromination in dichloromethane. A standard Suzuki coupling¹⁵ between **F1-Br** and the various aryl boronic acids in the presence of a Pd(0) catalyst thus afforded the corresponding **F1-Ar** which were purified by column chromatography over silica gel using an ethyl acetate/hexanes mixtures as the eluent. The various **F1-Ar** were prepared in excellent overall yields and their structures were confirmed by ¹H/¹³C NMR spectroscopy.

Scheme 8. Synthetic scheme for the preparation of various **F2-Ar** and **F1-Ar** derivatives in Figure 15.



Absorption/Emission Spectroscopy of F2-Ar and F1-Ar. With the various **F2-Ar** and **F1-Ar** derivatives at hand, we next recorded their absorption and emission spectra in dichloromethane at 22 °C (Figures 16 and 17). While the absorption bands of **F2-Ar** and **F1-Ar** were rather similar (Figure 16), the emission bands of cofacially stacked **F2-Ar**

derivatives were found to be relatively broad and bathochromically shifted (or red-shifted) in comparison to the model **F1-Ar** derivatives (see Figure 17 and Table 17).

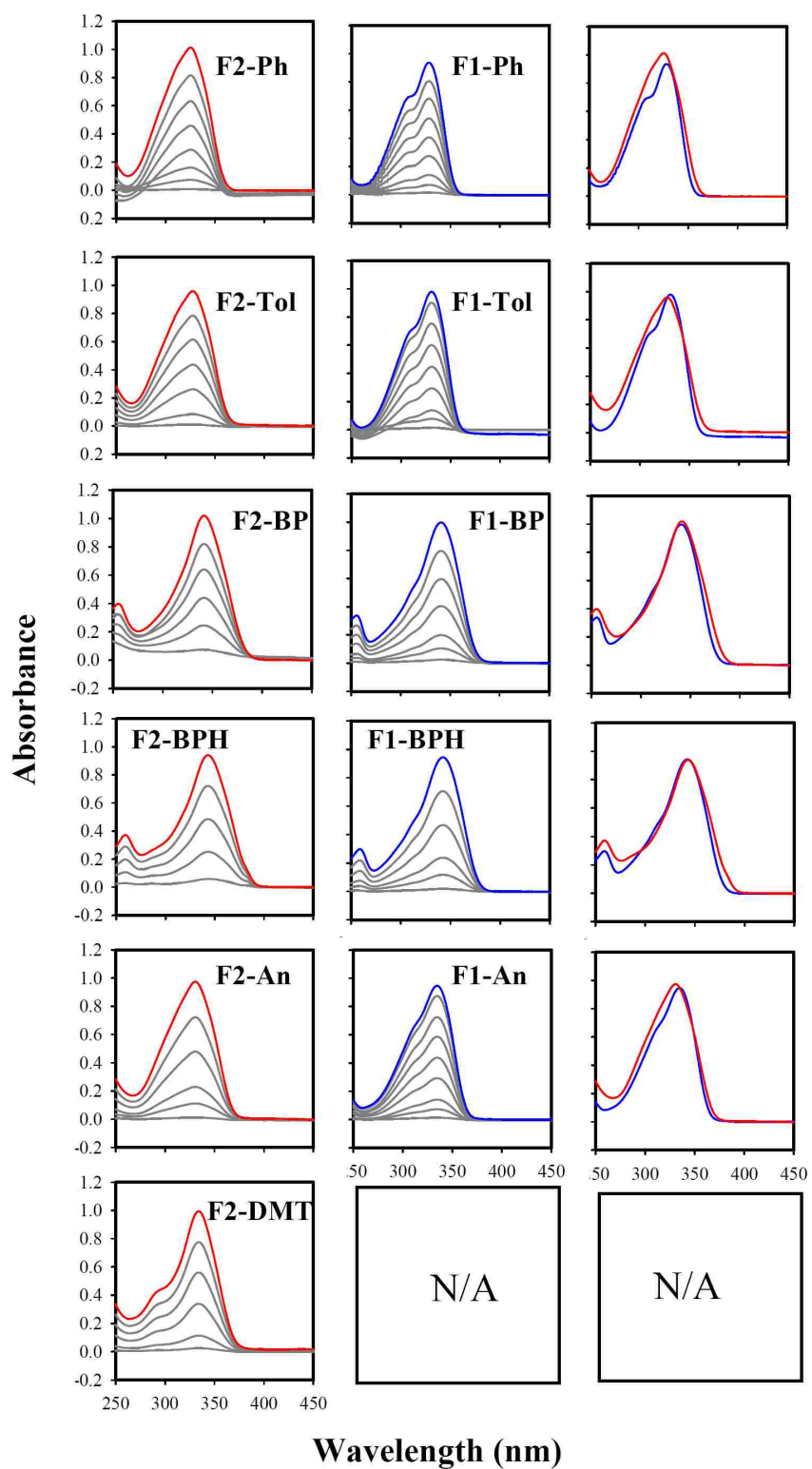


Figure 16. Electronic absorption spectra of various **F2-Ar** (left) and **F1-Ar** (middle) at varying concentrations in dichloromethane at 22 °C. (Right) Comparison of **F2-Ar** (left) and **F1-Ar** spectra.

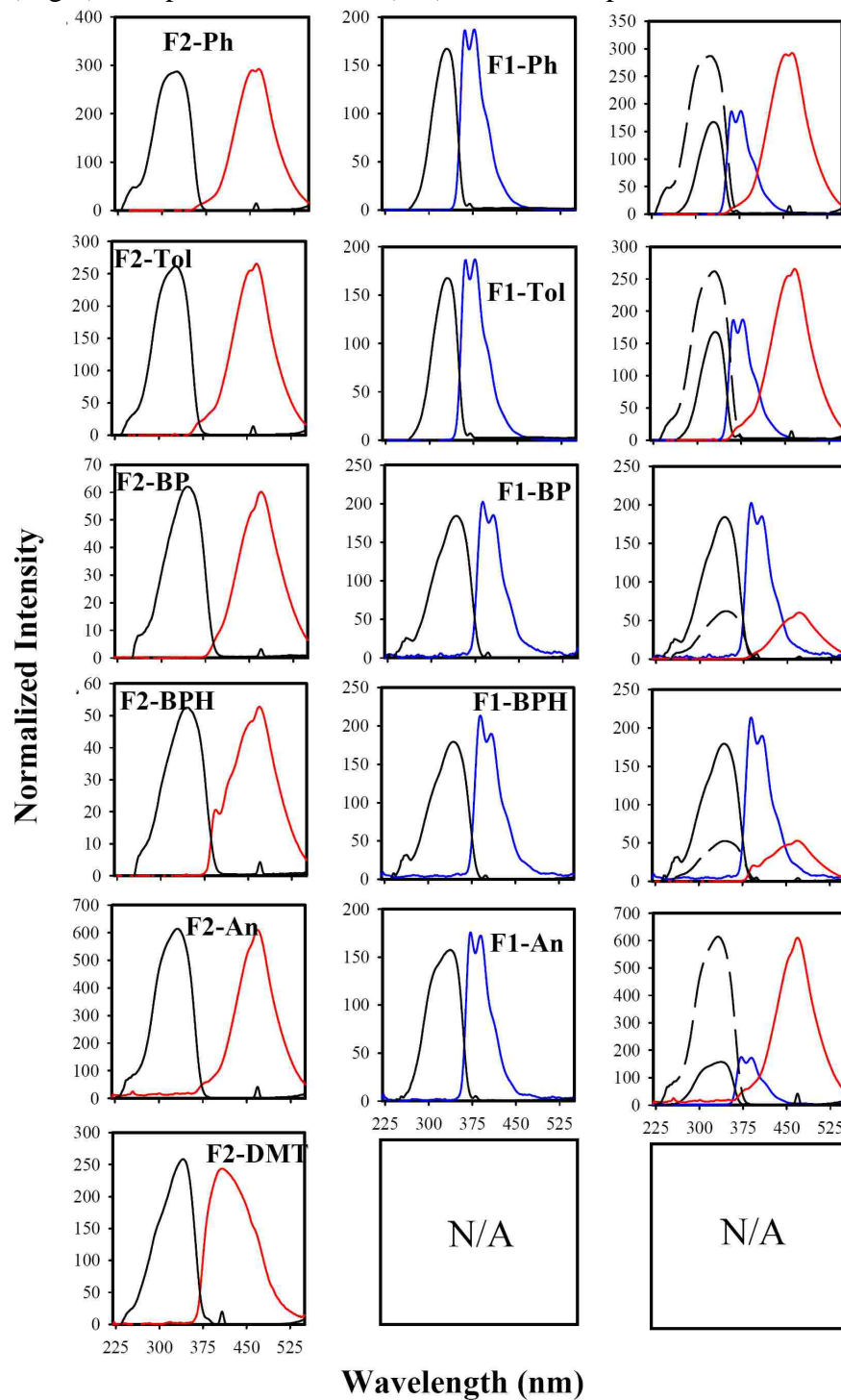


Figure 17. Emission (red and blue) and excitation (black) spectra of various **F2-Ar** (left) and **F1-Ar** (middle) at varying concentrations in

dichloromethane at 22 °C. (Right) Comparison of **F2-Ar** (left) and **F1-Ar** spectra.

Electrochemistry. Next, the redox properties of the **F2-Ar** and **F1-Ar** derivatives were evaluated by subjecting them to electrochemical oxidation at a platinum electrode as a 1×10^{-3} M solution in dichloromethane containing 0.1 M tetra-*n*-butylammonium hexafluorophosphate (*n*-Bu₄NPF₆) as the supporting electrolyte. The cyclic voltammograms of various derivatives in Figure 19 consistently met the reversibility criteria at various scan rates of 50-500 mV/s, as they all showed cathodic/anodic peak current ratios of $i_a/i_c=1.0$ (theoretical) at 22 °C (see Figure 18 for representative examples). The reversible oxidation potentials of various polyphenylene derivatives were calibrated with ferrocene as an internal standard ($E_{ox} = 0.45$ V vs SCE) and are compiled in Table 17.

Except the phenyl and the tolyl analogues (i.e. **F1-Ph** and **F1-Tol**), both of which only show one single reversible oxidation wave, the biphenyl (i.e. **F1-BP** and **F1-BPH**), anisyl (**F1-An**), and dimethoxytolyl (**F1-DMT**) derivatives showed two well defined 1- e^- oxidation waves, corresponding to the formation of mono cation radical and dication, respectively (see Figure 19, middle). In contrast, the first reversible oxidation wave of the phenyl and tolyl analogues of **F2** derivatives (i.e. **F2-Ph** and **F2-Tol**) consist of two closely spaced 1- e^- oxidation waves while the biphenyl (i.e. **F2-BP** and **F2-BPH**), anisyl (**F2-An**), and dimethoxytolyl (**F2-DMT**) derivatives showed a single 2- e^- oxidation wave. Except for **F2-DMT** which showed two well-defined 2- e^- oxidation waves, the second oxidation wave corresponding to the formation of a tetracation (i.e. 4- e^- oxidation)

was found to be quasi-reversible for **F2-BP**, **F2-BPH** and **F2-An** and was not observed for **F2-Ph** and **F2-Tol** [see Figure 19 (right) and Table 17].

The first 2- e^- oxidation event (corresponding to the first oxidation wave for **F2-Ar** derivatives) occurred at a relatively lower potential (by $\sim 170 \pm 10$ mV) as compared to the corresponding **F1-Ar** derivatives. As such, the lowering of the first oxidation potentials suggests that the cofacially-stacked difluorene derivatives (i.e. **F2-Ar**) stabilize a pimeric dication much more effectively as compared to the monomeric cation radical of the model **F1-Ar** derivatives.

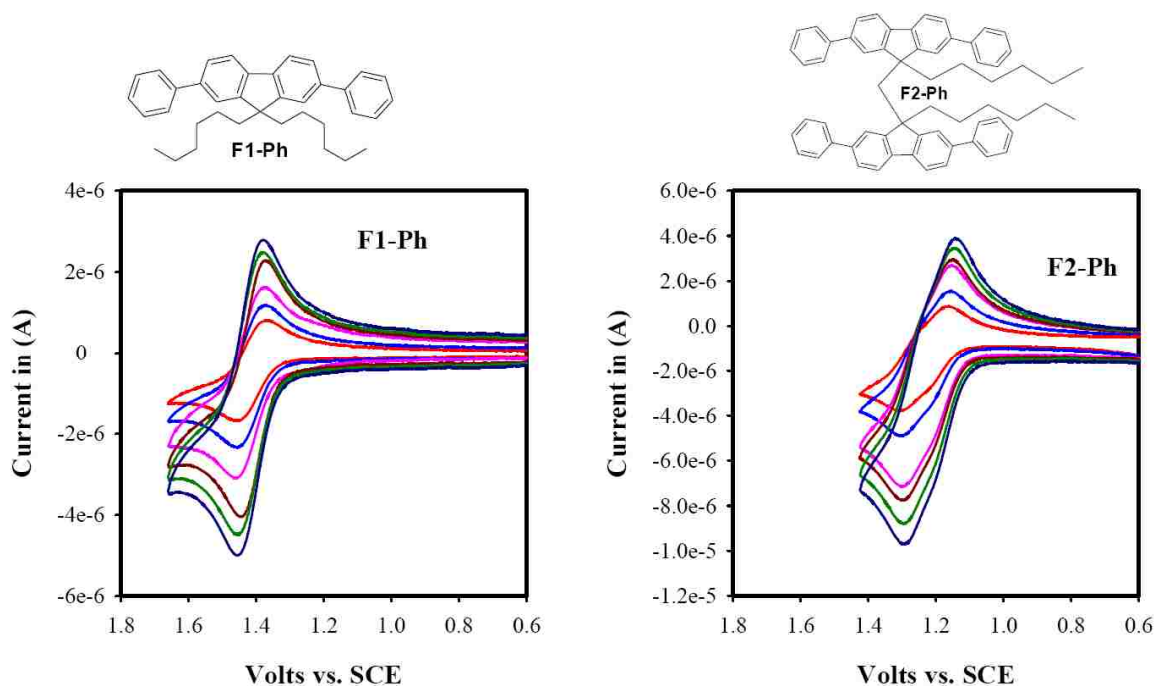


Figure 18. Cyclic voltammograms of 1×10^{-3} M **F1-Ph** and **F2-Ph** in CH_2Cl_2 containing 0.1 M $n\text{-Bu}_4\text{NPF}_6$ at scan rates between 50 and 500 mV s^{-1} at 22 $^\circ\text{C}$.

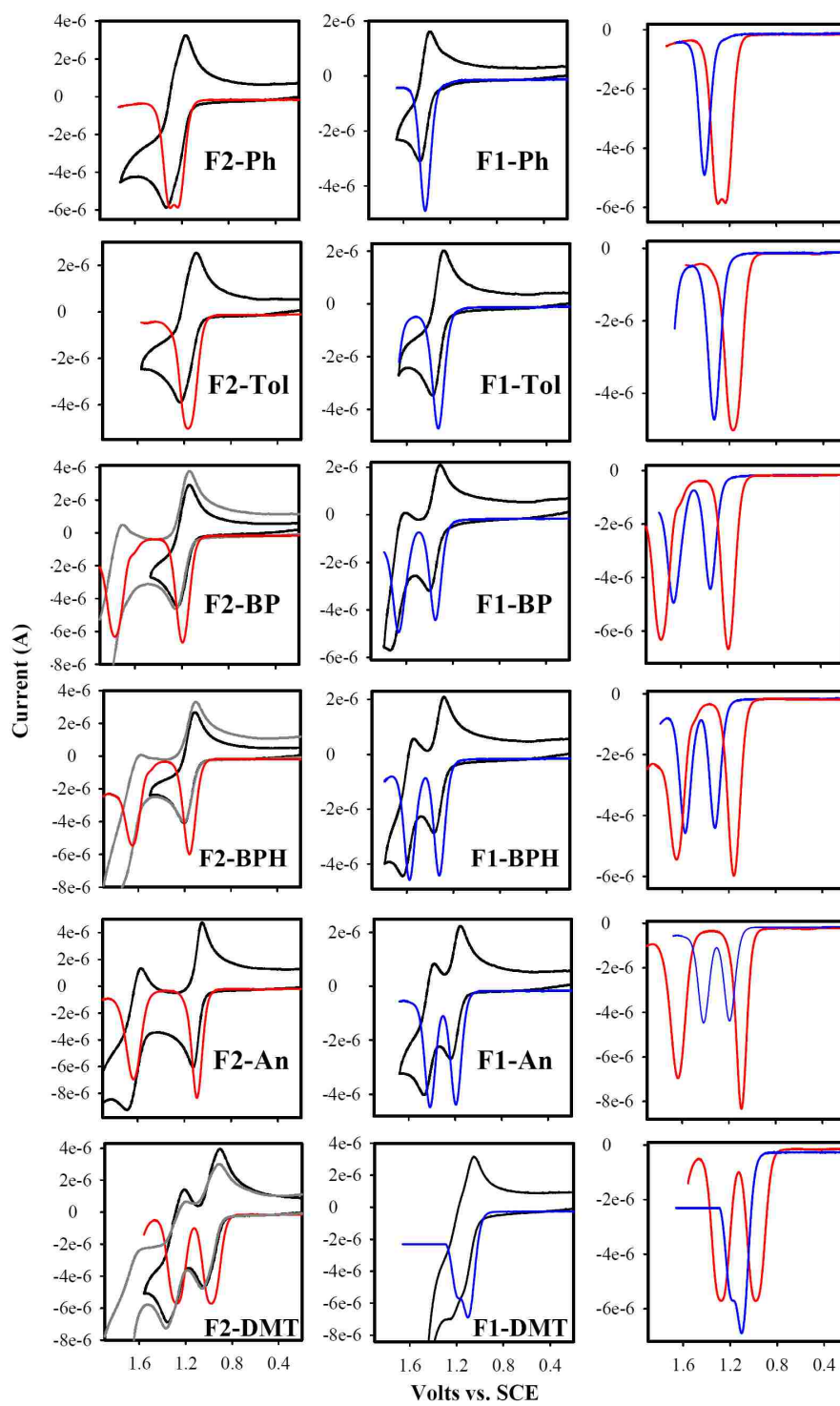


Figure 19. Cyclic voltammograms of 1×10^{-3} M **F2-Ar** (left) and **F1-Ar** (middle) in CH_2Cl_2 containing 0.1 M $n\text{-Bu}_4\text{NPF}_6$ at a scan rate of 200 mV s^{-1} at $22 \text{ }^\circ\text{C}$. (Right) Comparison of the square-wave voltammograms of **F2-Ar** (red) and **F1-Ar** (blue) derivatives.

Table 17. The optical and electrochemical data of **F2-Ar** and **F1-Ar** derivatives.

Properties	Units	F2-Ph (F1-Ph)	F2-Tol (F1-Tol)	F2-An (F1-An)	F2-DMT (F1-DMT)	F2-BP (F1-BP)	F2-BPH (F1-BPH)
E_{ox1} V vs. SCE	V	1.24 (1.42)	1.17 (1.33)	1.02 (1.20)	0.99 (1.16)	1.19 (1.35)	1.16 (1.32)
ΔE_{ox1} (F2-Ar - F1-Ar)	mV	180	160	180	170	160	160
E_{ox2} V vs. SCE	V	1.30 (1.90)	1.91 (1.74)	1.57 (1.42)	1.29 (-)	1.77 (1.62)	1.66 (1.57)
λ_{max} (UV-vis)	nm	326 (328)	327 (331)	331 (335)	334 (-)	341 (341)	343 (342)
ϵ_{max}	($\text{M}^{-1} \text{ cm}^{-1}$)	50,500 (40,870)	52,459 (44,545)	72,932 (42,727)	66,000 (-)	122,449 (59,880)	140,930 (70,677)
λ_{max} (emission)	nm	460 (370)	460 (370)	468 (381)	408 (-)	470 (397)	470 (399)
F2-Ar ⁺² (F1-Ar ⁺²) λ_{max}	nm	1026 (1062)	1116 (1158)	1288 (1346)	1900 (-)	1276 (1368)	1370 (1518)
F2-Ar ⁺² (F1-Ar ⁺²) ϵ_{max}	($\text{M}^{-1} \text{ cm}^{-1}$)	25,610 (21,973)	34,797 (69,515)	42,927 (55,603)	17,434 (-)	41,893 (33,869)	53,325 (49,956)

Generation of the **F2-Ar** and **F1-Ar** Cation Radicals and their Electronic

Spectroscopy. The reversibility of the first oxidation potentials of various **F2-Ar** and **F1-Ar** derivatives suggested that their pimeric dication and cation radicals, respectively, should be sufficiently stable, and may be generated using stable cation-radical salts [such as $\text{MA}^{+\bullet}$, $E_{\text{red}} = 1.14 \text{ V vs. SCE}$ and $\text{NAP}^{+\bullet}$, $E_{\text{red}} = 1.34 \text{ V vs. SCE}$]^{36,61} or a

dichlorodicyano-*p*-benzoquinone (DDQ)-acid system⁶² as one-electron aromatic oxidants in dichloromethane as follows.

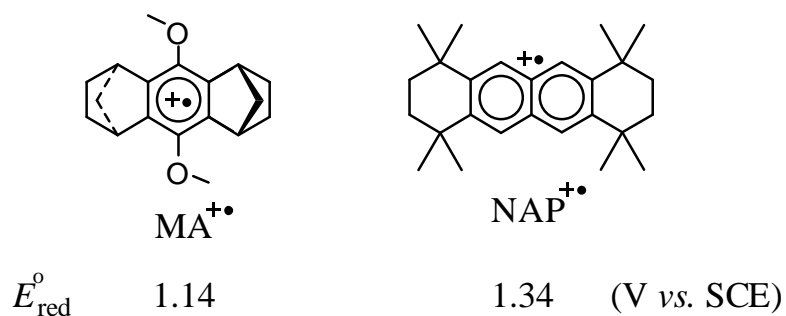
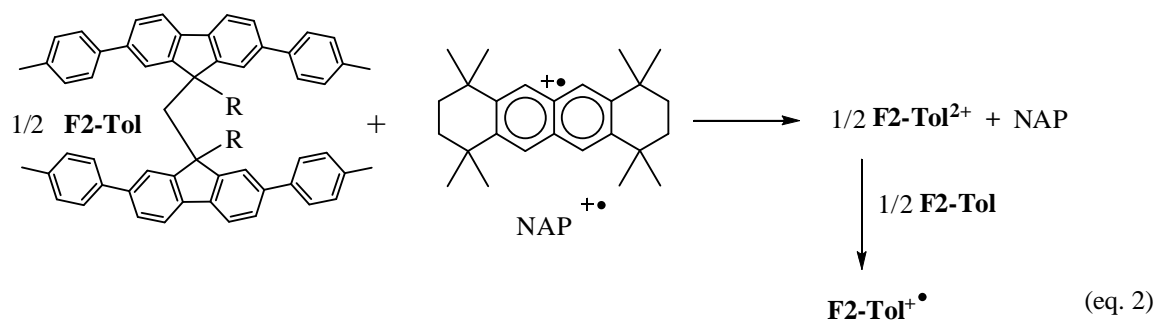


Figure 20. The structures and redox potentials of the aromatic oxidants used for the generation of pimeric dication (i.e. **F2-Ar**⁺²) and monomeric cation radicals (i.e. **F1-Ar**^{+•}).

Thus Figure 21 (left) shows the spectral changes attendant upon an incremental addition of sub-stoichiometric amounts of **F2-Ar** to a 2.7×10^{-5} M **NAP**^{+•} ($\lambda_{\text{max}} = 672, 616, 503, \text{ and } 396 \text{ nm}; \epsilon_{672} = 9300 \text{ M}^{-1} \text{ cm}^{-1}$)⁶¹ in dichloromethane at 22 °C. Furthermore a plot of formation of the **F2-Tol**²⁺ dication (i.e. increase in the absorbance at 1006 nm) against the increments of added neutral **F2-Tol** (see Figure 21, far left), established that **NAP**^{+•} was completely consumed after the addition of ½ equiv. of **F2-Tol**; and the resulting absorption spectrum of the dication **F2-Tol**²⁺ was transformed to the monocation radical **F2-Tol**^{+•} upon addition of another ½ equiv. of neutral **F2-Tol** (i.e. eq 2).



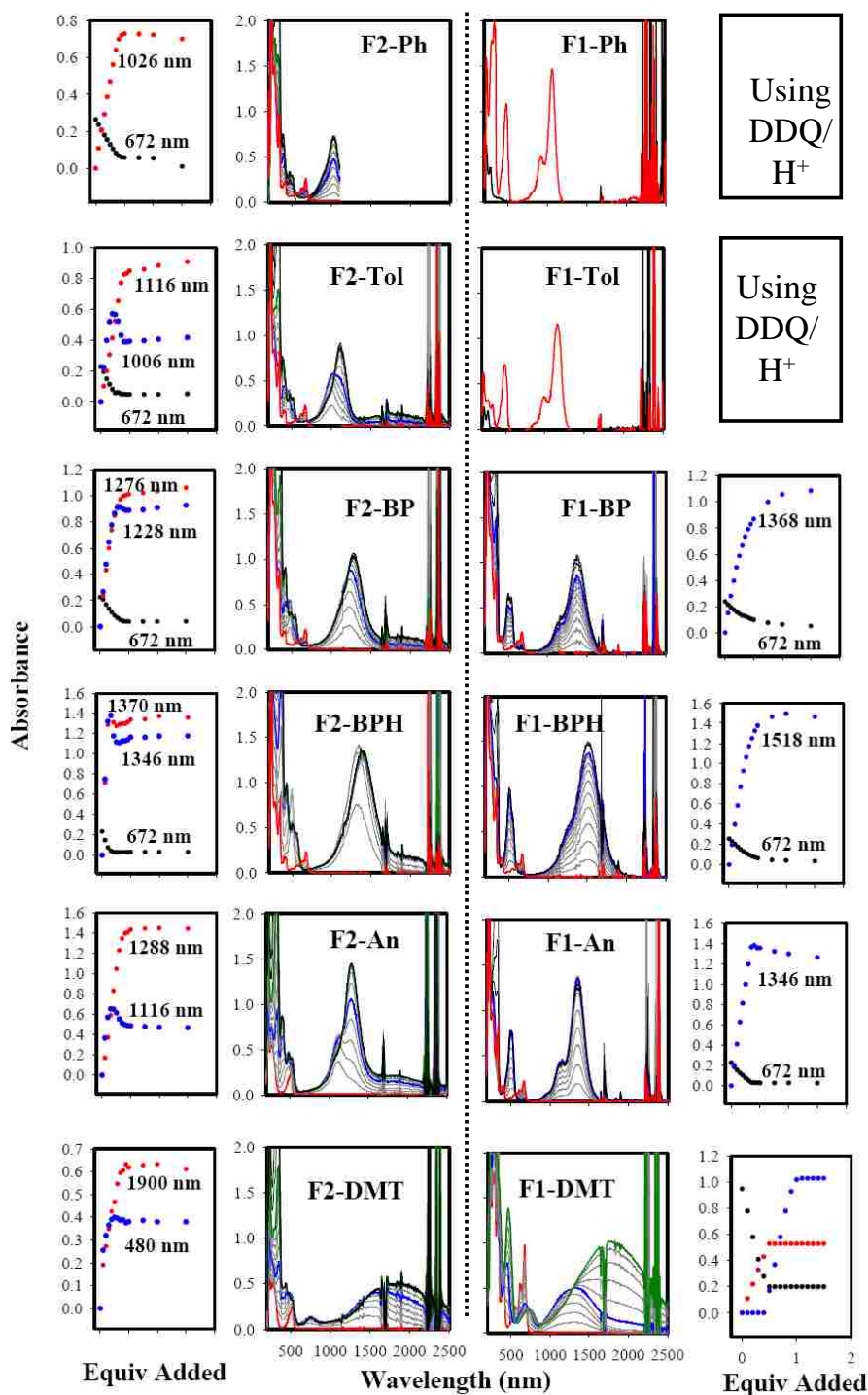


Figure 21. Spectral changes obtained upon the redox titrations of **F2-Ar** to **F2-Ar²⁺** (left) and **F1-Ar** to **F1-Ar⁺** (right) using **NAP⁺** (for **F2-Ph**, **F2-Tol**, **F2-BP**, **F2-BPH**, **F1-BP**, and **F1-BPH**), **MA⁺** (**F2-An** and **F2-DMT**), and a **DDQ/H⁺** system (i.e **F1-Ph** and **F1-Tol**) in dichloromethane at 22 °C.

Similarly, the dication and cation radicals of various **F2-Ar** and **F1-Ar** were generated using $\text{NAP}^{+\bullet}$, $\text{MA}^{+\bullet}$, or DDQ/H^+ (see Figure 21) and are further compared in Figure 22. The absorption spectra of the pimeric dications (i.e. F2-Ar^{2+}) were not profoundly different when compared to model mono cation radicals (i.e. $\text{F1-Ar}^{+\bullet}$), see Figure 22.

Red traces are F2-Ar^{2+} and blue traces are $\text{F1-Ar}^{+\bullet}$

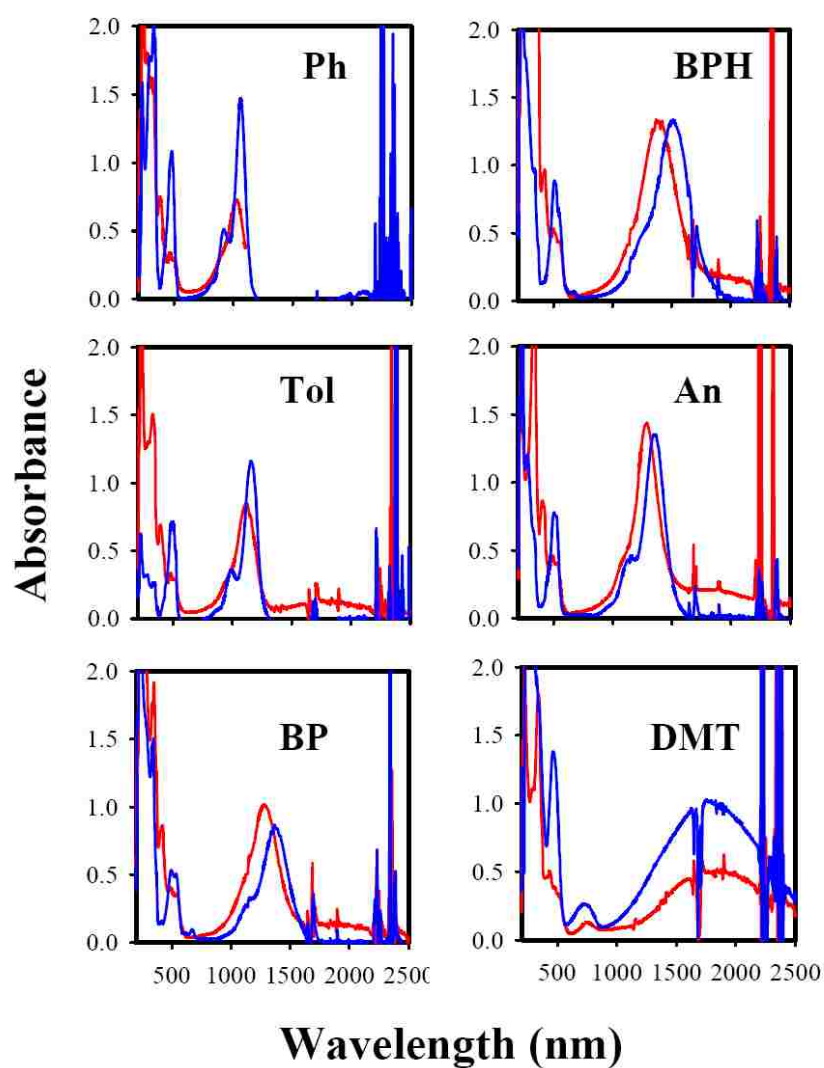


Figure 22. A comparison of the absorption spectra of F2-Ar^{2+} and $\text{F1-Ar}^{+\bullet}$

X-ray Crystallography of Neutral F2-Ar and its Dications. The **F2-Ar** dications, obtained according to eq 2, are highly persistent at ambient temperatures and did not show any decomposition during a 24 h period at 0 °C, as confirmed by UV-vis spectroscopy. The single crystals of various **F2-Ar**²⁺, suitable for X-ray crystallography, were obtained by a slow diffusion of toluene into the dichloromethane solutions of [**F2-Ph**²⁺ (SbCl₆⁻)₂], [**F2-Tol**²⁺ (SbCl₆⁻)₂], and [**F2-DMT**²⁺ (SbCl₆⁻)₂] at -10 °C during the course of 2 days.

The crystal structure of various neutral **F2-Ar** and the representative model **F1-Tol** were also determined and are compared in Figure 24. The expected cofacial arrangement of various poly-*p*-phenylene groups in the **F2-Ar** derivatives is based on the fact that these derivatives are built on the rigid framework of difluorene (i.e. **F2**) which is permitted to adapt a conformation where the fluoranyl moieties are oriented cofacially. Interestingly, however, the observed large distortions from the perfect cofacial arrangement of attached aryl groups on the **F2** framework in various **F2-Ar** derivatives arises, in part, due to the most common (stabilizing) aromatic-aromatic interactions (largely observed in solid state) between the two aromatic rings in neutral form, i.e. Figure 23.⁶³

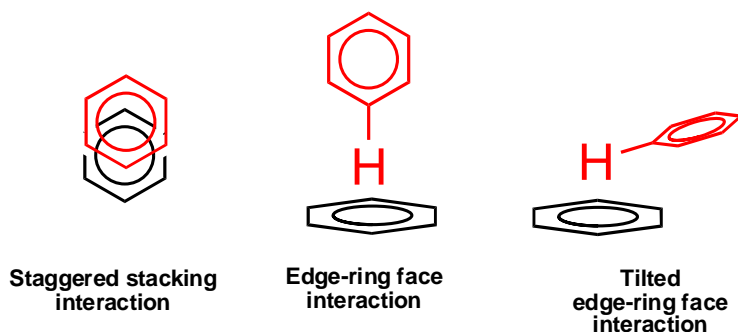


Figure 23. Typical aromatic-aromatic interactions observed in the solid state.

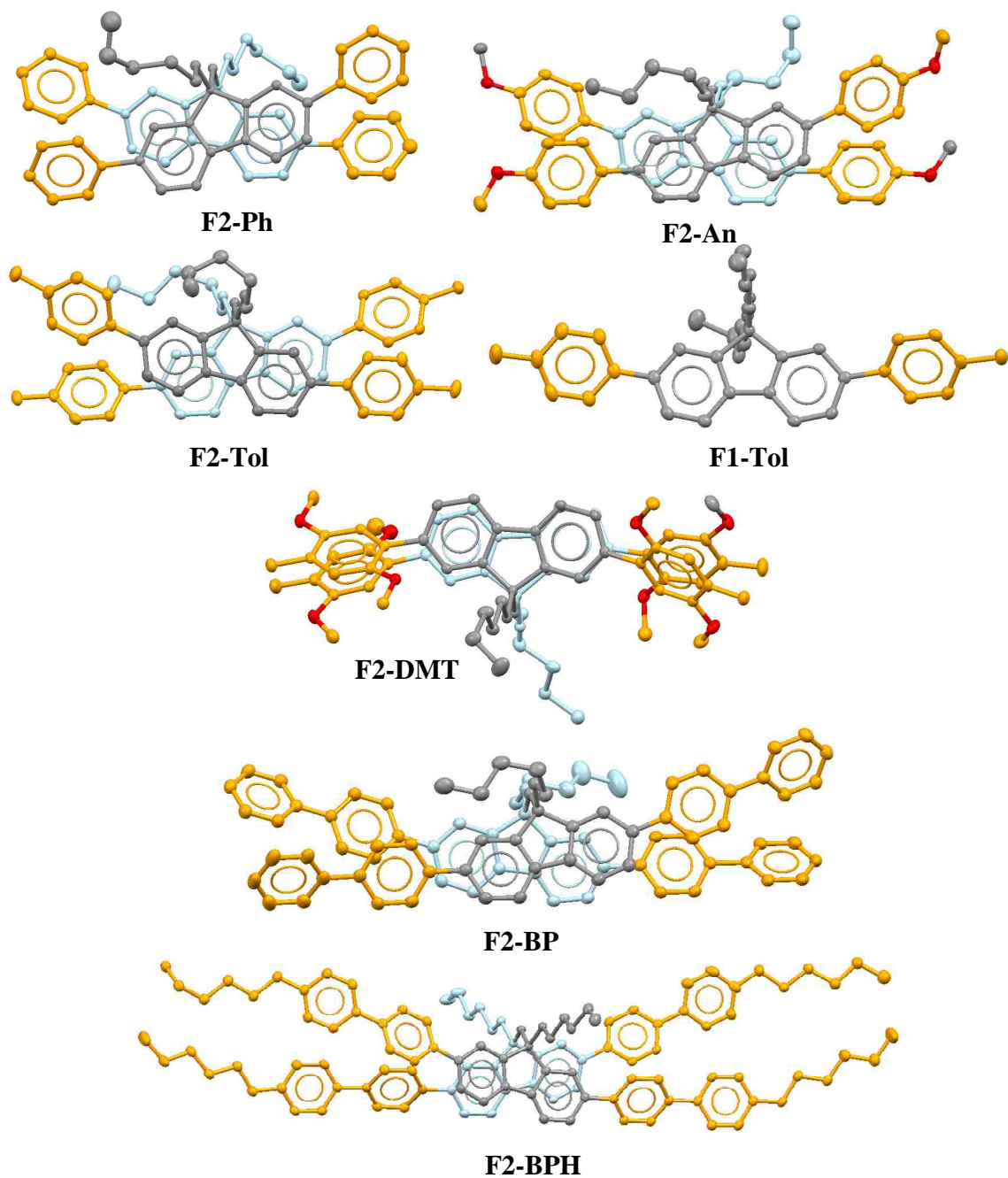


Figure 24. The molecular structures of various (neutral) **F2-Ar** and a model **F1-Ar** derivative (**F1-Tol**), obtained by X-ray crystallography, are compared.

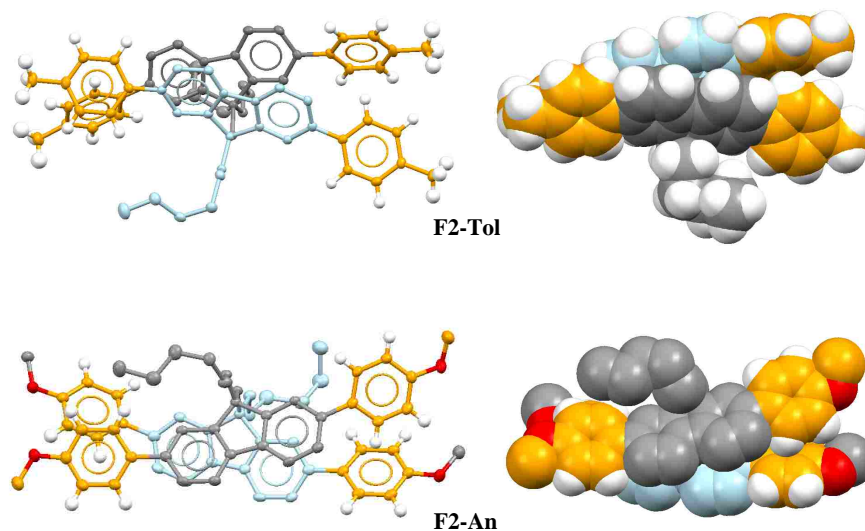


Figure 25. The representative structures of **F2-Tol** and **F2-An** showing that the conformations of various **F2-Ar** derivatives are controlled, in part, by effective intramolecular C-H- π interaction.

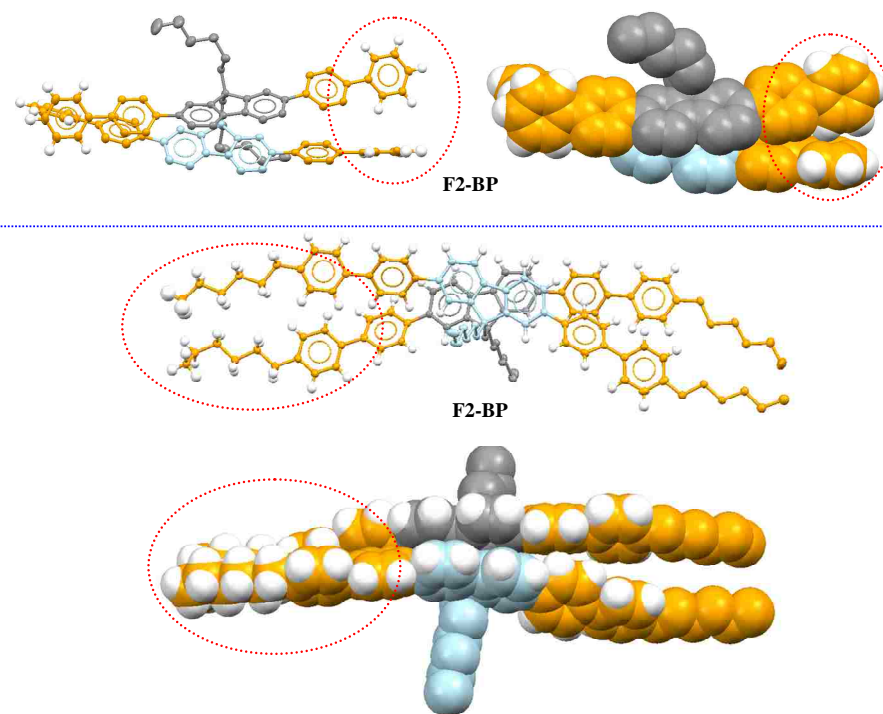


Figure 25. Conformations of **F2-BP** and **F2-BPH** showing that while the conformation of **F2-BP** is dominated by C-H- π interaction, the **F2-BPH** conformation is controlled by efficient stacking of the nonpolar hexyl groups connected to the polyphenylenes (shown by red circles).

Indeed, as shown in Figures 25 and 26, the conformations of various **F2-Ar** derivatives are dominated by these aromatic-aromatic interactions listed in Figure 23.

The molecular dicationic [**F2-Ph**²⁺ (SbCl₆⁻)₂], [**F2-Tol**²⁺ (SbCl₆⁻)₂], and [**F2-DMT**²⁺ (SbCl₆⁻)₂] are compared in Figure 27 and they all show almost perfect parallel arrangement of the cofacial poly-p-phenylene moieties.

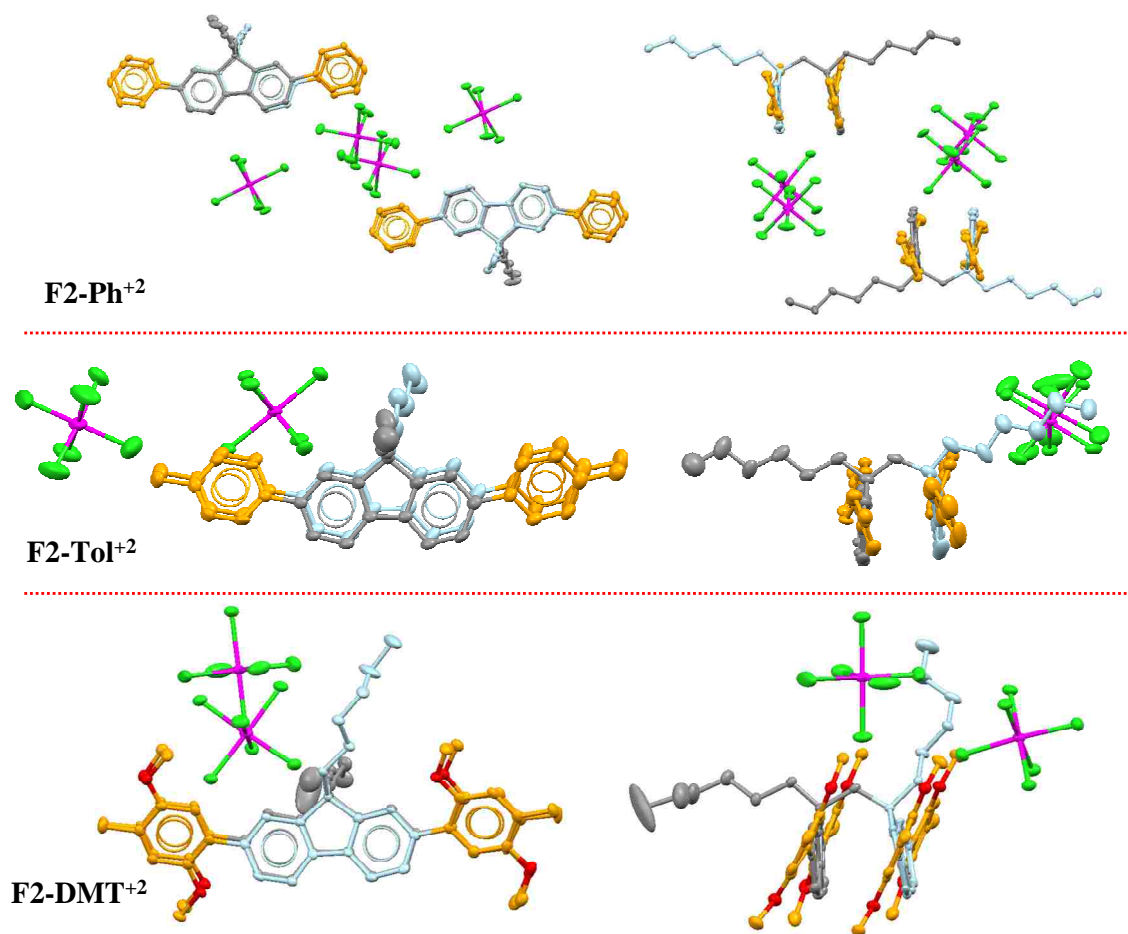


Figure 27. The molecular dicationic [**F2-Ph**²⁺ (SbCl₆⁻)₂], [**F2-Tol**²⁺ (SbCl₆⁻)₂], and [**F2-DMT**²⁺ (SbCl₆⁻)₂], obtained by X-ray crystallography.

Theoretically, the removal of one electron each from the opposing poly-*p*-phenylene moieties in the dicationic **F2-Ar** derivatives should result in a significant Coulombic repulsion between the positive charges of the cofacially-oriented poly-*p*-phenylene moieties. However, the X-ray structures of the dicationic [**F2-Ph**²⁺ (SbCl₆⁻)₂], [**F2-Tol**²⁺ (SbCl₆⁻)₂], and [**F2-DMT**²⁺ (SbCl₆⁻)₂] show that the coupling between the half-filled electronic orbitals of the two cation-radical moieties (from each poly-*p*-phenylene unit) provide an attractive/bonding force between them.

Apparently, after the 2-*e*⁻ oxidation, the coupling/attractive forces between the cationic poly-*p*-phenylene moieties is much stronger than the expected Coulombic repulsion between them. The resulting species are characterized by reduced values of their cleft angles as compared to the corresponding neutral derivatives. The almost eclipsed conformations of the two cofacial poly-*p*-phenylene moieties in dications as compared to neutral **F2-Ar** derivatives (compare Figures 24 and 27) further attest that two charges are effectively stabilized by the cofacial arrangement of the poly-*p*-phenylene moieties.

Unfortunately, the experimental precision of geometric parameters of the **F2-Ar** dications does not allow a detailed analysis of their bond lengths re-distribution upon a 2-*e*⁻ oxidation. However, it is easily seen that all of them have a characteristic quinonoidal distortion of their biphenyl fragments described by the contraction of the central C-C bond from 1.465 Å in neutral molecules to 1.437 Å in (**F2-DMT**²⁺) and to 1.414 and 1.419 Å in **F2-Tol**²⁺ and **F2-Ph**²⁺, respectively. The average precision of the bond lengths in various dications varies from 0.007 to 0.01 Å. Moreover, the reduced quinonoidal distortion in **F2-DMT**²⁺ along with an additional quinonoidal distortion in its peripheral

dimethoxytolyl groups (characterized by the shortening of C-O bonds from 1.376 to 1.362 Å) are a result of an extended delocalization of its positive charge, involving the outer Ar groups (see Figure 28).

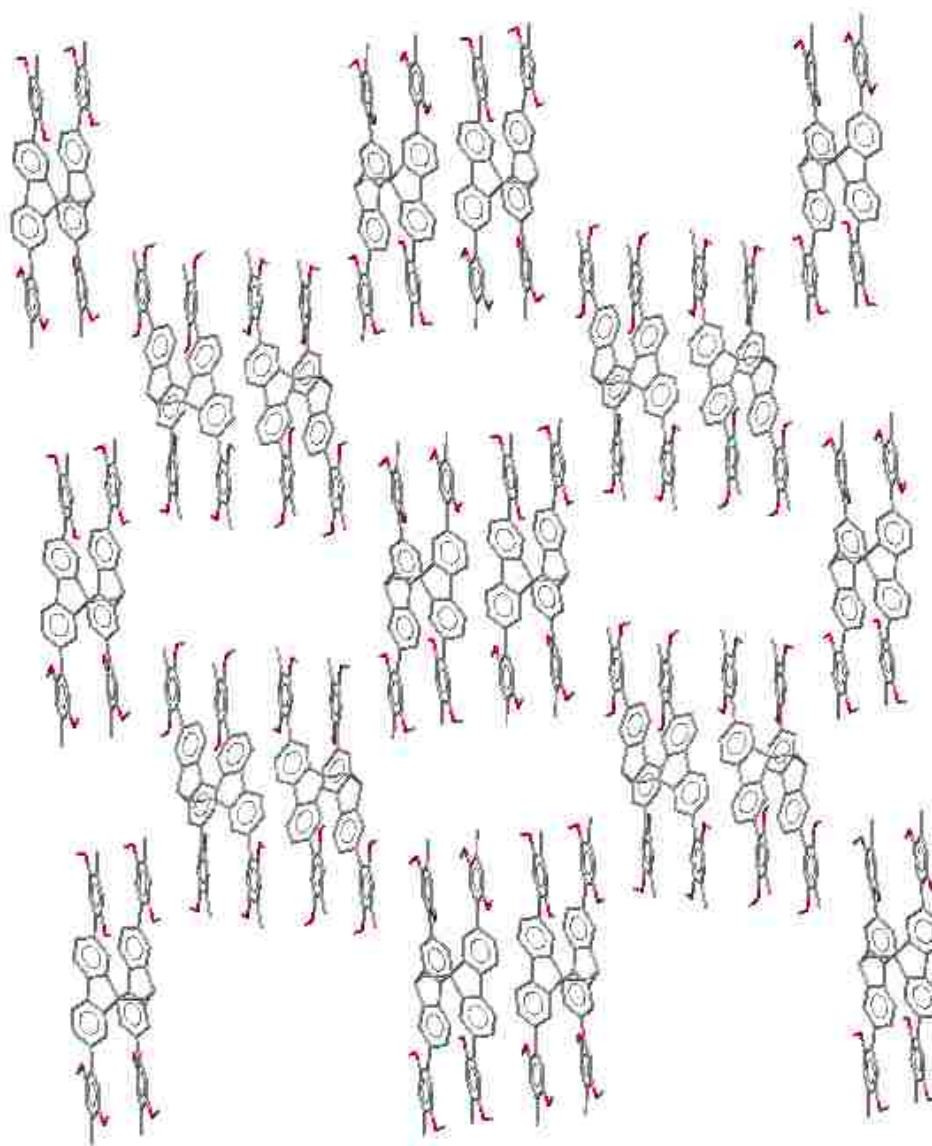


Figure 28. The packing arrangement of $[\text{F2-DMT}^{2+}(\text{SbCl}_6^-)_2]$ showing that dications form layers along the [101] crystallographic plane. In these layers, dications form anti-parallel dimers, which in turn are connected in a honeycomb 2-dimensional framework through close (3.3-3.4 Å) Ar...Ar contacts. Ar groups form infinite parallel stacks and SbCl_6^- anions and solvent molecules (together with hexyl groups are not shown for clarity) occupy positions between the layers.

3.3 SUMMARY and CONCLUSION

In summary, a novel series of cofacially-arrayed poly-*p*-phenylenes (**F2-Ar**) has shown that the X-ray structural characterization of the neutral molecules are largely dominated by effective intramolecular C-H- π interactions while the dicationic species display an almost perfect parallel arrangement of the cofacial poly-*p*-phenylene moieties (Figure 29).

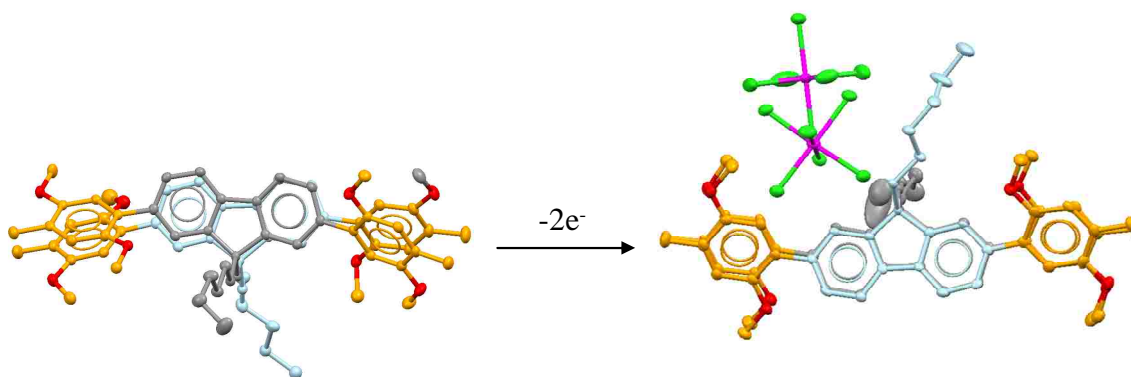


Figure 29. Comparing the neutral **F2-DMT** and dicationic [**F2-DMT**²⁺ (**SbCl6**⁻)₂] X-ray crystal structures.

Cyclic voltammetry of the various **F2-Ar** and **F1-Ar** consistently met the reversibility criteria at scan rates between 50 and 500 mV/s and the first 2 e⁻ oxidation event of the various **F2-Ar** occurred at a relatively lower potential ($\sim 170 \pm 10$ mV) as compared to the corresponding **F1-Ar**. The electronic absorption spectra of **F2-Ar** and **F1-Ar** were strikingly similar as opposed to their emission spectra which showed that the **F2-Ar** derivatives were relatively broad and bathochromically shifted in comparison to the model **F1-Ar** derivatives. The initial findings described herein will be further probed in the future and the results will be reported accordingly.

3.4 EXPERIMENTAL SECTION

General Experimental Methods and Materials. All reactions were performed under an argon atmosphere unless otherwise stated. Fluorene, *p*-formaldehyde, potassium *tert*-butoxide, N,N-dimethylformamide, 1-bromohexane, bromine, 4-bromobiphenyl, hexanoyl chloride, anhydrous aluminum chloride, carbon disulfide, hydrazine hydrate, potassium hydroxide, diethylene glycol, *n*-butyllithium, triisopropylborate, sulfuric acid, *tetrakis*(triphenylphosphine)palladium(0), 1,2-dimethoxyethane, anhydrous sodium carbonate, phenylboronic acid, 3,4-dimethoxyphenylboronic acid, 4-biphenylboronic acid, and anhydrous ferric chloride were all commercially available and used without further purification. 4-methylphenylboronic acid, 4-methoxyphenylboronic acid, and 2,5-dimethoxytolylboronic acid were all prepared according to standard literature procedures, **F1-DMT** was prepared according to a previously published work from our laboratory.

Anhydrous tetrahydrofuran (THF) was prepared by refluxing the commercial tetrahydrofuran over lithium tetrahydroaluminate under an argon atmosphere for 24 hours followed by distillation. It was stored under an argon atmosphere in a Schlenk flask equipped with a Teflon valve fitted with Viton *O*-rings. Dichloromethane (Aldrich) was repeatedly stirred with fresh aliquots of concentrated sulfuric acid (~10 % by volume) until the acid layer remained colorless. After separation it was washed successively with water, aqueous sodium bicarbonate, water, and aqueous sodium chloride and dried over anhydrous calcium chloride. The dichloromethane was distilled twice from P₂O₅ under an argon atmosphere and stored in a Schlenk flask equipped with a Teflon valve fitted with Viton *O*-rings. The hexanes and toluene were distilled from P₂O₅ under an argon

atmosphere and then refluxed over calcium hydride (~12 h). After distillation from CaH₂, the solvents were stored in Schlenk flasks under an argon atmosphere. NMR spectra were recorded on Varian 300 and 400 MHz NMR spectrometers.

Cyclic Voltammetry (CV). The CV cell was of an air-tight design with high vacuum Teflon valves and Viton O-ring seals to allow an inert atmosphere to be maintained without contamination by grease. The working electrode consisted of an adjustable platinum disk embedded in a glass seal to allow periodic polishing (with a fine emery cloth) without changing the surface area (~1 mm²) significantly. The reference SCE electrode (saturated calomel electrode) and its salt bridge were separated from the catholyte by a sintered glass frit. The counter electrode consisted of platinum gauze that was separated from the working electrode by ~3 mm. The CV measurements were carried out in a solution of 0.1 M supporting electrolyte (tetra-*n*-butylammonium hexafluorophosphate, TBAH) and 1-5 × 10⁻³ M substrate in dry dichloromethane under an argon atmosphere. All the cyclic voltammograms were recorded at a sweep rate of 200 mV sec⁻¹, unless otherwise specified and were IR compensated. The oxidation potentials ($E_{1/2}$) were referenced to SCE, which was calibrated with added (equimolar) ferrocene ($E_{1/2} = 0.450$ V vs. SCE). The $E_{1/2}$ values were calculated by taking the average of anodic and cathodic peak potentials in the reversible cyclic voltammograms.

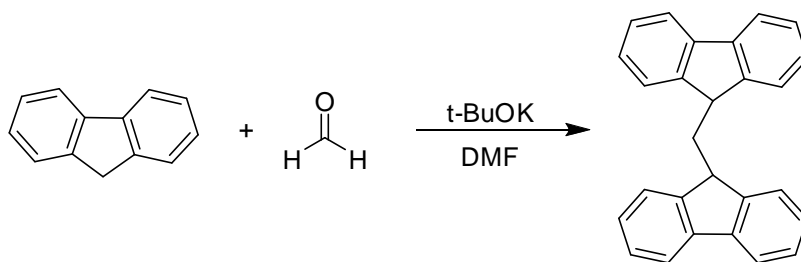
Procedure for the Spectral Titration of MA⁺ SbCl₆⁻ with F2-Ar. An orange-red solution of MA⁺ SbCl₆⁻ in dichloromethane (3 mL, 3.4 × 10⁻⁵ M) was transferred under an argon atmosphere in a 1-cm quartz cuvette at room temperature. A dichloromethane solution (1 × 10⁻³ M) of F2-Ar in 10 μL increments was added to this

solution. The UV-vis spectra of the resulting solutions, after the addition of each increment, were recorded at 22 °C.

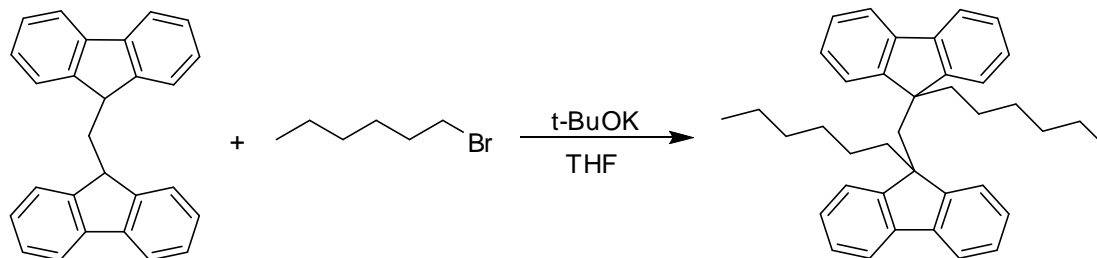
Procedure for the Spectral Titration of $\text{NAP}^{++} \text{SbCl}_6^-$ with F2-Ar and F1-Ar.

A dark blue solution of $\text{NAP}^{++} \text{SbCl}_6^-$ in dichloromethane (3 mL, 2.7×10^{-5} M) was transferred under an argon atmosphere in a 1-cm quartz cuvette at room temperature. A dichloromethane solution (8.1×10^{-4} M) of **F2-Ar** or **F1-Ar** in 10 μL increments was added to this solution. The UV-vis spectra of the resulting solutions, after the addition of each increment, were recorded at 22 °C.

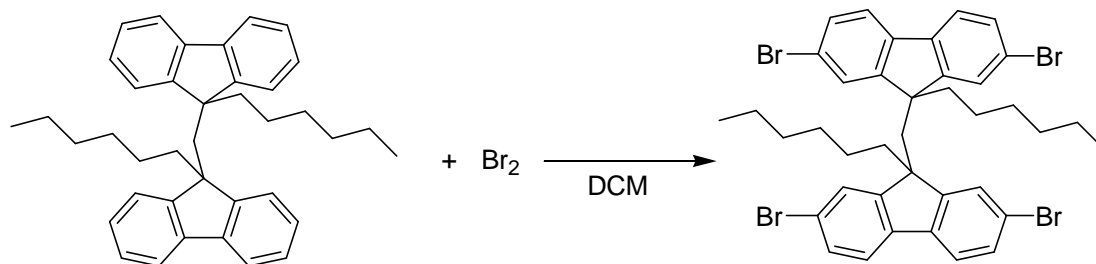
Synthesis of F2-H2.



In an oven dried schlenk flask under argon fluorene (5.0 g, 30 mmol) is dissolved in N,N-dimethylformamide (40 mL). To this solution, potassium *tert*-butoxide (0.17 g, 1.5 mmol) is added and allowed to stir for 5 minutes after which *para*-formaldehyde (0.45 g, 15mmol) is added to the solution which is allowed to stir for 20 minutes at room temp. The resulting solution is then poured into a 5% HCl solution (100 mL), filtered, washed with water (3 x 30 mL), and dried under vacuum to afford a beige solid. Yield (5.01 g, 97%); mp: 203-206 °C; ^1H NMR (CDCl_3) δ : 2.25 (t, 2H), 4.42 (t, 2H), 7.30 (t, 4H, $J = 7.4$ Hz), 7.41 (t, 4H, $J = 7.4$ Hz) 7.57 (d, 4H, $J = 7.6$ Hz), 7.83 (d, 4H, $J = 7.6$ Hz). ^{13}C NMR (CDCl_3) δ : 39.03, 46.05, 120.29, 125.21, 127.18, 127.46, 141.16, 147.64.

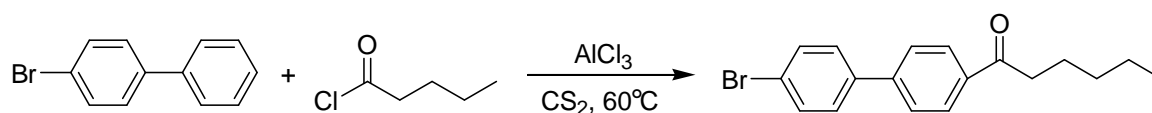
Synthesis of F2.

In an oven dried schlenk flask under argon F2-H2 (5.01 g, 14.5 mmol) is dissolved in tetrahydrofuran (125 mL). To this solution, potassium *tert*-butoxide (3.58 g, 31.9 mmol) and 1-bromohexane (5.27 g, 31.9 mmol) are added sequentially, the resulting purple solution is allowed to stir for 1 hour at room temperature. The solution is then quenched with water (100 mL) and extracted with dichloromethane (3 x 20 mL). The combined organic extracts are dried over anhydrous magnesium sulfate, filtered, evaporated under reduced pressure and dried under vacuum to produce a yellow liquid that is used without further purification. Yield (7.4 g, >99%); ^1H NMR (CDCl_3) δ : 0.26 (m, 6H), 0.71 (t, 6H), 0.91 (m, 8H), 1.02 (m, 4H), 1.81 (m, 4H), 3.04 (s, 2H), 6.77 (d, 4H, $J = 7.7$ Hz), 6.81 (td, 4H, $J = 7.5$ Hz, 1.2 Hz), 6.97 (td, 4H, $J = 7.5$ Hz, 1.2 Hz), 7.06 (d, 4H, $J = 7.7$ Hz). ^{13}C NMR (CDCl_3) δ : 14.17, 22.73, 29.68, 31.54, 42.96, 49.47, 53.53, 119.01, 123.50, 125.82, 125.85, 140.95, 148.90.

Synthesis of F2-Br.

To a solution of F2 (7.38 g, 14.4 mmol) in dichloromethane (125 mL), a solution of bromine (9.67 g, 60.5 mmol) in dichloromethane (20 mL) is added dropwise. The resulting dark red solution is allowed to stir for 90 minutes after which time it is quenched with concentrated aqueous potassium hydroxide (100 mL) and extracted with dichloromethane (3 x 20 mL). The combined organic extracts were dried over anhydrous magnesium sulfate and filtered. The solvent was evaporated under reduced pressure and the beige solid is dried under vacuum. Recrystallization from a dichloromethane/methanol mixture produces a white solid that is used without further purification. Yield (7.63 g, 64%); mp: 166-169 °C; ^1H NMR (CDCl_3) δ : 0.18 (m, 4H), 0.73 (t, 6H), 0.93 (m, 8H), 1.03 (m, 4H), 1.82 (m, 4H), 2.89 (s, 2H), 6.90 (d, 4H, $J = 8.1$ Hz), 6.96 (d, 4H, $J = 1.7$ Hz), 7.17 (dd, 4H, $J = 8.1$ Hz, 1.7 Hz). ^{13}C NMR (CDCl_3) δ : 14.15, 22.45, 22.71, 29.47, 31.49, 42.24, 49.26, 54.05, 120.37, 121.09, 127.07, 130.44, 138.77, 150.03.

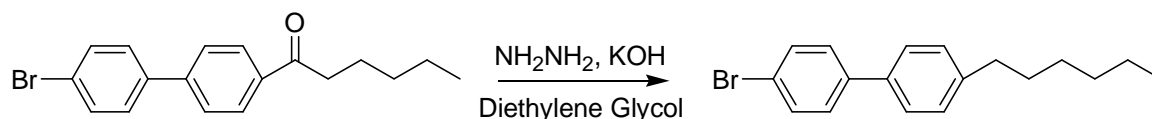
Synthesis of 1-(4'-Bromobiphenyl-4-yl)-hexan-1-one.



In a 500 mL schlenk flask equipped with a dropping funnel and condenser, hexanoyl chloride (6.73 g, 50 mmol), is dissolved in carbon disulfide (100 mL) at 0°C under an argon atmosphere. To this solution, anhydrous aluminum chloride (8.67 g, 65 mmol) is added portion wise over 20 minutes after which time a solution of 4-bromobiphenyl (11.66 g, 50 mmol) in carbon disulfide (50 mL) is added dropwise over the course of 20 minutes while maintaining the 0°C temperature. The resulting solution is heated at 60°C overnight, after which time it is allowed to come to room temp and cooled using a dry ice

– acetone bath, quenched with a 10% HCl solution (40 mL), and extracted with dichloromethane (3 x 30 mL). The combined organic extracts were dried over anhydrous magnesium sulfate, evaporated, and dried under vacuum to produce an off white solid that was used without further purification. Yield (15.03 g, 91%); mp: 96-98 °C; ¹H NMR (CDCl₃) δ: 0.92 (t, 3H), 1.38 (m, 4H), 1.76 (m, 2H), 2.99 (t, 2H), 7.48 (d, 2H, *J* = 8.6 Hz), 7.59 (d, 2H, *J* = 8.6 Hz), 7.64 (d, 2H, *J* = 8.6 Hz), 8.03 (d, 2H, *J* = 8.6 Hz). ¹³C NMR (CDCl₃) δ: 14.19, 22.75, 24.29, 31.75, 38.85, 122.77, 127.19, 128.95, 128.99, 132.27, 136.23, 138.99, 144.40, 200.26.

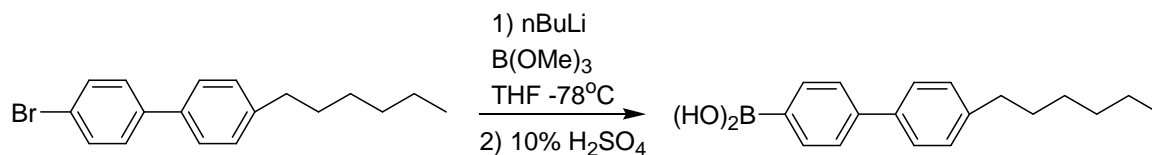
Synthesis 4-Bromo-4'-hexylbiphenyl



In a schlenk flask under argon, 1-(4'-bromobiphenyl-4-yl)-hexan-1-one (15.03 g, 45.4 mmol) is dissolved in diethylene glycol (125 mL) with stirring. Hydrazine hydrate (6.6 mL, 136.2 mmol) and potassium hydroxide (10.16 g, 181.6 mmol) are then added to the solution which is allowed to reflux for 24 hours. The resulting yellow solution is cooled to room temperature, quenched with a 5% HCl solution (50 mL), and extracted with dichloromethane (3 x 30 mL). The combined organic extracts were dried over anhydrous magnesium sulfate, evaporated, and dried under vacuum to give a white solid that was purified by filtering over a short pad of silica gel using 5% ethyl acetate/hexanes as the eluent. Yield (13.6 g, 94%); mp: 88-89 °C; ¹H NMR (CDCl₃) δ: 0.89 (m, 3H), 1.33 (m, 6H), 1.64 (m, 2H), 2.64 (t, 2H), 7.25 (d, 2H, *J* = 8.3 Hz), 7.43-7.48 (m, 4H), 7.55 (d, 2H,

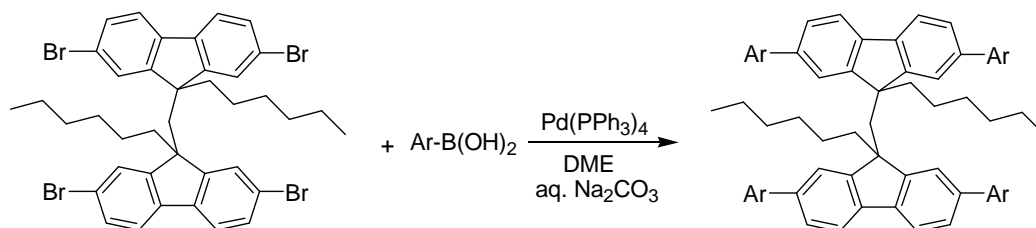
$J = 8.6$ Hz). ^{13}C NMR (CDCl_3) δ : 14.33, 22.84, 29.25, 31.64, 31.96, 35.83, 121.36, 126.95, 128.73, 129.15, 131.99, 137.46, 140.27, 142.77

Synthesis of 4'-hexyl-4-biphenylboronic acid



In a schlenk flask under argon, 4-bromo-4'-hexylbiphenyl (7.5 g, 23.6 mmol) is dissolved in anhydrous tetrahydrofuran (225 mL) and cooled to -78 °C. To this solution, *n*-butyllithium (14.2 mL, 35.5 mmol) is added dropwise and the resulting solution is allowed to stir for 1 hour after which time triisopropylborate (8.2 mL, 35.5 mmol) is added. After stirring overnight, the solvent is evaporated and 10% H_2SO_4 (100 mL) is added to the solution which is then allowed to stir for 3 hours after which time it is extracted with diethyl ether (3 x 20 mL) and dried over anhydrous magnesium sulfate. The combined organic extracts are then concentrated and triturated with hexanes to produce a beige colored precipitate which is filtered, dried under vacuum, and used without further purification. Yield (5.8 g, 87%); mp: 117-119 °C; ^1H NMR (CD_3OD) δ : 0.82 (m, 3H), 1.23 (m, 6H), 1.53 (m, 2H), 2.52 (t, 2H), 7.12 (d, 2H, $J = 8.1$ Hz), 7.42 (d, 2H, $J = 8.3$ Hz), 7.47 (d, 2H, $J = 8.1$ Hz), 7.69 (d, 2H, $J = 6.7$ Hz). ^{13}C NMR (CD_3OD) δ : 14.60, 23.83, 30.22, 32.79, 33.03, 36.69, 127.00, 127.93, 130.01, 135.52, 139.68, 143.50, 143.99.

General Procedure for the Synthesis of Various F2-Ar



Solid F2-Br and the corresponding aryl boronic acid (5 equiv.) were dissolved in anhydrous 1,2-dimethoxyethane (DME) (30 mL) in an oven dried Schlenk flask under an argon atmosphere and the flask was evacuated and filled with argon (3x). In another oven dried Schlenk flask a solution of anhydrous sodium carbonate (5.0 g) in water (20 mL) was prepared under an argon atmosphere and the flask was also evacuated and filled with argon (3x). To the DME solution, $\text{Pd(PPh}_3)_4$ (50 mg) and the salt solution were added sequentially under a strict argon atmosphere followed by evacuation and filling the flask with argon (3x) after each addition. The flask was covered with foil and the solution was allowed to reflux overnight. The resulting solution was cooled to room temperature, quenched with 5% HCl (50 mL) and extracted with dichloromethane (3 x 20 mL). The organic layer was dried over anhydrous magnesium sulfate, evaporated and dried under vacuum. The various F2-Ar were purified by column chromatography using an ethyl acetate/hexanes mixture as the eluent to afford the pure F2-Ar.

F2-Ph: Yield (1.12 g, 76%) clear solid; mp: 196-198 °C; $^1\text{H NMR}$ (CDCl_3) δ : 0.31 (m, 4H), 0.70 (t, 6H), 0.95 (broad m, 12H), 1.94 (m, 4H), 3.16 (s, 2H), 7.02 (s, 4H), 7.08 (dd, 4H, $J = 7.8$ Hz, 1.4 Hz), 7.14 (d, 4H, $J = 8.4$ Hz), 7.20-7.23 (m, 8H), 7.29-7.32 (m, 12H). $^{13}\text{C NMR}$ (CDCl_3) δ : 14.15, 22.60, 22.66, 29.56, 31.40, 42.80, 50.45, 53.79, 119.25, 122.12, 125.88, 126.69, 127.42, 128.64, 139.00, 140.22, 141.82, 149.70.

F2-Tol: Yield (0.90 g, 85%) yellow solid; mp: 173-175 °C; ^1H NMR (CDCl_3) δ : 0.32 (m, 4H), 0.69 (t, 6H), 0.94 (broad m, 12H), 1.90 (m, 4H), 2.42 (s, 12H), 3.12 (s, 2H), 6.97 (s, 4H), 7.03 (d, 4H, $J = 7.8$ Hz), 7.07-7.14 (broad m, 20H). ^{13}C NMR (CDCl_3) δ : 14.15, 21.35, 22.60, 22.67, 29.57, 31.40, 42.79, 53.73, 119.09, 122.03, 125.67, 127.37, 129.27, 136.29, 138.86, 139.13, 140.03, 149.61.

F2-BP: Yield (0.58 g, 43%) yellow solid; mp: 279-281 °C; ^1H NMR (CDCl_3) δ : 0.36 (m, 4H), 0.71 (t, 6H), 0.99 (broad m, 12H), 2.02 (m, 4H), 3.24 (s, 2H), 7.13 (s, 4H), 7.18 (m, 8H), 7.34 (d, 8H, $J = 8.2$ Hz), 7.38 (d, 4H $J = 7.1$ Hz), 7.44 (m, 8H), 7.51 (d, 8H, $J = 8.2$ Hz), 7.58 (d, 8H, $J = 7.8$ Hz). ^{13}C NMR (CDCl_3) δ : 14.17, 22.67, 29.61, 31.43, 35.70, 42.80, 50.35, 53.87, 119.34, 121.99, 125.73, 127.11, 127.25, 127.37, 127.58, 129.00, 138.24, 139.40, 140.26, 140.54, 140.91, 149.65.

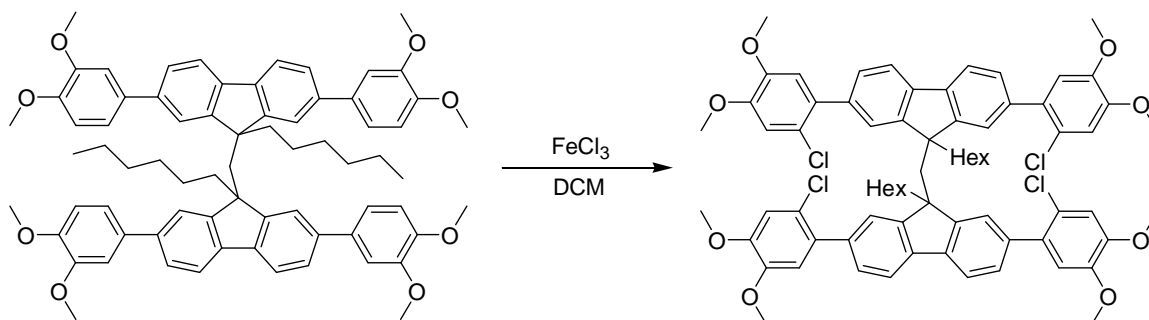
F2-BPH: Yield (0.37 g, 42%) white solid; mp: 182-185 °C; ^1H NMR (CDCl_3) δ : 0.40 (m, 4H), 0.73 (t, 6H), 0.97 (m, 24H), 1.41 (m, 24H), 1.73 (m, 8H), 2.03 (m, 4H), 2.72 (t, 8H), 3.25 (s, 2H), 7.14 (s, 4H), 7.18 (m, 8H), 7.28 (d, 8H, $J = 8.1$ Hz), 7.33 (d, 8H, $J = 8.3$ Hz), 7.52 (d, 8H, $J = 8.3$ Hz), 7.53 (d, 8H, $J = 8.1$ Hz). ^{13}C NMR (CDCl_3) δ : 14.17, 14.39, 22.68, 22.91, 29.40, 29.61, 31.43, 31.82, 32.04, 35.93, 42.79, 53.84, 119.29, 121.96, 125.69, 126.97, 127.07, 127.55, 129.04, 138.24, 138.32, 139.36, 140.22, 140.26, 142.20, 149.64.

F2-An: Yield (0.85 g, 50 %) yellow solid; mp: 169-171 °C; ^1H NMR (CDCl_3) δ : 0.34 (m, 4H), 0.68 (t, 6H), 0.94 (m, 12H), 1.93 (m, 4H), 3.14 (s, 2H), 3.81 (s, 12H), 6.83 (d, 8H, $J = 8.7$ Hz), 6.99 (s, 4H), 7.02 (d, 4H, $J = 7.8$ Hz), 7.08 (d, 4H, $J = 7.8$ Hz), 7.17 (d, 8H, $J = 8.7$ Hz). ^{13}C NMR (CDCl_3) δ : 14.14, 22.59, 22.66, 29.59, 31.40, 42.88, 50.32, 53.73, 55.49, 113.96, 119.07, 121.72, 125.30, 128.34, 134.49, 138.33, 139.73, 149.55, 158.81.

F2-DMT: Yield (0.40 g, 70%) clear solid; mp: 150-153 °C; ^1H NMR (CDCl_3) δ : 0.49 (m, 4H), 0.70 (t, 6H), 0.94 (m, 12H), 1.80 (m, 4H), 2.24 (s, 12H), 2.96 (s, 2H), 3.63 (s, 12H), 3.78 (s, 12H), 6.55 (s, 4H), 6.71 (s, 4H), 7.10 (m 8H), 7.30 (d, 4H, $J = 8.1$ Hz). ^{13}C NMR (CDCl_3) δ : 14.16, 16.40, 22.81, 23.21, 29.90, 31.61, 42.51, 54.28, 56.26, 56.75, 113.67, 115.51, 118.62, 125.60, 126.04, 127.68, 129.54, 136.17, 139.54, 149.51, 150.43, 152.00.

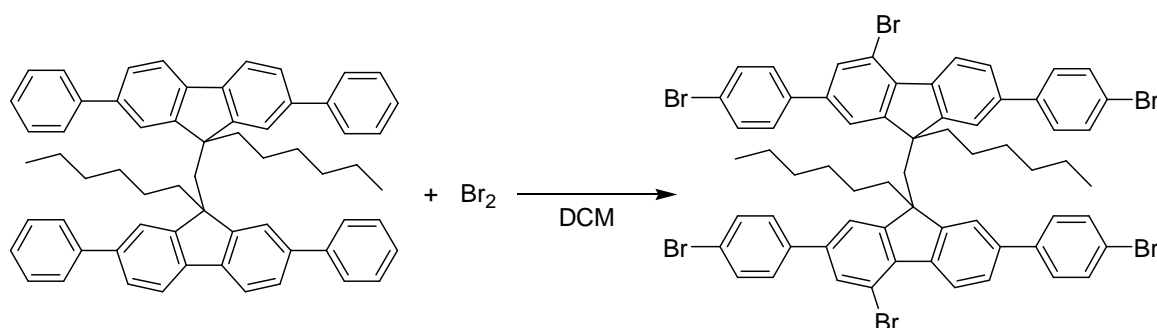
F2-Ver: Yield (0.50 g, 82%) beige solid; mp: 148-150 °C; ^1H NMR (CDCl_3) δ : 0.37 (m, 4H), 0.70 (t, 6H), 0.95 (broad m, 12H), 1.93 (m, 4H), 3.16 (s, 2H), 3.92 (s, 24H), 6.77 (s, 8H), 6.88 (s, 4H), 7.01 (s, 4H), 7.06 (d, 4H, $J = 7.8$ Hz), 7.15 (d, 4H, $J = 7.8$ Hz). ^{13}C NMR (CDCl_3) δ : 14.12, 22.61, 29.50, 31.37, 42.83, 53.89, 56.14, 56.21, 110.66, 111.31, 119.15, 119.72, 121.87, 125.37, 134.73, 138.57, 139.77, 148.40, 149.05, 149.73.

Attempted cyclization of F2-Ver with FeCl₃.



To a stirred solution of F2-Veratrole (0.40 g, 0.38 mmol) in dichloromethane (50 mL), anhydrous ferric chloride (0.49 g, 3.04 mmol) is added and the resulting solution is allowed to stir overnight. The reaction is then quenched with methanol (30 mL) and washed with water (3 x 50 mL). The organic layer is then separated, dried over anhydrous magnesium sulfate, passed over a short pad of silica gel, evaporated, and dried under vacuum. The crude solid was recrystallized from a dichloromethane/methanol mixture to give a brown solid. Yield (0.37 g, 93%); mp: 100-102 °C; ¹H NMR (CDCl₃) δ: 0.45 (m, 4H), 0.70 (t, 6H), 0.94 (m, 12H), 1.84 (m, 4H), 3.14 (s, 2H), 3.88 (s, 12H), 3.90 (s, 12H), 6.62 (s, 4H), 6.90 (s, 4H), 6.99 (m, 8H), 7.28 (m, 4H). ¹³C NMR (CDCl₃) δ: 14.13, 22.64, 23.03, 29.59, 31.57, 43.31, 53.62, 53.95, 56.39, 113.03, 114.49, 118.84, 123.61, 125.33, 127.90, 133.08, 136.99, 139.98, 147.71, 148.63, 149.54.

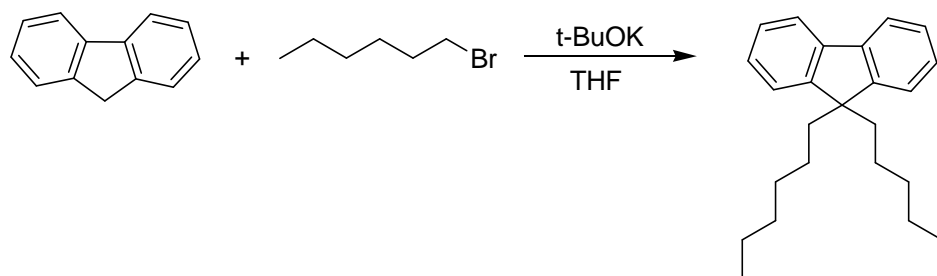
Procedure for the Synthesis of F2-Ph-Br₆



With the intentions of synthesizing higher homologues of the **F2-Ar** series via a tetrabromo **F2-Ph** derivative, the bromination of **F2-Ph** was carried out as follows. In a Schlenk flask equipped with a dropping funnel, **F2-Ph** (0.50 g, 0.61 mmol) was dissolved in dichloromethane (25 mL). To this a solution of bromine (0.40 g, 2.5 mmol) in dichloromethane (5 mL) was added dropwise and the resulting dark red solution was allowed to stir for 2 hours after which time it was quenched with aqueous potassium hydroxide (50 mL) and extracted with dichloromethane (3 x 20 mL). The combined organic extracts were dried over anhydrous magnesium sulfate, evaporated and dried under vacuum. The resulting solid was recrystallized from a dichloromethane/methanol mixture to afford a beige colored solid which was confirmed to be a mixture of both the *cis* and *trans* hexabrominated **F2-Ph** derivative as established by $^1\text{H}/^{13}\text{C}$ NMR

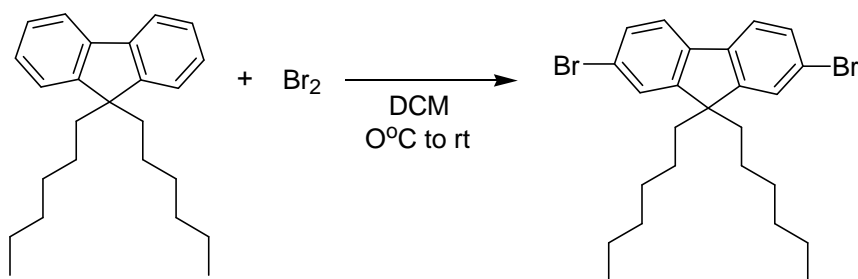
Spectroscopy as well as X-ray crystallography. Yield (0.63 g, 80%); ^1H NMR (CDCl_3) δ : 0.23 (m, 4H), 0.70 (t, 6H), 0.94 (m, 12H), 1.97 (m, 4H), 3.08 (s, 2H), 6.90 (d, 4H, $J = 10.6$ Hz), 7.03 (t, 6H, $J = 7.6$ Hz), 7.12 (d, 2H, $J = 8.2$ Hz), 7.27 (s, 2H), 7.48 (m, 8H), 8.04 (d, 2H, $J = 8.2$ Hz). ^{13}C NMR (CDCl_3) δ : 14.13, 22.36, 22.60, 29.40, 31.32, 42.30, 53.81, 116.69, 120.29, 121.24, 121.46, 121.95, 122.88, 125.62, 128.54, 128.86, 130.97, 131.85, 132.01, 138.08, 138.26, 138.43, 138.57, 139.42, 139.95, 149.65, 152.21.

Preparation of **F1**.



In an oven dried schlenk flask under argon, fluorene (10 g, 60.2 mmol) is dissolved in tetrahydrofuran (250 mL). To this solution, potassium *tert*-butoxide (14.85 g, 132.44 mmol) and 1-bromohexane (21.8 g, 132.44 mmol) are added sequentially, the resulting light blue solution is allowed to stir for 2 hours at room temperature. The solution is then quenched with water (200 mL) and extracted with dichloromethane (3 x 30 mL). The combined organic extracts are dried over anhydrous magnesium sulfate, filtered, evaporated under reduced pressure and dried under vacuum to produce a yellow liquid that is used without further purification. Yield (20.13 g, >99%); ^1H NMR (CDCl_3) δ : 0.74 (m, 4H), 0.86 (t, 6H), 1.15 (m, 12H), 2.07 (m, 4H), 7.37-7.43 (m, 6H), 7.79 (m, 2H). ^{13}C NMR (CDCl_3) δ : 14.22, 22.80, 23.93, 29.96, 31.72, 40.65, 55.19, 119.83, 122.99, 126.88, 127.18, 141.31, 150.84

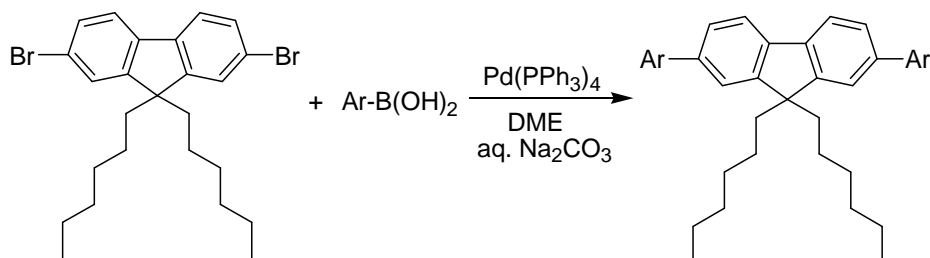
Preparation of F1-Br.



In an oven dried schlenk flask equipped with a dropping funnel, F1 (10.0 g, 29.9 mmol) is dissolved in dichloromethane (100 mL) and cooled to 0°C using an ice bath. A solution of bromine (9.55 g, 59.8 mmol) in dichloromethane (10 mL) is added dropwise. The resulting dark red solution is taken off the ice bath and allowed to stir for 1 hour after which time it is quenched with aqueous potassium hydroxide (100 mL) and extracted with dichloromethane (3 x 20 mL). The combined organic extracts were dried over

anhydrous magnesium sulfate, evaporated, and dried under vacuum to give a yellow oil which is recrystallized from a dichloromethane/methanol mixture to afford a yellow solid that is used without further purification. Yield (12.0 g, 82%); mp: 62-64 °C; ^1H NMR (CDCl_3) δ : 0.60 (m, 4H), 0.79 (t, 6H), 1.06 (m, 12H), 1.93 (m, 4H), 7.44-7.47 (m, 4H), 7.52 (d, 2H, $J = 8.6$ Hz). ^{13}C NMR(CDCl_3) δ : 14.21, 22.78, 23.84, 29.78, 31.65, 40.40, 55.87, 121.32, 121.67, 126.35, 130.34, 139.24, 152.73.

Synthesis of Various F1-Ar.



Solid F1-Br and the corresponding aryl boronic acid (3 equiv.) were dissolved in anhydrous 1,2-dimethoxyethane (DME) (30 mL) in an oven dried Schlenk flask under an argon atmosphere and the flask was evacuated and filled with argon (3x). In another oven dried Schlenk flask a solution of anhydrous sodium carbonate (5.0 g) in water (20 mL) was prepared under an argon atmosphere and the flask was also evacuated and filled with argon (3x). To the DME solution, $\text{Pd(PPh}_3)_4$ (50 mg) and the salt solution were added sequentially under a strict argon atmosphere followed by evacuation and filling the flask with argon (3x) after each addition. The flask was covered with foil and the solution was allowed to reflux overnight. The resulting solution was cooled to room temperature, quenched with 5% HCl (50 mL) and extracted with dichloromethane (3 x 20 mL). The organic layer was dried over anhydrous magnesium sulfate, evaporated and dried under

vacuum. The various F1-Ar were purified by column chromatography over silica gel using an ethyl acetate/hexanes mixture as the eluent to afford the pure F1-Ar.

F1-Ph: Yield (0.77 g, 78%) colorless solid; mp: 47-49 °C; ^1H NMR (CDCl_3) δ : 0.85 (m, 10H), 1.15 (m, 12H), 2.14 (m, 4H), 7.44 (t, 2H, $J = 7.3$ Hz), 7.56 (t, 4H, $J = 7.9$ Hz), 7.68 (m, 4H), 7.77 (d, 4H, $J = 7.9$ Hz), 7.86 (d, 2H, $J = 8.3$ Hz). ^{13}C NMR (CDCl_3) δ : 14.22, 22.80, 24.01, 29.94, 31.68, 40.70, 55.47, 120.21, 121.72, 126.26, 127.32, 127.40, 128.99, 140.26, 140.27, 141.90, 151.86.

F1-Tol: Yield (0.83 g, 79%) white solid; mp: 83-85 °C; ^1H NMR (CDCl_3) δ : 0.81 (m, 10H), 1.12 (m, 12H), 2.09 (m, 4H), 2.47 (s, 6H), 7.34 (d, 4H, $J = 7.7$ Hz), 7.63 (m, 8H), 7.80 (d, 2H, $J = 7.6$ Hz). ^{13}C NMR (CDCl_3) δ : 14.22, 21.34, 22.80, 23.99, 29.94, 31.67, 40.69, 55.40, 120.10, 121.53, 126.00, 127.23, 129.70, 137.07, 139.05, 140.06, 140.09, 151.80.

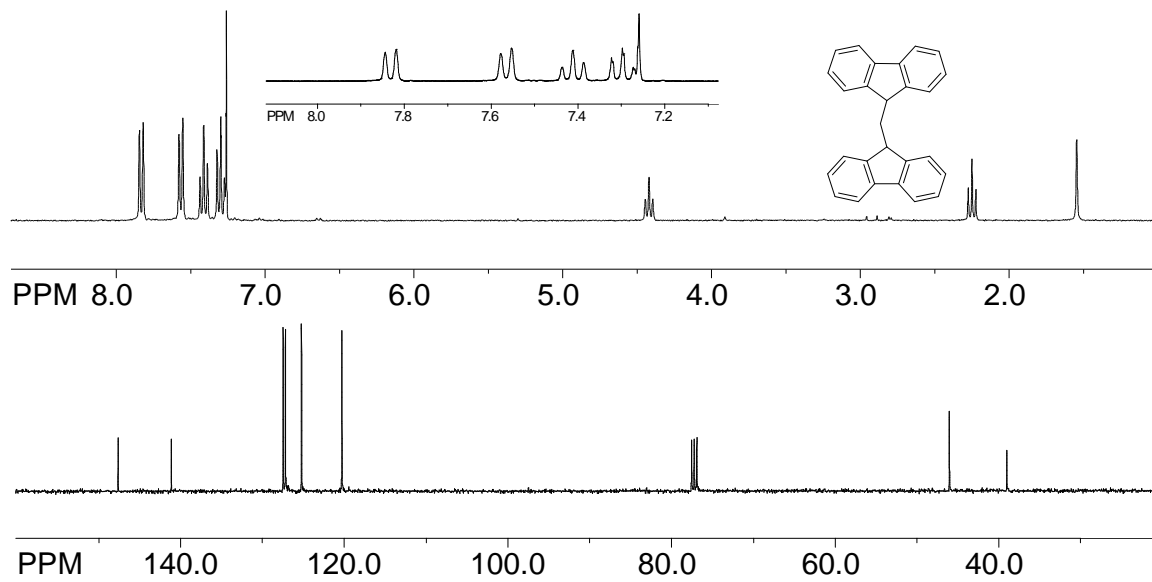
F1-BP: Yield (1.04 g, 80%) yellow solid; mp: 168-170 °C; ^1H NMR (CDCl_3) δ : 0.77 (m, 10H), 1.09 (m, 12H), 2.08 (m, 4H), 7.39 (t, 2H, $J = 7.2$ Hz), 7.49 (t, 4H, $J = 7.2$ Hz), 7.64 (d, 4H, $J = 5.9$ Hz), 7.68 (d, 4H, $J = 8.5$ Hz), 7.73 (d, 4H, $J = 8.5$ Hz), 7.79 (d, 4H, $J = 8.5$ Hz), 7.81 (d, 2H, $J = 7.9$ Hz). ^{13}C NMR (CDCl_3) δ : 14.23, 22.82, 24.03, 29.95, 31.70, 40.73, 55.52, 120.29, 121.61, 126.16, 127.27, 127.56, 127.75, 129.06, 139.72, 140.20, 140.37, 140.79, 140.97, 151.95.

FI-BPH: Yield (0.60 g, 49%) white solid; mp: 104-106 °C; ^1H NMR(CDCl_3) δ : 0.77 (m, 10H), 0.92 (m, 6H), 1.07 (m, 12H), 1.36 (m, 12H), 1.68 (m, 4H), 2.08 (m, 4H), 2.68 (t, 4H), 7.30 (d, 4H, $J = 8.2$ Hz), 7.60 (d, 4H, $J = 8.0$ Hz), 7.63-7.67 (m, 4H), 7.72 (d, 4H, $J = 8.4$ Hz), 7.77 (d, 4H, $J = 8.4$ Hz), 7.80 (d, 2H, $J = 7.8$ Hz). ^{13}C NMR (CDCl_3) δ : 14.23, 14.36, 22.82, 22.86, 24.03, 29.31, 29.96, 31.70, 31.74, 31.99, 35.88, 40.74, 55.50, 120.25, 121.57, 126.12, 127.09, 127.56, 127.68, 129.12, 138.25, 139.77, 140.17, 140.32, 140.46, 142.47, 151.92.

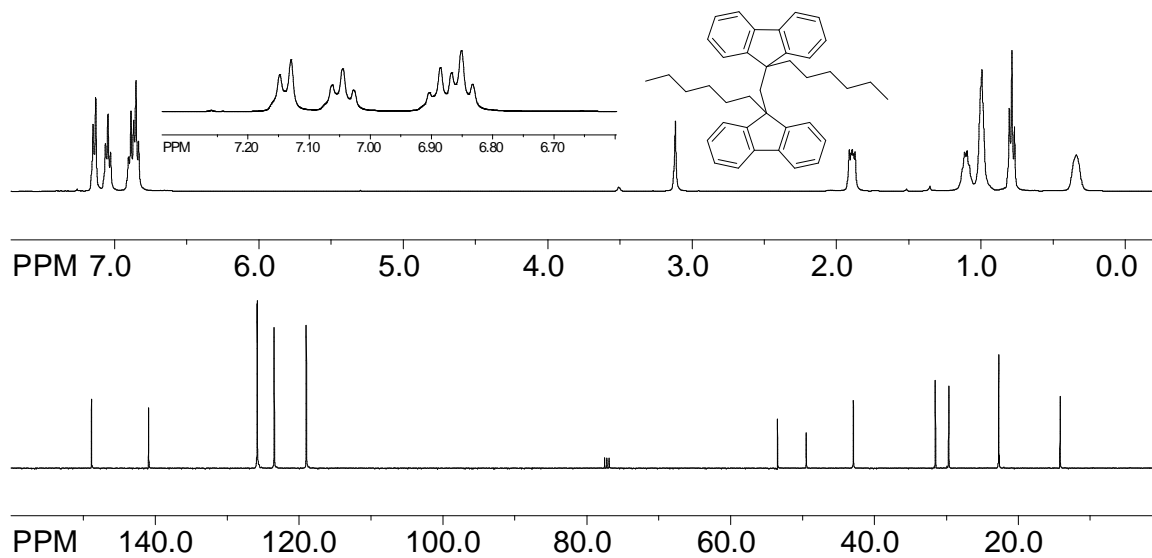
FI-An: Yield (0.62 g, 86%) yellow solid; mp: 101-102 °C; ^1H NMR (CDCl_3) δ : 0.76 (m, 10H), 1.07-1.17 (m, 12H), 2.03 (m, 4H), 3.87 (s, 6H), 7.02 (d, 4H, $J = 8.8$ Hz), 7.53 (d, 4H, $J = 8.8$ Hz), 7.62 (d, 4H, $J = 8.8$ Hz), 7.73 (d, 4H, $J = 7.7$ Hz). ^{13}C NMR (CDCl_3) δ : 14.22, 22.80, 23.99, 29.94, 31.67, 40.67, 55.37, 55.58, 114.41, 120.05, 121.25, 125.75, 128.38, 131.48, 139.71, 139.77, 151.77, 159.23.

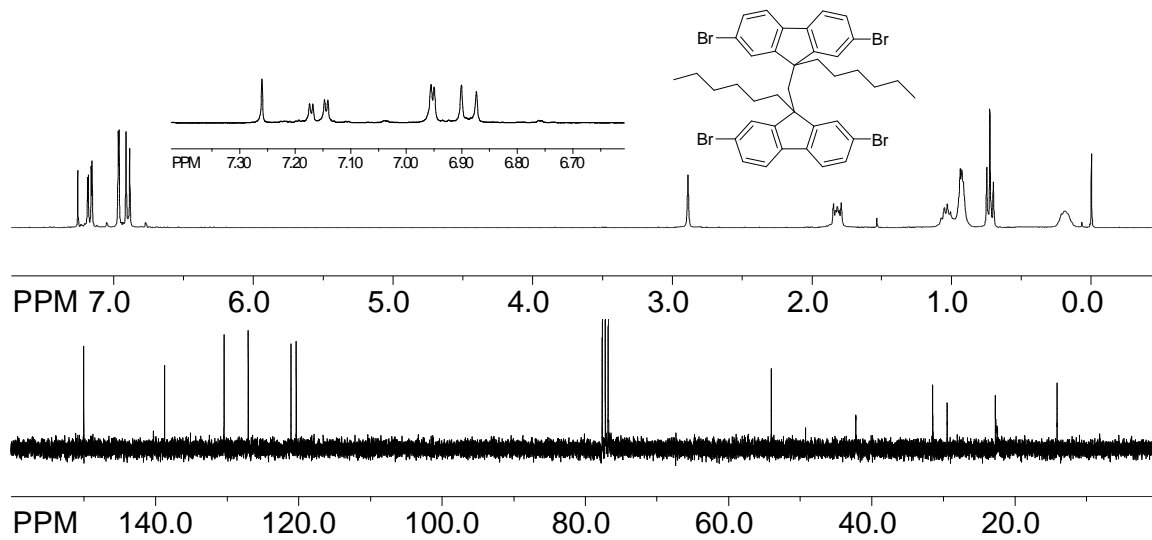
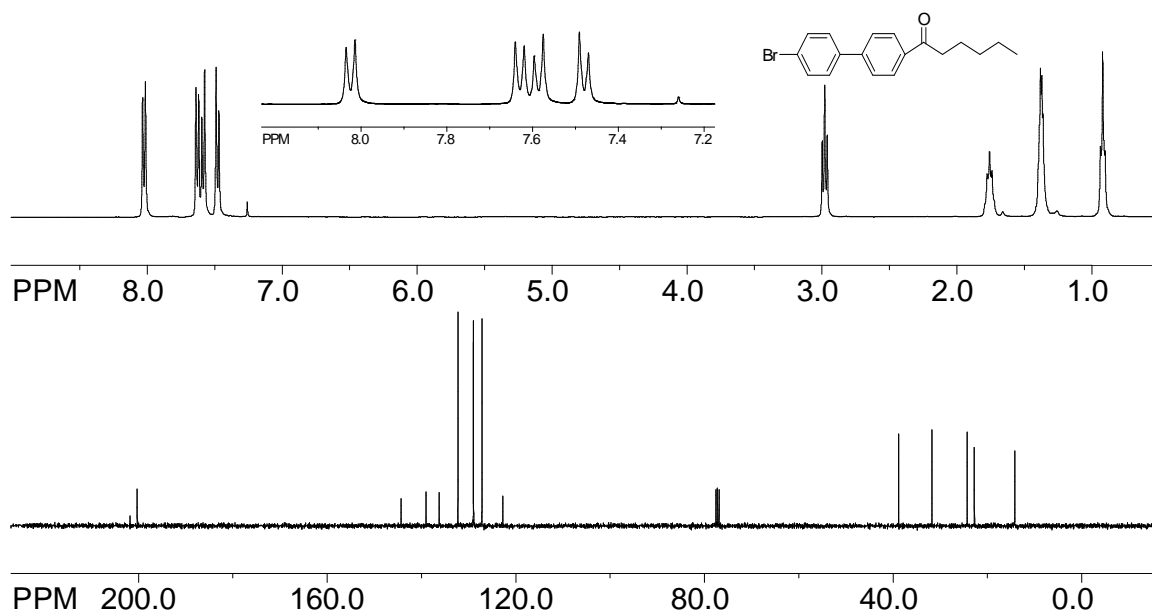
3.5 EXPERIMENTAL SPECTRA

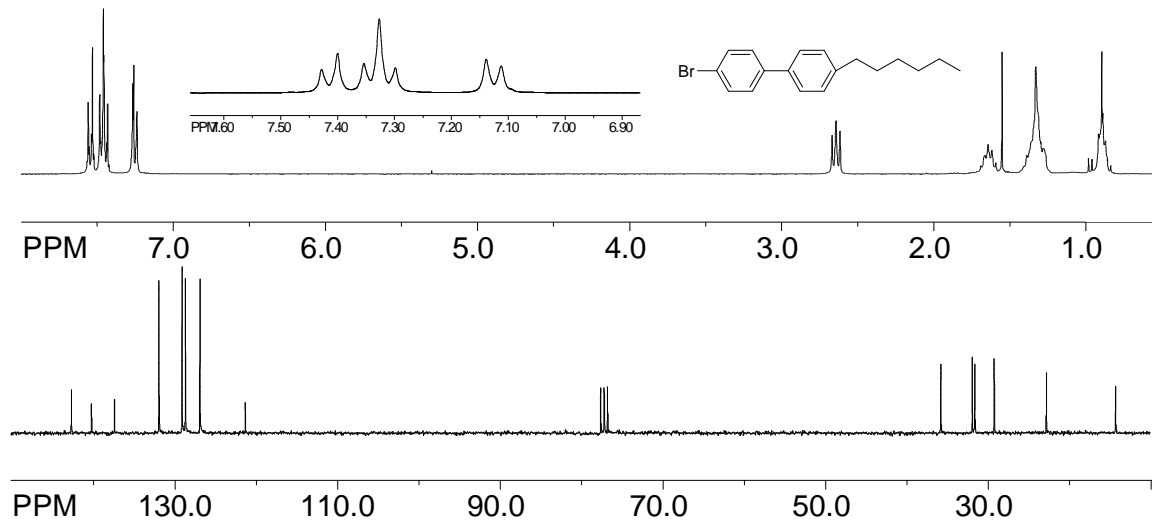
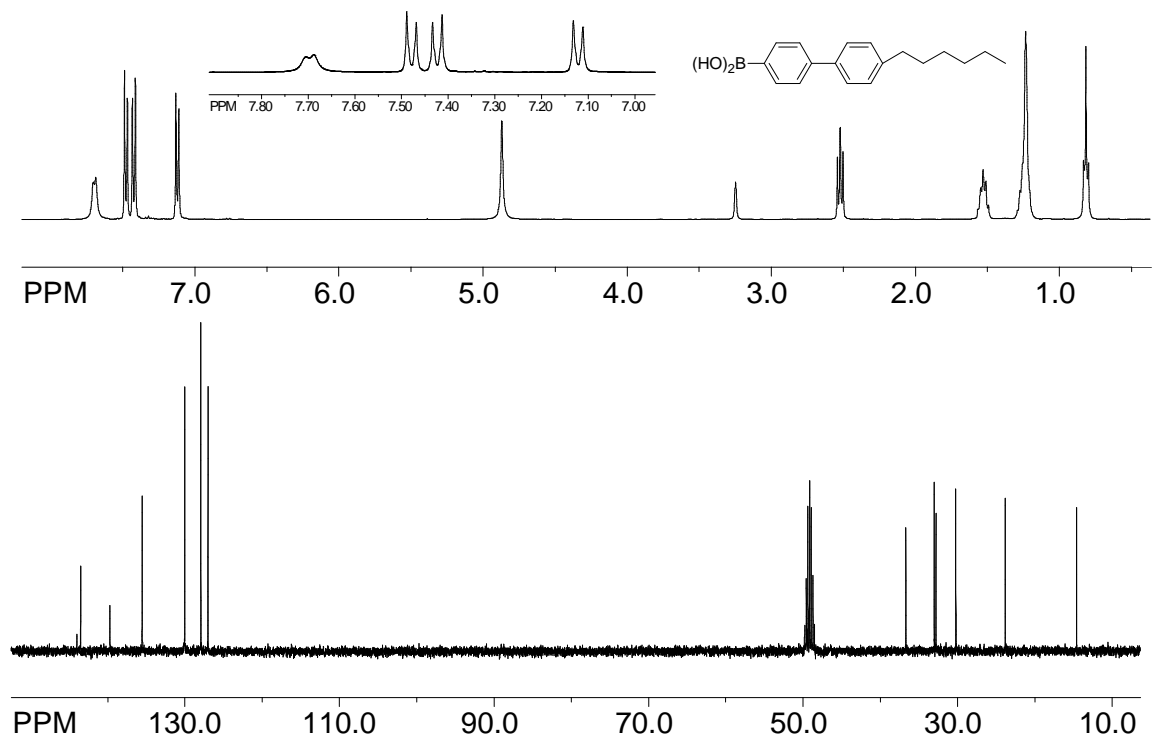
^1H and ^{13}C NMR Spectra of F2-H2

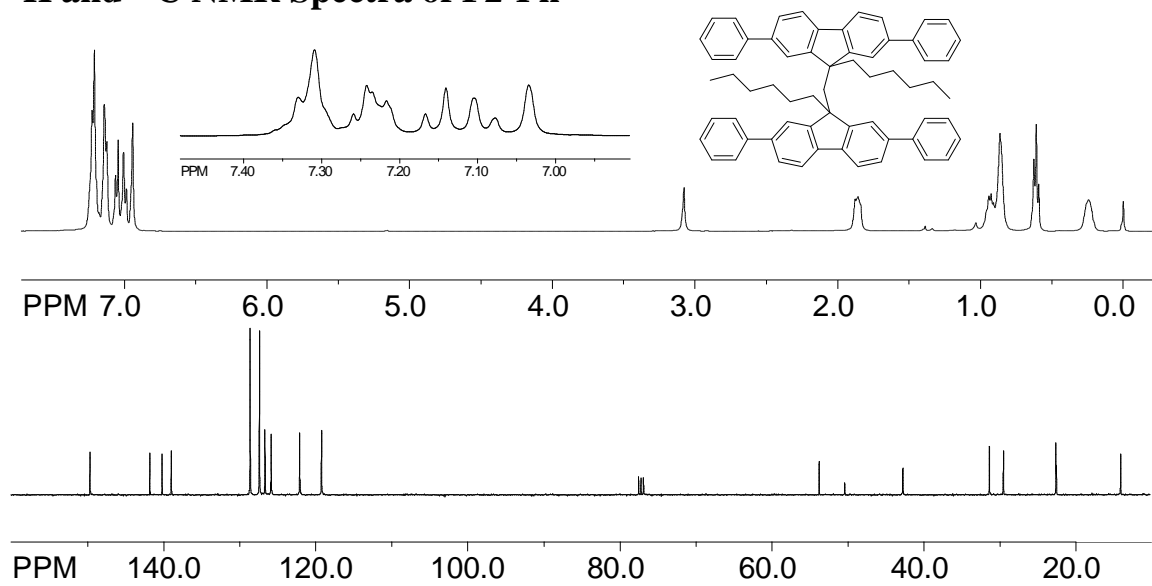
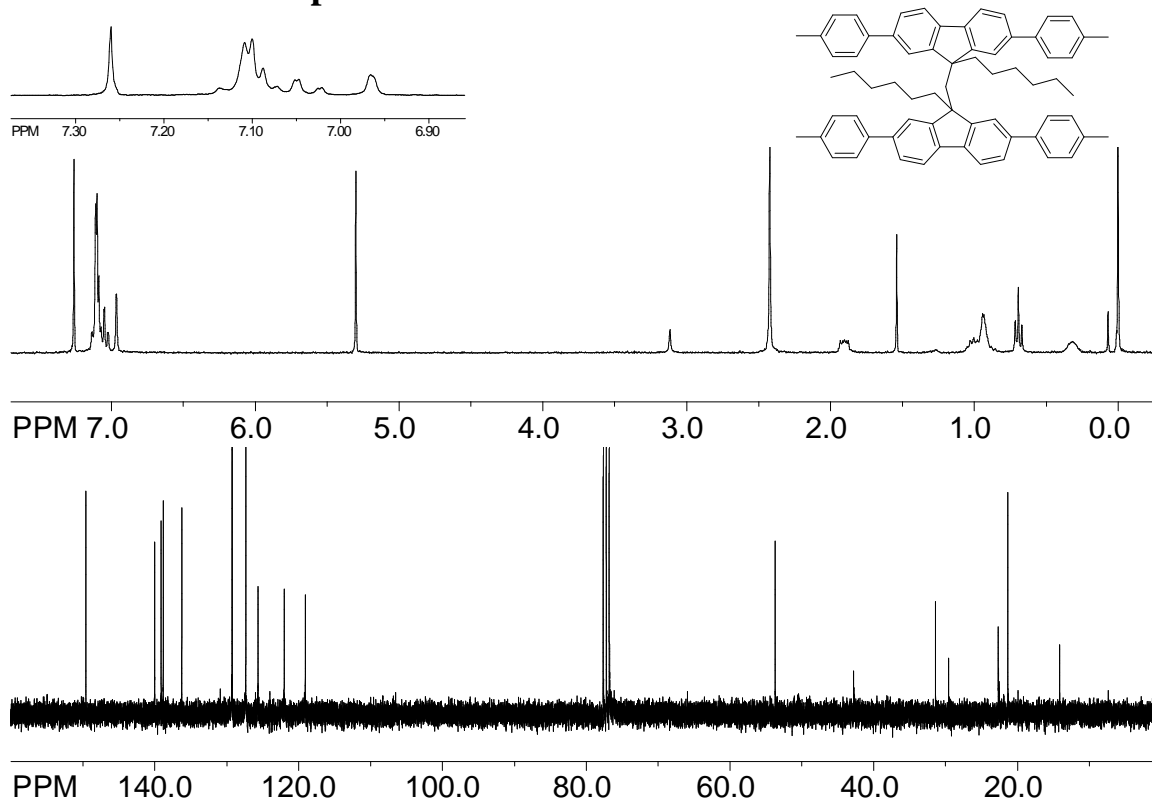


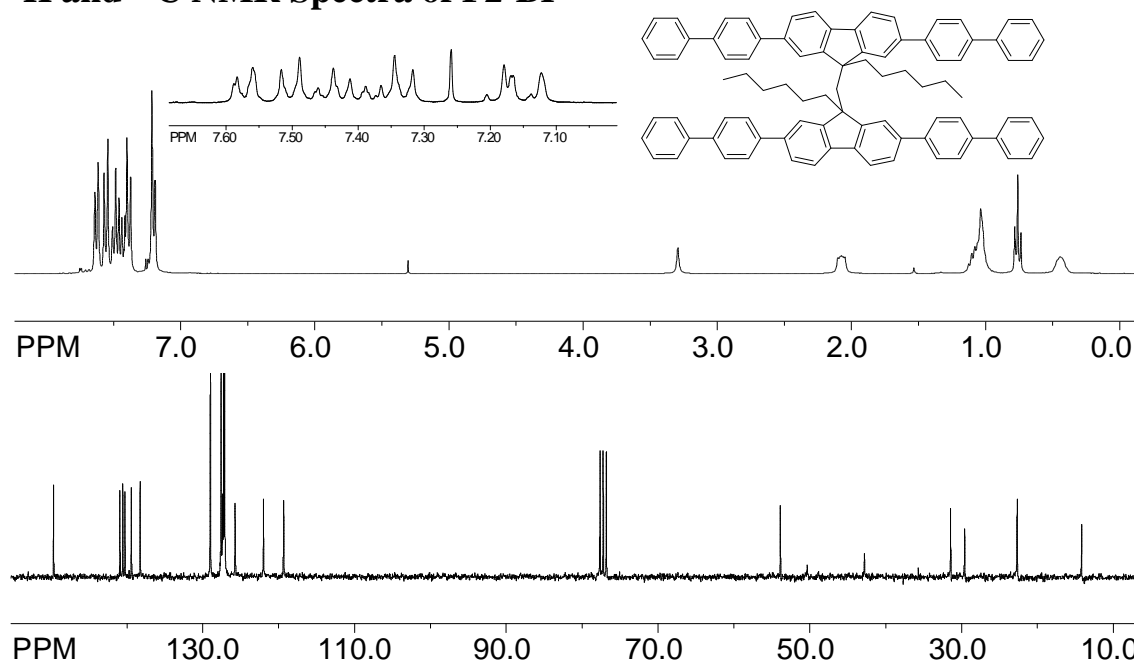
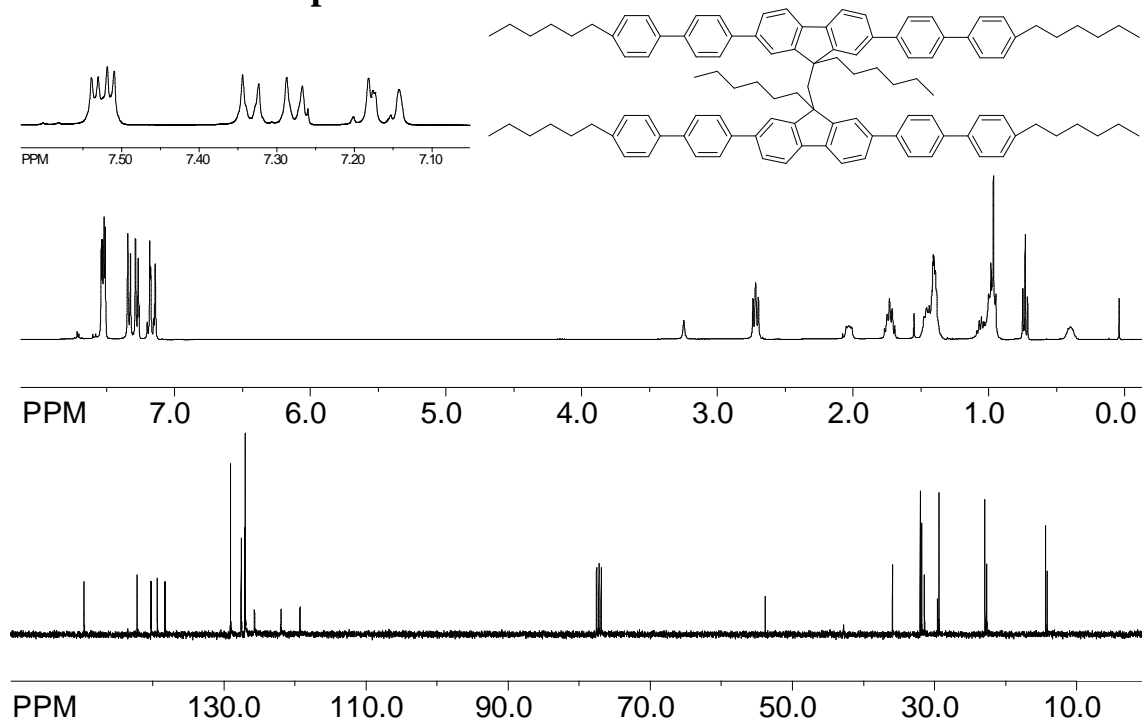
^1H and ^{13}C NMR Spectra of F2



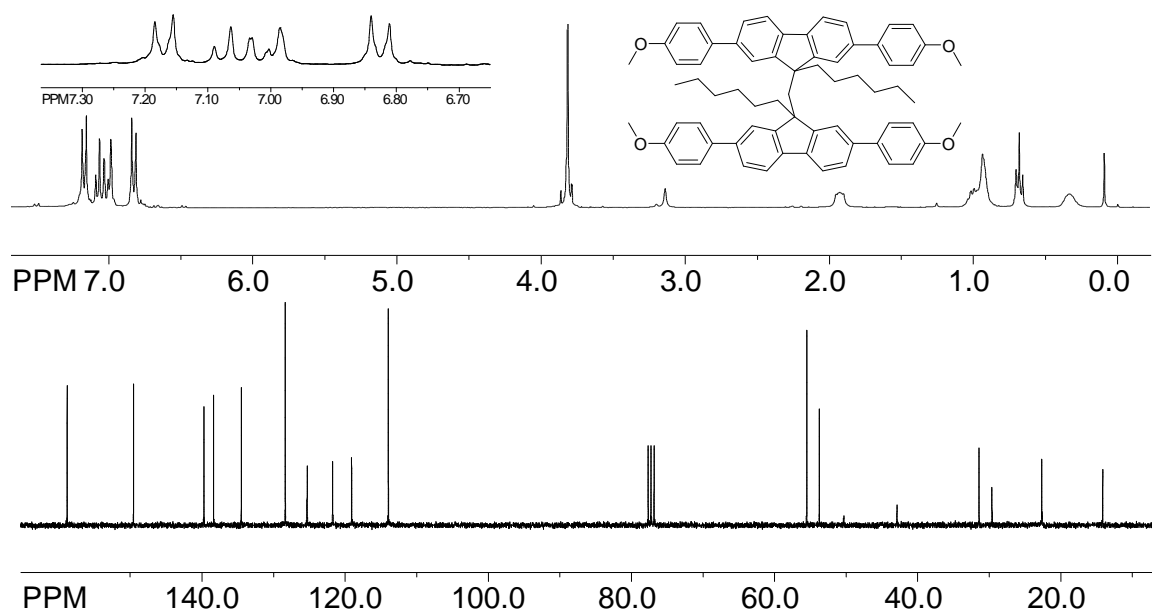
^1H and ^{13}C NMR Spectra of F2-Br **^1H and ^{13}C NMR Spectra of 1-(4'-Bromobiphenyl-4-yl)-hexan-1-one**

^1H and ^{13}C NMR Spectra of 4-Bromo-4'-hexylbiphenyl **^1H and ^{13}C NMR Spectra of 4'-hexyl-4-biphenylboronic acid**

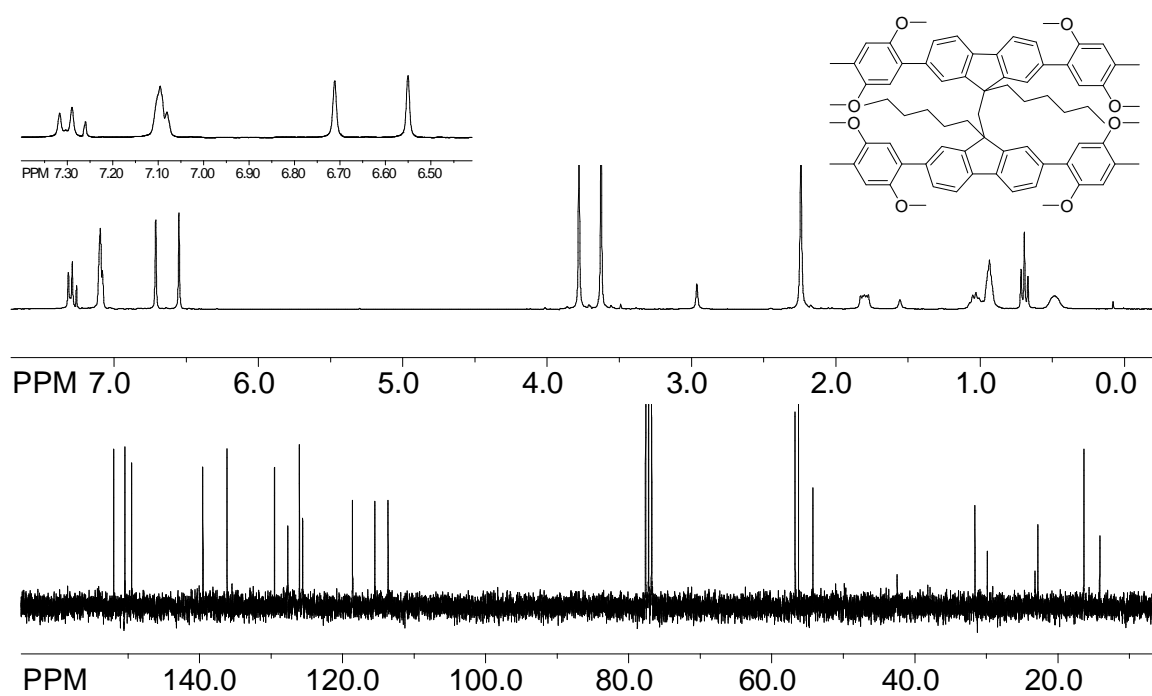
^1H and ^{13}C NMR Spectra of F2-Ph **^1H and ^{13}C NMR Spectra of F2-Tol**

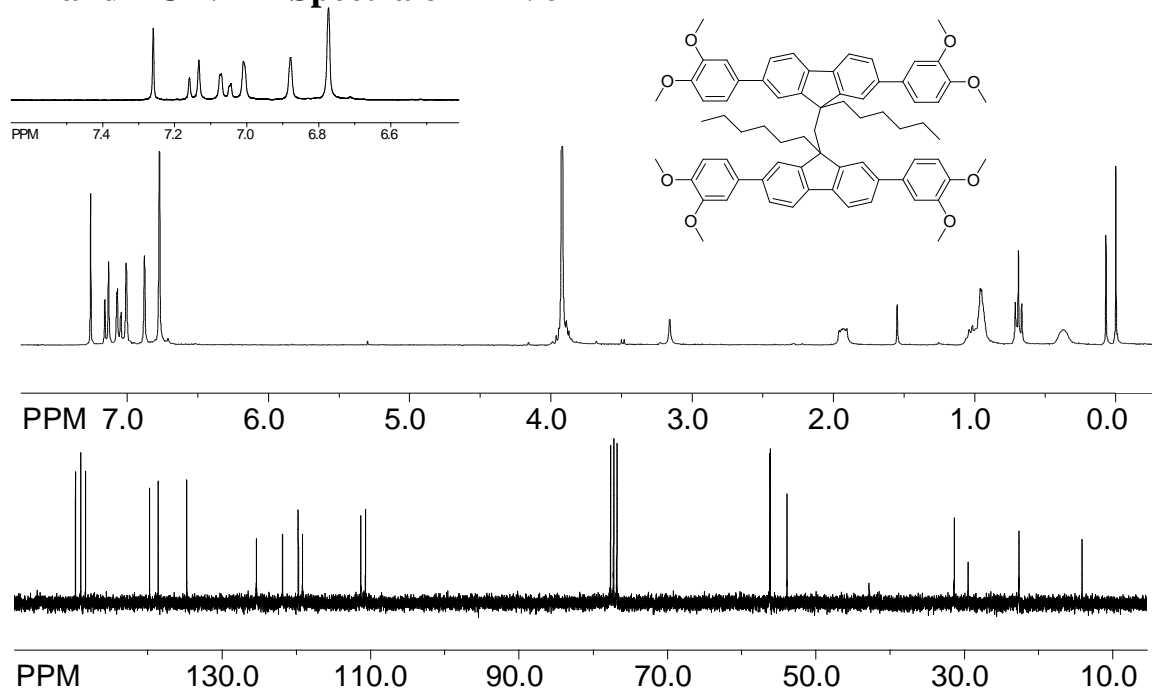
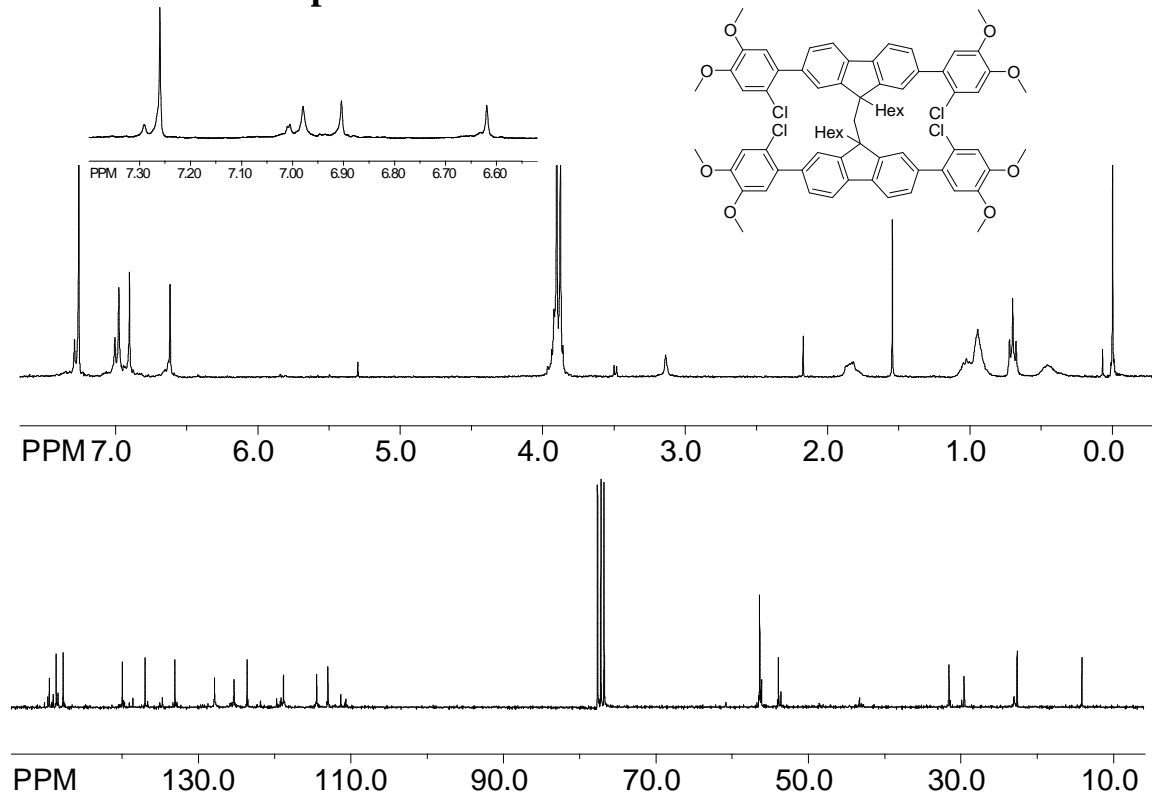
^1H and ^{13}C NMR Spectra of F2-BP **^1H and ^{13}C NMR Spectra of F2-BPH**

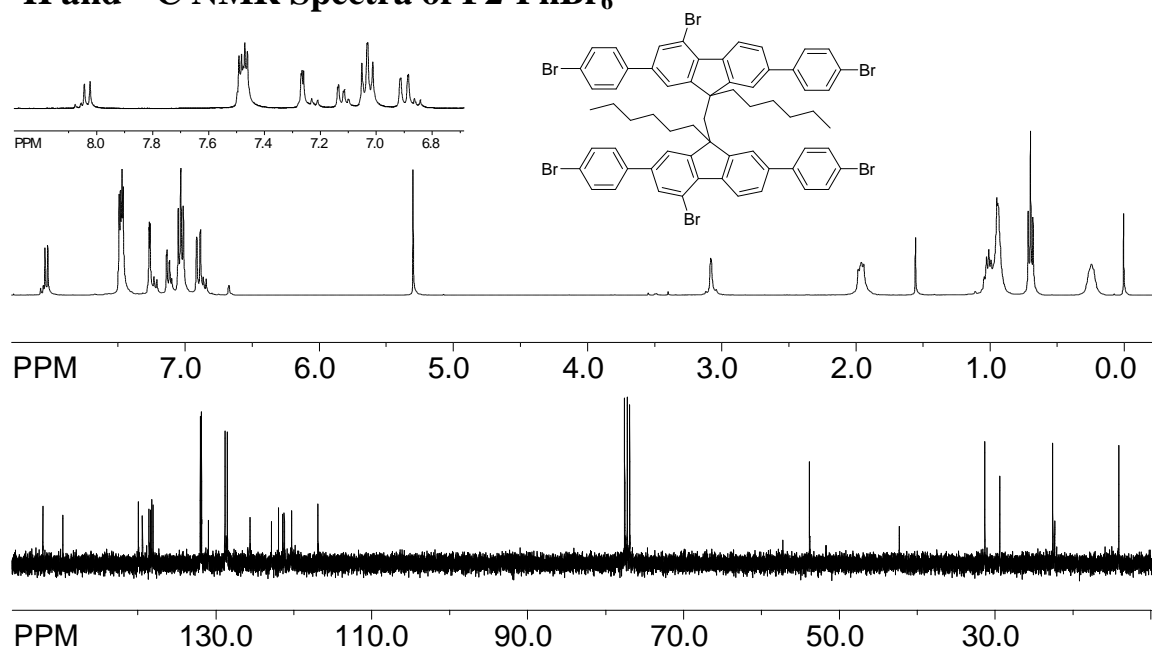
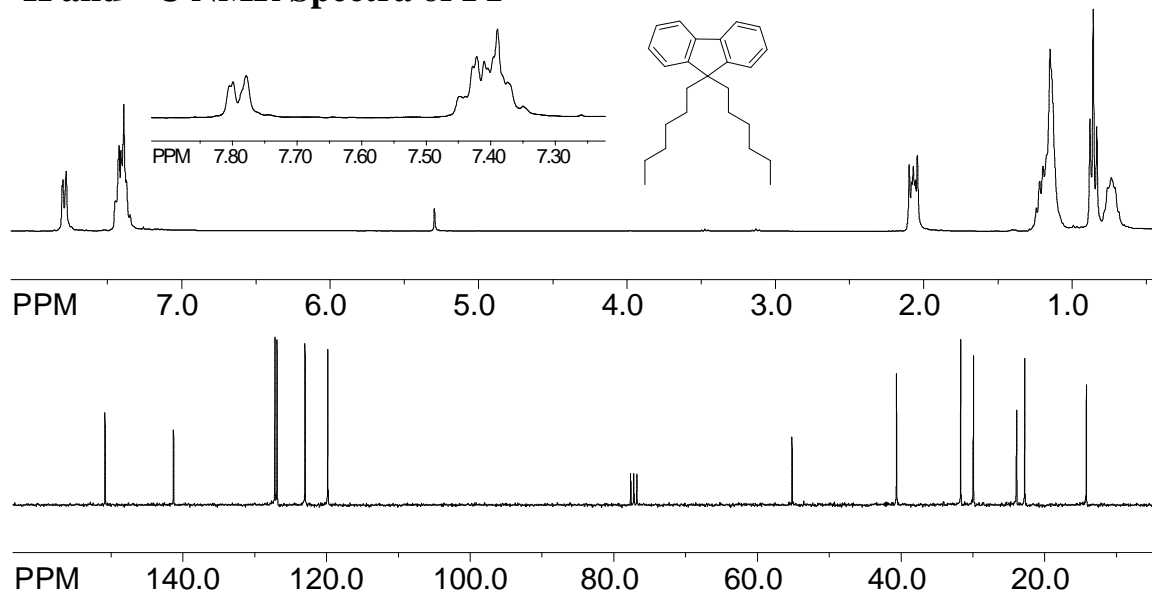
^1H and ^{13}C NMR Spectra of F2-An

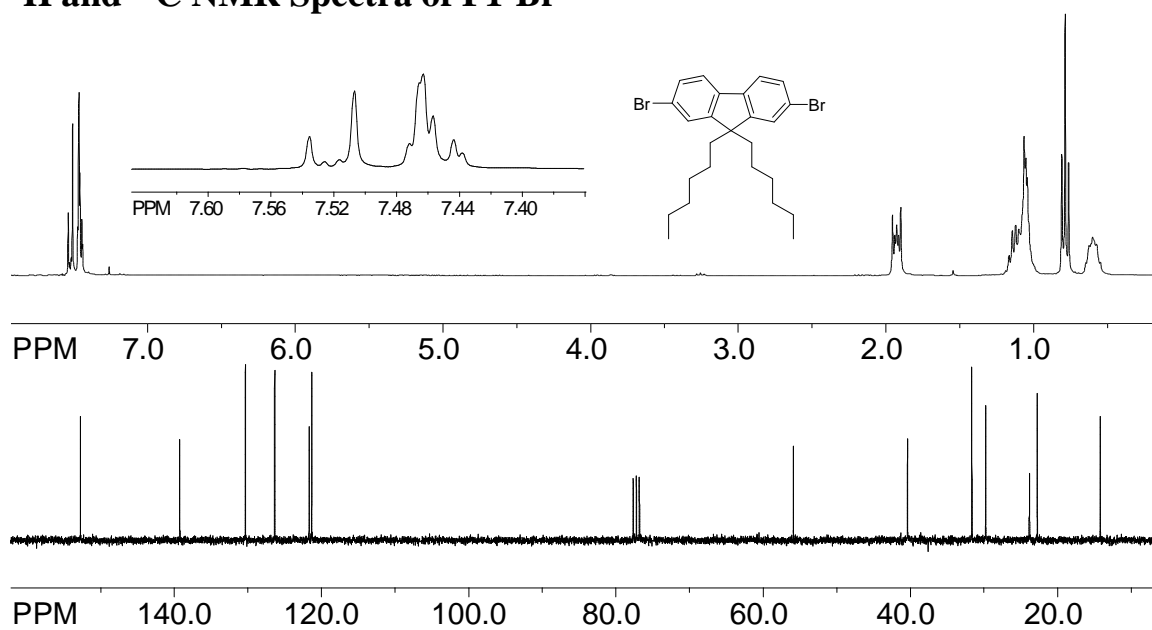
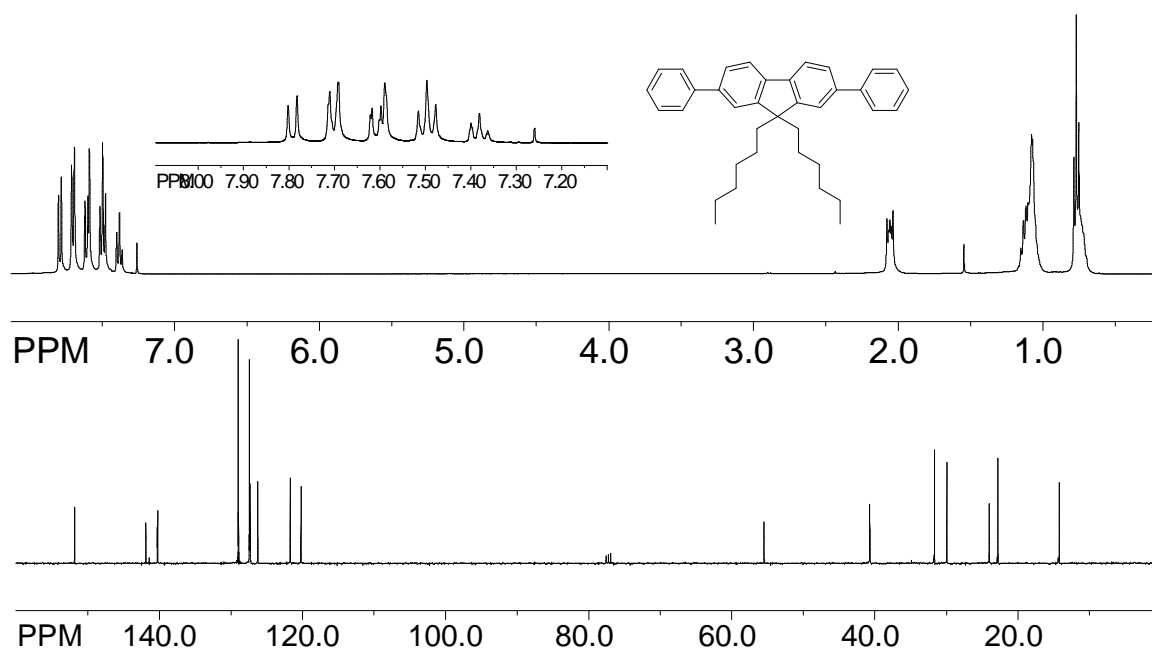


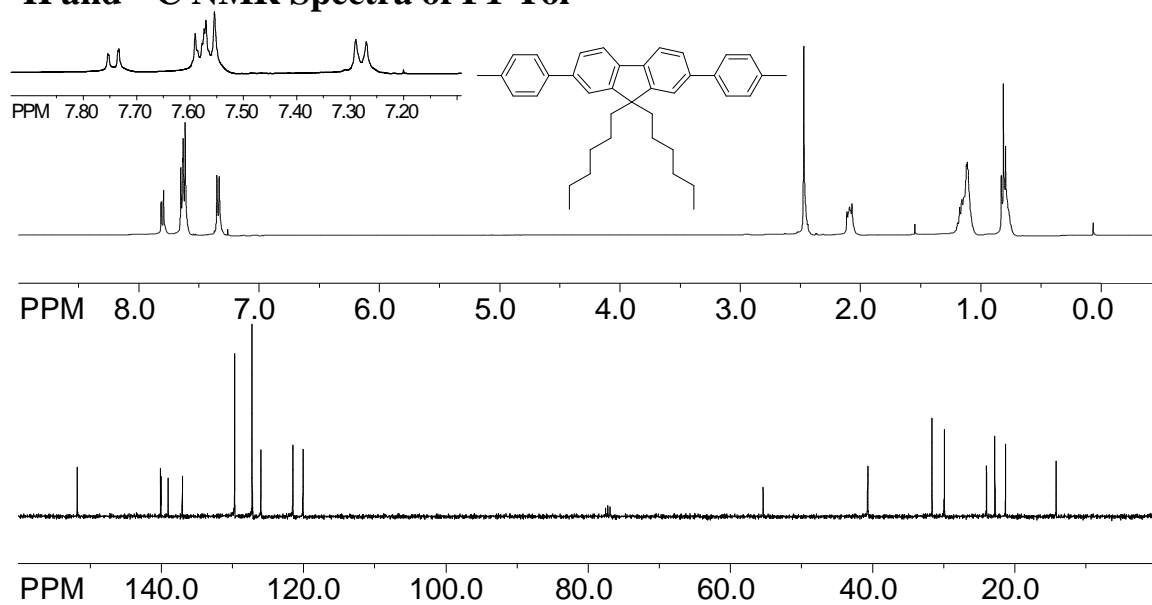
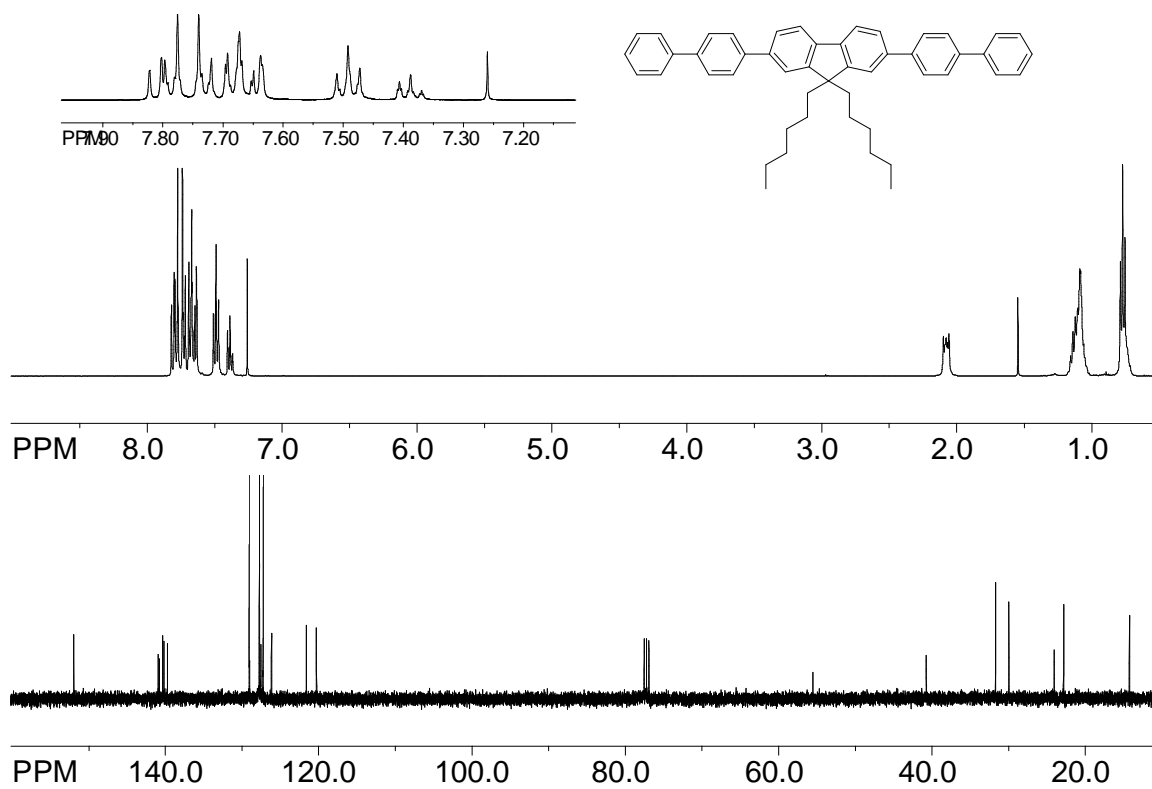
^1H and ^{13}C NMR Spectra of F2-DMT



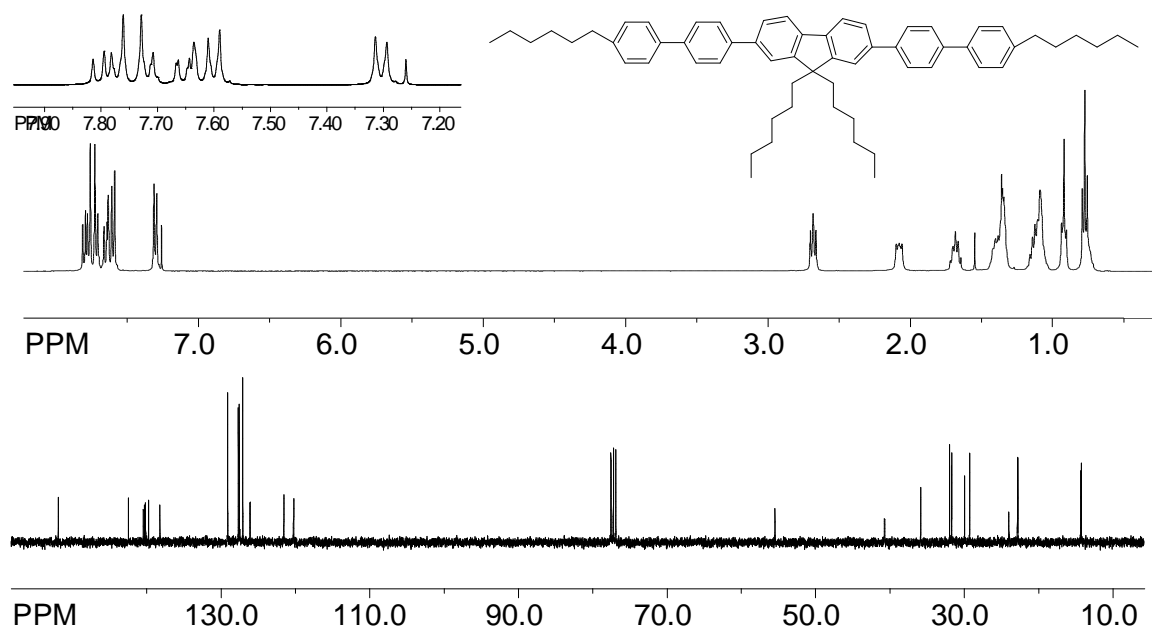
^1H and ^{13}C NMR Spectra of F2-Ver **^1H and ^{13}C NMR Spectra of F2-Ver-Cl**

^1H and ^{13}C NMR Spectra of F2-PhBr₆ **^1H and ^{13}C NMR Spectra of F1**

^1H and ^{13}C NMR Spectra of F1-Br **^1H and ^{13}C NMR Spectra of F1-Ph**

^1H and ^{13}C NMR Spectra of F1-Tol **^1H and ^{13}C NMR Spectra of F1-BP**

^1H and ^{13}C NMR Spectra of F1-BPH



^1H and ^{13}C NMR Spectra of F1-An

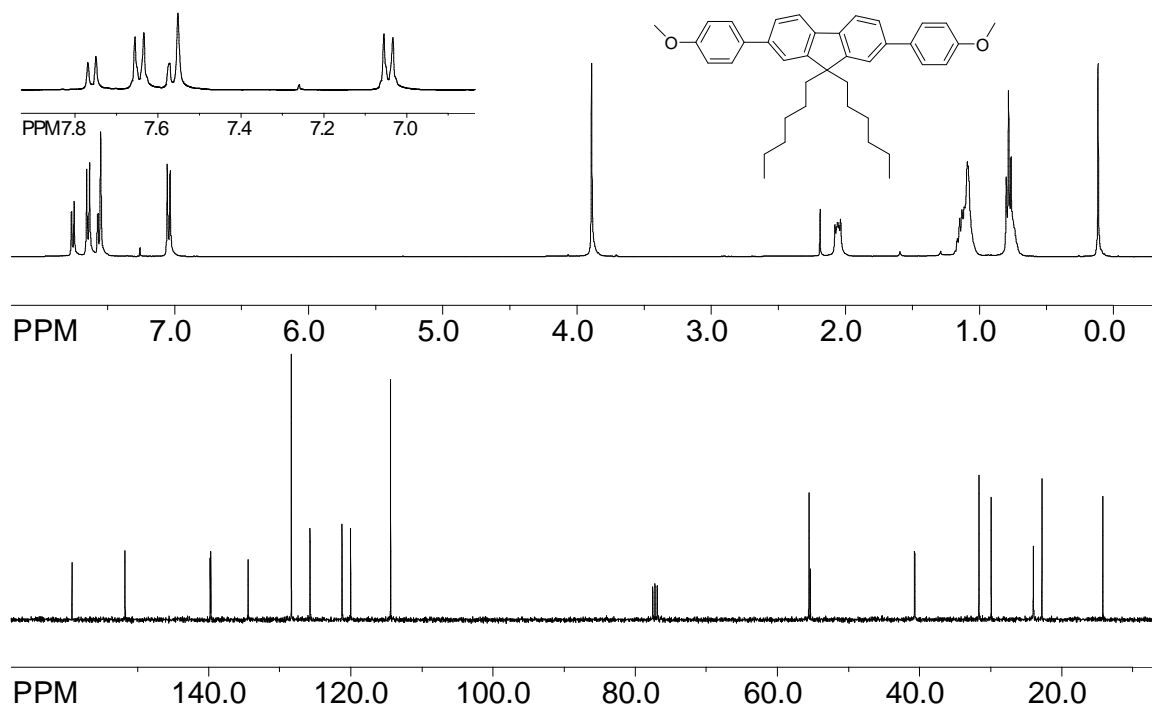
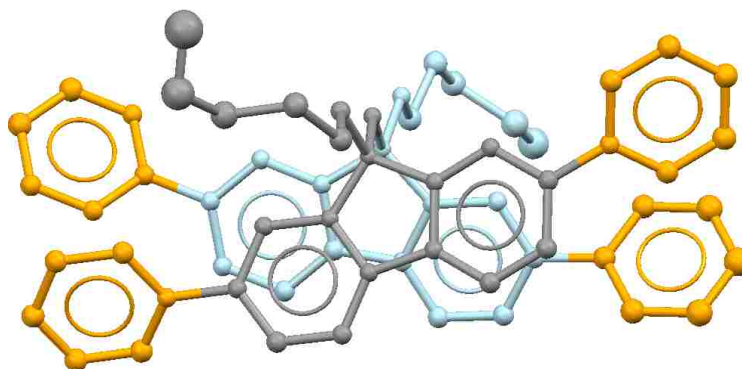
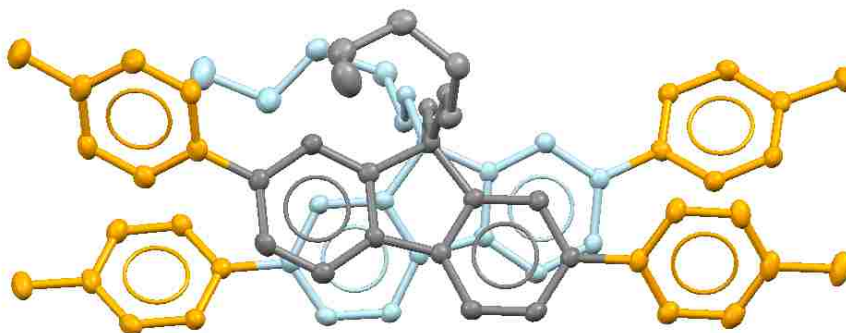
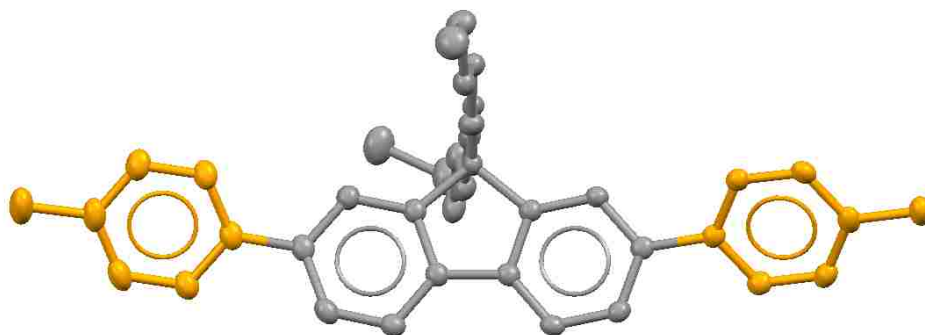


Table 18. Crystal data and structure refinement for raj11b (F2-Ph).

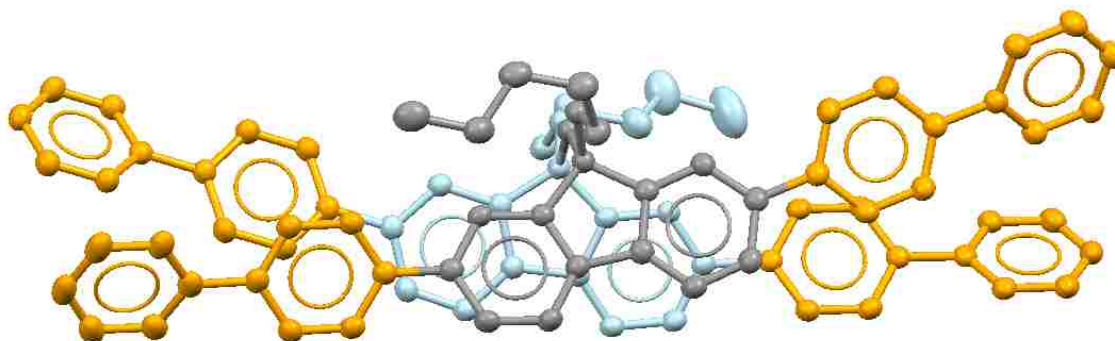
Identification code	raj11b	
Empirical formula	C ₆₃ H ₆₀	
Formula weight	817.11	
Temperature	100(2) K	
Wavelength	0.71073 Å	
Crystal system	Monoclinic	
Space group	P 2/n	
Unit cell dimensions	a = 17.048(2) Å	α = 90°.
	b = 21.875(3) Å	β = 91.537(2)°.
	c = 24.758(3) Å	γ = 90°.
Volume	9229.4(18) Å ³	
Z	8	
Density (calculated)	1.176 Mg/m ³	
Absorption coefficient	0.066 mm ⁻¹	
F(000)	3504	
Crystal size	0.23 x 0.21 x 0.21 mm ³	
Theta range for data collection	0.93 to 32.12°.	
Index ranges	-25 ≤ h ≤ 25, 0 ≤ k ≤ 32, 0 ≤ l ≤ 37	
Reflections collected	151550	
Independent reflections	30595 [R(int) = 0.0546]	
Completeness to theta = 32.12°	98.5 %	
Absorption correction	Semi-empirical from equivalents	
Max. and min. transmission	0.9863 and 0.9850	
Refinement method	Full-matrix least-squares on F ²	
Data / restraints / parameters	30595 / 363 / 1027	
Goodness-of-fit on F ²	1.035	
Final R indices [I > 2σ(I)]	R1 = 0.1020, wR2 = 0.2484	
R indices (all data)	R1 = 0.1475, wR2 = 0.2734	
Largest diff. peak and hole	0.743 and -0.496 e.Å ⁻³	

Table 19. Crystal data and structure refinement for raj111 (F2-Tol).

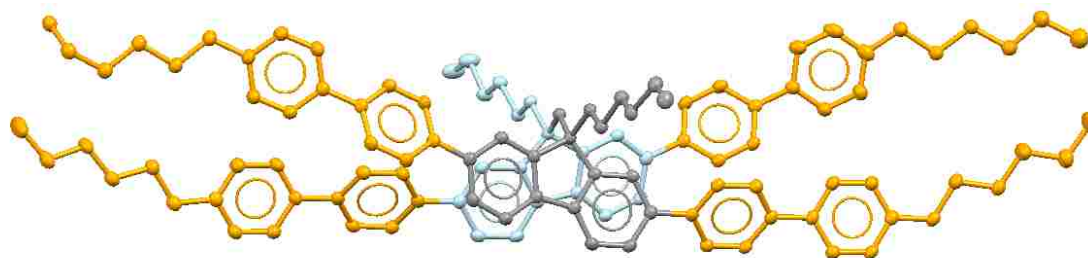
Identification code	raj111	
Empirical formula	C _{68.91} H _{71.82} Cl _{3.82}	
Formula weight	1035.54	
Temperature	100(2) K	
Wavelength	1.54178 Å	
Crystal system	Monoclinic	
Space group	P 21/c	
Unit cell dimensions	a = 23.6767(15) Å	α = 90°.
	b = 12.4995(8) Å	β = 106.411(4)°.
	c = 19.5888(12) Å	γ = 90°.
Volume	5561.1(6) Å ³	
Z	4	
Density (calculated)	1.237 Mg/m ³	
Absorption coefficient	2.165 mm ⁻¹	
F(000)	2201	
Crystal size	0.60 x 0.30 x 0.08 mm ³	
Theta range for data collection	3.89 to 67.74°.	
Index ranges	-27 ≤ h ≤ 25, 0 ≤ k ≤ 14, 0 ≤ l ≤ 22	
Reflections collected	43082	
Independent reflections	9690 [R(int) = 0.0509]	
Completeness to theta = 67.74°	98.2 %	
Absorption correction	Semi-empirical from equivalents	
Max. and min. transmission	0.8459 and 0.3567	
Refinement method	Full-matrix least-squares on F ²	
Data / restraints / parameters	9690 / 3 / 678	
Goodness-of-fit on F ²	1.005	
Final R indices [I > 2σ(I)]	R1 = 0.0684, wR2 = 0.1596	
R indices (all data)	R1 = 0.0746, wR2 = 0.1622	
Largest diff. peak and hole	0.577 and -0.567 e.Å ⁻³	

Table 20. Crystal data and structure refinement for raj16m (F1-Tol).

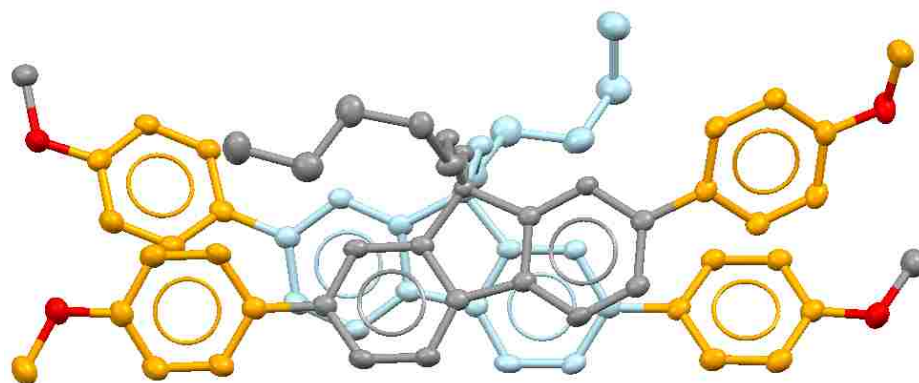
Identification code	raj16m	
Empirical formula	C ₄₆ H ₃₆ O ₄	
Formula weight	652.75	
Temperature	100(2) K	
Wavelength	1.54178 Å	
Crystal system	Monoclinic	
Space group	P 21/n	
Unit cell dimensions	a = 9.7701(2) Å	α = 90°.
	b = 24.4149(5) Å	β = 91.6700(10)°.
	c = 14.1159(3) Å	γ = 90°.
Volume	3365.72(12) Å ³	
Z	4	
Density (calculated)	1.288 Mg/m ³	
Absorption coefficient	0.639 mm ⁻¹	
F(000)	1376	
Crystal size	0.33 x 0.14 x 0.07 mm ³	
Theta range for data collection	3.62 to 67.94°.	
Index ranges	-11 ≤ h ≤ 11, 0 ≤ k ≤ 29, 0 ≤ l ≤ 16	
Reflections collected	28063	
Independent reflections	5928 [R(int) = 0.0177]	
Completeness to theta = 67.94°	98.7 %	
Absorption correction	Semi-empirical from equivalents	
Max. and min. transmission	0.9566 and 0.8169	
Refinement method	Full-matrix least-squares on F ²	
Data / restraints / parameters	5928 / 0 / 456	
Goodness-of-fit on F ²	1.012	
Final R indices [I > 2σ(I)]	R1 = 0.0329, wR2 = 0.0891	
R indices (all data)	R1 = 0.0342, wR2 = 0.0902	
Extinction coefficient	0.00076(10)	
Largest diff. peak and hole	0.209 and -0.161 e.Å ⁻³	

Table 21. Crystal data and structure refinement for raj11s (F2-BP).

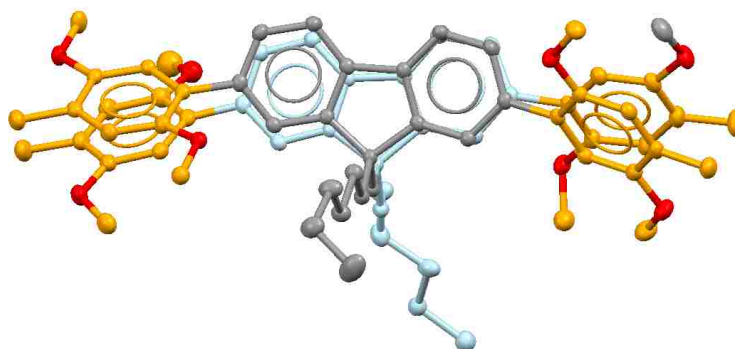
Identification code	raj11s
Empirical formula	C _{87.13} H _{76.25} Cl _{0.25}
Formula weight	1132.20
Temperature	100(2) K
Wavelength	1.54178 Å
Crystal system	Monoclinic
Space group	P 2/n
Unit cell dimensions	a = 30.1607(9) Å α = 90°. b = 29.6275(8) Å β = 112.7550(10)°. c = 31.1218(9) Å γ = 90°.
Volume	25645.5(13) Å ³
Z	16
Density (calculated)	1.173 Mg/m ³
Absorption coefficient	0.590 mm ⁻¹
F(000)	9653
Crystal size	0.44 x 0.25 x 0.04 mm ³
Theta range for data collection	2.29 to 68.29°.
Index ranges	-36 ≤ h ≤ 33, 0 ≤ k ≤ 34, 0 ≤ l ≤ 37
Reflections collected	214741
Independent reflections	46096 [R(int) = 0.0580]
Completeness to theta = 68.29°	98.0 %
Absorption correction	Semi-empirical from equivalents
Max. and min. transmission	0.9768 and 0.7813
Refinement method	Full-matrix least-squares on F ²
Data / restraints / parameters	46096 / 78 / 3162
Goodness-of-fit on F ²	1.059
Final R indices [I > 2σ(I)]	R1 = 0.0632, wR2 = 0.1710
R indices (all data)	R1 = 0.0894, wR2 = 0.1860
Largest diff. peak and hole	1.016 and -0.687 e.Å ⁻³

Table 22. Crystal data and structure refinement for raj11x (F2-BPH).

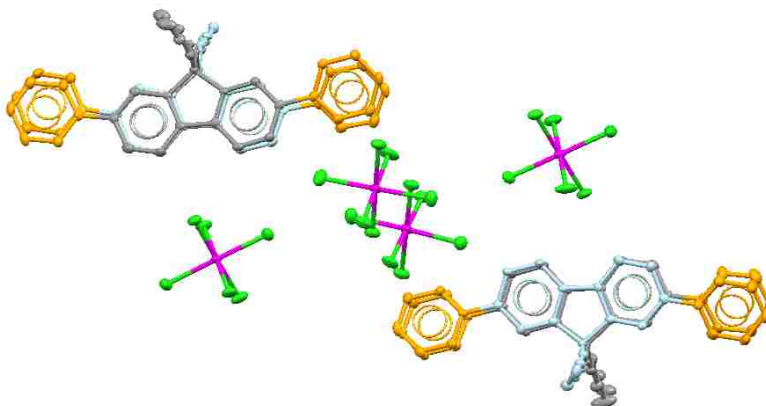
Identification code	raj11x	
Empirical formula	C ₁₁₁ H ₁₂₄	
Formula weight	1458.10	
Temperature	100(2) K	
Wavelength	1.54178 Å	
Crystal system	Monoclinic	
Space group	P 21/n	
Unit cell dimensions	a = 14.57620(10) Å	α = 90°.
	b = 48.1622(5) Å	β = 99.6950(10)°.
	c = 24.4636(2) Å	γ = 90°.
Volume	16928.7(3) Å ³	
Z	8	
Density (calculated)	1.144 Mg/m ³	
Absorption coefficient	0.475 mm ⁻¹	
F(000)	6320	
Crystal size	0.25 x 0.10 x 0.06 mm ³	
Theta range for data collection	2.59 to 68.33°.	
Index ranges	-17 ≤ h ≤ 17, 0 ≤ k ≤ 57, 0 ≤ l ≤ 29	
Reflections collected	145022	
Independent reflections	30438 [R(int) = 0.0288]	
Completeness to theta = 68.33°	97.9 %	
Absorption correction	Semi-empirical from equivalents	
Max. and min. transmission	0.9720 and 0.8904	
Refinement method	Full-matrix least-squares on F ²	
Data / restraints / parameters	30438 / 9 / 2007	
Goodness-of-fit on F ²	1.008	
Final R indices [I > 2σ(I)]	R1 = 0.0459, wR2 = 0.1136	
R indices (all data)	R1 = 0.0589, wR2 = 0.1203	
Largest diff. peak and hole	0.338 and -0.312 e.Å ⁻³	

Table 23. Crystal data and structure refinement for raj11fn (F2-An).

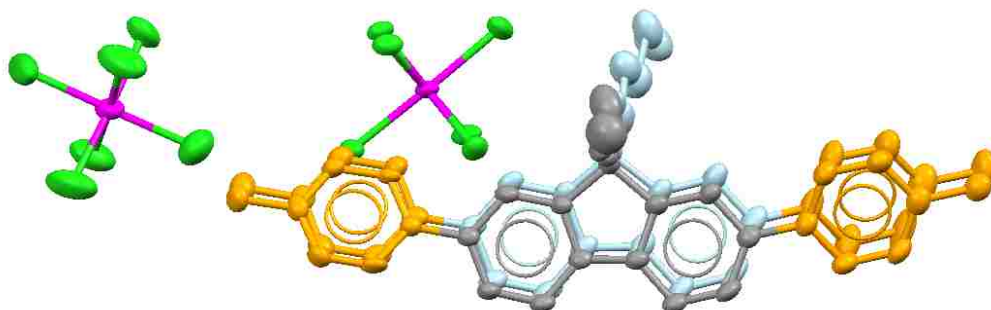
Identification code	raj11fn
Empirical formula	C ₆₇ H ₆₈ O ₄
Formula weight	937.21
Temperature	100(2) K
Wavelength	1.54178 Å
Crystal system	Monoclinic
Space group	P n
Unit cell dimensions	a = 17.3016(3) Å α = 90°. b = 9.8397(2) Å β = 104.5870(10)°. c = 31.1932(6) Å γ = 90°.
Volume	5139.23(17) Å ³
Z	4
Density (calculated)	1.211 Mg/m ³
Absorption coefficient	0.567 mm ⁻¹
F(000)	2008
Crystal size	0.50 x 0.36 x 0.09 mm ³
Theta range for data collection	2.68 to 67.74°.
Index ranges	-20 ≤ h ≤ 20, 0 ≤ k ≤ 11, 0 ≤ l ≤ 37
Reflections collected	42040
Independent reflections	9142 [R(int) = 0.0206]
Completeness to theta = 67.74°	98.1 %
Absorption correction	Semi-empirical from equivalents
Max. and min. transmission	0.9507 and 0.7647
Refinement method	Full-matrix least-squares on F ²
Data / restraints / parameters	9142 / 2 / 1291
Goodness-of-fit on F ²	1.011
Final R indices [I > 2σ(I)]	R1 = 0.0406, wR2 = 0.1113
R indices (all data)	R1 = 0.0416, wR2 = 0.1124
Absolute structure parameter	0.03(19)
Largest diff. peak and hole	0.489 and -0.250 e.Å ⁻³

Table 24. Crystal data and structure refinement for raj16f (F2-DMT).

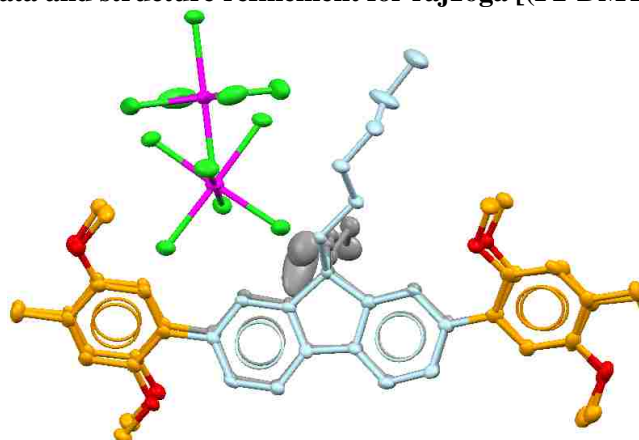
Identification code	raj16f
Empirical formula	C ₇₅ H ₈₄ O _{8.40}
Formula weight	1119.90
Temperature	100(2) K
Wavelength	1.54178 Å
Crystal system	Monoclinic
Space group	P 21/n
Unit cell dimensions	a = 17.8132(4) Å α = 90°. b = 11.2790(2) Å β = 102.9640(10)°. c = 31.9469(6) Å γ = 90°.
Volume	6255.0(2) Å ³
Z	4
Density (calculated)	1.189 Mg/m ³
Absorption coefficient	0.598 mm ⁻¹
F(000)	2405
Crystal size	0.53 x 0.21 x 0.08 mm ³
Theta range for data collection	2.62 to 67.88°.
Index ranges	-21 ≤ h ≤ 20, 0 ≤ k ≤ 13, 0 ≤ l ≤ 37
Reflections collected	52249
Independent reflections	11185 [R(int) = 0.0196]
Completeness to theta = 67.88°	98.3 %
Absorption correction	Semi-empirical from equivalents
Max. and min. transmission	0.9537 and 0.7422
Refinement method	Full-matrix least-squares on F ²
Data / restraints / parameters	11185 / 0 / 767
Goodness-of-fit on F ²	0.998
Final R indices [I > 2σ(I)]	R1 = 0.0421, wR2 = 0.1069
R indices (all data)	R1 = 0.0454, wR2 = 0.1096
Extinction coefficient	0.00011(3)
Largest diff. peak and hole	0.504 and -0.428 e.Å ⁻³

Table 25. Crystal data and structure refinement for raj13aa [(F2-Ph)²⁺ (SbCl₆)₂].

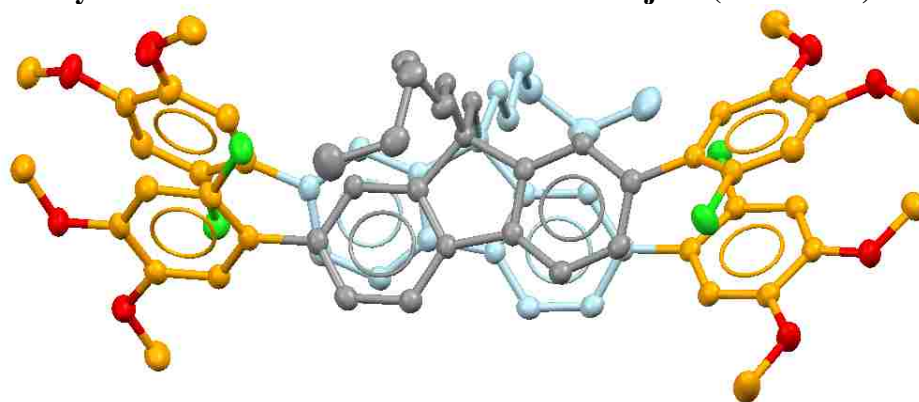
Identification code	raj13aa
Empirical formula	C ₇₇ H ₇₃ Cl ₁₂ Sb ₂
Formula weight	1667.25
Temperature	100(2) K
Wavelength	1.54178 Å
Crystal system	Monoclinic
Space group	P 21/c
Unit cell dimensions	a = 25.9123(6) Å α = 90°. b = 23.5515(5) Å β = 114.5170(10)°. c = 26.4084(6) Å γ = 90°.
Volume	14663.3(6) Å ³
Z	8
Density (calculated)	1.510 Mg/m ³
Absorption coefficient	10.194 mm ⁻¹
F(000)	6728
Crystal size	0.18 x 0.09 x 0.03 mm ³
Theta range for data collection	2.63 to 68.07°.
Index ranges	-31 ≤ h ≤ 28, 0 ≤ k ≤ 28, 0 ≤ l ≤ 31
Reflections collected	122759
Independent reflections	26344 [R(int) = 0.0646]
Completeness to theta = 68.07°	98.5 %
Absorption correction	Numerical
Max. and min. transmission	0.7496 and 0.2612
Refinement method	Full-matrix least-squares on F ²
Data / restraints / parameters	26344 / 150 / 1637
Goodness-of-fit on F ²	1.023
Final R indices [I > 2σ(I)]	R1 = 0.0532, wR2 = 0.1205
R indices (all data)	R1 = 0.0883, wR2 = 0.1338
Largest diff. peak and hole	2.015 and -0.753 e.Å ⁻³

Table 26. Crystal data and structure refinement for raj16ja [(F2-Tol)²⁺ (SbCl₆)₂].

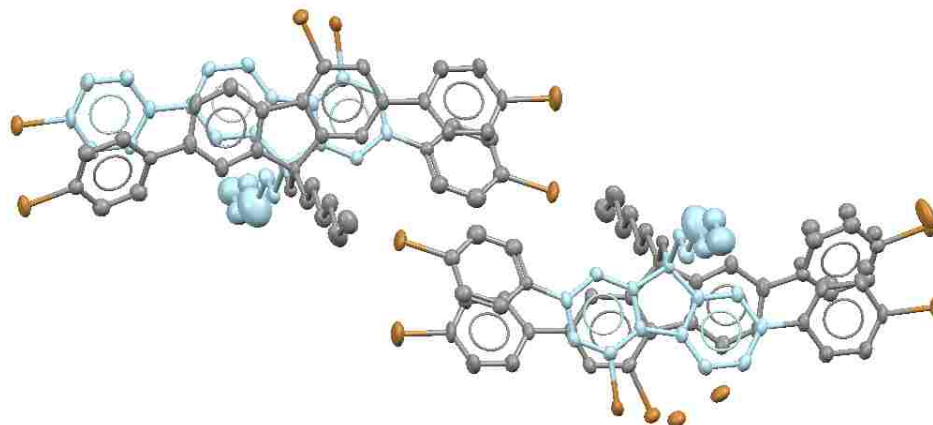
Identification code	raj16ja	
Empirical formula	C ₇₄ H ₇₆ Cl ₁₂ Sb ₂	
Formula weight	1634.25	
Temperature	100(2) K	
Wavelength	1.54178 Å	
Crystal system	Triclinic	
Space group	P -1	
Unit cell dimensions	a = 12.3732(5) Å	α = 71.830(2)°.
	b = 15.0430(6) Å	β = 86.905(2)°.
	c = 21.9499(9) Å	γ = 68.804(2)°.
Volume	3611.2(3) Å ³	
Z	2	
Density (calculated)	1.503 Mg/m ³	
Absorption coefficient	10.333 mm ⁻¹	
F(000)	1652	
Crystal size	0.71 x 0.09 x 0.03 mm ³	
Theta range for data collection	3.32 to 67.60°.	
Index ranges	-14 ≤ h ≤ 13, -16 ≤ k ≤ 17, 0 ≤ l ≤ 26	
Reflections collected	29041	
Independent reflections	12127 [R(int) = 0.0531]	
Completeness to theta = 67.60°	98.0 %	
Absorption correction	Numerical	
Max. and min. transmission	0.7607 and 0.0511	
Refinement method	Full-matrix least-squares on F ²	
Data / restraints / parameters	12127 / 36 / 814	
Goodness-of-fit on F ²	1.001	
Final R indices [I > 2σ(I)]	R1 = 0.0788, wR2 = 0.1892	
R indices (all data)	R1 = 0.1120, wR2 = 0.2139	
Largest diff. peak and hole	2.042 and -0.999 e.Å ⁻³	

Table 27. Crystal data and structure refinement for raj16ga [(F2-DMT)²⁺ (SbCl₆)₂].

Identification code	raj16ga	
Empirical formula	C _{77.01} H _{88.01} Cl _{116.01} O ₈ Sb ₂	
Formula weight	1952.81	
Temperature	100(2) K	
Wavelength	1.54178 Å	
Crystal system	Monoclinic	
Space group	P 21/n	
Unit cell dimensions	a = 17.0139(7) Å	α = 90°.
	b = 23.5773(10) Å	β = 91.232(2)°.
	c = 21.4402(9) Å	γ = 90°.
Volume	8598.6(6) Å ³	
Z	4	
Density (calculated)	1.508 Mg/m ³	
Absorption coefficient	9.971 mm ⁻¹	
F(000)	3953	
Crystal size	0.56 x 0.09 x 0.03 mm ³	
Theta range for data collection	2.79 to 67.87°.	
Index ranges	-20 ≤ h ≤ 20, 0 ≤ k ≤ 28, 0 ≤ l ≤ 25	
Reflections collected	70707	
Independent reflections	15257 [R(int) = 0.0587]	
Completeness to theta = 67.87°	98.6 %	
Absorption correction	Numerical	
Max. and min. transmission	0.7280 and 0.0717	
Refinement method	Full-matrix least-squares on F ²	
Data / restraints / parameters	15257 / 3 / 983	
Goodness-of-fit on F ²	1.019	
Final R indices [I > 2σ(I)]	R1 = 0.0590, wR2 = 0.1427	
R indices (all data)	R1 = 0.0782, wR2 = 0.1526	
Largest diff. peak and hole	1.452 and -1.007 e.Å ⁻³	

Table 28. Crystal data and structure refinement for raj11c (F2-Ver-Cl).

Identification code	raj11c	
Empirical formula	C ₇₁ H ₇₂ Cl ₄ O ₈	
Formula weight	1195.09	
Temperature	100(2) K	
Wavelength	1.54178 Å	
Crystal system	Triclinic	
Space group	P -1	
Unit cell dimensions	a = 13.5163(4) Å	α = 83.4080(10)°.
	b = 14.6913(4) Å	β = 88.474(2)°.
	c = 15.4938(4) Å	γ = 80.116(2)°.
Volume	3010.86(14) Å ³	
Z	2	
Density (calculated)	1.318 Mg/m ³	
Absorption coefficient	2.247 mm ⁻¹	
F(000)	1260	
Crystal size	0.43 x 0.25 x 0.18 mm ³	
Theta range for data collection	2.87 to 66.64°.	
Index ranges	-15 ≤ h ≤ 15, -17 ≤ k ≤ 17, 0 ≤ l ≤ 18	
Reflections collected	23541	
Independent reflections	9795 [R(int) = 0.0214]	
Completeness to theta = 66.64°	98.1 %	
Absorption correction	Semi-empirical from equivalents	
Max. and min. transmission	0.6879 and 0.4450	
Refinement method	Full-matrix least-squares on F ²	
Data / restraints / parameters	9795 / 0 / 748	
Goodness-of-fit on F ²	1.070	
Final R indices [I > 2σ(I)]	R1 = 0.0512, wR2 = 0.1410	
R indices (all data)	R1 = 0.0623, wR2 = 0.1506	
Largest diff. peak and hole	0.930 and -0.289 e.Å ⁻³	

Table 29. Crystal data and structure refinement for raj12qa (F2-Ph-Br6).

Identification code	raj12qa
Empirical formula	C _{64.85} H _{57.70} Br ₆ Cl _{11.70}
Formula weight	1376.83
Temperature	100(2) K
Wavelength	1.54178 Å
Crystal system	Monoclinic
Space group	P 21/c
Unit cell dimensions	a = 14.7051(3) Å α = 90°. b = 26.6887(5) Å β = 101.4120(10)°. c = 14.5892(3) Å γ = 90°.
Volume	5612.48(19) Å ³
Z	4
Density (calculated)	1.629 Mg/m ³
Absorption coefficient	6.221 mm ⁻¹
F(000)	2743
Crystal size	0.52 x 0.28 x 0.12 mm ³
Theta range for data collection	3.31 to 67.79°.
Index ranges	-17 ≤ h ≤ 17, 0 ≤ k ≤ 31, 0 ≤ l ≤ 17
Reflections collected	46029
Independent reflections	9987 [R(int) = 0.0336]
Completeness to theta = 67.79°	98.0 %
Absorption correction	Numerical
Max. and min. transmission	0.5223 and 0.1403
Refinement method	Full-matrix least-squares on F ²
Data / restraints / parameters	9987 / 69 / 670
Goodness-of-fit on F ²	1.130
Final R indices [I > 2σ(I)]	R1 = 0.0725, wR2 = 0.1687
R indices (all data)	R1 = 0.0795, wR2 = 0.1721
Largest diff. peak and hole	1.114 and -1.006 e.Å ⁻³

Bibliography

1. Kiupel, B.; Niederalt, C.; Nieger, M.; Grimme, S.; Vogtle, F. *Angew. Chem. Int. Ed.* **1998**, *37*, 3031-3034.
2. Grimme, S.; Harren, J.; Sobanski, A.; Vogtle, F. *Eur. J. Org. Chem.* **1998**, 1491-1509.
3. Hill, D. J.; Mio, M. J.; Prince, R. B.; Hughes, T. S.; Moore, J. S. *Chem. Rev.* **2001**, *101*, 3893-4011.
4. Kočovský, P.; Vyskočil, S.; Smrčina, M. *Chem. Rev.* **2003**, *103*, 3213-3245.
5. Jeulin, S.; de Paule, S. D.; Ratovelomanana-Vidal, V.; Genêt, J.-P.; Champion, N.; Dellis, P. *PNAS*, **2004**, *101*, 5799-5804.
6. Vachon, J.; Perollier, C.; Monchaud, D.; Marsol, C.; Ditrich, K.; Lacour, J. *J. Org. Chem.* **2005**, *70*, 5903-5911.
7. Goncalves-Farbos, M.-H.; Vial, L.; Lacour, J. *Chem. Commun.* **2008**, 829-831.
8. Griffin, G. W.; Horn, K. A. *Org. Prep. Proc. Int.* **1985**, *17*, 187-190.
9. Muellen, K.; Heinz, W.; Klaemer, F. G.; Roth, W. R.; Kindermann, I.; Adamczak, O.; Wette, M.; Lex, J. *Chem. Ber.* **1990**, *123*, 2349-2371.
10. Pomerantz, M.; Dassanayake, N. L.; McManus, T. R.; Reynolds, C. H. *J. Org. Chem.* **1984**, *49*, 4029-4032.
11. Jaime, C.; Font, J. *J. Org. Chem.* **1990**, *55*, 2637-2644.
12. Mislow, K.; Glass, M. A. W.; Hopps, H. B.; Simon, E.; Wahl, G.H., Jr. *J. Am. Chem. Soc.* **1964**, *86*, 1710-1733.
13. Sonogashira, K. In *Comprehensive Organic Synthesis*; Trost, B. M., Fleming, I., Eds.; Pergamon: Oxford, 1991; Volume 3, pp 521-548.
14. Chanteau, S. H.; Tour, J. M. *J. Org. Chem.* **2003**, *68*, 8750-8766.
15. Suzuki, A. *Chem. Commun.* **2005**, 4759-4763.
16. Hassan, J.; Sevignon, M.; Gozzi, C.; Schulz, E.; Lemaire, M. *Chem. Rev.* **2002**, *102*, 1359-1469.
17. Rathore, R.; Abdelwahed, S. H.; Guzei, I. A. *J. Am. Chem. Soc.* **2003**, *125*, 8712.

18. Rathore, R.; Burns, C. L. *J. Org. Chem.* **2003**, *68*, 4071-4074.
19. Franco, G.; Alberti, A.; Guerra, M.; Seconi, G.; Vivarelli, P. *J. Chem. Soc., Perkin Trans. 2*, **1976**, 173 – 178.
20. Banerjee, M.; Shukla, R.; Rathore, R. *J. Am. Chem. Soc.* **2009**, *131*, 1780-1786.
21. Ebersson, L. *Electron-Transfer Reactions in Organic Chemistry*; Springer: New York, 1987.
22. Yoshida, K. *Electrooxidation in Organic Chemistry. The Role of Cation Radicals as Synthetic Intermediates*; Wiley: New York, 1984.
23. Rathore, R.; Kochi J. K. *Adv. Phys. Org. Chem.* **2000**, *35*, 193.
24. Shirota, Y.; Kageyama, H. *Chem. Rev.* **2007**, *107*, 953.
25. Carroll, R. L.; Gorman, C. B. *Angew. Chem. Int. Ed.* **2002**, *41*, 4378.
26. Miller, J. S.; Epstein, A. J.; Reiff, W.M. *Science* **1988**, *240*, 40.
27. Rovira, C. *Chem. Rev.* **2004**, *104*, 5289.
28. Segura, J. L.; Martín, N.; Guldi, D. M. *Chem. Soc. Rev.* **2005**, *34*, 31.
29. Chebny, V. J.; Shukla, R.; Lindeman, S. V.; Rathore, R. *Org. Lett.* **2009**, *11*, 1939.
30. Chebny, V. J.; Navale, T. S.; Shukla, R.; Lindeman, S. V.; Rathore, R. *Org. Lett.* **2009**, *11*, 2253.
31. Davidson, I. M.; Musgrave, O. C. *J. Chem. Soc.* **1963**, 3154.
32. Zhu, X.-Z.; Chen, C.-F. *J. Am. Chem. Soc.* **2005**, *127*, 13158.
33. Zhu, X.-Z.; Chen, C.-F. *J. Org. Chem.* **2005**, *70*, 917.
34. *Introduction to Molecular Electronics*, Petty, M. C., Bryce, M. R., Bloor, D., Eds.; Oxford Univ. Press: New York, 1995.
35. *Organic Electronics*; Klauk, H., Ed.; Wiley-VCH: Weinheim, 2006.
36. Rathore, R.; Burns, C. L.; Deselnicu, M. I. *Org. Synth.* **2005**, *82*, 1.
37. Rathore, R.; Burns, C. L.; Deselnicu, M. I. *Org. Lett.* **2001**, *3*, 2887.

38. Le Magueres, P., Lindeman, S.V., Kochi, J. K. *Org. Lett.* **2000**, 2, 3567.
39. Lee, S.; Chen, B.; Fredrickson, D. C.; DiSalvo, F. J.; Lobkovsky, E.; Adams, J. A. *Chem. Mater.* **2003**, 15, 1420.
40. Schlesener, C. J.; Amatore, C.; Kochi, J. K. *J. Am. Chem. Soc.* **1984**, 106, 7472.
41. Parker, V. D.; Ebersson, L. *Tetrahedron Lett.* **1969**, 2839.
42. Parker, V. D.; Ebersson, L. *Acta Chem. Scand.* **1970**, 24, 3542.
43. Wadumethrige, S. H.; Rathore, R. *Org. Lett.* **2008**, 10, 5139.
44. Becker, H. D.; Sanchez, D. J. *J. Org. Chem.* **1979**, 44, 1787.
45. Dekker, C.; Ratner, M. A. *Physics World* **2001**, 14, 29.
46. Maiya, B. G.; Ramasarma, T. *Current Science* **2001**, 80, 1523.
47. Grinstaff, M. W. *Angew. Chem. Int. Ed. Engl.* **1999**, 38, 3629.
48. Kelley, S. O.; Barton, J. K. *Metal Ions in Biological Systems* **1999**, 36, 211.
49. Barton, J. K. *Pure Appl. Chem.* **1998**, 70, 873.
50. Lewis, F. D.; Wu, T.; Liu, X.; Letsinger, R. L.; Greenfield, S. R.; Miller, S. E.; Wasielewski, M. R. *J. Am. Chem. Soc.* **2000**, 122, 2889.
51. Lewis, F. D.; Liu, X.; Wu, Y.; Miller, S. E.; Wasielewski, M. R.; Letsinger, R. L.; Sanishvili, R.; Joachimiak, A.; Tereshko, V.; Egli, M. *J. Am. Chem. Soc.* **1999**, 121, 9905.
52. Kan, Y.; Schuster, G. B. *J. Am. Chem. Soc.* **1999**, 121, 11607.
53. Lewis, F. D.; Letsinger, R.L.; Wasielewski, M.R. *Acc. Chem. Res.* **2001**, 34, 159.
54. Anthony, J. E.; Brooks, J. S.; Eaton, D. L.; Parkin, S. R. *J. Am. Chem. Soc.* **2001**, 123, 9482-9483.
55. Swartz, C. R.; Parkin, S. R.; Bullock, J. E.; Anthony, J. E.; Mayer, A. C.; Malliaras, G. G. *Org. Lett.* **2005**, 7, 3163-3166.
56. Banerjee, M.; Lindemann, S. V.; Rathore, R. *J. Am. Chem. Soc.* **2007**, 129, 8070.
57. Feringa, B. L.; Jager, W. F.; Lange, B. de *Tetrahedron* **1993**, 49, 8267.

58. Fabbrizzi, L.; Poggi, A. *Chem. Soc. Rev.* **1995**, 198.
59. Watson, M. D.; Fechtenkotter, A.; Mullen, K. *Chem. Rev.* **2001**, *101*, 1267.
60. Rathore, R.; Le Magueres, P.; Lindeman, S.V.; Kochi, J.K. *Angew. Chem. Int. Ed. Engl.* **2000**, *39*, 809.
61. Rathore, R.; Burns, C. L.; Abdelwahed, S. A. *Org. Lett.* **2004**, *6*, 1689-1692.
62. Zhai, L.; Shukla, R.; Rathore, R. *Org. Lett.* **2009**, *11*, 3474.
63. Burley, S.K.; Petsko, A. *J. Am. Chem. Soc.* **1986**, *108*, 7995-8001.

